DEVELOPMENT OF TAILOR-MADE CATALYST LIBRARIES FOR THE CONSTRUCTION OF CHIRAL C-X (X= C, N AND O) BONDS. APPLICATION TO THE SYNTHESIS OF COMPLEX MOLECULES

Joan Saltó de la Torre

UNIVERSITAT ROVIRA i VIRGILI

Development of tailor-made catalyst libraries for the construction of chiral C-X (X= C, N and O) bonds. Application to the synthesis of complex molecules

Joan Saltó de la Torre

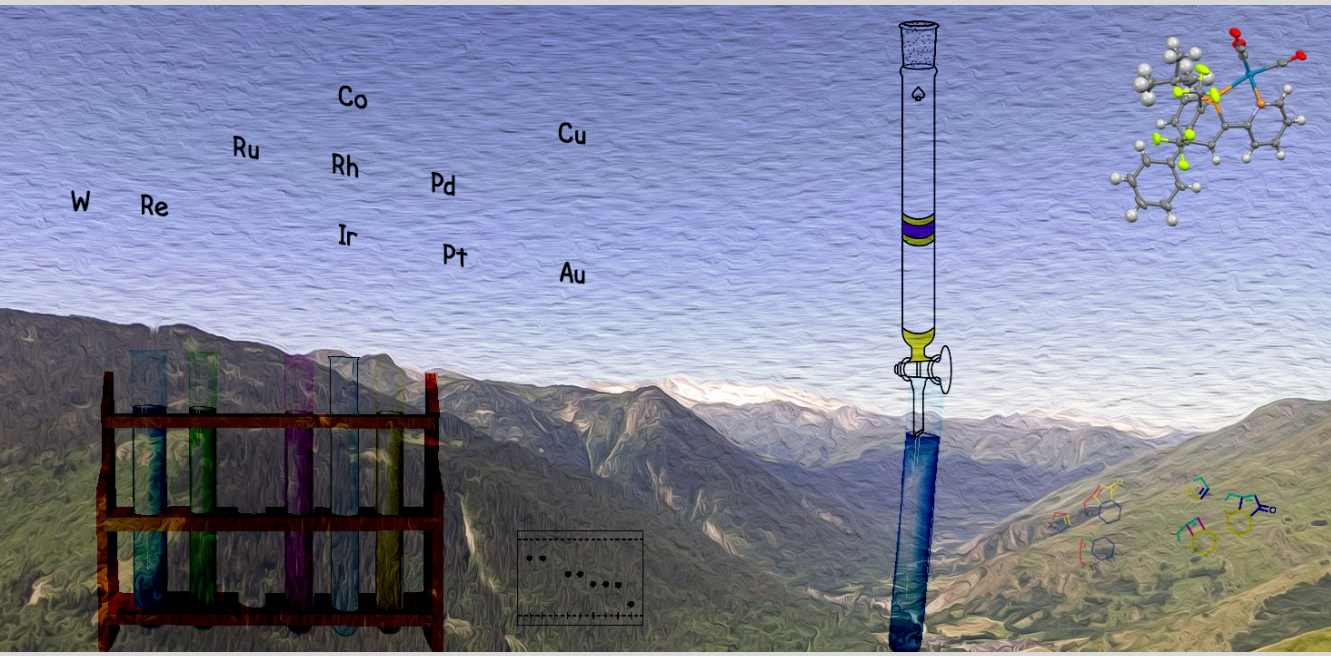

DOCTORAL THESIS
2021

UNIVERSITAT ROVIRA I VIRGILI
DEVELOPMENT OF TAILOR-MADE CATALYST LIBRARIES FOR THE CONSTRUCTION OF CHIRAL C-X (X= C, N AND O) BONDS. APPLICATION TO THE SYNTHESIS OF COMPLEX MOLECULES
Joan Saltó de la Torre

UNIVERSITAT ROVIRA I VIRGILI
DEVELOPMENT OF TAILOR-MADE CATALYST LIBRARIES FOR THE CONSTRUCTION OF CHIRAL C-X (X= C, N AND O) BONDS. APPLICATION TO THE SYNTHESIS OF COMPLEX MOLECULES
Joan Saltó de la Torre

UNIVERSITAT ROVIRA I VIRGILI
DEVELOPMENT OF TAILOR-MADE CATALYST LIBRARIES FOR THE CONSTRUCTION OF CHIRAL C-X (X= C, N AND O) BONDS. APPLICATION TO THE SYNTHESIS OF COMPLEX MOLECULES
Joan Saltó de la Torre

Joan Saltó de la Torre

Development of tailor-made catalyst libraries for the construction of chiral C-X (X = C, N and O) bonds. Application to the synthesis of complex molecules

PhD-Thesis

Supervised by Prof. Montserrat Diéguez Fernández and Prof. Oscar Pàmies Ollé

Departament de Química Física i Inorgànica

UNIVERSITAT ROVIRA i VIRGILI

Tarragona, November of 2021

UNIVERSITAT ROVIRA I VIRGILI
DEVELOPMENT OF TAILOR-MADE CATALYST LIBRARIES FOR THE CONSTRUCTION OF CHIRAL C-X (X= C, N AND O) BONDS. APPLICATION TO THE SYNTHESIS OF COMPLEX MOLECULES
Joan Saltó de la Torre

UNIVERSITAT ROVIRA i VIRGILI

PROF. MONTSERRAT DIÉGUEZ FERNÁNDEZ and PROF. OSCAR PÀMIES OLLÉ, full professors of the Departament de Química Física i Inorgànica at Universitat Rovira i Virgili

WE STATE:

That the present thesis, entitled "**Development of tailor-made catalyst libraries for the construction of chiral C-X (X = C, N and O) bonds. Application to the synthesis of complex molecules**", presented by JOAN SALTÓ DE LA TORRE for the award of the degree of Doctor, has been carried out at the Departament de Química Física i Inorgànica of this university. We also state that this work fulfills all requirements to be eligible for the International Doctorate Award.

Tarragona, November of 2021,

Prof. Montserrat Diéguez Fernández

Prof. Oscar Pàmies Ollé

UNIVERSITAT ROVIRA I VIRGILI
DEVELOPMENT OF TAILOR-MADE CATALYST LIBRARIES FOR THE CONSTRUCTION OF CHIRAL C-X (X= C, N AND O) BONDS. APPLICATION TO THE SYNTHESIS OF COMPLEX MOLECULES
Joan Saltó de la Torre

Acknowledgements/Agraïments

Ja ha plogut des de que vaig començar la tesi i fer aquesta part és potser, la més difícil. Molt de temps, masses vivències bones i dolentes però una experiència àmpliament satisfactòria.

En primer lloc, als meus supervisors, la Prof. Montserrat Diéguez i el Prof. Oscar Pàmies, gràcies per tot, per aguantar-me, per corregir-me i per confiar en mi. Moltes gràcies per les mil correccions, papers, presentacions, etc.... i per ajudar-me a créixer científicament i com a persona. Mil gràcies.

I would also to thank Prof. Müller for the collaboration we have started this year. It was a pleasure working at FU Berlin with your group.

També voldria mencionar tots els tècnics que fan possible la recerca en aquesta universitat, en especial al Josep, la Raquel i al Ramón. Raquel moltes gràcies per estar sempre disposada a ajudar encara que estiguis molt enfeinada. Josep, gràcies per tenir cura dels solvents, gràcies hem pogut fer un munt de columnes! Ramón, el millor tècnic de RMN del món sencer, gràcies per arreglar-me els *shims*, *tunejar* les mostres sempre que ha calgut i per estar sempre disposat a ajudar. És una sort per a la universitat tenir un tècnic com tu! També voldria mencionar i donar les gràcies a tot el personal de la Universitat que no tenint contacte tan directe han estat disposats sempre a ajudar.

Durant aquesta vivència he viscut amb dos grups diferents. En primer lloc començaré pels antics. Carlota, gràcies per ficar-me al meu lloc quan ha calgut i fer-me baixar a terra, això m'ha fet créixer. Moltíssima sort amb la teva nova família que en pocs mesos tindràs! Moltes ganes de veure a l'Artur! Maria, et desitjo molta sort en la nova aventura que començaràs aviat a la URV! Segur podràs amb tot el que et proposis. Zahra, it was nice and funny work with you, I will always remember you with a smile. Jordi R. i Núria, moltíssima sort amb la vostra família que tindreu aviat, segur que sereu uns pares fantàstics, va ser un plaer treballar amb vosaltres. Myriam, I also wish both of you good luck, thank you for being so kind. Albert F, Efrem, Fran va ser un plaer treballar amb vosaltres.

En segon lloc, al nou grup, Jordi, m'ho he passat molt bé amb tu tots aquests anys ha sigut un plaer discutir de química orgànica amb tu com ha sigut un plaer compartir sopars, dinars, berenars, ets un crack! Moltíssima sort amb el que t'espera. Lola qué te voy a decir, que muchas gracias por todo ha sido un placer compartir tiempo contigo, nos hemos reído mucho. La padrina Jèssica, la més veterana del grup! Ets una de les molt bona xiqueta, no canviïs mai i molta sort en la teva nova aventura industrial. Pol, molta sort en el terreny personal i científic, segur que si t'ho proposes aconseguiràs al que vulguis. Moltes gràcies per introduir-me a la "*vida moderna*" ara sé moltes coses més. Daniel, you have arrived later but anyway, I will wish you good luck in this new adventure you are about to start now. I must tell you that you should speak more. Don't be shy!

Acknowledgements

Als borillos. Oriol, ha sigut un plaer compartir temps amb tu tant laboralment com personalment, m'ho he passat genial! Richi! Hemos ido a la par estos años. ¡Muchas gracias por todo! ¡Suerte con tu defensa! Paula, ha sigut un plaer coincidir amb tu també, m'ho he passat molt bé esmorzant i discutint per qui va primer al *rotavap*. Mireia, molta sort amb el màster i amb les columnes! Sara, que decirte, que eres el toque de color del 216, sin ti y tus estilos el laboratorio 216 no sería lo mismo.

Joris, I wish you good luck in la France! It was a pleasure learning French from you! I have laughed a lot. I wish to see you soon. ¡¡¡Pequeño Javi, te deseo mucha suerte!!!

De los de arriba, ¡Aaron "*gracias*" por venirme a molestar por el hidrogeno y por el tiempo que hemos pasado juntos! ¡Me lo he pasado muy bien!

To my German friends, I would not forget to mention them. Without them, my stage in Berlin would have not been the same. I must mention especially *Tavarish* Andrei who taught me a lot of Russian stuff, communism and all the time we had spent together. I will always remember a lot of Russian songs, and the funny time spent in the lab! Tim and Alex, I wish you good luck in all, and remember the German idiosyncrasy: Germans always suffer...

No puc deixar-me els meus amics... Sergi i Ivet, gràcies per tot i molta sort que segur que la tindreu! Leila, Irene y Jordi gràcies per aguantar-me i ajudar a aixecar-me quan he no he estat bé. Dona gust tenir uns amics com vosaltres.

No puc deixar de banda, la part més important de totes, la família. Especialment agrair a la meva mare la comprensió durant aquest temps que he estat més enfeinat i per fer-me la vida més fàcil. També mencionar als que ja no hi son, sempre us tinc presents.

Gràcies a tots per tot.

I gratefully acknowledge financial support of the Ministry of Science and Technology of the Spanish government by an FPI grant (BES-2017-079670).

List of publications

1. Biosca, M.; Margalef, J.; Caldentey, X.; Besora, M.; Rodríguez-Escrich, C.; Saltó, J.; Cambeiro, X. C.; Maseras, F.; Pàmies, O.; Diéguez, M.; Pericàs, M. A., Computationally Guided Design of a Readily Assembled Phosphite–Thioether Ligand for a Broad Range of Pd-Catalyzed Asymmetric Allylic Substitutions. *ACS Catalysis* **2018**, *8*, 3587-3601.

2. Biosca, M.; Saltó, J.; Magre, M.; Norrby, P.-O.; Pàmies, O.; Diéguez, M., An Improved Class of Phosphite-Oxazoline Ligands for Pd-Catalyzed Allylic Substitution Reactions. *ACS Catalysis* **2019**, *9*, 6033-6048.

3. Saltó, J.; Pàmies, O.; Diéguez, M.; Synthetic applications of Pd-allylic substitution products for the synthesis of chiral complex molecules. *Manuscript in preparation*.

UNIVERSITAT ROVIRA I VIRGILI
DEVELOPMENT OF TAILOR-MADE CATALYST LIBRARIES FOR THE CONSTRUCTION OF CHIRAL C-X (X= C, N AND O) BONDS. APPLICATION TO THE SYNTHESIS OF COMPLEX MOLECULES
Joan Saltó de la Torre

Summary of the thesis

The thesis is divided into 7 Chapters.

Chapter 1. *Introduction*. This Chapter first presents the relevance of enantioselective metal catalysis in the preparation of enantiomerically pure compounds. An important step in their preparation is the design of chiral ligands. Among them, two families of heterodonor phosphite/phosphinite-thioether and phosphite-oxazoline containing ligands are developed in this thesis for application in the Pd-catalyzed allylic substitution reaction. For this reaction, the antecedents, performance, and main achievements are discussed in this introduction Chapter, with special emphasis on the most successful P-oxazoline/thioether ligand families. The state-of-the-art and current needs in this field justify the objectives of the thesis.

Chapter 2. *Objectives*. Based on the aspects discussed in Chapter 1, this Chapter presents the objectives of the thesis. These involve the synthesis and application in the Pd-catalyzed allylic substitution reaction of two families of heterodonor P-X ligands (X= thioether and oxazoline). It also includes a further derivatization of some of the substitution products for the synthesis of complex molecules. Finally, the objectives also include the design and synthesis of phosphabarrelene/5-phosphasemibullvalene-pyridine ligands, specially designed to be applied in the near future in enantioselective allylic and propargylic catalyzed substitution reactions, as well as metal-catalyzed asymmetric hydrogenations.

Chapter 3. *DFT-guided synthesis of a new family of P-S ligands based on indene for Pd-catalyzed asymmetric allylic substitution reactions*. This Chapter, which has been done in a collaboration framework with the groups of M. A. Pericàs and F. Maseras (ICIQ), contains the development and application of a phosphite/phosphinite-thioether ligand library in Pd-catalyzed allylic substitution reactions. These ligands have been prepared in only three steps from cheap indene. The combination of experimental and theoretical studies has led to the design of an optimal, solid, and air-stable phosphite-anthracenethiol derivative with excellent behavior in the reaction of choice. Improving most approaches reported to date, this ligand presents a broad substrate and nucleophile scope. Excellent enantioselectivities have been achieved for a range of linear and cyclic allylic substrates using a large number of C-, N-, and O-nucleophiles (40 compounds in total). The species responsible for the catalytic activity have been also further studied by NMR to clearly establish the origin of the enantioselectivity. The results included in this Chapter has been published in *ACS Catalysis* **2018**, 8, 3587. I have participated in the synthesis of part of the ligand library and in part of the catalysts screening.

Chapter 4. *Application of a phosphite-oxazoline ligand library for Pd-catalyzed asymmetric allylic substitution reactions.* This Chapter, which has been done in collaboration with Prof. P-O Norrby from AstraZeneca in Sweden, includes the design of a phosphite-oxazoline ligand library for Pd-catalyzed asymmetric allylic substitution reactions. By selecting the substituents at the alkyl backbone chain of the ligand backbone and at the oxazoline group, as well as the configuration of the biaryl phosphite group, high activities (TOF > 8000 mol substrate × (mol Pd × h)$^{-1}$) and excellent enantioselectivities (*ee*'s up to 99%) have been achieved for many substrates with a wide range of C-, O-, and N-nucleophiles (73 substitution products in total). These results surpass the best one reported so far, even the family of ligands included in Chapter 3. The results included in this Chapter has been published in *ACS Catalysis* **2019**, 9, 6033. I have participated in the synthesis of part of the ligand library and most of the catalysts screening.

Chapter 5. *Synthetic applications of the resulting Pd-catalyzed allylic substitution products.* In this Chapter we have derivatized some of the products obtained in Chapters 3 and 4. In this regard, we submitted the chiral alkylation products to Grubbs' metathesis, to Pauson-Khand reactions and to metal catalyzed cycloisomerization to achieve chiral functionalized (poly)carbocyclic and heterocyclic compounds.

Chapter 6. *Synthesis of heterodonor phosphabarralene/5-phosphasemibullvalene-pyridine ligands and their metal complexes.* This Chapter includes the work done during my stage of 7 months in the group of Prof. C. Müller at Freie Universität in Germany. During the stage I have been able to successfully synthesize several phosphabarrelene-pyridine and 5-phosphasemibullvalene-pyridine ligands from their corresponding phosphinine-pyridine compounds. We have also studied their coordination chemistry.

Chapter 7. *General conclusions*. This Chapter presents the conclusions of the work presented in this thesis.

Index

Chapter 1

Introduction

The preparation of enantiopure compounds is nowadays a must in several industries such as agrochemical, pharmaceutical, among others.[1] Since the thalidomide case in the 60's, where one of the enantiomers of this drug had the desired antiemetic properties the other one had teratogenic effects, the regulations on the drug marked have increased and nowadays the preparation of single stereoisomers is fundamental. In this respect, asymmetric catalysis is one of the most valuable tools since with the proper choose of the catalytic system high levels of conversion and enantioselectivities can be obtained.[1] Moreover, asymmetric catalytic processes are more straightforward as well as more sustainable since they do not require the use of, for example, chiral auxiliaries or the resolution of enantiomers.[1] In this regard, metal-catalyzed asymmetric reactions have proved to be a reliable tool for the construction of new stereogenic centers.[1] Therefore, its importance has been reflected by the myriad of publications in this field as well as the Nobel Prize award in 2001 to W. S. Knowles, K. B. Sharpless and R. Noyori as well as to E. Negishi, R. F. Heck and A. Suzuki in 2010.[2]

To have the best performing system in enantioselective metal-catalyzed reactions several variables should be optimized. In this respect, one of the most crucial is the correct choose of the chiral ligand.[1, 3] The ideal ligand should be synthesized in few steps, preferentially from the chiral pool, be easy to handle (an air stable solid) and to present a modular scaffold that facilitates to find the best performing ligand. In the last decades heterodonor ligands have emerged as an increasingly used ligand class, since the different electronic and steric properties of these heteroatoms are powerful stereocontrol elements.[3] The two functionalities also smooth catalyst optimization since both functionalities can be independently varied for improved catalyst performance. Among heterodonor ligands, P-N ligands have been the most used, being P-oxazoline the most studied ones due to their availability and modular preparation. Among the thousands of ligands prepared, a few stand out for their broad applicability.[3a,c-f] A large reaction and substrate scope are desirable to minimize the time devoted to ligand finding and preparation.

In this aspect, this thesis is focused in finding suitable chiral ligands for metal-catalyzed asymmetric reactions. Concretely, two libraries of heterodonor ligands have been designed to overcome the substrate specificity in Pd-catalyzed asymmetric allylic substitution (AAS) reactions. Thus, air stable and modular P-thioether and P-oxazoline ligand libraries have been prepared from readily available starting materials and applied on Pd-AAS (see chapters 3 and 4). The synthetic applications of these new P-S and P-N ligand libraries have been demonstrated by their use in the synthesis of more complex chiral molecules (see chapter 5). To continue the improvement of finding ligands with a large reaction and substrate scope, in chapter 6 we include the development of a new type of heterodonor P-N ligands, the phosphabarralene/5-phosphasemibullvalene-pyridine ones, specially designed for a future application in Pd-AAS but also in propargylic substitution, hydrogenation among other reactions. Below, we describe the background in the Pd-catalyzed asymmetric allylic substitution with special emphasis on

the most successful bidentate heterodonor P-oxazoline and P-thioether ligand families applied in this process.

1.1. Pd-catalyzed asymmetric allylic substitution

The formation of new chiral C-C and C-heteroatom bonds is of high importance on the field of organic chemistry. In this regard, the Pd-catalyzed asymmetric allylic substitution has proved to be one of the most efficient strategies since it has a high functional group tolerance, it works under mild reaction conditions and usually the levels of stereoinduction achieved are high.[4] This process involves the reaction between a racemic allylic substrate, which contains a leaving group (carbonate or acetate), and a nucleophile. In enantioselective Pd-catalyzed allylic substitution reactions we can find two different classes depending on the type of substrate (Scheme 1.1). Type A reaction involves the formation of a symmetrical π-allyl intermediate from the corresponding racemic substrates (either linear or cyclic). Therefore, in this case the enantioselectivity is ruled by the regioselectivity of the nucleophilic attack and therefore it depends on the ability of the chiral ligand to differentiate the two corresponding allylic terminal carbons. In type B reactions the racemic or prochiral substrate, with two identical geminal substituents at one terminal allyl carbon, react via the π-allyl intermediate which can isomerize though a π-σ-π mechanism. Therefore, the enantioselection can occur either in the ionization step, leading to the allyl intermediate, or in the nucleophilic attack. For this substrate type, the regioselectivity is also a problem since a mixture of regioisomers can be obtained. Most of the Pd-catalyst developed until now favour the obtention of the undesired achiral linear product rather than the chiral branched isomer, in contrast to what was found with Ir- and Cu-catalytic systems.[4]

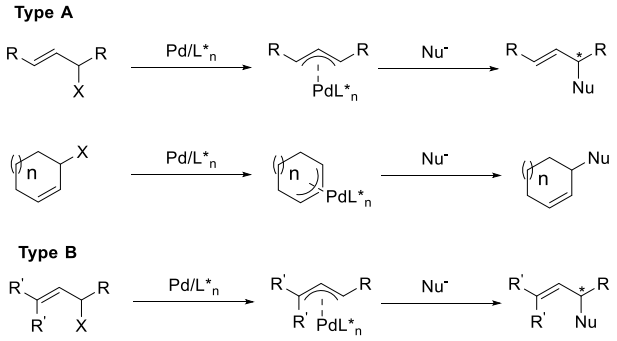

Scheme 1.1. Classification of Pd-catalyzed asymmetric allylic substitution reactions.

In this reaction the variety of substrates (linear or cyclic) is wide, being the *rac*-(*E*)-1,3-diphenylallyl acetate the benchmark substrate (Figure 1.1). Among the nucleophiles used, stabilized carbon nucleophiles, such as carbanions derived from 1,3-dicarbonyl

compounds, maintain a prominent position in enantioselective Pd-catalyzed allylic substitutions. Apart from malonates and related stabilized C-nucleophiles including various functionalized malonates, β-diketones, 2-cyanoacetates, pyrroles, nitromethane, etc., N- and O-nucleophiles and to a lesser extent P- and S-nucleophiles have been used.[4] Among the reactions studied the alkylation of *rac*-(*E*)-1,3-diphenylallyl acetate using malonates, and especially dimethyl malonate as the nucleophile, continues to serve as benchmark reaction to evaluate the potential of new ligands in asymmetric catalysis. Accordingly, since 2008, a large number of papers on the development of new ligands for the alkylation of this benchmark substrate with malonate derivatives have been published.[4a]

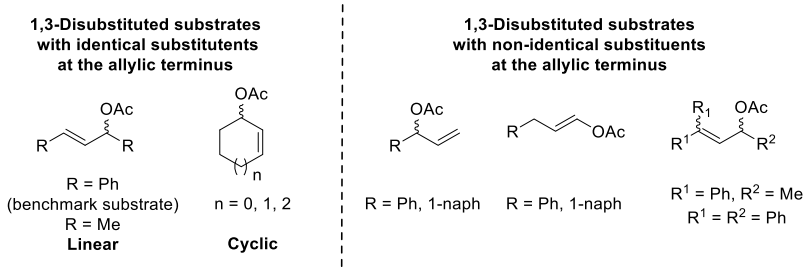

Figure 1.1. Types of substrates used on Pd-catalyzed asymmetric allylic substitutions.

1.1.1. Mechanism

The catalytic cycle for Pd-catalyzed allylic substitution reactions using stabilized C-nucleophiles and heteronucleophiles has been studied widely.[4] The catalytic cycle involves four steps (Scheme 1.2).

The first step is the coordination of the allylic substrate **B** to the Pd^0 specie **A**. Then, an oxidative addition take place to form the Pd π-allyl intermediates **D**, identical for ligands with C_2 symmetry, and usually minor, *syn*,*anti* and *anti*,*anti* isomers. Intermediates **D** in presence of nucleophiles can suffer a nucleophilic attack in one of the two allyl carbon terminus (C-1 or C-3) preferentially. After this, the formation of an unstable Pd^{II} complex **E** leads to the readily dissociation to the final substituted product **F** and the formation again of Pd^0 specie **A** which restart the catalytic cycle.

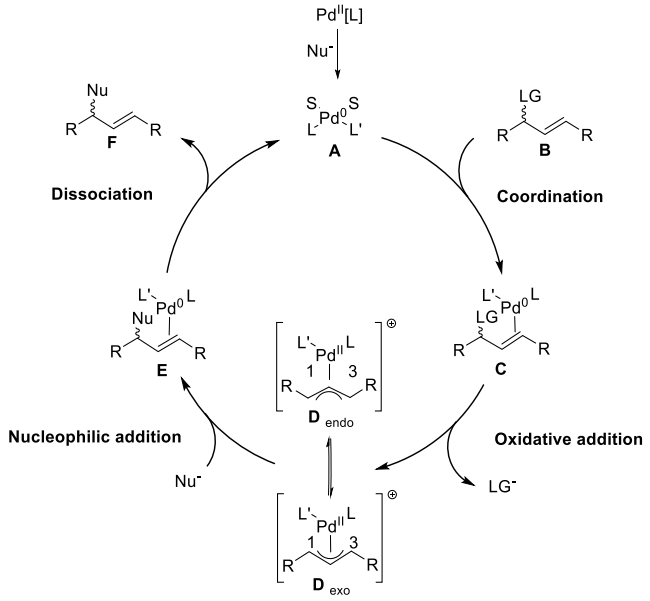

Scheme 1.2. Catalytic cycle for Pd-catalyzed allylic substitution reaction.

For substrates with enantiotopic leaving groups (in geminal or 1,3-positions), the enantiodiscriminating step is the oxidative addition whereas for substrates with identical substituents at the 1- and 3-positions, enantiodiscrimination occurs during nucleophilic attack at one of the diastereotopic sites (enantiotopic in the presence of achiral ligands). For other substrates, the relative rates of the different steps, including interconversion of isomeric allyl complexes, govern in which step the enantioselectivity is determined. Use of prochiral nucleophiles, finally, may also lead to enantiodiscrimination.[4]

1.1.2. Ligands

The ligands used for this transformation are mainly based in the use of four different strategies (Figure 1.2). The first one developed by Hayahi *et al.* is based on directing the nucleophile to one of the allyl terminal carbon atoms by a secondary interaction between the nucleophile and a side chain of the ligand.[5] The second one, developed by Trost and coworkers, is based on bidentate diphosphine ligands with a large bite angle that are able to create a chiral pocket between the ligand and the metal center where the allyl system accommodates perfectly.[6] Ligands of this type represent one of the most effective ligand families for asymmetric allylic substitution of unhindered substrates, which has found widespread use in natural product synthesis. The originally mechanistic

model proposed that the enantioselectivity results from steric interactions with the four P-phenyl groups forming the chiral cavity, which block one of the allylic termini against nucleophilic attack.[6] A refined model reported in 2009 found the presence of secondary interactions between the ligand and the nucleophile that directs the attack.[7] Therefore, the enantioselectivity induced by Trost's ligands results from an interplay between steric interactions imposed by the chiral cavity of the ligand and H-bond and electrostatic interactions of the amide groups with the nucleophile. The third strategy is based on the use of heterodonor ligands which create an electronic differentiation between both allylic carbon terminal atoms due to the different trans influences of both donor groups. In this respect, Helmchen, Ptaltz and Williams developed the phosphine-oxazoline ligands (PHOX ligands) which have provided high enantioselectivities for the benchmark linear hindered substrate *rac*-(*E*)-1,3-diphenylallyl acetate.[8] After this work, a wide range of heterodonor P-N ligands, mainly P-oxazolines, have been prepared by modifying the ligands backbone. Unfortunately, phosphine-oxazoline ligands give poor *ee'*s when less sterically demanding or cyclic substrates are used.[8] In this respect, the phosphine/phosphinite-N ligands and the Trost diphosphine ligands have a complementary scope. Other mixed bidentate donor ligands, such P-S ligands, are emerging as alternative to P-N ligands.[3a-c]

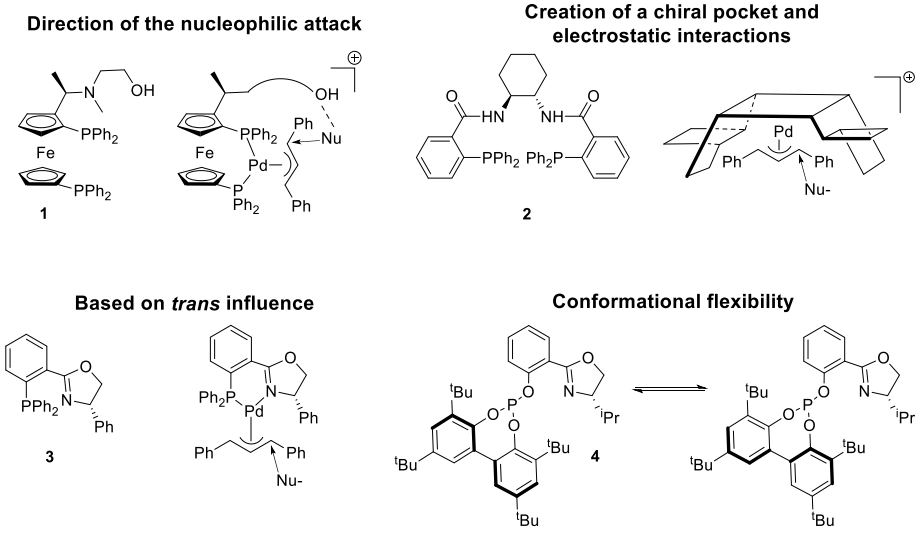

Figure 1.2. Schematic representation of the four main ligand design' strategies used in Pd-AAS.

A fourth design principle, which has emerged from the search for ligands displaying wider substrate scope, focuses on conformational flexibility.[9] Traditionally, chiral ligands were designed based on conformationally rigid structural elements that allow straightforward prediction of steric interactions with a substrate. However, more recently evidence has been accumulated that a certain degree of flexibility can be beneficial for inducing enantioselectivity. In this respect, our group was pioneering and

found that the introduction of a flexible biaryl phosphite group was advantageous in overcoming the high substrate specificity and reaction rates of this process. The first example of this approach was the replacement of the phosphine group on PHOX ligands by biaryl phosphite moieties.[10] Pd complexes of these ligands proved to be very effective catalysts for reactions of both hindered and unhindered linear and cyclic substrates with a large number of C-, N- and O-nucleophiles (48 substitution products in total), outperforming Pd-PHOX catalysts. Moreover, excellent activities (TOFs up to >2400 mol substrate x (mol Pd x h)$^{-1}$), higher than with PHOX ligands were achieved due to the π-acceptor capacity of the phosphite moiety. The wide substrate scope was rationalized by NMR and DFT studies of its Pd-η^3-olefin and Pd-η^3-allyl complexes. This studies indicate that the broad substrate scope of Pd/biaryl phosphite-oxazoline systems results from their capacity to adjust the size of the binding pocket to the substrate type, a feature that also explains their excellent performance in other asymmetric reactions.[11] In addition, the presence of a biaryl phosphite group increase the regioselectivity to the branched isomer when the more challenging monosubstituted substrates were used, thanks to its π-acceptor ability and bulkiness, phosphite moiety increase the density of the most substituted allyl terminal carbon via trans influence, favouring the nucleophilic attack to this carbon. Therefore, with these ligands we could also reach high regio- and enantioselectivities for monosubstituted substrates.[10a,c]

It should be mentioned that although many new heterodonor ligands have been designed during the last decades, several recent studies on more challenging substrates and/or nucleophiles were tested with well-established ligand scaffolds or slight modifications of them (e.g., PHOX and Trost's ligand).[4a] Although bidentate ligands continue to have a prominent position, we must highlight that some of monodentate ligands have recently provided excellent results when using specific type of substrates.[12]

In the next sections we summarize and discuss the most successful P-oxazoline and P-thioether ligands developed in Pd-catalyzed asymmetric allylic substitution reactions.

1.1.2.1. P-oxazoline ligands

Derived from PHOX ligands, several other P-oxazoline based ligands have been developed.[3d] In this sense these modifications on the PHOX ligands can be grouped in: (a) modifications of the oxazoline ring, (b) modifications on the ligand backbone and (c) the replacement of the phosphine by other phosphorous groups.

Concerning the modifications of the oxazoline ring (Figure 1.3), it can been found the introduction of a sugar moiety or other chiral groups with the development of ligands **5**[13], **6**[14] (with R = OH, OMe) and **7**[15] (R = Me, Bn, $CHPh_2$, CPh_3, CH_2CH_2OMe). Both, ligands **5** and **6**, provided comparable results then the PHOX ligands for the hindered linear benchmark substrate *rac*-(*E*)-1,3-diphenylallyl acetate (up to 98% and >99% *ee,* respectively) and low enantioselectivities for less sterically demanding substrates (up to 66% and 59% *ee*, respectively).

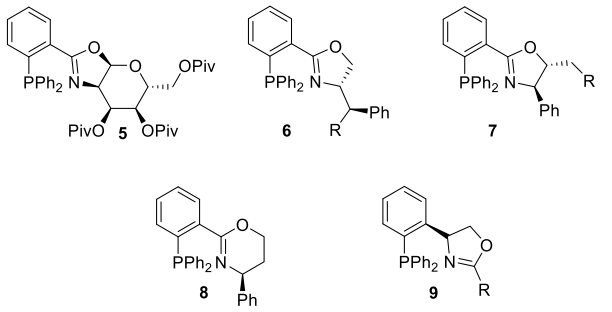

Figure 1.3. Selected modifications of the oxazoline ring in phosphine-oxazoline ligands.

Ligands **7** with two stereogenic groups in the oxazoline ring provided high enantioselectivities when using the benchmark linear substrate (*ee* up to 97%) and trisubstituted ones (*ee* up to 94 %), but low with non-hindered substrates.[15] Notably, these ligands also performed well for monosubstituted substrates obtaining high regioselectivity towards the branched isomer (up to 93%) with enantioselectivies up to 82%.

Another modification is the replacement of the 5-membered ring of the oxazoline by a 6-membered ring with ligand **8**.[16] The results with benchmark substrate were excellent (*ee* up to 99%) whereas for the benchmark non-hindered linear substrate, *rac*-1,3-dimethylallyl acetate, the enantioselectivities attained were low (*ee* up to 50%). Moreover, the activities obtained with this catalytic system were much lower than those achieved with PHOX ligands.

Finally, the conformationally rigid phosphine-oxazoline **9** (R = ^{t}Bu, $CHPh_2$, 3,5-di-^{t}Bu-Ph, Ad) has been also applied in Pd-AAS.[17] Its application provided high *ee* for the benchmark hindered substrate (*ee* up to 98%) but, for cyclic substrates as well as for linear non-symmetric substrates the *ee*'s achieved were lower (*ee's* up to 34%) indicating that this ligand is also highly substrate specific.

Several modifications on the ligand backbone have been performed (Figure 1.4). In this regard, the replacement of the *o*-penylene tether on PHOX ligands by a ferrocenyl moiety has been studied with ligands **10** (R = ^{t}Bu, ^{i}Pr)[18] and **11** (R = ^{t}Bu, ^{i}Pr, Ph)[19]. Both ligands provided high enantioselectivities in the Pd-catalyzed asymmetric allylic alkylation of the benchmark hindered substrate *rac*-(*E*)-1,3-diphenylallyl acetate using dimethyl malonate (*ee*'s up to 99% and 95%, respectively). Moreover, the allylic alkylation of benchmark unhindered linear substrate *rac*-(*E*)-dimethylallyl acetate using ligand **10** and dimethyl malonate as nucleophile provided high levels of enantioinduction (*ee* up to 98%). With these ligands, the authors found that the planar chirality exerted an important control over the Pd-allyl complexes formed and therefore on the enantiomeric excesses observed.

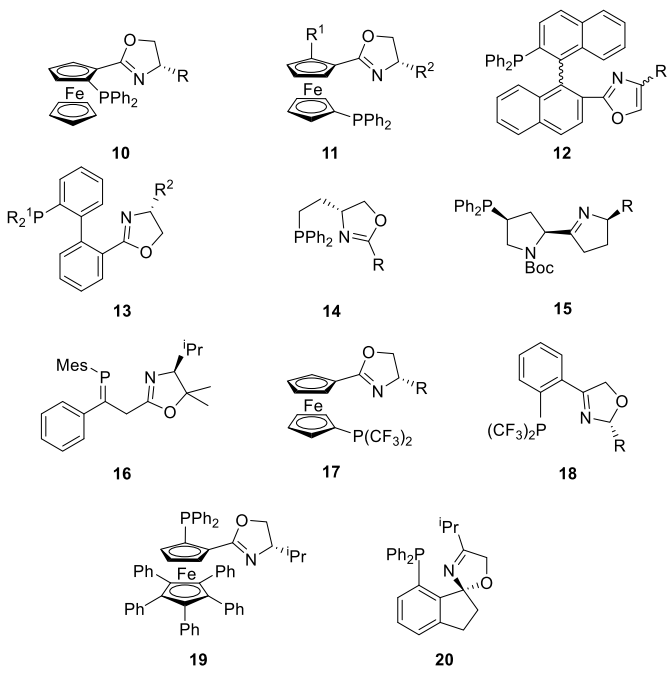

Figure 1.4. Selected modifications on the ligand backbone for phosphine-oxazoline ligands.

The introduction of biaryl phosphine groups was studied with ligands **12** (R = ^{i}Pr, ^{t}Bu)[20] and **13**[21]. For **12** the replacement the *o*-phenylene tether group on PHOX ligand by a binaphthyl moiety provided good results for the alkylation of the benchmark hindered substrate using dimethyl malonate (*ee*'s up to 97%) as well as amination using benzylamines as nucleophiles (*ee*'s up to 99%). Furthermore, the configuration on the binaphthyl moiety determinates the configuration of the substituted product. Ligands **13** (R^1 = Ph, 4-MeOPh, 3,5-$^{t}Bu_2$Ph, 3,5-$^{t}Bu_2$-4-MeOPh, R^2 = ^{i}Pr, ^{t}Bu, Ph) with an achiral biaryl phosphine provided also high enantiomeric excess for the hindered model linear substrate (*ee*'s up to 92%).

Ligands **14** (R = Ph, Ad, 2,4-di^{t}BuPh, 2,4-di^{t}Bu-3-OMePh, CPh_3, anthryl, 7-OEt-naphtyl) provided excellent enantioselectivities for the benchmark linear substrate (*ee's* up to 98%) whereas for both, cyclic *rac*-cyclohex-2-en-1-yl acetate and linear non-hindered substrate, *rac*-(*E)*-dimethylallyl acetate, the enantioselectivities attained were moderate *(ee*'s up to 79% and 82%, respectively).[22]

The proline-derived ligands **15** (R = ^{i}Pr, ^{t}Bu, Ph) have been successfully used for the alkylation of cyclic substrates.[23] where the tendency on enantioselectivities was the opposite as the usually observed since the *ee*'s increased when reducing the size of the cyclic substrate. Nevertheless, their application in the benchmark hindered substrate attained very low enantioselectivities (*ee'*s up to 30%).

The replacement of the phosphine for a phosphaalkene has been studied with ligand **16**.[24] The use of this ligand allowed the alkylation of the benchmark hindered substrate using malonates (including substituted ones) as well as acetylacetone as nucleophiles

(*ee*'s up to 92%). Moreover, the alkene-containing alkylated products were derivatized by ring closing metathesis reaction to give the corresponding carbocycles without loss of the chiral information.

The introduction of more π-acceptor electro withdrawing phosphines has been studied with ligands **17**[25] (R = Ph, Bn, ^{i}Pr, ^{t}Bu) and **18**[26] (R = Ph, Bn, ^{i}Pr, ^{t}Bu). In this regard, the use of these ligands seems to be limited to the alkylation of monosubstituted acetates providing regioselectivities up to 99% with enantioselectivities up to 94%.

Among the modifications on the backbone, two of the most successful modifications are represented by the introduction of a bulky pentaphenylferrocene, with ligand **19**[27], and highly rigid spiro-indane-based phosphine-oxazoline ligand **20**[28]. Ligand **19** was specifically designed for improve the enantioselectivity achieved with PHOX ligands for cyclic substrates. In this case, high *ee*'s were attained even with the more challenging cyclopentenyl acetate substrate (*ee*'s up to 91%). On the other hand, ligand **20** provided a delightful catalytic activity on the alkylation of the benchmark hindered substrate *rac*-(*E*)-1,3-diphenylallyl acetate using several malonates (including substituted ones) as well as with indoles and alkyl alcohols (*ee*'s up to >99%).[29]

The replacement of the phosphine group by a phosphinite has been also studied on this transformation. Nevertheless, in contrast to phosphinite-thioether ligand counterparts (see below), the use phosphinite-oxazoline ligands in this transformation is not common (Figure 1.5). There are two examples of them (Figure 1.5). In this regard, the phosphinite-oxazoline ligands **21** (R = Me, ^{i}Pr, ^{t}Bu, ^{i}Bu, Ph, Bn) derived from D-glucosamine provided high enantioselectivity for the hindered benchmark substrate (*ee* up to 96%) and moderate for the unhindered lineal and cyclic ones (*ee's* up to 74%).[30] Another family of phosphinite-oxazoline ligands developed has been ligands **22** (R = ferrocene, cobaltocene, Ad, Ph) (which is a modification of **14**). Enantioselectivities up to 96% were attained for the allylic alkylation of the benchmark substrate *rac*-(*E*)-1,3-diphenylallyl acetate. Nevertheless, their application in linear non-hindered benchmark substrate as well as for the cyclic benchmark substrate provided very low results (*ee*'s up to 36% and 25%, respectively).[31]

Figure 1.5. Phosphinite-oxazoline ligands developed for Pd-catalyzed allylic alkylation.

As mentioned before, the replacement of the phosphine by a biaryl phosphite group in P-oxazoline ligands has been highly beneficial in terms of nucleophile and substrate scope as well as for regioselectivity issues.[10b, c] Thus, aside of ligand **4**, some other families of phosphite-oxazoline ligands have been developed (Figure 1.6). In this respect we can highlight phosphite-oxazoline ligands **23** (R^1 = ^{t}Bu, ^{i}Pr, Ph, R^2 = (S^{ax}): H, Me, (R^{ax}): H) which were intended to overcome the problem of regioselectivity in the allylic alkylation of monosubstituted linear substrates.[32] In this case, a delightful

regioselectivity (up to 95%) to the chiral branched isomer and excellent enantioselectivities (up to 94%) were achieved for a range of monosubstituted hindered substrates. In contrast, moderate results were obtained for symmetrically hindered and unhindered substrates (60% and 70% *ee,* respectively).

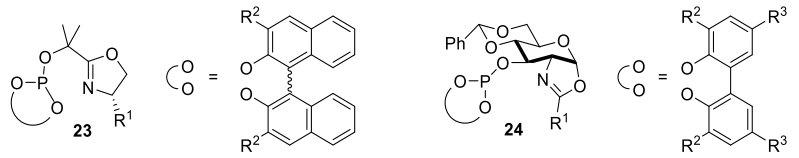

Figure 1.6. Phosphite-oxazoline ligands used in Pd-AAS.

After our successful family of **4**, we have developed other phosphite-oxazoline ligand families. In this regard, ligands **24** (R^1 = Ph, ^{i}Pr, ^{t}Bu, Me, R^2 = ^{t}Bu, H, $SiMe_3$, R^3 = ^{t}Bu, OMe, H) based on sugar have been developed and successfully applied on Pd-catalyzed allylic alkylation providing excellent results in the alkylation of mono- and disubstituted hindered and unhindered linear and cyclic substrates (*ee*'s up to 99%).[33] In comparation with the phosphinite version **21**, the phosphite counterpart **24** provided better results in terms of substrate scope.

1.1.2.2. P-thioether ligands

P-thioether ligands have also attracted attention since they take advantage of the electronic disparity between the two donor atoms: sulfur is a poor σ-donor and a poor π-acceptor in comparison with the better σ-donor and π-acceptor nature of phosphorus. In addition, the thioether group adds the advantage of higher chemical stability when compared with oxazolines and phosphines. The early successful work by Kang,[34] Pregosin[35] and Evans[36] among others,[3c,37] with P-thioether ligands in Pd-catalyzed allylic alkylation and other asymmetric reactions put the focus on this type of ligands and spurred their development. Since then, many P-S ligands have been developed, but only a few of them have shown to be successfully applicable to mechanistically unrelated asymmetric reactions and with high substrate/reagent scope.[3c] Compared to P-N ligands, the lower impact of P-S analogues in metal-catalyzed asymmetric reactions has been mainly attributed to the difficulty to control the diastereomeric metal-sulfur mixtures formed in solution. More recently, it has been found that the configuration of the thioether group can be controlled by the selection of an adequate ligand backbone, and this has led to the recent discovery of P-thioether ligand families.[3c] In next section we collect the families of P-thioether ligands that have been applied with most success. We focus on recent works and a quick overview of previous reports is also briefly incorporated when relevant.

In 1995, Kang et al. reported the first application of the P-thioether ligand in the Pd-catalyzed allylic alkylation of the benchmark linear hindered substrate with dimethyl

malonate (Figure 1.7) with a 91% *ee* and 65% yield.[34] They applied the binaphthalene-based phosphine-thioether ligand **25** (R= Me), analogue to the *R*-BINAP. The group of Shi et al. could increase the catalytic performance of Pd/**25** (96% yield and 96% ee) after optimizing the conditions of use.[38] Binaphthyl-based P–thioether ligands, where the chiral axis is the only stereogenic element, have found limited application and only Hagiwara *et al.* have reported some further applications. They prepared a range of BINAP's ligands with new thioether alkyl and aryl substituent, ligands **25** (R = Ph, 2-^{i}PrPh, 2-Naph, 3,5-Xyl and Cy), that allowed to extend the range of nucleophiles tested to the less studied indoles.[39] With ligand **25** (R= 2-^{i}PrPh), a broad range of simple and substituted indoles could be successfully introduced (up to 95% *ee*), but the substrate scope was still limited to the hindered benchmark substrate.

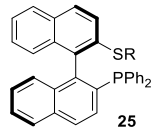

25

Figure 1.7. 1.1'-Binaphthalene-based phosphine-thioether ligands **25**.

Ferrocene-based compounds have been widely used as ligands in metal-catalyzed asymmetric reactions. In 1996, Pregosin et *al.* were the first to develop an heterodonor P-S ferrocene-based ligands (Figure 1.8, ligand **26**) with a thioglucoside moiety, that provided 88% *ee* in the alkylation of *rac*-(*E*)-diphenylallyl acetate with dimethyl malonate as nucleophile.[35] Since then, a broad range of P–thioether ferrocenyl ligands have been developed, frequently combining central and planar chirality. Among them, three families can be highlighted. The first one is the N–phosphine-thioether FerroNPS type ligands **27**-**29** (Figure 1.8). Ligands **27** (R = Et, ^{t}Bu, Ph, Cy), with mixed planar/central chirality, have provided good results in the allylic substitution of the benchmark hindered substrate with dimethyl malonate, benzylamine and less studied benzylic alcohols as nucleophiles (*ee*'s up to 96%).[40]

Then, the families of ligands **28** (R = Ph, *p*-tol, Me, Et, ^{i}Pr, ^{t}Bu, Cy) and **29**, related to FerroNPS and bearing imidazole or benzimidazole moieties, were applied in the allylic substitution of not only the benchmark linear substrate but also in two cyclic substrates (*ee* up to 87%) using indoles as nucleophiles, with enantioselectivities up to 96% ee.[41] Although the problem of substrate and nucleophile scope was still not solved, the promising results with other substrates different from the benchmark hindered linear substrate and with other nucleophiles, indicated that P-S ligands could be good candidates for further optimization.

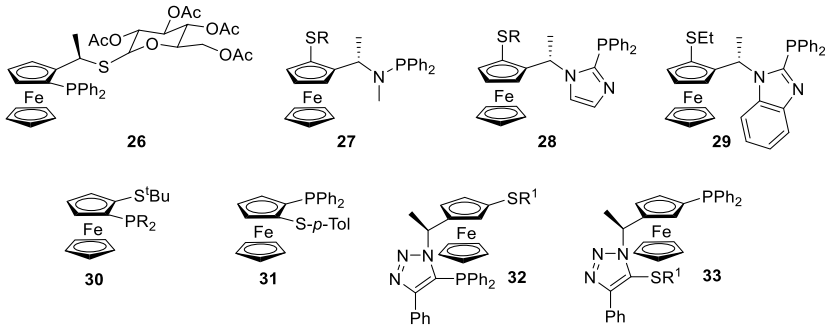

Figure 1.8. Most successful ferrocene-containing P-S ligand families used for Pd-catalyzed asymmetric allylic substitution.

The second family of ferrocene-based P-thioether ligands to be highlighted for Pd-allylic substitution is the Fesulphos ligands **30** and **31** (R = Ph, 4-F-Ph, 4-CF_3-Ph, 2-Fur, Cy) developed by Carretero group. Enantioselectivities up to 98% at -20 ^oC were attained with benchmark hindered substrate using both carbon and nitrogen nucleophiles.[42] Sterically demanding thioethers and electronically poor phosphines provided the best results (ligands **30**, R= 4-FPh, 4-CF_3Ph). Finally, the third family is the thioClick-Ferrophos ligands **32** and **33** that provided enantioselectivities up to 90% in the Pd-catalyzed allylic substitution of the linear benchmark substrate with dimethyl malonate, benzylamine and some benzylic alcohols.[43]

Another group of relevant P-S ligands are those involving two carbon atoms between the two donor functionalities (Figure 1.9).[3c, 37, 44] Among them we can highlight the phosphinite-thioether ligands **34** and **35,**[36b, 45] and the more recent families of phosphite–thioether **36**[46] and the phosphoramidite-thioether ligands **37**[47]. The Evan's ligand family **34** and **35** (R^1 = Ph, 4-MeOPh, 2,3,5,6-tetra-FPh, 4-^{t}BuPh, 3,5-diMePh, 1-Nap, 2-Nap, Bn, Cy, ^{t}Bu; R^2 = Ph, 4-MeOPh, 2-MeOPh, 4-F-Ph, 3,5-di-(CF_3)Ph, 3,5-diMePh, 1-Nap, Cy; R^3 = H, Me, R^4 = H, Me) provided enantioselectivities up to 98% in the Pd-catalyzed allylic alkylation and amination of the benchmark hindered substrate and of some cyclic substrates, but only moderate enantioselectivity (*ee* up to 65%) could be achieved for the less hindered linear substrate, *rac*-(*E*)-1,3-dimethylallyl acetate.[36b,45] These catalytic systems required to work at low temperatures (-20 °C).

The phosphite-thioether ligand family **36** (Ar = Ph, Mes, R^1 = 3,5-diMePh, 2,6-diMePh, 4-OMePh, 4-BrPh, 4-^{t}BuPh, 2-Nap, ^{i}Pr, Cy, ^{t}Bu, Ad, R^2 = Me, Bn, $CHPh_2$, CPh_3) synthesized from arylglycidols have been successfully applied in the Pd-allylic substitution of the benchmark linear substrate with C-, N-, and the less studied O-nucleophiles (*ee* up to 99%). Furthermore, they also attained good results in the alkylation of trisubstituted substrates *rac*-1,3,3-triphenylallyl acetate and *rac*-4,4-diphenylbut-3-en-2-yl acetate (up to 97% *ee*). Compared with the previous Evan's ligands, they provided comparable enantioselectivities working at room temperature with shorter reaction times.[46]

The last family of P-S ligand with two carbon atoms between both functionalities is the (*R*)-BINOL-based ligands **37** (R^1 = CH_2Cy, R^2 = 4-BrPh, R^3 = Ph, H, Me, I) that were applied in the Pd-catalyzed allylic alkylation of disubstituted linear substrates with a range of indoles with excellent enantioselectivities (up to 98% *ee*). Furthermore, these ligands also performed well in the etherification and amination of hindered substrate providing high enantioselectivities (98% and 97% *ee*, respectively).[48]

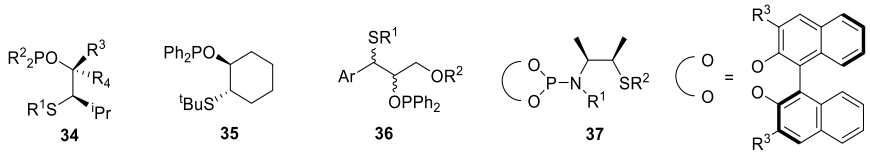

Figure 1.9. Selected P-thioether ligands featuring two carbon atoms between the two donor functionalities.

Another group of P-thioether ligands studied are those derived from sugars. Carbohydrates are a cheap and a readily available source of chiral backbones for ligand synthesis with a modular backbone.[49] The application of chiral sugar P-thioether ligands in catalysis was already introduced by Khiar *et al*. in 2005, with phosphinite-thioether ligands **38** (R^1 = 2-OMePh, 4-MePh, ^{t}Bu, R^2 = Ac, H, TBDMS) and **39** (Figure 1.10). They were applied in the Pd-catalyzed allylic substitution of the hindered model substrate (*ee's* up to 96%).[50] In addition, both enantiomers of the products could be obtained by using pseudo-enantiomeric ligands (**38** vs **39**), rather than preparing the corresponding P-S ligand from the expensive L-sugar derivative. However, still a narrow substrate and reagents scope was observed.

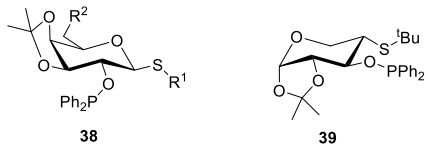

Figure 1.10. Phosphinite-thioglycoside ligands **38** and **39**.

In P-thioether based ligands derived from carbohydrates, our group have recently contributed with two extensive ligand libraries (Figure 1.11). The first family was derived from D-xylose and after carefully optimization of the ligand parameters (configuration of C-3 of the sugar backbone, position of the thioether group at C-3 or C-5 and thioether and phosphite groups) high enantioselectivities were attained in the substitution of a range of substrate types (hindered and unhindered, cyclic and linear) using a wide range of C–, N– and O–nucleophiles with ligands **40** and **41** (R = Ph, 2,6-diMePh, 1-Naph).[51] While ligand **40** with an (*S*) configuration at C-3 provided the best enantioselectivities in the alkylation of cyclic and hindered linear substrates, for unhindered linear substrates the best enantioselectivities were achieved with ligand **41** with an (*R*) configuration at C-3. Therefore, the configuration of C-3 helps to adjust the size of the chiral pocked to

the steric demands of the substrate. We must highlight that the excellent enantioselectivities attained in the etherification of linear and cyclic substrates represent the first example of successful etherification of both substrate types. A DFT computational study indicated that the enantiodetermining steps agrees with an early transition state. Further studies on the π-allylpalladium intermediates indicated that for the achievement of high enantioselectivities, the ligand parameters need to be correctly combined so that either the fastest reacting Pd-intermediate is predominantly formed (for linear hindered and unhindered linear substrates) and/or one of the *syn*/*syn* (*endo* or *exo*) isomers is predominantly formed (for unhindered cyclic derivative).

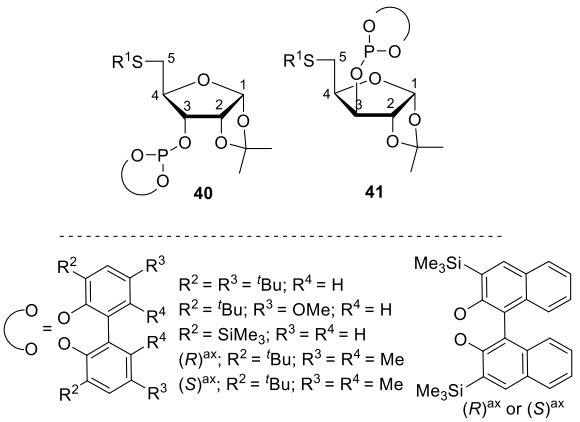

Figure 1.11. Furanoside-based P-thioether ligand library **40** and **41**.

The second family of phosphite-thioether ligands are those prepared from L-(+)-tartaric acid and D-(+)-mannitol (ligands **42** and **43;** R^1 = Ph, Me, ^{t}Bu, 2,6-diMePh, Ad, 1-Naph, 2-Naph; R^2 = H, Ph; R^3 = H, Me; R^4 = H, Me; R^5 = H, Me, $CH_2OTBDMS$, CH_2OTr; Figure 1.12). [52] Their high modular nature allows up to 61 possible combinations by the proper choose of the ligand parameters. Excellent enantioselectivities were attained for a range of hindered and unhindered substrates (*ee*'s up to 99% and 91%, respectively).[52] Furthermore, the catalytic system was able to efficiently introduce several C-, N- and O-nucleophiles. To obtain the highest enantioselectivities, a (*R*)-configured bulky alkyl group next to the phosphite moiety and an enantiopure biaryl phosphite moiety were needed. However, while an (*S*)-biaryl phosphite group was needed for hindered linear substrates (**43a**), an (*R*)-chiral biaryl phosphite group (**43b**) was preferred, for the less sterically demanding linear substrate *rac*-(*E*)-1,3-dimethylallyl acetate. In addition, for cyclic substrates both enantiomers of the product could be obtained by setting up the desired configuration of the biaryl phosphite group. Finally, studies of the key π-allylpalladium intermediates showed that for high enantioselectivity, the ligand parameters needed to be properly combined to either enhance the difference in the population of π-allylpalladium isomers formed or enhance the electronic differentiation between the most electrophilic allylic terminus carbon atoms of the isomeric intermediates formed.

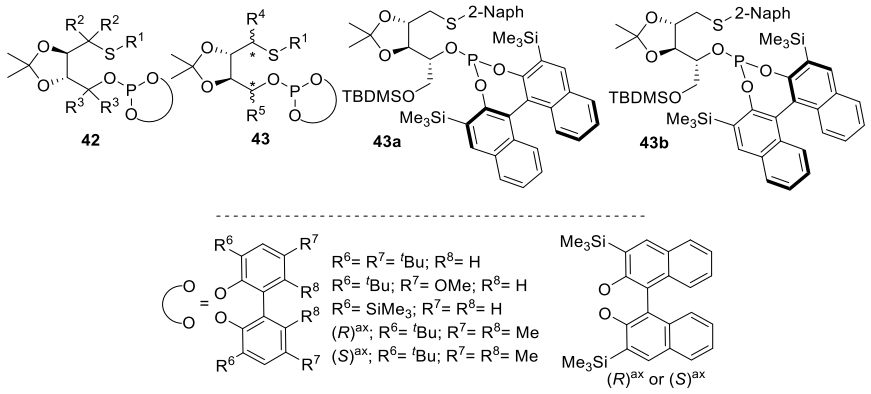

Figure 1.12. L-Tartaric acid and D-manitol derived ligand library **42** and **43**.

1.2. References

1. (a) *Asymmetric Catalysis in Industrial Scale: Challenges, Approaches, and Solutions*. Balser, H. U.; Federsel, H. J., Wiley: Weinheim, 2010; (b) *Catalytic Asymmetric Synthesis*. Ojima, I., John Wiley & Sons, Inc.: Hoboken, 2010; (c) *Applied Homogeneous Catalysis with Organometallics Compounds*. Cornils, B.; Hermann, W. A., Wiley-VCH: Weinhein, 2002; (d) *Comprehensive Asymmetric Catalysis*. Jacobsen, E. N.; Pfaltz, A.; Yamamoto, H., Springer-Verlag: Berlin, 1999; (e) Noyori, R.,·*Asymmetric Catalysis in Organic Synthesis*. 1994.

2. (a) Johansson Seechurn, C. C. C.; Kitching, M. O.; Colacot, T. J.; Snieckus, V., Palladium-Catalyzed Cross-Coupling: A Historical Contextual Perspective to the 2010 Nobel Prize. *Angewandte Chemie International Edition* **2012**, *51*, 5062-5085; (b) Negishi, E.-i., Magical Power of Transition Metals: Past, Present, and Future (Nobel Lecture). *Angewandte Chemie International Edition* **2011**, *50*, 6738-6764; (c) Knowles, W. S., Asymmetric Hydrogenations (Nobel Lecture). *Angewandte Chemie International Edition* **2002**, *41*, 1998-2007; (d) Sharpless, K. B., Searching for New Reactivity (Nobel Lecture). *Angewandte Chemie International Edition* **2002**, *41*, 2024-2032; (e) Noyori, R., Asymmetric Catalysis: Science and Opportunities (Nobel Lecture). *Angewandte Chemie International Edition* **2002**, *41*, 2008-2022.

3. (a) *Chiral Ligands. Evolution of Ligand Libraries for Asymmetric Catalysis.* Diéguez, M., CRC Press: New York, 2021; (b) Margalef, J.; Biosca, M.; de la Cruz Sánchez, P.; Faiges, J.; Pàmies, O.; Diéguez, M., Evolution in heterodonor P-N, P-S and P-O chiral ligands for preparing efficient catalysts for asymmetric catalysis. From design to applications. *Coordination Chemistry Reviews* **2021**, *446*, 214120; (c) Margalef, J.; Pàmies, O.; Pericàs, M. A.; Diéguez, M., Evolution of phosphorus–thioether ligands for asymmetric catalysis. *Chemical Communications* **2020**, *56*, 10795-10808; (d) Connon, R.; Roche, B.; Rokade, B. V.; Guiry, P. J., Further Developments and Applications of Oxazoline-Containing Ligands in Asymmetric Catalysis. *Chemical Reviews* **2021**, *121*, 6373-6521; (e) *Privileged Chiral Ligands and Catalysts*. Zhou, Q.-L., Wiley-VCH Verlag & Co. KGaA: Weinheim, 2011; (f) *Phosphorus Ligands in Asymmetric Catalysis: Synthesis and Applications*. Börner, A., Wiley-VCH: Weinheim, 2008; (g) Sommer, W.; Weibel, D., Asymmetric Catalysis, Privileged Ligands and Complexes. *Sigma Aldrich's Chemfiles* **2008**, *2*, 1-91.

4. (a) Pàmies, O.; Margalef, J.; Cañellas, S.; James, J.; Judge, E.; Guiry, P. J.; Moberg, C.; Bäckvall, J.-E.; Pfaltz, A.; Pericàs, M. A.; Diéguez, M., Recent Advances in Enantioselective Pd-

Catalyzed Allylic Substitution: From Design to Applications. *Chemical Reviews* **2021**, *121*, 4373-4505; (b) Trost, B. M., Pd- and Mo-catalyzed asymmetric allylic alkylation. *Organic Process Research & Development* **2012**, *16*, 185-194; (c) Trost, B. M.; Zhang, T.; Sieber, J. D., Catalytic Asymmetric Allylic Alkylation Employing Heteroatom Nucleophiles: a Powerful Method for C–X Bond Formation. *Chemical Science* **2010**, *1*, 427-440; (d) Lu, Z.; Ma, S., Metal-Catalyzed Enantioselective Allylation in Asymmetric Synthesis. *Angewandte Chemie International Edition* **2008**, *47*, 258-297; (e) Trost, B. M.; Crawley, M. L., Asymmetric transition-metal-catalyzed allylic alkylations: applications in total synthesis. *Chemical Reviews* **2003**, *103*, 2921-2944; (f) *Palladium Reagents and Catalysis: Innovations in Organic Synthesis*. Tsuji, J., Wiley: New York, 1995; (g) Johannsen, M.; Jorgensen, K. A., Allylic Amination. *Chemical Reviews* **1998**, *98*, 1689-1708.

5. (a) Hayashi, T.; Yamamoto, A.; Ito, Y.; Nishioka, E.; Miura, H.; Yanagi, K., Asymmetric Synthesis Catalyzed by Chiral Ferrocenylphosphine - Transition-metal Complexes. 8. Palladium-catalyzed Asymmetric Allylic Amination. *Journal of the American Chemical Society* **1989**, *111*, 6301–6311; (b) Hayashi, T.; Yamamoto, A.; Hagihara, T.; Ito, Y., Modification of optically active ferrocenylphosphine ligands for palladium-catalyzed asymmetric allylic alkylation. *Tetrahedron Letters* **1986**, *27*, 191-194.

6. (a) Trost, B. M.; Bunt, R. C., Asymmetric induction in allylic alkylations of 3-(acyloxy)cycloalkenes. *Journal of the American Chemical Society* **1994**, *116*, 4089–4090; (b) Trost, B. M.; Van Vranken, D. L.; Bingel, C., A modular approach for ligand design for asymmetric allylic alkylations via enantioselective palladium-catalyzed ionizations. *Journal of the American Chemical Society* **1992**, *114*, 9327–9343.

7. Butts, C. P.; Filali, E.; Lloyd-Jones, G. C.; Norrby, P. O.; Sale, D. A.; Schramm, Y., Structure-Based Rationale for Selectivity in the Asymmetric Allylic Alkylation of Cycloalkenyl Esters Employing the Trost 'Standard Ligand' (TSL): Isolation, Analysis and Alkylation of the Monomeric form of the Cationic η^3-Cyclohexenyl Complex $[(\eta^3\text{-c-}C_6H_9)Pd(TSL)]^+$. *Journal of the American Chemical Society* **2009**, *131*, 9945–9957.

8. (a) von Matt, P.; Lloyd-Jones, G. C.; Minidis, A. B. E.; Pfaltz, A.; Macko, L.; Neuburger, M.; Zehnder, M.; Ruegger, H.; Pregosin, P. S., Enantioselective Allylic Substitution Catalyzed by Chiral [Bis(dihydrooxazole)]palladium Complexes: Catalyst Structure and Possible Mechanism of Enantioselection. *Helvetica Chimica Acta* **1995**, *78*, 265-284; (b) Sprinz, J.; Helmchen, G., Phosphinoaryl- and Phosphinoalkyloxazolines as New Chiral Ligands for Enantioselective Catalysis: Very High Enantioselectivity in Palladium Catalyzed Allylic Substitutions. *Tetrahedron Letters* **1993**, *34*, 1769-1772; (c) Dawson, G. J.; Frost, C. G.; Williams, J. M. J.; Coote, S. J., Asymmetric Palladium Catalysed Allylic Substitution Using Phosphorus Containing Oxazoline Ligands. *Tetrahedron Letters* **1993**, *34*, 3149-3150.

9. Diéguez, M.; Pàmies, O.; Moberg, C., Self-Adaptable Tropos Catalysts. *Accounts of Chemical Research* **2021**, *54*, 3252-3263.

10. (a) Biosca, M.; Saltó, J.; Magre, M.; Norrby, P.-O.; Pàmies, O.; Diéguez, M., An Improved Class of Phosphite-Oxazoline Ligands for Pd-Catalyzed Allylic Substitution Reactions. *ACS Catalysis* **2019**, *9*, 6033-6048; (b) Bellini, R.; Magre, M.; Biosca, M.; Norrby, P. O.; Pàmies, O.; Diéguez, M.; Moberg, C., Conformational Preferences of a Tropos Biphenyl Phosphinooxazoline–a Ligand with Wide Substrate Scope. *ACS Catalysis* **2016**, *6*, 1701–1712; (c) Pàmies, O.; Diéguez, M.; Claver, C., New Phosphite−Oxazoline Ligands for Efficient Pd-Catalyzed Substitution Reactions. *Journal of the American Chemical Society* **2005**, *127*, 3646-3647.

11. (a) Mazuela, J.; Norrby, P.-O.; Andersson, P. G.; Pàmies, O.; Diéguez, M., Pyranoside Phosphite–Oxazoline Ligands for the Highly Versatile and Enantioselective Ir-Catalyzed Hydrogenation of Minimally Functionalized Olefins. A Combined Theoretical and Experimental Study. *Journal of the American Chemical Society* **2011**, *133*, 13634-13645; (b) Biosca, M.; Magre, M.; Coll, M.; Pàmies, O.; Diéguez, M., Alternatives to Phosphinooxazoline (t-BuPHOX) Ligands in the Metal-Catalyzed Hydrogenation of Minimally Functionalized

Olefins and Cyclic β-Enamides. *Advanced Synthesis & Catalysis* **2017**, *359*, 2801-2814; (c) Magre, M.; Biosca, M.; Pàmies, O.; Diéguez, M., Filling the Gaps in the Challenging Asymmetric Hydroboration of 1,1-Disubstituted Alkenes with Simple Phosphite-Based Phosphinooxazoline Iridium Catalysts. *ChemCatChem* **2015**, *7*, 114-120; (d) Mazuela, J.; Pàmies, O.; Diéguez, M., Biaryl Phosphite–Oxazoline Ligands from the Chiral Pool: Highly Efficient Modular Ligands for the Asymmetric Pd-Catalyzed Heck Reaction. *Chemistry: A European Journal* **2010**, *16*, 3434-3440; (e) Pàmies, O.; Diéguez, M., Adaptable P–X Biaryl Phosphite/Phosphoroamidite-Containing Ligands for Asymmetric Hydrogenation and C–X Bond-Forming Reactions: Ligand Libraries with Exceptionally Wide Substrate Scope. *The Chemical Record* **2016**, *16*, 2460-2481.

12. (a) Khan, S.; Shah, B. H.; Khan, I.; Li, M.; Zhang, Y. J., Pd-catalyzed regio- and enantioselective allylic substitution with 2-pyridones. *Chemical Communications* **2019**, *55*, 13168-13171; (b) Khan, S.; Li, H.; Zhao, C.; Wu, X.; Zhang, Y. J., Asymmetric allylic etherification of vinylethylene carbonates with diols via Pd/B cooperative catalysis: a route to chiral hemi-crown ethers. *Organic Letters* **2019**, *21*, 9457-9462; (c) Cai, A.; Kleij, A. W., Regio- and enantioselective preparation of chiral allylic sulfones featuring elusive quaternary stereocenters. *Angewandte Chemie International Edition* **2019**, *58*, 14944-14949; (d) Khan, A.; Khan, S.; Khan, I.; Zhao, C.; Mao, Y.; Chen, Y.; Zhang, Y. J., Enantioselective construction of tertiary C-O bond via allylic substitution of vinylethylene carbonates with water and alcohols. *Journal of the American Chemical Society* **2017**, *139*, 10733-10741; (e) Guo, W.; Cai, A.; Xie, J.; Kleij, A. W., Asymmetric synthesis of α,α-disubstituted allylic amines through palladium-catalyzed allylic substitution. *Angewandte Chemie International Edition* **2017**, *56*, 11797-11801; (f) Gao, R. D.; Xu, Q. L.; Zhang, B.; Gu, Y.; Dai, L. X.; You, S. L., Palladium(0)-catalyzed intermolecular allylic dearomatization of indoles by a formal [4+2] cycloaddition reaction. *Chemistry – A European Journal* **2016**, *22*, 11601-11604; (g) Wei, X.; Liu, D.; An, Q.; Zhang, W., Hydrogen-bond directed regioselective pd-catalyzed asymmetric allylic alkylation: the construction of chiral α-amino acids with vicinal tertiary and quaternary stereocenters. *Organic Letters* **2015**, *17*, 5768-5771; (h) Banerjee, D.; Junge, K.; Beller, M., Cooperative catalysis by palladium and a chiral phosphoric acid: enantioselective amination of racemic allylic alcohols. *Angewandte Chemie International Edition* **2014**, *53*, 13049-13053; (i) Audisio, D.; Gopakumar, G.; Xie, L. X.; Alves, L. G.; Wirtz, C.; Martins, A. M.; Thiel, W.; Farès, C.; Maulide, N., Palladium-catalyzed allylic substitution at four-membered-ring systems: formation of η^1-allyl complexes and electrocyclic ring opening. *Angewandte Chemie International Edition* **2013**, *52*, 6313-6316; (j) Ohmatsu, K.; Ito, M.; Kunieda, T.; Ooi, T., Exploiting the modularity of ion-paired chiral ligands for palladium- catalyzed enantioselective allylation of benzofuran-2(3H)-ones. *Journal of the American Chemical Society* **2013**, *135*, 590-593; (k) Audisio, D.; Luparia, M.; Oliveira, M. T.; Klütt, D.; Maulide, N., Diastereodivergent de-epimerization in catalytic asymmetric allylic alkylation. *Angewandte Chemie International Edition* **2012**, *51*, 7314-7317; (l) Luparia, M.; Oliveira, M. T.; Audisio, D.; Frébault, F.; Goddard, R.; Maulide, N., Catalytic asymmetric diastereodivergent deracemization. *Angewandte Chemie International Edition* **2011**, *50*, 12631-12635.

13. Gläser, B.; Kunz, H., Enantioselective Allylic Substitution Using a Novel (Phosphino-α-d-glucopyrano-oxazoline)palladium Catalyst. *Synlett* **1998**, *1998*, 53-54.

14. Frölander, A.; Lutsenko, S.; Privalov, T.; Moberg, C., Conformational Preferences and Enantiodiscrimination of Phosphino-4-(1-hydroxyalkyl)oxazoline−Metal−Olefin Complexes Resulting from an OH−Metal Hydrogen Bond. *The Journal of Organic Chemistry* **2005**, *70*, 9882-9891.

15. Popa, D.; Puigjaner, C.; Gómez, M.; Benet-Buchholz, J.; Vidal-Ferran, A.; Pericàs, M. A., Phosphinooxazolines Derived from 3-Amino-1,2-diols: Highly Efficient Modular P-N Ligands. *Advanced Synthesis & Catalysis* **2007**, *349*, 2265-2278.

16. Liu, S.; Müller, J. F. K.; Neuburger, M.; Schaffner, S.; Zehnder, M., Synthesis, X-Ray Crystal-Structure Analysis, and NMR Studies of (η3-Allyl)palladium(II) Complexes Containing

a Novel Dihydro(phosphinoaryl)oxazine Ligand: Application in Palladium-Catalyzed Asymmetric Synthesis. *Helvetica Chimica Acta* **2000**, *83*, 1256-1267.
17. Liu, D.; Dai, Q.; Zhang, X., A new class of readily available and conformationally rigid phosphino-oxazoline ligands for asymmetric catalysis. *Tetrahedron* **2005**, *61*, 6460-6471.
18. (a) You, S.-L.; Hou, X.-L.; Dai, L.-X.; Yu, Y.-H.; Xia, W., Role of Planar Chirality of S,N- and P,N-Ferrocene Ligands in Palladium-Catalyzed Allylic Substitutions. *The Journal of Organic Chemistry* **2002**, *67*, 4684-4695; (b) Zhang, W.; Yoneda, Y.-i.; Kida, T.; Nakatsuji, Y.; Ikeda, I., Novel chiral P,N-ferrocene ligands in palladium-catalyzed asymmetric allylic alkylations. *Tetrahedron: Asymmetry* **1998**, *9*, 3371-3380; (c) Ahn, K. H.; Cho, C.-W.; Park, J.; Lee, S., Pd-catalyzed asymmetric allylic alkylations using various diphenylphosphino(oxazolinyl)ferrocene ligands. *Tetrahedron: Asymmetry* **1997**, *8*, 1179-1185.
19. Deng, W.-P.; You, S.-L.; Hou, X.-L.; Dai, L.-X.; Yu, Y.-H.; Xia, W.; Sun, J., Importance of Planar Chirality in Chiral Catalysts with Three Chiral Elements: The Role of Planar Chirality in 2'-Substituted 1,1'-P,N-Ferrocene Ligands on the Enantioselectivity in Pd-Catalyzed Allylic Substitution. *Journal of the American Chemical Society* **2001**, *123*, 6508-6519.
20. (a) Selvakumar, K.; Valentini, M.; Wörle, M.; Pregosin, P. S.; Albinati, A., Palladium(0) Olefin Complexes and Enantioselective Allylic Amination/Alkylation with a P,N-Auxiliary. *Organometallics* **1999**, *18*, 1207-1215; (b) Imai, Y.; Zhang, W.; Kida, T.; Nakatsuji, Y.; Ikeda, I., Diphenylphosphinooxazoline ligands with a chiral binaphthyl backbone for Pd-catalyzed allylic alkylation. *Tetrahedron Letters* **1998**, *39*, 4343-4346.
21. Tian, F.; Yao, D.; Zhang, Y. J.; Zhang, W., Phosphine-oxazoline ligands with an axial-unfixed biphenyl backbone: the effects of the substituent at oxazoline ring and P phenyl ring on Pd-catalyzed asymmetric allylic alkylation. *Tetrahedron* **2009**, *65*, 9609-9615.
22. (a) Hou, D.-R.; Reibenspies, J. H.; Burgess, K., New, Optically Active Phosphine Oxazoline (JM-Phos) Ligands: Syntheses and Applications in Allylation Reactions. *The Journal of Organic Chemistry* **2001**, *66*, 206-215; (b) Hou, D.-R.; Burgess, K., JM-PHOS Ligands: Second-Generation Phosphine Oxazolines for Asymmetric Catalysis. *Organic Letters* **1999**, *1*, 1745-1747.
23. Gilbertson, S. R.; Xie, D.; Fu, Z., Proline-Based P, N Ligands in Asymmetric Allylation and the Heck Reaction. *The Journal of Organic Chemistry* **2001**, *66*, 7240-7246.
24. Dugal-Tessier, J.; Dake, G. R.; Gates, D. P., Chiral Phosphaalkene-Oxazoline Ligands for the Palladium-Catalyzed Asymmetric Allylic Alkylation. *Organic Letters* **2010**, *12*, 4667-4669.
25. Lai, Z. W.; Yang, R. F.; Ye, K. Y.; Sun, H.; You, S. L., Synthesis of 1-[bis(trifluoromethyl)phosphine]-1'-oxazolinylferrocene ligands and their application in regio- and enantioselective Pd-catalyzed allylic alkylation of monosubstituted allyl substrates. *Beilstein Journal of Organic Chemistry* **2014**, *10*, 1261-1266.
26. Hu, Z.; Li, Y.; Liu, K.; Shen, Q., Bis(perfluoroalkyl) phosphino-oxazoline: a modular, stable, strongly π-accepting ligand for asymmetric catalysis. *Journal of Organic Chemistry* **2012**, *77*, 7957-7967.
27. Ayerbe Garcia, M. A.; Frey, W.; Peters, R., Sterically demanding planar chiral P,N ligands by diastereoselective ortho lithiation of pentaphenylferrocenyloxazolines and their application to palladium-catalyzed substitutions with cyclic allylic acetates. *Organometallics* **2014**, *33*, 1068-1078.
28. Qiu, Z.; Sun, R.; Teng, D., Synthesis of highly rigid phosphine-oxazoline ligands for palladium-catalyzed asymmetric allylic alkylation. *Organic & Biomolecular Chemistry* **2018**, *16*, 7717-7724.
29. Qiu, Z.; Sun, R.; Yang, K.; Teng, D., Spiro Indane-based phosphine-oxazolines as highly efficient P,N ligands for enantioselective Pd-catalyzed allylic alkylation of indoles and allylic etherification. *Molecules* **2019**, *24*, 1575.
30. (a) Yonehara, K.; Hashizume, T.; Mori, K.; Ohe, K.; Uemura, S., Palladium-catalysed asymmetric allylic alkylation using new chiral phosphinite–nitrogen ligands derived from D-

glucosamine. *Chemical Communications* **1999**, 415-416; (b) Yonehara, K.; Hashizume, T.; Mori, K.; Ohe, K.; Uemura, S., Palladium-Catalyzed Asymmetric Allylic Substitution Reactions Using New Chiral Phosphinite−Oxazoline Ligands Derived from d-Glucosamine. *The Journal of Organic Chemistry* **1999**, *64*, 9374-9380.

31. (a) Jones, G.; Richards, C. J., (*S*)-Serine derived N–O and N–P oxazoline ligands for asymmetric catalysis. *Tetrahedron: Asymmetry* **2004**, *15*, 653-664; (b) Jones, G.; Richards, C. J., Simple phosphinite–oxazoline ligands for asymmetric catalysis. *Tetrahedron Letters* **2001**, *42*, 5553-5555.

32. Prétôt, R.; Pfaltz, A., New Ligands for Regio- and Enantiocontrol in Pd-Catalyzed Allylic Alkylations. *Angewandte Chemie International Edition* **1998**, *37*, 323-325.

33. (a) Mata, Y.; Diéguez, M.; Pàmies, O.; Claver, C., New Carbohydrate-Based Phosphite-Oxazoline Ligands as Highly Versatile Ligands for Palladium-Catalyzed Allylic Substitution Reactions. *Advanced Synthesis & Catalysis* **2005**, *347*, 1943-1947; (b) Mata, Y.; Pàmies, O.; Diéguez, M., Pyranoside Phosphite-Oxazoline Ligand Library: Highly Efficient Modular P,N Ligands for Palladium-Catalyzed Allylic Substitution Reactions. A Study of the Key Palladium Allyl Intermediates. *Advanced Synthesis & Catalysis* **2009**, *351*, 3217-3234.

34. Kang, J. Y., S. Kin, K. Cho, H., Catalytic Asymmetric Allylic Alkylation with A Novel P-S Bidentate Ligand. *Bulletin of the Korean Chemical Society* **1995**, *16*, 439-441.

35. Albinati, A.; Pregosin, P. S.; Wick, K., A New P,S-Chiral Auxiliary Derived from Thioglucose. X-ray Structure of a Palladium 1,3-Diphenylallyl Complex with a Strongly Rotated Allyl Ligand. *Organometallics* **1996**, *15*, 2419-2421.

36. (a) Evans, D. A.; Campos, K. R.; Tedrow, J. S.; Michael, F. E.; Gagné, M. R., Chiral Mixed Phosphorus/Sulfur Ligands for Palladium-Catalyzed Allylic Alkylations and Aminations. *The Journal of Organic Chemistry* **1999**, *64*, 2994-2995; (b) Evans, D. A.; Campos, K. R.; Tedrow, J. S.; Michael, F. E.; Gagné, M. R., Application of Chiral Mixed Phosphorus/Sulfur Ligands to Palladium-Catalyzed Allylic Substitutions. *Journal of the American Chemical Society* **2000**, *122*, 7905-7920.

37. (a) Arrayás, R. G.; Carretero, J. C., Chiral Thioether-Based Catalysts in Asymmetric Synthesis: Recent Advances. *Chemical Communications* **2011**, *47*, 2207-2211; (b) Lam, F. L.; Kwong, F. Y.; Chan, A. S. C., Recent developments on chiral P,S-type ligands and their applications in asymmetric catalysis. *Chemical Communications* **2010**, *46*, 4649-4667; (c) Lam, F. L.; Kwong, F. Y.; Chan, A. S. C., Recent developments on chiral P,S-type ligands and their applications in asymmetric Catalysis. *Chemical Communications* **2010**, *46*, 4649-4667; (d) Martin, E.; Diéguez, M., Thioether Containing Ligands for Asymmetric Allylic Substitution Reactions. *Comptes Rendus Chimie* **2007**, *10*, 188-205; (e) Mellah, M.; Voituriez, A.; Schulz, E., Chiral Sulfur Ligands for Asymmetric Catalysis. *Chemical Reviews* **2007**, *107*, 5133-5209; (f) Masdeu-Bultó, A. M.; Diéguez, M.; Martin, E.; Gómez, M., Chiral thioether ligands: coordination chemistry and asymmetric catalysis. *Coordination Chemistry Reviews* **2003**, *242*, 159-201; (g) Bayón, J. C.; Claver, C.; Masdeu-Bultó, A. M., Homogeneous catalysis with transition metal complexes containing sulfur ligands. *Coordination Chemistry Reviews* **1999**, *193-195*, 73-145.

38. Zhang, W.; Shi, M., Axially chiral P,S-heterodonor ligands with a binaphthalene framework for palladium-catalyzed asymmetric allylic substitutions: experimental investigation on the reversal of enantioselectivity between different alkyl groups on sulfur atom. *Tetrahedron: Asymmetry* **2004**, *15*, 3467-3476.

39. Hoshi, T.; Sasaki, K.; Sato, S.; Ishii, Y.; Suzuki, T.; Hagiwara, H., Highly enantioselective Pd-catalyzed allylic alkylation of indoles using sulfur-MOP ligand. *Organic Letters* **2011**, *13*, 932-935.

40. (a) Lam, F. L.; Au-Yeung, T. T. L.; Kwong, F. Y.; Zhou, Z.; Wong, K. Y.; Chan, A. S. C., Palladium–(*S*,p*R*)-FerroNPS-Catalyzed Asymmetric Allylic Etherification: Electronic Effect of Nonconjugated Substituents on Benzylic Alcohols on Enantioselectivity. *Angewandte Chemie International Edition* **2008**, *47*, 1280-1283; (b) Lam, F. L.; Au-Yeung, T. T. L.; Cheung, H. Y.;

Kok, S. H. L.; Lam, W. S.; Wong, K. Y.; Chan, A. S. C., Easily accessible ferrocenyl N-P/S type ligands and their applications in asymmetric allylic substitutions. *Tetrahedron: Asymmetry* **2006**, *17*, 497-499.

41. (a) Cheung, H. Y.; Yu, W. Y.; Au-Yeung, T. T. L.; Zhou, Z. A.; Chan, S. C., Effective Chiral Ferrocenyl Phosphine-Thioether Ligands in Enantioselective Palladium-Catalyzed Allylic Alkylations. *Advanced Synthesis & Catalysis* **2009**, *351*, 1412-1422; (b) Cheung, H. Y.; Yu, W. Y.; Lam, F. L.; Au-Yeung, T. T. L.; Zhou, Z.; Chan, T. H.; Chan, A. S. C., Enantioselective Pd-catalyzed allylic alkylation of indoles by a new class of chiral ferrocenyl P/S ligands. *Organic Letters* **2007**, *9*, 4295-4298.

42. (a) Mancheño, O. G.; Priego, J.; Cabrera, S.; Arrayás, R. G.; Llamas, T.; Carretero, J. C., 1-Phosphino-2-sulfenylferrocenes as Planar Chiral Ligands in Enantioselective Palladium-Catalyzed Allylic Substitutions. *The Journal of Organic Chemistry* **2003**, *68*, 3679-3686; (b) Priego, J.; Mancheño, O. G.; Cabrera, S.; Arrayás, R. G.; Llamas, T.; Carretero, J. C., 1-Phosphino-2-sulfenylferrocenes: efficient ligands in enantioselective palladium-catalyzed allylic substitutions and ring opening of 7-oxabenzonorbornadienes. *Chemical Communications* **2002**, 2512-2513.

43. Kato, M.; Nakamura, T.; Ogata, K.; Fukuzawa, S. I., Synthesis of Novel Ferrocenyl-Based P,S Ligands (ThioClickFerrophos) and Their Use in Pd-Catalyzed Asymmetric Allylic Substitutions. *European Journal of Organic Chemistry* **2009**, *2009*, 5232-5238.

44. Gavrilov, K. N.; Chuchelkin, I. V.; Zheglov, S. V.; Firsin, I. D.; Zimarev, V. S.; Gavrilov, V. K.; Maximychev, A. V.; Perepukhov, A. M.; Goulioukina, N. S., First P*,S-bidentate diamidophosphite ligand in Pd-catalyzed asymmetric reactions. *Mendeleev Communications* **2020**, *30*, 31-33.

45. Evans, D. A.; Campos, K. R.; Tedrow, J. S.; Michael, F. E.; Gagné, M. R., Chiral Mixed Phosphorus/Sulfur Ligands for Palladium-Catalyzed Allylic Alkylations and Aminations. *The Journal of Organic Chemistry* **1999**, *64*, 2994-2995.

46. Caldentey, X.; Pericàs, M. A., Modular P,S-Ligands for Pd-Catalyzed Asymmetric Allylic Substitutions. *The Journal of Organic Chemistry* **2010**, *75*, 2628-2644.

47. Feng, B.; Pu, X. Y.; Liu, Z. C.; Xiao, W. J.; Chen, J. R., Highly enantioselective Pd-catalyzed indole allylic alkylation using binaphthyl-based phosphoramidite-thioether ligands. *Organic Chemistry Frontiers* **2016**, *3*, 1246-1249.

48. Lu, B.; Feng, B.; Ye, H.; Chen, J. R.; Xiao, W. J., Pd/phosphoramidite thioether complex-catalyzed asymmetric N-allylic alkylation of hydrazones with allylic acetates. *Organic Letters* **2018**, *20*, 3473-3476.

49. (a) Woodward, S.; Diéguez, M.; Pàmies, O., Use of sugar-based ligands in selective catalysis: Recent developments. *Coordination Chemistry Reviews* **2010**, *254*, 2007-2030; (b) Benessere, V.; Del Litto, R.; De Roma, A.; Ruffo, F., Carbohydrates as building blocks of privileged ligands. *Coordination Chemistry Reviews* **2010**, *254*, 390-401; (c) Boysen, M. M. K., Carbohydrates as Synthetic Tools in Organic Chemistry. *Chemistry – A European Journal* **2007**, *13*, 8648-8659; (d) Diéguez, M.; Pàmies, O.; Claver, C., Ligands Derived from Carbohydrates for Asymmetric Catalysis. *Chemical Reviews* **2004**, *104*, 3189-3216.

50. (a) Khiar, N.; Suárez, B.; Stiller, M.; Valdivia, V.; Fernández, I., Mixed S/P Ligands from Carbohydrates: Synthesis and Utilization in Asymmetric Catalysis. *Phosphorus, Sulfur, and Silicon and the Related Elements* **2005**, *180*, 1253-1258; (b) Khiar, N.; Suárez, B.; Valdivia, V.; Fernández, I., Phosphinite Thioglycosides Derived from Natural d-Sugars as Useful P/S Ligands for the Synthesis of Both Enantiomers in Palladium-Catalyzed Asymmetric Substitution. *Synlett* **2005**, *2005*, 2963-2967.

51. (a) Coll, M.; Pàmies, O.; Diéguez, M., Highly Versatile Pd–Thioether–Phosphite Catalytic Systems for Asymmetric Allylic Alkylation, Amination, and Etherification Reactions. *Organic Letters* **2014**, *16*, 1892-1895; (b) Margalef, J.; Coll, M.; Norrby, P. O.; Pàmies, O.; Diéguez, M., Asymmetric Catalyzed Allylic Substitution Using a Pd/P–S Catalyst Library with Exceptional

High Substrate and Nucleophile Versatility: DFT and Pd-π-allyl Key Intermediates Studies. *Organometallics* **2016**, *35*, 3323-3335.

52. Margalef, J.; Borràs, C.; Alegre, S.; Pàmies, O.; Diéguez, M., A readily accessible and modular carbohydrate-derived thioether/selenoether-phosphite ligand library for Pd-catalyzed asymmetric allylic substitutions. *Dalton Transactions* **2019**, *48*, 12632-12643.

Chapter 2

Objectives

The main objective of this thesis is to develop new chiral compounds for their application as chiral ligands in relevant enantioselective metal-catalyzed reactions. The more specific aims are:

1. The design of two new heterodonor ligand libraries to overcome the substrate specificity and the still low activities in the Pd-catalyzed asymmetric allylic substitution. In this respect, air stable and modular phosphite/phosphinite-thioether (**L1**-**L8a**-**c**,**f**-**i**) and phosphite-oxazoline (**L9**-**L15a**,**d**-**e**) ligand libraries will be prepared and tested (Figure 2.1). In addition, some of the substitution products will we further derivatized for the synthesis of more complex chiral Molecules.

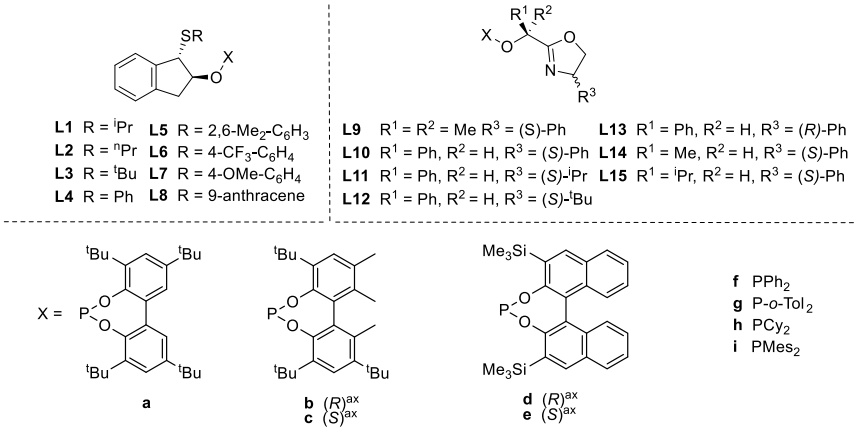

Figure 2.1. Phosphite/phosphinite-thioether (**L1**-**L8a**-**c**,**f**-**i**) and phosphite-oxazoline (**L9**-**L15a**,**d**-**e**) ligand libraries developed for this thesis.

2. The preparation of phosphabarralene/5-phosphasemibullvalene-pyridine ligands **L16**-**L21** to be applied in the near future in enantioselective allylic and propargylic catalyzed substitutions, as well as metal-catalyzed asymmetric hydrogenations (Figure 2.2).

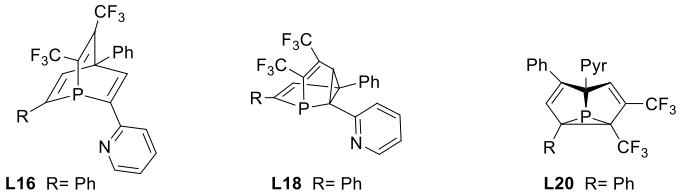

Figure 2.2. The phosphabarralene/5-phosphasemibullvalene-pyridine ligands **L16**-**L21** developed for this thesis.

Chapter 3

DFT-guided synthesis of a new family of P-S ligands based on indene for Pd-catalyzed asymmetric allylic substitution reactions

3.1. Introduction

The production of new chemicals should bear in mind the principles of green chemistry. In this respect, reducing the amount of waste, energy consumption and reaction by-products is nowadays a must. For this reason, catalysis has become a reliable strategy according of the principles of green chemistry.[1]

Concretely, in the production enantiopure products which are present in many pharmaceuticals and agrochemicals, asymmetric catalysis is one of the more used strategies since with the proper choose of the catalytic system, high levels of conversion and enantiopurity can be achieved.[2] In this regard, Pd-catalyzed allylic asymmetric substitution is very convenient since allows the creation of new C-C, C-heteroatom bonds with high levels of stereoinduction from readily available starting materials. Furthermore, this transformation allows the process in the presence of other functional groups and requires very mild reaction conditions. In addition, the presence of an alkene allows its further derivatization in several possibilities.[3] In this reaction, one of the most crucial parameters to optimize is the correct choose of them. For this reason, several ligands have been studied to evaluate the yield, selectivity, and the substrate scope. Among all ligands studied, heterodonor P-oxazoline ligands (such as PHOX ligands) have proved to be more advantageous than their homodonor analogs since *trans* effect plays a crucial role differentiating between the two allylic carbons. When heterodonor ligands are used, the nucleophilic addition takes place the carbon *trans* to the more donor group (which has a strong *trans* effect). In this respect, our group has developed several ligands containing a biaryl-phosphite. The introduction of this group has proved to be advantageous since biaryl-phosphite groups are fluxional enough to accommodate several different substrates with different steric demands and therefore, favoring the substrate scope.[4]

Although uncountable Pd-asymmetric allylic substitution studies have been published there is still several issues about this process. For example, the more successful ligands for this reaction (such as Trost and PHOX ligands) work well for either hindered or unhindered substrates and give poor *ee's* for the other substrate type. Moreover, they scarcely tolerate a broad range of nucleophiles. Thus, the application of this reaction in new substrates or nucleophiles usually requires an optimization process to find the best performing ligand which is in general time consuming. As result, the search of a ligand that tolerates several different substrates and nucleophiles is still highly needed. Furthermore, this search should consider that the ligand must be easy to synthesize from readily available chiral synthons (i.e., from chiral pool) and easy to handle (i.e, air stable solids).[3]

Among other heterodonor ligands, the replacement of the oxazoline group by a thioether moieties have been also studied. In general, P-thioether ligands are more robust and easier to synthesize than the oxazoline counterparts.[5] Nevertheless, most of the P-thioether ligand applications have a limited substrate and nucleophile scope. A plausible explanation can be found in the fact than when thioether groups are

coordinated, they become a new stereogenic center that in most cases produce diastereomeric mixtures in solution that affect to the performance of the system.[6] However, if the ligand scaffold can control the configuration on sulfur atom when coordinated to the metal center, this provides a new chiral center closer to the metal that in most cases can be beneficial in terms of enantioselectivity. In this regard, our group has also has successfully applied several heterodonor P-S ligands in Pd-AAS.[5e, 7] For example, in 2014 our group disclose a Pd/phosphite-thioether furasonide-based system in Pd-AAS that were able to generate C-C and C-heteroatom bonds with either hindered or unhindered substrates with a range of C, N, and O-nucleophiles. The results in terms of enantioselectivities and yields were comparable to the best performing systems in the literature. Although the ligands were synthesized from unexpensive D-xylose, the synthesis required from many steps.[7c, 8] For this reason, and having in mind all these considerations, we decided to give a push to P-heterodonor-based catalytic systems by designing a new P-thioether ligand library (Ligands **L1**-**L8a-c**,**f-i** Figure 3.1) from unexpensive indene for Pd-catalyzed asymmetric allylic substitution reactions.

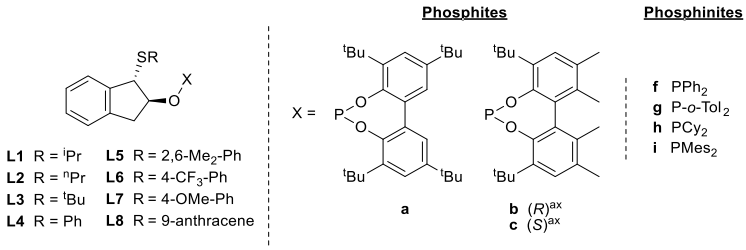

Figure 3.1. Phosphite/phosphinite-thioether ligand library **L1**-**L8a**-**c**,**f-i**.

The ligand design has several advantages compared to other P-S ligand libraries. The first one is that the preparation of this ligand library requires only three steps. The second advantage is that Jacobsen epoxidation of indene guarantees that both indene oxide stereoisomers are available with high enantiomeric excesses (>99%). The third one is that ring opening reaction with the corresponding thioether allows selectively the synthesis of a myriad of different thioethers.[9] And finally, the resulting *trans*-alcohol allows the installation of either a phosphite or a phosphinite moiety. This step wise synthesis allows the systematic furnish of each module (first thioether group and then phosphite/phosphinite moiety) which is highly beneficial to synthesize several candidates for a screening. In this case, the performance of this system was studied systematically by varying the electronics and sterics on thioether group, the P group (phosphite-*vs*-phosphinite), and the configuration of the biaryl phosphite moiety.

Moreover, the simplicity of the ligand backbone should facilitate the identification of the key intermediates by NMR (fewer overlapping signals) and DFT studies. Both DFT and the study of the intermediates by NMR were crucial to fully understand the origin of the enantioselectivity and therefore find the optimal ligand. The optimal ligand was applied to a broad range of nucleophiles (C-, N- and O-) and substrates (in total 26

products). In order to test the system in a more sustainable way, we also tested it in propylene carbonate that in contrast with dichloromethane is more environmentally friendly.[10]

3.2. Results and discussion

3.2.1. Ligand synthesis and first screening

The corresponding phosphite/phosphinite-thioether ligands were straightforward prepared in only three steps from inexpensive indene **1** (ca. 17 €/kg) (Scheme 3.1).

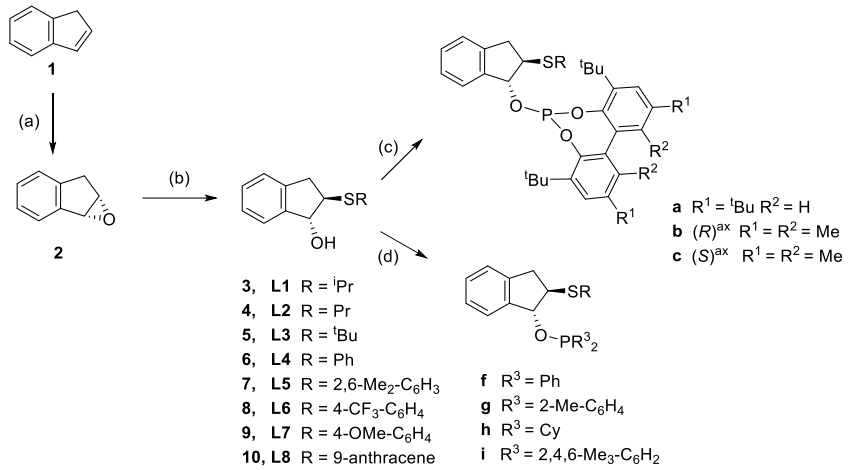

(a) (*R,R*)-Mn-salen catalyst, 4-PPNO, aq NaClO, CH_2Cl_2;[11] (b) RSH, NaOH, dioxane/water (10:1);[12] (c) $ClP(OR^1R^2)_2$ for **a**-**c**, Pyr, toluene; (d) $ClPR^3_2$ for **f**-**i**, TEA, toluene.

Scheme 3.1. Synthesis of phosphite/phosphinite-thioether ligands **L1-L8a-c**,**f-i** from indene.

First, epoxidation of indene **1** with Jacobsen catalyst and subsequently recrystallization afforded the enantiopure indene oxide in high yields and excellent enantioselectivity (>99% *ee*).[11, 13] Then, the chiral epoxide **2** was opened in a stereo- and regioselective manner with the corresponding thiol in basic media in dioxane/water as solvent.[12] Initially, seven different thiols with different electronic and steric properties were introduced (compounds **3**-**9**). The hydroxy group allowed to synthesize either phosphinite or phosphite moieties in only 1 more step from the corresponding chlorophosphine or chlorophosphite. The ligands were obtained in high yields as white solids in case of phosphites (**L1-L7a-c**) and colorless oils in the case of phosphinites (**L1-L7f-i**). Whereas all phosphite-containing ligands were stable, the phosphinite analogues showed slow decomposition even when they were stored at -20 °C.

With the ligands **L1-L7a-c**,**f-i** in hand, we evaluated them in the Pd-catalyzed allylic alkylation of two substrates, the hindered *rac*-(*E*)-1,3-diphenylallyl acetate (**S1**) and the more challenging cyclic unhindered *rac*-cyclohex-2-en-1-yl acetate (**S2**) using dimethyl malonate as nucleophile. The results are summarized in Table 3.1 Our system showed a promising catalytic activity obtaining full conversions (except **L1h**) with *ee* values up to 97% in the case of **S1** and up to 88% in case of **S2**. Moreover, our system was extremely active observing TOF values around 2000 mol substrate × (mol Pd × h)$^{-1}$).

Table 3.1. Selected results for the Pd-catalyzed allylic alkylation of model substrates **S1** and **S2** with dimethyl malonate using the ligand library **L1**-**La**-**c**,**f-i**.[a]

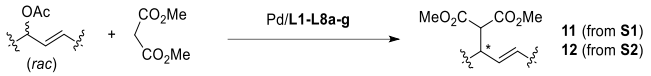

		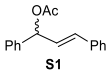 S1		 S2	
Entry	L	% Conv (h)[b]	%ee[c]	% Conv (h)[b]	%ee[c]
1	**L1a**	100 (0.5)	17 (*R*)	100 (2)	15 (*S*)
2	**L1b**	100 (0.5)	90 (*R*)	100 (2)	66 (*R*)
3	**L1c**	100 (0.5)	75 (*S*)	100 (2)	61 (*S*)
4	**L1f**	100 (0.5)	50 (*R*)	100 (2)	28 (*S*)
5	**L1g**	100 (0.5)	25 (*R*)	100 (2)	11 (*S*)
6	**L1h**	5 (0.5)	32 (*R*)	10 (2)	28 (*S*)
7	**L1i**	100 (0.5)	4 (*R*)	100 (2)	14 (*R*)
8	**L2b**	100 (0.5)	90 (*R*)	100 (2)	62 (*R*)
9	**L3b**	100 (0.5)	84 (*R*)	100 (2)	60 (*R*)
10	**L3g**	100 (0.5)	63 (*R*)	100 (2)	77 (*S*)
11	**L4b**	100 (0.5)[d]	97 (*R*)	100 (2)	85 (*R*)
12	**L5b**	100 (0.5)	96 (*R*)	100 (2)	86 (*R*)
13	**L5c**	100 (0.5)	80 (*S*)	100 (2)	84 (*S*)
14	**L5f**	100 (0.5)	28 (*R*)	100 (2)	13 (*S*)
15	**L5g**	100 (0.5)	40 (*R*)	100 (2)	11 (*S*)
16	**L6b**	100 (0.5)	96 (*R*)	100 (2)	88 (*R*)
17	**L7b**	100 (0.5)	97 (*R*)	100 (2)	87 (*R*)
18[e]	**L5b**	100 (0.5)	96 (*R*)	100 (2)	85 (*R*)

[a] 0.5 mol% $[PdCl(\eta^3\text{-}C_3H_5)]_2$, ligand (0.011 mmol), substrate (1 mmol), CH_2Cl_2 (2 ml), BSA (3 eq), dimethyl malonate (3 eq), KOAc (pinch) at rt for the indicated time. [b] Conversion percentage determined by ^{1}H-NMR. [c] Enantiomeric excesses determined by HPLC for **S1** and GC for **S2**. Absolute configuration drawn in parentheses. [d] TOF calculated is 2000 mol/h using 0.25% mol of Pd precursor. [e] Propylene carbonate was used as solvent and the reaction temperature was 40 °C.

To analyze the contribution of P-donor groups on this catalytic system we compared the effect of having a phosphinite or a phosphite. Whereas by using phosphite groups we could attain enantioselectivities up to 97% and 87% for **S1** and **S2,** respectively (entry 17, ligand **L7b**), lower enantiomeric excesses were found when phosphinite analogues were used (entries 4-7). After that, we compared the phosphite ligands each other (entries 1-3). In this aspect, it drives our attention that phosphite ligands with axial chirality in the biaryl phosphite group (**b** and **c**) showed better performance in terms of

ee values than those analogues with an achiral biaryl group (**a**) (entry 1 *vs* entries 2-3). For **S1**, we could observe cooperative effect between the configurations of the backbone and the biaryl phosphite group, being the match cases those which have (*R*) configuration on the biaryl phosphite group (**c**). In contrast, when **S2** was alkylated, no cooperative effect was observed.

Another aspect to analyze is the contribution of the nature of thioether groups. In this respect, ligands containing alkyl groups showed lower levels of enantioinduction than their aryl-thioether analogs (ligands **L1**-**L3** *vs* **L4**-**L7**, entries 1-10 and 4-18, respectively).

To sum up, the best enantiomeric excesses for **S1** (up to 97% *ee*) were obtained using ligands which have an aryl thioether group and a (*R*) configuration on the biaryl phosphite moiety (entries 11-12 and 16-17). In contrast, for **S2** the best *ee* values (up to 88%) were achieved by using ligands with an aryl thioether group regardless the configuration on the biaryl phosphite used (entries 16-17). Interestingly, both enantiomers of the alkylated product from **S2** are easily accessible by just changing the configuration of the biaryl phosphite group (entries 12-13).

To improve the sustainability of this transformation, we also tested our catalytic system with propylene carbonate as greener solvent than dichloromethane. Despite its advantages, it has been scarcely used in Pd-AAS and the only examples found are with the benchmark substrate **S1**.[10b, 14] To our delight, when **S1** and **S2** were alkylated in propylene carbonate, the corresponding products were obtained in high yields and enantioselectivities comparable to those obtained with dichloromethane as solvent (entries 12 and 18).

3.2.2. Optimization of ligand parameters by DFT calculations

In order to fine-tuning the ligand and with the aim of improve the enantioselectivities achieved, we further performed DFT studies. Previous calculations on this reaction have shown that the enantioselective step is the nucleophilic attack on the Pd-allyl complex. Transition states in this process can be either early or late depending on several parameters such as, the ligand used, the nucleophile and the reaction conditions. In the case of late transition state, the TS resembles on the Pd-olefin complexes.[15]

For this reason, we calculated the TS's and the Pd-olefin complexes relative energies using the model hindered substrate **S1** with dimethyl malonate as nucleophile and using ligands **L5b** and **L5c** that differ on the configuration of the biaryl phosphite (Table 3.1, entries 12 and 13). The contribution of more energetic species such as *anti-anti* and *syn-anti* was not considered and only the more stable *syn-syn* allyl species were calculated.[3c] In the calculations, the configuration on the thioether was considered as well as the attack of the nucleophile *trans* to P and S. The reason for this is that the *trans* effect of P-S ligands is usually less exacerbated than their P,N-ligands counterpart and little differences in electronics and sterics can change the *trans* preference in the TS.[8, 16] As

we can see in Table 3.2, the relative energies of calculated TS's matched with the experimental results. The calculated enantioselectivity values for **L5b** (ee_{cal} > 99% (*R*)) were higher than for **L5c** (96% (*S*)), following the same trend than the experimental values (96% *ee* (*R*) for **L5b** and 80% *ee* (*S*) for **L5c**).

Table 3.2. Relative energies and representation of most stable *R*- and *S*- transition states and the most stable *R*- and *S*- Pd-π-olefins for **S1** with dimethyl malonate and **L5b-c** as ligands.

	Transition States				Pd-olefin complexes			
L	$TS_{(R)}$	$TS_{(S)}$	% *ee* cal	% *ee* exp	$Pd\text{-olefin}_{(R)}$	$Pd\text{-olefin}_{(S)}$	% *ee* cal	% *ee* exp
L5b	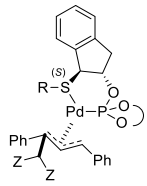 *endo* 0 kJmol^{-1}	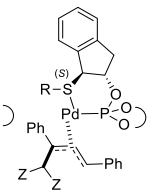 *exo* 28 kJmol^{-1}	>99 (*R*)	96 (*R*)	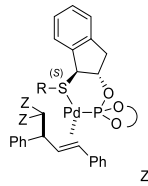 0 kJmol^{-1}	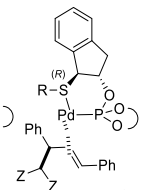 38.1 kJmol^{-1}	>99 (*R*)	96 (*R*)
L5c	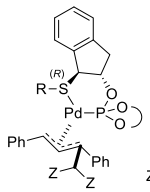 *exo* 10.8 kJmol^{-1}	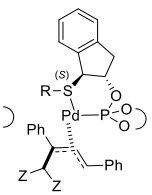 *exo* 0 kJmol^{-1}	96 (*S*)	80 (*S*)	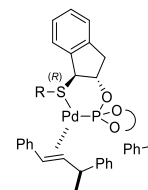 0 kJmol^{-1}	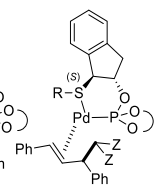 18.1 kJmol^{-1}	>99 (*R*)	80 (*S*)

Z = CO_2Me

Furthermore, the DFT studies show that the change of the configuration on the biaryl phosphite moiety leads to the preferential formation of the opposite enantiomer which is in agreement with the experimental results. Also, in contrast with the results obtained for **L5b**, with ligand **L5c** both enantiomers come from TSs with *exo* coordination of the substrate, where the nucleophile attacks *trans* to P (minor enantiomer) or *trans* to S (major enantiomer). It is also evident that results for Pd-olefin intermediates do not correlate with the experimental results as for both ligands the major product should be (*R*) with calculated *ee* values of more of 99%.

The origin of enantioselectivities for Pd/**L5b** and Pd/**L5c** catalytic systems was difficult to elucidate. Furthermore, the distortion/interaction analysis was neither conclusive. Fortunately, the quadrant analysis was more informative (Figure 3.2). The repulsion between one phenyl substituent of **S1** and the biaryl phosphite group seems to be crucial. Thus, the difference configuration on the biaryl phosphite moiety in both ligands, place the sterics on a different quadrant, therefore, giving the opposite

enantiomers. But it is not only the phosphite sterics that plays a role on enantiodiscrimination. The thioether bulk plays also an important role since its substituent push closer the substrate and the catalyst and therefore it increases the enantioselectivity.

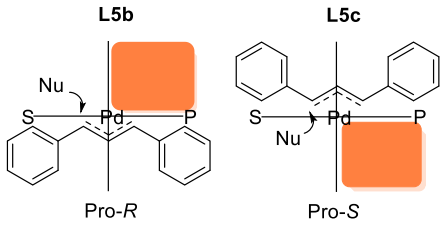

Figure 3.2. Schematic representation of quadratic model of the most stable TSs for ligands **L5b** and **L5c.** Steric effects from the phosphite are represented by the orange boxes.

Taking into account the role of the steric bulk exerted by the thioether substituent, we further investigated if a fine tuning on the sulfur bulkiness could be beneficial to increase the *ee*'s values for alkylation of cyclic unhindered substrate **S2**. For this, we performed the corresponding TS's calculation using the ligand **L5b** (with thioether containing 2,6-dimethylphenyl group) as well as related ligands with a 2,6-^{i}Pr-C_6H_4 and an anthryl group respectively (Table 3.3). In this case, ammonia was used as nucleophile to speed up the calculations.[17]

Table 3.3. Results for the calculated enantioselectivities for **S2** and the corresponding obtained experimentally.[a]

R—S	L	$\Delta\Delta G^{\ddagger}_{cal}$ (kJmol^{-1})	$\%ee_{cal}$	$\%ee_{exp}$
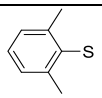	**L5b**	1.2	9 (*R*)	86 (*R*)
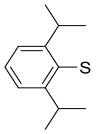		2.1	35 (*R*)	
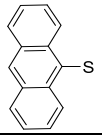	**L8b**	6.8	74 (*R*)	94 (*R*)[a]

[a] 0.5 mol% [PdCl(η^3-C_3H_5)]$_2$, ligand (0.011 mmol), substrate (1 mmol), CH_2Cl_2 (2 ml), BSA (3 eq), dimethyl malonate (3 eq), KOAc (pinch) at rt for 2 h. The alkylation with **L8c** gave 93% ee (*S*).

The results shown in Table 3.3, clearly showed that by increasing the rigidity of the thioether group, the energy difference between the TS's leading to opposite enantiomers increased. As result, the computational calculations suggested that the introduction of an anthryl group should have a positive effect on enantioselectivity.

Encouraged by these results, we synthesized and applied the new ligand with an anthryl thioether group (**L8b**). The application of Pd/**L8b** in the allylic alkylation of **S2** lead to an increment of *ee* value from 88% to 94%, which agrees with the computational results. This result is comparable to the best one reported for this substrate. To our delight, when **L8b** was also applied in the alkylation of **S1** the enantioselectivity increased from 97% (**L7b**) to 99% (*R*).

3.2.3. Allylic substitution with Pd/L8b system using several different nucleophiles

After ligand optimization, we next tested our best performing ligand **L8b** with several different C-, N- and O-nucleophiles. First, we started with the alkylation of **S1** with Pd/**L8b** catalytic system with several carbon nucleophiles. The results are summarized in Table 3.4.

Non-substituted malonates were alkylated in high yields and excellent enantioselectivities (up to 99% *ee*, entries 1 and 2). Then, we tested a set of different substituted malonates, such as allyl-, butenyl, pentenyl-, or propargyl-substituted malonates that are by far more interesting in a synthetic point of view and challenging in Pd-asymmetric allylic alkylation than the non-substituted ones. Interestingly, the substituted malonates were alkylated from very good to excellent yields and with excellent enantiomeric excesses regardless substitution pattern in the malonate (up to 99% *ee*, entries 3-7). Then, we further tested other C-nucleophiles rather than malonates. In the case of acetylacetone and malonitrile we obtain the alkylated product with high level of enantiocontrol (entries 8 and 9). In the case of isopropyl cyanoacetate, we could achieve excellent *ee* values albeit with low diastereomeric control.[18] Finally, two pyrroles were also tested as nucleophiles the alkylation of **S1**. Pyrroles are interesting from medicinal chemistry point of view as they have been found in several biologically active molecules.[19] Their use in Pd-catalyzed allylic alkylation has been reported in only one reference with **S1**-type substrates requiring low temperatures (-20 °C) to attain high *ee's*.[20] It must be mentioned that systems using privileged ligands such Trost ligands are not compatible with the use of pyrroles.[20] To our delight, our P-S ligand was able to alkylate **S1** with very good yields and excellent *ee* values (up to >99% *ee*, entries 11 and 12).

Table 3.4. Pd-catalyzed allylic substitution of **S1** with optimal ligand **L8b** several different C-nucleophiles.[a]

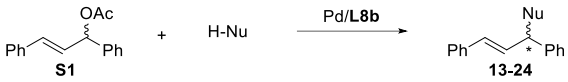

Entry	Product	% Yield[b]	% *ee*[c]	Entry	Product	% Yield	% *ee*
1	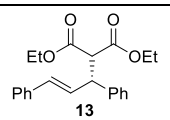 **13**	94	99 ®	7	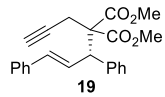 **19**	90	99 (*S*)
2	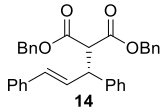 **14**	92	98 ®	8	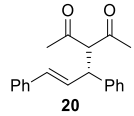 **20**	88	98 (*S*)
3	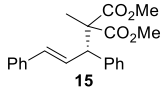 **15**	92	97 (*S*)	9	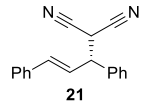 **21**	84	98 (*R*)
4	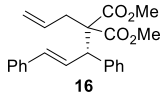 **16**	93	98 (*S*)	10	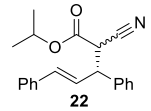 **22**	82 (3:2 dr)	98/97
5	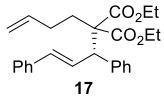 **17**	89	98 (*S*)	11[d]	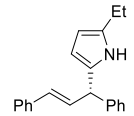 **23**	87	96 (*S*)
6	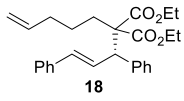 **18**	91	95 (*S*)	12[d]	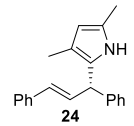 **24**	85	>99 (*S*)

[a] 0.5 mol% $[PdCl(\eta^3\text{-}C_3H_5)]_2$, ligand (0.011 mmol), substrate (1 mmol), CH_2Cl_2 (2 ml), BSA (3 eq), Nucleophile (3 eq), KOAc (pinch) at rt for 30 min. [b] Full conversion. [c] Determined by HPLC. [d] 2 mol % $[PdCl(\eta^3\text{-}C_3H_5)]_2$, 4.4 mol % ligand CH_2Cl_2 (2 ml), K_2CO_3 (2 equiv) at rt for 18 h.

We then moved to the allylic substitution using amines as nucleophiles (Table 3.5). Amines are present in myriad of pharmaceutically active compounds and represent one of the most valuable nucleophile group in this transformation[3l].

First, we tested benzylamine obtaining a very good yield and an excellent enantioselectivity (entry 1, 99% *ee*). After that, we further tested substituted benzylamines such as those furnished with *p*-methoxy and *p*-trifluoromethane groups. In both cases, good yields and excellent enantioselectivities were obtained (entries 2 and 3). Our Pd/**L8b** catalytic system was able to attain excellent enantiocontrol when using furfurylamine, morpholine or even allylamine which contains another double bound that can be further derivatized for the synthesis of more complex chiral molecules (entries 4-6).

Table 3.5. Pd-catalyzed allylic substitution of **S1** with optimal ligand **L8b** several N- and O-nucleophiles.[a]

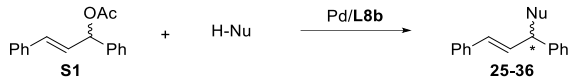

Entry	Product	% Yield[b]	% *ee*[c]	Entry	Product	% Yield[b]	% *ee*[c]
1	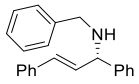 **25**	88	99 (*S*)	7[d]	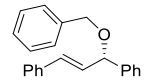 **31**	92	99 (*S*)
2	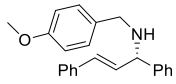 **26**	81	99 (*S*)	8[d]	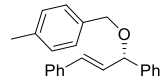 **32**	90	98 (*S*)
3	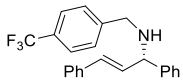 **27**	78	99 (*S*)	9[d]	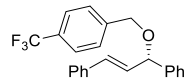 **33**	91	98 (*R*)
4	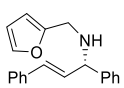 **28**	83	97 (*S*)	10[d]	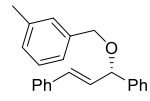 **34**	93	98 (S)
5	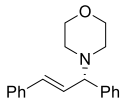 **29**	87	98 (*S*)	11[d]	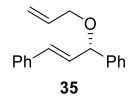 **35**	83	96 (*S*)
6	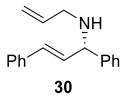 **30**	79	97 (*S*)	12[d]	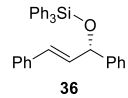 **36**	78	>99 (*S*)

[a] 0.5 mol% $[PdCl(\eta^3\text{-}C_3H_5)]_2$, ligand (0.011 mmol), substrate (1 mmol), CH_2Cl_2 (2 ml), BSA (3 eq), Nucleophile (3 eq), KOAc (pinch) at rt for 30 min. [b] Full conversion. [c] Determined by HPLC. [d] 2 mol % $[PdCl(\eta^3\text{-}C_3H_5)]_2$, 4.4 mol % ligand CH_2Cl_2 (2 ml), Cs_2CO_3 (3 equiv) at rt for 18 h.

Encouraged by the enantiomeric control that our Pd/**L8b** catalytic system showed, we further tested it in allylic etherification of **S1** (Table 3.5). It is worth to mention that Pd-catalyzed allylic etherification has been less studied, and the examples found mostly deal with phenols that have, by far, a lower pK_a value than the corresponding alkyl-alcohols.[21] To prove our catalytic system we focused in the use of alkyl alcohols. Thus, we choose benzyl and allyl substituted alcohols. To our delight, high yields and enantioselectivities were attained regardless the alcohol used. Nevertheless, it was required to increase the catalyst loading and the use of Cs_2CO_3 as base to obtain these excellent results (entries 7-11). We also achieved high yield and enantioselectivity in the etherification of **S1** using triphenylsilanol which after alkylation gave the corresponding chiral silyl ether (entry 12). This route allows then the obtention of chiral silyl-protected alcohols which are interesting for organic synthesis. To sum up, enantioselectivities obtained when alcohols were used as nucleophiles have remained as high as those obtained with dimethyl malonate.

Next, we tested our Pd/**L8b** catalytic system in the allylic alkylation of other hindered substrates with different electronic and steric properties than **S1**. The results are summarized in Table 3.6. We were able to alkylate them from very good to excellent yields and in all cases excellent enantioselectivities regardless their electronic properties (entries 1-4) as well as the steric properties (entries 5-6).

Table 3.6. Pd-catalyzed allylic alkylation of substrates other hindered substrates **S3**-**S7** using carbon nucleophiles.[a]

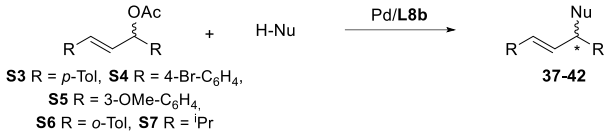

S3 R = *p*-Tol, **S4** R = 4-Br-C_6H_4, **S5** R = 3-OMe-C_6H_4, **S6** R = *o*-Tol, **S7** R = ^{i}Pr

37-42

Entry	Substrate	Product	% Yield[b]	% *ee*[c]
1	**S3**	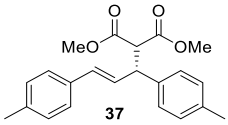 **37**	98	98 (*R*)
2	**S3**	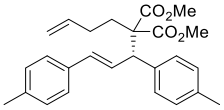 **38**	87	97 (*R*)
3	**S4**	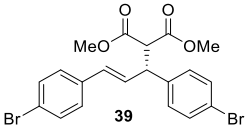 **39**	89	96 (*R*)
4	**S5**	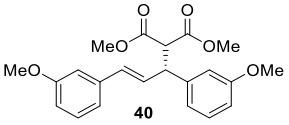 **40**	91	97 (*R*)
5	**S6**	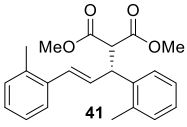 **41**	87	99 (*R*)
6	**S7**	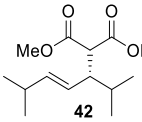 **42**	91	>95% (*R*)

[a] 0.5 mol% [$PdCl(\eta^3$-$C_3H_5)]_2$, ligand (0.011 mmol), substrate (1 mmol), CH_2Cl_2 (2 ml), BSA (3 eq), dimethyl malonate (3 eq), KOAc (pinch) at rt for 2 h. [b] Full conversion. [d] Measured by HPLC.

Next, as previously mentioned, catalytic systems able to alkylate both hindered and unhindered substrates with good *ee* values are very difficult to find. Thus, we tested our Pd/**L8b** catalytic system in the alkylation of three unhindered substrates: **S2**, **S8** and **S9** which differ in the ring size. The results are summarized in Table 3.7. For cyclohexenyl

derivative **S2**, we could attain high enantioselectivities regardless the nucleophile used (entries 1-6, *ee's* up to 97%). Interestingly, the excellent catalytic performance was maintained with the 7-membered cyclic substrate **S9** (entries 9 and 10, *ee's* up to 96%), as well as for the more challenging 5-membered cyclic substrate **S8** (entries 7 and 8, *ee's* up to 85%).

Table 3.7. Allylic alkylation of unhindered cyclic substrates using different carbon nucleophiles.[a]

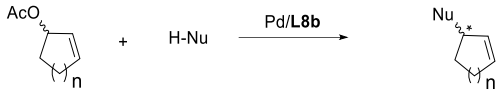

S2 (n = 2)
S8 (n = 1)
S9 (n = 3)

43-52

Entry	S.	Product	% Yield[b]	% *ee*[c]	Entry	S.	Product	% Yield[b]	% *ee*[c]
1	**S2**	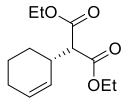 **43**	87	95 (*R*)	6	**S2**	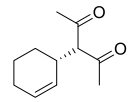 **48**	82	90 (-)
2	**S2**	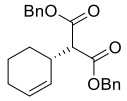 **44**	84	95 (*R*)	7	**S8**	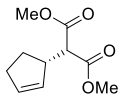 **49**	80	84 (-)
3	**S2**	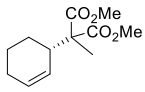 **45**	87	91 (*R*)	8	**S8**	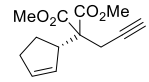 **50**	83	85 (-)
4	**S2**	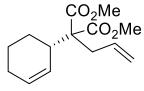 **46**	84	94 (*R*)	9	**S9**	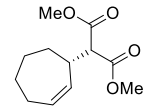 **51**	90	96 (*R*)
5	**S2**	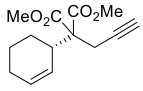 **47**	86	87 (*R*)	10	**S9**	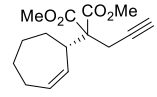 **52**	92	96 (*R*)

[a] 0.5 mol% $[PdCl(\eta^3\text{-}C_3H_5)]_2$, ligand (0.011 mmol), substrate (1 mmol), CH_2Cl_2 (2 ml), BSA (3 eq), dimethyl malonate (3 eq), KOAc (pinch) at rt for 2 h. [b] Full conversion. [e] Measured by HPLC or GC.

3.2.4. Study of Pd-allyl intermediates by NMR

To fully understand the catalytic process we also synthesized, characterized and studied the relative reactivity toward the nucleophile of the Pd-allyl intermediates [Pd(η^3-allyl)(P-S)]BF_4 with the ligands **L5b** and **L5c**.

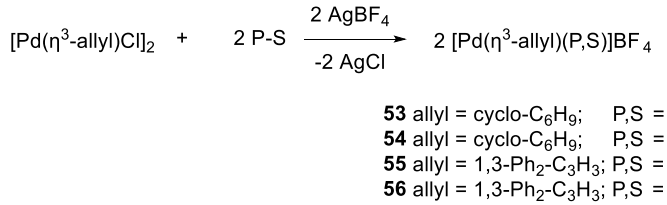

Scheme 3.2. Synthesis of the [Pd(η^3-allyl)(P-S **= L5b-c**)]BF_4 intermediates **53**-**56**.

All complexes were synthesized in as previously reported[22] and fully characterized by ^{1}H, ^{13}C and ^{31}P{^{1}H} NMR spectroscopy as well as by ESI-TOF-HRMS. Unfortunately, we were not able to grow suitable crystals for x-ray structure determination.

To understand the relation between the configuration of the alkylated product and the configuration of biaryl phosphite group in the allylic substitution of **S2**, we compared **53** (Pd/**L5b**) with **54** (Pd/**L5c**). In VT-NMR study (30 °C to -80 °C) we observed the presence of almost one single isomer (ratio 95:5, Scheme 2.1.3). We could assign unambiguously by NOE that the preferential coordination mode of the allyl group was *exo* for **53** and *endo* for **54** respectively. In both cases, the configuration of the thioether of both intermediates was (*S*). DFT calculations agreed with the assignment of the complexes. The results showed that **53** the Pd(η^3-*exo*) isomer was 9.5 kJmol^{-1} more stable than the Pd(η^3-*endo*) while for **54** the difference between *endo* and *exo* isomers is 7.3 kJ/mol. It is also worth to mention that ^{13}C NMR shifts indicates for both complexes **53** and **54** that the more electrophilic carbon was *trans* to phosphite group. Thus, assuming that nucleophilic attack takes place at the more electrophilic allyl carbon terminus, the diastereomeric ratio of Pd-allyl intermediates matches with the enantioselectivity observed (86% *ee* (*R*) for **L5b** and 84% *ee* (*R*) for **L5c**). That indicates that both intermediates react at a similar rate. To sum up, in the allylic substitution of **S2**, the *endo* and *exo* population of the Pd-allyl intermediates determines the stereochemical outcome of the reaction.

To further understand the relation of the configuration of phosphite moiety and the enantioselectivity observed for **S1**, we compared complex **55** (Pd/**L5b**) and complex **56** (Pd/**L5c**). In this case, the enantioselectivities achieved indicate that **L5b** provides higher enantioselectivity than **L5c** which differs from **S2**. The VT-NMR (from 30 °C to -80 °C) of complexes **55** and **56** indicated the presence of two *syn*/*syn* isomers in solution at ratios of 93:7 and 70:30, respectively. Nevertheless, NOE experiments did not allow the complete elucidation of the 3D structures of the Pd-allyl intermediates. The assignment was carried out by DFT studies as well as by the reactivity study of the Pd-allyl complexes

with sodium malonate at low temperature. These studies indicated that for complex **55**, the minor *endo* isomer reacts around 20 times faster than the major *exo* isomer. Whereas for complex **56**, the major *exo* isomer reacts 3.5 times faster than the minor *endo* isomer. Therefore, for **S1** the enantioselectivity seems to be controlled by the different reactivity of allyl intermediates towards nucleophilic attack.

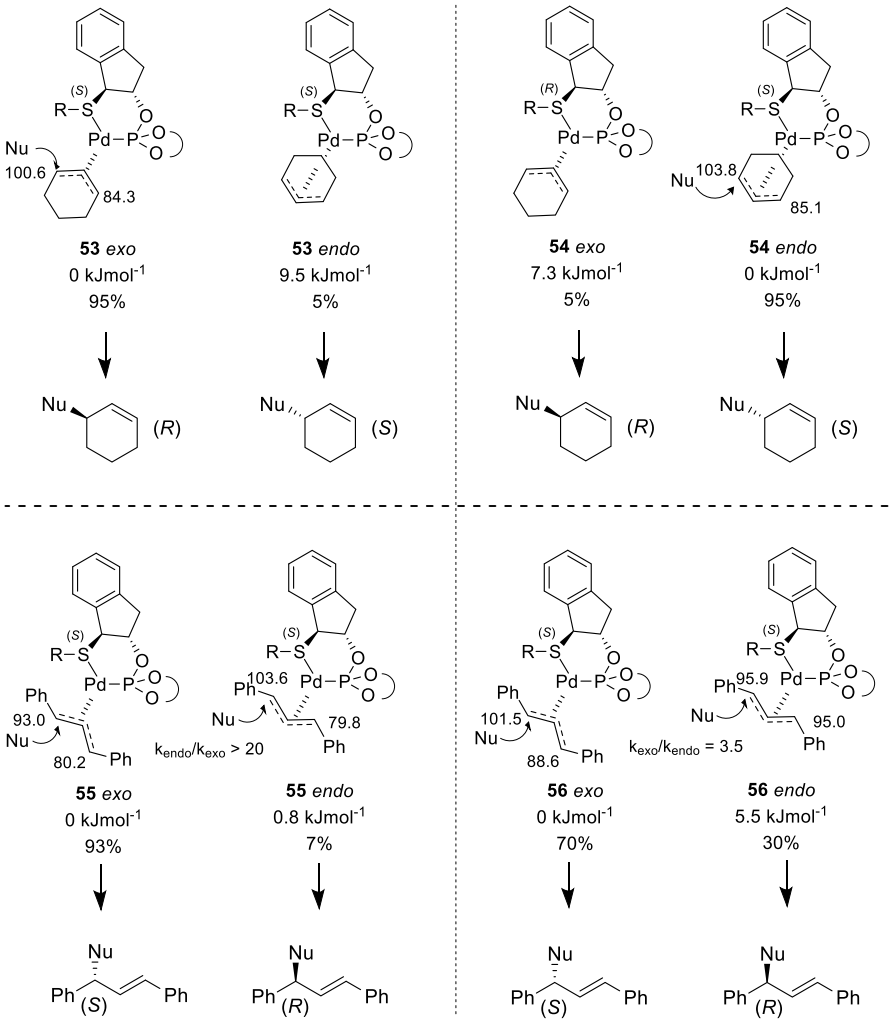

Scheme 3.3. Diastereomeric pairs of Pd-allyl intermediates for **S1** and **S2** and computed relative energies by DFT.

.

3.3. Conclusions

We have designed a small but reliable P-S ligand library for Pd-catalyzed asymmetric allylic substitution. These ligands were synthesized in only three steps from unexpensive indene. The combination of experimental and theoretical studies has led to the design of an optimal, solid, and air-stable phosphite-anthracenethiol derivative with excellent behavior in Pd-catalyzed allylic substitution reactions. Improving the results reported to date, this ligand presents a broad substrate and nucleophile scope. Excellent enantioselectivities have been achieved for a range of linear and cyclic allylic substrates using a large number of C-, N-, and O-nucleophiles (40 compounds in total). The species responsible for the catalytic activity have been also further studied by NMR to clearly establish the origin of the enantioselectivity.

3.4. Experimental part

All reactions were carried out using standard Schlenk techniques under an argon atmosphere. Commercial chemicals were used as received. Solvents were dried by means of standard procedures and stored under argon. ^{1}H, $^{13}C\{^{1}H\}$ and $^{31}P\{^{1}H\}$ NMR spectra were recorded using a Varian Mercury-400 MHz spectrometer. Chemical shifts are relative to that of $SiMe_4$ (^{1}H and $^{13}C\{^{1}H\}$) as an internal standard. Racemic substrates **S1**-**S9** and Ligands L1f and L5f are known compounds and they were prepared as previously reported.[23] The NMR copies can be found in the electronic supporting information provided with this thesis.

3.4.1. General procedure for the regio- and stereospecific ring opening of 2. Preparation of thioether alcohols 3–10

A solution of (−)-indene oxide **2** (2 mmol, 264 mg) in dioxane (4.5 ml/mmol of indene oxide) is treated with the corresponding thiol (3 mmol). Then, a solution of NaOH (3 mmol, 120 mg) in water (0.45 ml/mmol of indene oxide) is added dropwise. The reaction mixture is capped and stirred at 55 °C until the epoxide is consumed according to TLC analysis (ca. 45–60 min). After this, the mixture is cooled to room temperature, diluted with water, and extracted with CH_2Cl_2 (3 × 20 ml). The combined organic layers are dried over Na_2SO_4 and concentrated to give a residue that is purified by flash chromatography on silica gel to give the desired thioether alcohol.

3.4.2. Characterization details for the thioether alcohols 3-10

(*1S*,2*S*)-1-(Isopropylthio)-2,3-dihydro-1*H*-inden-2-ol (3). Yield: 308 mg (74%), white solid. SiO_2-chromatography (gradient from cyclohexane/EtOAc = 100:0 to

cyclohexane/EtOAc = 80:20). ^{1}H NMR (400 MHz, $CDCl_3$): δ= 1.34 (d, 3H, CH_3, ^{i}Pr, $^3J_{H-H}$ =6.7 Hz), 1.38 (d, 3H, CH_3, ^{i}Pr, $^3J_{H-H}$ =6.7 Hz), 2.07 (bs, 1H, OH), 2.86 (dd, 1H, CH_2, $^2J_{H-H}$ =16.1, $^3J_{H-H}$ =4.4 Hz), 3.14 (hept, 1H, CH, ^{i}Pr, $^3J_{H-H}$ =6.7 Hz), 3.38 (dd, 1H, CH_2, $^2J_{H-H}$ =16.1, $^3J_{H-H}$ =6.2 Hz), 4.13 (d, 1H, CH-S, $^3J_{H-H}$ =4.1 Hz), 4.46-4.49 (m, 1H, CH-O), 7.22 (bs, 3H, CH=), 7.36 (m , 1H, CH=).^{13}C NMR (100.6 MHz, $CDCl_3$): δ= 23.8 (CH_3), 24.2 (CH_3), 35.5 (CH), 39.9 (CH_2), 55.9 (CH-S), 79.9 (CH-O), 125.1 (CH=), 125.4 (CH=), 127.1 (CH=), 127.9 (CH=), 140.0 (C), 141.3 (C).

(1*S*,2*S*)-1-(Propylthio)-2,3-dihydro-1*H*-inden-2-ol (4). Yield: 325 mg (78%), white solid. SiO_2-chromatography (gradient from cyclohexane/EtOAc = 100:0 to cyclohexane/EtOAc = 80:20). ^{1}H NMR (400 MHz, $CDCl_3$): δ= 1.01 (t, 3H, CH_3, ^{n}Pr, $^3J_{H-H}$ =7.3 Hz), 1.66 (sext, 2H, CH_2, ^{n}Pr, $^3J_{H-H}$ =7.3 Hz), 2.10 (bs, 1H, OH), 2.53 (dt, 1H, CH_2, $^2J_{H-H}$ =12.3, $^3J_{H-H}$ =7.3 Hz), 2.60 (dt, 1H, CH_2, $^2J_{H-H}$ =12.3, $^3J_{H-H}$ =7.3 Hz), 2.87 (dd, 1H, CH_2, $^2J_{H-H}$ =16.1, $^3J_{H-H}$ =4.7 Hz), 3.37 (dd, 1H, CH_2, $^2J_{H-H}$ =16.1, $^3J_{H-H}$ =6.3 Hz), 4.09 (d, 1H, CH-S, $^3J_{H-H}$ =4.3 Hz), 4.49 (quint, 1H, CH-O, $^3J_{H-H}$ =5.0 Hz), 7.32-7.40 (m, 1H, CH=), 7.20-7.25 (m, 3H, CH=). ^{13}C NMR (100.6 MHz, $CDCl_3$): δ= 13.6 (CH_3), 23.2 (CH_2), 33.0 (CH_2), 39.8 (CH_2), 57.0 (CH-S), 79.3 (CH-O), 125.1 (CH=), 125.3 (CH=), 127.1 (CH=), 127.9 (CH=), 140.1 (C), 140.6 (C).

(1*S*,2*S*)-1-(*tert*-Butylthio)-2,3-dihydro-1*H*-inden-2-ol (5). Yield: 320 mg (72%), pale orange solid. SiO_2-chromatography (gradient from cyclohexane/EtOAc = 100:0 to cyclohexane/EtOAc = 80:20). ^{1}H NMR (400 MHz, $CDCl_3$): δ= 1.45 (s, 3H, CH_3, ^{t}Bu), 2.29 (bs, 1H, OH), 2.86 (dd, 1H, CH_2, $^2J_{H-H}$ =15.8, $^3J_{H-H}$ =5.6 Hz), 3.32 (dd, 1H, CH_2, $^2J_{H-H}$ =15.8, $^3J_{H-H}$ =6.4 Hz), 4.03 (d, 1H, CH-S, $^3J_{H-H}$ =5.3 Hz), 4.39-4.44 (m, 1H, CH-O), 7.19-7.25 (m, 3H, CH=), 7.38 (m, 1H, CH=), 7.36 (m , 1H, CH=).^{13}C NMR (100.6 MHz, $CDCl_3$): δ= 31.7 (CH_3, ^{t}Bu), 39.9 (CH_2), 43.7 (C, ^{t}Bu), 54.6 (CH-S), 80.8 (CH-O), 124.8 (CH=), 125.6 (CH=), 127.2 (CH=), 127.7 (CH=), 139.7 (C), 142.0 (C).

(1*S*,2*S*)-1-(Phenylthio)-2,3-dihydro-1*H*-inden-2-ol (6). Yield: 373 mg (77%), white solid. SiO_2-chromatography (gradient from cyclohexane/EtOAc = 100:0 to cyclohexane/EtOAc = 80:20). ^{1}H NMR (400 MHz, $CDCl_3$): δ= 2.09 (bs, 1H, OH), 2.82 (dd, 1H, CH_2, $^2J_{H-H}$ =16.3, $^3J_{H-H}$ =3.5 Hz), 3.32 (dd, 1H, CH_2, $^2J_{H-H}$ =16.3, $^3J_{H-H}$ =6.2 Hz), 4.50 (dt, 1H, CH-O, $^3J_{H-H}$ =6.2 Hz, $^3J_{H-H}$ =3.4 Hz), 4.55 (d, 1H, CH-S, $^3J_{H-H}$ =3.3 Hz), 7.19-7.24 (m, 4H, CH=), 7.26-7.31 (m, 2H, CH=), 7.34-7.37 (m, 1H, CH=), 7.40-7.43 (m, 2H, CH=).^{13}C NMR (100.6 MHz, $CDCl_3$): δ= 39.9 (CH_2), 59.1 (CH-S), 79.6 (CH-O), 125.2 (CH=), 125.7 (CH=), 126.9 (CH=), 127.2 (CH=), 128.3 (CH=), 129.0 (CH=), 130.9 (CH=), 135.2 (CH=), 139.9 (CH=), 135.2 (C), 139.9 (C), 140.6 (C).

(1*S*,2*S*)-1-((2,6-Dimethylphenyl)thio)-2,3-dihydro-1*H*-inden-2-ol (7). Yield: 427 mg (79%), white solid. SiO_2-chromatography (gradient from cyclohexane/EtOAc = 100:0 to cyclohexane/EtOAc = 80:20). ^{1}H NMR (400 MHz, $CDCl_3$): δ= 1.75 (bs, 1H, OH), 2.47 (s, 6H, CH_3), 2.82 (dd, 1H, CH_2, $^2J_{H-H}$ =16.6, $^3J_{H-H}$ =2.1 Hz), 3.52 (dd, 1H, CH_2, $^2J_{H-H}$ =16.6, $^3J_{H-H}$ =5.5 Hz), 4.32 (d, 1H, CH-S, $^3J_{H-H}$ =2.0 Hz), 4.36 (tt, 1H, CH-O, $^3J_{H-H}$ =5.5 Hz, $^3J_{H-H}$ =2.1 Hz), 6.94 (d, 1H, CH=, $^3J_{H-H}$ =7.5 Hz), 7.06-7.16 (m, 4H, CH=), 7.18-7.26 (m, 2H, CH=). ^{13}C NMR (100.6 MHz, $CDCl_3$): δ= 21.9 (CH_3), 40.3 (CH_2), 58.8 (CH-S), 78.5 (CH-O), 125.3 (CH=), 125.4 (CH=), 126.7 (CH=), 128.1 (CH=), 128.2 (CH=), 128.7 (CH=), 132.0 (CH=), 140.4 (C), 140.7 (C), 143.6 (C).

(1*S*,2*S*)-1-((4-(Trifluoromethyl)phenyl)thio)-2,3-dihydro-1*H*-inden-2-ol (8). Yield: 478 mg (77%), yellow oil. SiO_2-chromatography (gradient from cyclohexane/EtOAc = 100:0 to cyclohexane/EtOAc = 80:20). ^{1}H NMR (400 MHz, $CDCl_3$): δ= 2.06 (d, 1H, OH, $^3J_{H-H}$ =4.9 Hz), 2.91 (dd, 1H, CH_2, $^2J_{H-H}$ =16.5, $^3J_{H-H}$ =3.5 Hz), 3.42 (dd, 1H, CH_2, $^2J_{H-H}$ =16.5, $^3J_{H-H}$ =6.0 Hz), 4.55 (m, 1H, CH-O), 4.69 (d, 1H, CH-S, $^3J_{H-H}$ =3.2 Hz), 7.21-7.30 (m, 3H, CH=), 7.36-7.41 (m, 1H, CH=), 7.46-7.57 (m, 4H, CH=). ^{13}C NMR (100.6 MHz, $CDCl_3$): δ= 40.2 (CH_2), 58.0 (CH-S), 78.6 (CH-O), 124.1 (CH=), 125.4 (CH=), 125.7 (CH=), 125.8 (q, CH=, $^3J_{H-F}$ =3.8 Hz), 127.4 (CH=), 128.2 (q, C, $^2J_{H-F}$ =32.8 Hz), 128.7 (CH=), 128.8 (CH=), 139.0 (C), 140.6 (C), 141.3 (C).

(1*S*,2*S*)-1-((4-Methoxyphenyl)thio)-2,3-dihydro-1*H*-inden-2-ol (9). Yield: 541 mg (79%), yellow oil. SiO_2-chromatography (gradient from cyclohexane/EtOAc = 100:0 to cyclohexane/EtOAc = 75:25). ^{1}H NMR (400 MHz, $CDCl_3$): δ= 1.97 (d, 1H, OH, $^3J_{H-H}$ =5.2 Hz), 2.81 (dd, 1H, CH_2, $^2J_{H-H}$ =16.3, $^3J_{H-H}$ =3.5 Hz), 3.25 (dd, 1H, CH_2, $^2J_{H-H}$ =16.3, $^3J_{H-H}$ =6.1 Hz), 3.79 (s, 3H, CH_3O), 4.38 (d, 1H, CH-S, $^3J_{H-H}$ =3.3 Hz), 4.50 (tt, 1H, CH-O, $^3J_{H-H}$ =6.1 Hz, $^3J_{H-H}$ =3.5 Hz), 6.82 (d, 2H, CH=, $^3J_{H-H}$ =8.7 Hz), 7.19-7.27 (m, 3H, CH=), 7.35-7.42 (m, 3H, CH=). ^{13}C NMR (100.6 MHz, $CDCl_3$): δ= 39.9 (CH_2), 55.3 (CH-S), 60.6 (CH_3O), 78.6 (CH-O), 114.6 (CH=), 124.4 (CH=), 125.2 (CH=), 125.6 (CH=), 127.0 (CH=), 128.1 (CH=), 135.1 (C), 140.2 (C), 140.6 (C), 159.6 (C).

(1*S*,2*S*)-1-(Anthracen-9-ylthio)-2,3-dihydro-1*H*-inden-2-ol (10). Yield: 308 mg (45%), yellow solid. SiO_2-chromatography (gradient from cyclohexane/EtOAc = 100:0 to cyclohexane/EtOAc = 80:20).. ^{1}H NMR (400 MHz, $CDCl_3$): δ= 1.33 (d, 1H, OH, $^3J_{H-H}$ =5.1 Hz), 2.80 (dd, 1H, CH_2, $^2J_{H-H}$ =16.4, $^3J_{H-H}$ =2.6 Hz), 3.58 (dd, 1H, CH_2, $^2J_{H-H}$ =16.4, $^3J_{H-H}$ =5.6 Hz), 4.40 (m, 1H, CH-O), 4.55 (d, 1H, CH-S, $^3J_{H-H}$ =2.2 Hz), 7.16 (t, 1H, CH=, $^3J_{H-H}$ =7.5 Hz), 7.24 (t, 1H, CH=, $^3J_{H-H}$ =7.5 Hz), 7.25-7.30 (m , 2H, CH=), 7.52 (ddd, 2H, CH=, $^3J_{H-H}$ =8.0 Hz, $^3J_{H-H}$ =6.5 Hz, $^4J_{H-H}$ =1.1 Hz), 7.61 (ddd, 2H, CH=, $^3J_{H-H}$ =8.9 Hz, $^3J_{H-H}$ =6.5 Hz, $^4J_{H-H}$ =1.0 Hz), 8.05 (d, 2H, CH=, $^3J_{H-H}$ =8.4 Hz), 8.54 (s, 1H, CH=), 8.98 (dq, 2H, CH=, $^3J_{H-H}$ =8.9, $^4J_{H-H}$ =1.0 Hz).^{13}C NMR (100.6 MHz, $CDCl_3$): δ= 40.1 (CH_2), 61.2 (CH-S), 78.7 (CH-O), 125.3 (CH=), 125.4 (CH=), 125.7 (CH=), 126.6 (CH=), 126.9 (CH=), 127.0 (CH=), 127.7 (CH=), 128.4 (CH=), 129.1 (CH=), 129.6 (C), 131.8 (C), 134.9 (C), 140.2 (C), 140.8 (C).

3.4.3. Preparation of phosphite-thioether ligands L1-L8a-c

The corresponding phosphorochloridite (1.1 mmol) produced *in situ* was dissolved in toluene (5 ml), and pyridine (0.3 ml, 3.9 mmol) was added. The corresponding thioether-hydroxyl compound (1 mmol) was azeotropically dried with toluene (3 x 2 ml) and then dissolved in toluene (5 ml) to which pyridine (0.3 ml, 3.9 mmol) was added. The alcohol solution was transferred slowly to a solution of phosphorochloridite. The reaction mixture was stirred at 80ºC for 90 min, after which the pyridine salts were removed by filtration. Evaporation of the solvent gave a white foam, which was purified by flash chromatography in silica (Hexane/Toluene/NEt_3 = 7/3/1) to produce the corresponding ligands as white solids.

3.4.4. Preparation of phosphinite–thioether ligands L1–L8g–i

The corresponding thioether–hydroxyl compound (0.5 mmol) and DMAP (6.7 mg, 0.055 mmol) were dissolved in toluene (1 ml), and triethylamine was added (0.09 ml, 0.65 mmol) at rt, followed by the addition of the corresponding chlorophosphine (0.55 mmol) via syringe. The reaction was stirred for 20 min at room temperature. The solvent was removed in vacuo, and the product was purified by flash chromatography on alumina (toluene/NEt3 = 100/1) to produce the corresponding ligand as an oil.

3.4.5. Characterization details for ligands L1-L8a-c,g-i

L1a. Yield: 320.8 mg (50%). ^{31}P NMR (161.9 MHz, C_6D_6): δ=141.5 (s). ^{1}H NMR (400 MHz, C_6D_6): δ=1.09 (d, 3H, CH_3, ^{i}Pr, $^{3}J_{H-H}$ =6.4 Hz), 1.07 (d, 3H, CH_3, ^{i}Pr, $^{3}J_{H-H}$ =6.8 Hz), 1.26 (s, 9H, CH_3, ^{t}Bu), 1.28 (s, 9H, CH_3, ^{t}Bu), 1.54 (s, 9H, CH_3, ^{t}Bu), 1.56 (s, 9H, CH_3, ^{t}Bu), 2.90-2.96 (m, 2H, CH_2, CH ^{i}Pr), 3.23 (dd, 1H, CH_2, $^{2}J_{H-H}$ =16.4 Hz, $^{3}J_{H-H}$ =5.6 Hz), 4.57 (b, 1H, CH-S), 5.18 (m, 1H, CH-OP), 6.94-7.12 (m, 3H, CH=), 7.31 (s, 1H, CH=), 7.33 (d, 1H, CH=, $^{4}J_{H-H}$ =2.8 Hz), 7.34 (d, 1H, CH=, $^{4}J_{H-H}$ =2.4 Hz), 7.57 (d, 1H, CH=, $^{4}J_{H-H}$ =2.4 Hz), 7.59 (d, 1H, CH=, $^{4}J_{H-H}$ =2.4 Hz), ^{13}C NMR (100.6 MHz, C_6D_6): δ=23.4 (CH_3, ^{i}Pr), 23.8 (CH_3, ^{i}Pr), 31.0 (d, CH_3, ^{t}Bu, J_{C-P} =7.6 Hz), 31.1 (CH_3, ^{t}Bu), 34.2 (C, ^{t}Bu), 34.9 (C, ^{t}Bu), 35.3 (CH, ^{i}Pr), 39.1 (CH_2), 54.7 (CH-S), 82.8 (CH-OP), 124.1-146.6 (aromatic carbons). MS HR-ESI [found 669.3498, $C_{40}H_{55}O_3PS$ $(M-Na)^+$ requires 669.3502].

L1b. Yield: 220.8 mg (37%). ^{31}P NMR (161.9 MHz, C_6D_6): δ=130.2 (s). ^{1}H NMR (400 MHz, C_6D_6): δ=1.03 (d, 3H, CH_3, ^{i}Pr, $^{3}J_{H-H}$ =6.8 Hz), 1.23 (d, 3H, CH_3, ^{i}Pr, $^{3}J_{H-H}$ =6.4 Hz), 1.49 (s, 9H, CH_3, ^{t}Bu), 1.53 (s, 9H, CH_3, ^{t}Bu), 1.64 (s, 3H, CH_3), 1.76 (s, 3H, CH_3), 2.01 (s, 3H, CH_3), 2.07 (s, 3H, CH_3), 2.71-2.77 (m, 1H, CH, ^{i}Pr), 2.88 (d, 1H, CH_2, $^{2}J_{H-H}$ =16.4 Hz), 3.27 (dd, 1H, CH_2, $^{2}J_{H-H}$ =16.4 Hz, $^{3}J_{H-H}$ =4.8 Hz), 4.81 (b, 1H, CH-S), 4.92 (m, 1H, CH-OP), 6.89-7.12 (m, 3H, CH=), 7.19 (m, 2H, CH=), 7.35 (d, 1H, CH=, $^{3}J_{H-H}$ =8.8 Hz). ^{13}C NMR (100.6 MHz, C_6D_6): δ=16.3 (CH_3), 16.6 (CH_3), 20.0 (CH_3), 20.1 (CH_3), 23.3 (CH_3, ^{i}Pr), 24.2 (CH_3, ^{i}Pr), 31.3 (CH_3, ^{t}Bu), 31.4 (d, CH_3, ^{t}Bu, J_{C-P} =5.3 Hz), 34.6 (C, ^{t}Bu), 34.7 (C, ^{t}Bu), 34.8 (CH, ^{i}Pr), 39.3 (CH_2), 55.0 (CH-S), 82.9 (CH-OP), 124.9-146.4 (aromatic carbons). MS HR-ESI [found 613.2903, $C_{36}H_{47}O_3PS$ $(M-Na)^+$ requires 613.2876].

L1c. Yield: 202.0 mg (34%). ^{31}P NMR (161.9 MHz, C_6D_6): δ=139.4 (s). ^{1}H NMR (400 MHz, C_6D_6): δ=1.09 (d, 3H, CH_3, ^{i}Pr, $^{3}J_{H-H}$ =6.8 Hz), 1.12 (d, 3H, CH_3, ^{i}Pr, $^{3}J_{H-H}$ =6.8 Hz), 1.47 (s, 9H, CH_3, ^{t}Bu), 1.61 (s, 9H, CH_3, ^{t}Bu), 1.69 (s, 3H, CH_3), 1.75 (s, 3H, CH_3), 2.05 (s, 6H, CH_3), 2.85-2.91 (m, 1H, CH, ^{i}Pr), 3.37 (d, 1H, CH_2, $^{2}J_{H-H}$ =16.4 Hz), 3.38 (dd, 1H, CH_2, $^{2}J_{H-H}$ =16.8 Hz, $^{3}J_{H-H}$ =6.0 Hz), 4.24 (d, 1H, CH-S, $^{3}J_{H-H}$ =4.8 Hz), 5.07-5.11 (m, 1H, CH-OP), 6.95-7.03 (m, 3H, CH=), 7.18 (s, 1H, CH=), 7.23 (2H, CH=). ^{13}C NMR (100.6 MHz, C_6D_6): δ=16.3 (CH_3, ^{i}Pr), 16.5 (CH_3, ^{i}Pr), 20.1 (CH_3), 23.5 (CH_3), 23.9 (CH_3), 31.3 (CH_3, ^{t}Bu), 31.4 (d, CH_3, ^{t}Bu, J_{C-P} =5.3 Hz), 34.6 (C, ^{t}Bu), 34.8 (CH, ^{i}Pr), 39.7 (CH_2), 54.7 (CH-S), 82.7 (d, CH-OP, $^{2}J_{C-P}$ =6.1 Hz), 124.9-145.5 (aromatic carbons). MS HR-ESI [found 613.2869, $C_{36}H_{47}O_3PS$ $(M-Na)^+$ requires 613.2876].

L1g. Yield: 257.8 mg (61%). ^{31}P NMR (161.9 MHz, C_6D_6): δ=98.2 (s). ^{1}H NMR (400 MHz, C_6D_6): δ=1.08 (d, 3H, CH_3, ^{i}Pr, $^{3}J_{H-H}$=6.8 Hz), 1.21 (d, 3H, CH_3, ^{i}Pr, $^{3}J_{H-H}$=6.4 Hz), 2.37 (s, 3H, CH_3, *o*-Tol), 2.41 (s, 3H, CH_3, *o*-Tol), 2.91-3.01 (m, 2H, CH ^{i}Pr, CH_2), 3.30 (dd, 1H, CH_2, $^{2}J_{H-H}$=16.4 Hz, $^{3}J_{H-H}$=6.0 Hz), 4.49 (b, 1H, CH-S), 4.82 (m, 1H, CH-OP), 6.91-7.15 (m, 9H, CH=), 7.36 (d, 1H, CH=, $^{3}J_{H-H}$=6.8 Hz), 7.52 (m, 2H, CH=). ^{13}C NMR (100.6 MHz, C_6D_6): δ=20.3 (d, CH_3, *o*-Tol, $^{3}J_{C-P}$=4.0 Hz), 20.5 (d,CH_3, *o*-Tol, $^{3}J_{C-P}$=4.4 Hz), 23.2 (CH_3, ^{i}Pr), 23.8 (CH_3, ^{i}Pr), 35.3 (CH, ^{i}Pr), 39.1 (d, CH_2, $^{3}J_{C-P}$=6.1 Hz), 54.7 (d, CH-S, $^{3}J_{C-P}$=6.1 Hz), 87.7 (d, CH-OP, $^{2}J_{C-P}$=20,7 Hz), 124.8-141.4 (aromatic carbons).

L1h. Yield: 128.9 mg (61%). ^{31}P NMR (161.9 MHz, C_6D_6): δ=140.4 (s). ^{1}H NMR (400 MHz, C_6D_6): δ=1.08-1.20 (m, 6H, CH_2, Cy), 1.22 (d, 3H, CH_3, ^{i}Pr, $^{3}J_{H-H}$=6.4 Hz), 1.25-1.35 (m, 5H, CH_2, Cy), 1.38 (d, 3H, CH_3, ^{i}Pr, $^{3}J_{H-H}$=6.4 Hz), 1.48-1.61 (m, 5H, CH_2, Cy), 1.69 (b, 5H, CH, CH_2, Cy), 1.86 (m, 2H, CH_2, Cy), 2.98 (d, 1H, CH_2, $^{2}J_{H-H}$=16.0 Hz), 3.10-3.17 (m, 1H, CH ^{i}Pr), 3.41 (dd, 1H, CH_2, $^{2}J_{H-H}$=16.4 Hz, $^{3}J_{H-H}$=5.6 Hz), 4.51-4.54 (m, 2H, CH-S, CH-OP), 6.99-7.15 (m, 3H, CH=), 7.40 (d, 1H, CH=, $^{3}J_{H-H}$=8.0 Hz), 7.52 (m, 2H, CH=). ^{13}C NMR (100.6 MHz, C_6D_6): δ=23.3 (CH_3, ^{i}Pr), 24.0 (CH_3, ^{i}Pr), 26.5-27.1 (CH_2, Cy), 28.1 (CH_2, Cy), 28.3 (CH_2, Cy), 28.5 (CH_2, Cy), 35.2 (CH, ^{i}Pr), 37.6 (d, CH, $^{1}J_{C-P}$=8.5 Hz), 37.8 (d, CH, $^{1}J_{C-P}$=9.9 Hz), 39.3 (d, CH_2, $^{3}J_{C-P}$=6.1 Hz), 54.8 (d, CH-S, $^{3}J_{C-P}$=6.1 Hz), 87.7 (d, CH-OP, $^{2}J_{C-P}$=18.4 Hz), 124.8-141.5 (aromatic carbons).

L1i. Yield: 129.9 mg (54%). ^{31}P NMR (161.9 MHz, C_6D_6): δ=114.5 (s). ^{1}H NMR (400 MHz, C_6D_6): δ=1.11 (d, 3H, CH_3, ^{i}Pr, $^{3}J_{H-H}$=6.8 Hz), 1.22 (d, 3H, CH_3, ^{i}Pr, $^{3}J_{H-H}$=6.4 Hz), 2.04 (s, 3H, *p*-CH_3, Mes), 2.06 (s, 3H, *p*-CH_3, Mes), 2.39 (s, 12H, *o*-CH_3, Mes), 2.85-2.99 (m, 2H, CH ^{i}Pr, CH_2), 3.33 (dd, 1H, CH_2, $^{2}J_{H-H}$=16.4 Hz, $^{3}J_{H-H}$=5.6 Hz), 4.46 (b, 1H, CH-S), 4.66 (m, 1H, CH-OP), 6.63 (s, 1H, CH=), 6.64 (s, 1H, CH=), 6.65 (s, 1H, CH=), 6.66 (s, 1H, CH=), 6.94-7.05 (m, 2H, CH=), 7.12 (m, 1H, CH=), 7.31 (m, 1H, CH=). ^{13}C NMR (100.6 MHz, C_6D_6): δ=20.6 (*p*-CH_3, Mes), 22.1 (d, *o*-CH_3, Mes, $^{3}J_{C-P}$=3.0 Hz), 22.2 (d, *o*-CH_3, Mes, $^{3}J_{C-P}$=3.1 Hz), 23.2 (CH_3, ^{i}Pr), 23.9 (CH_3, ^{i}Pr), 35.2 (CH, ^{i}Pr), 38.9 (d, CH_2, $^{3}J_{C-P}$=6.8 Hz), 54.6 (d, CH-S, $^{3}J_{C-P}$=7.6 Hz), 87.6 (d, CH-OP, $^{2}J_{C-P}$=22,1 Hz), 124.7-141.6 (aromatic carbons).

L2b. Yield: 352.2 mg (59%). ^{31}P NMR (161.9 MHz, C_6D_6): δ=132.4 (s). ^{1}H NMR (400 MHz, C_6D_6): δ=0.82 (pt, 3H, CH_3, Pr, $^{3}J_{H-H}$=7.2 Hz), 1.41-1.53 (m, 2H, CH_2, Pr), 1.53 (s, 9H, CH_3, ^{t}Bu), 1.58 (s, 9H, CH_3, ^{t}Bu), 1.69 (s, 3H, CH_3), 1.80 (s, 3H, CH_3), 2.05 (s, 3H, CH_3), 2.09 (s, 3H, CH_3), 2.23-2.30 (m, 1H, CH_2, Pr), 2.44-2.50 (m, 2H, CH_2, Pr), 2.93 (d, 1H, CH_2, $^{2}J_{H-H}$=16.8 Hz), 3.25 (dd, 1H, CH_2, $^{2}J_{H-H}$=16.4 Hz, $^{3}J_{H-H}$=5.2 Hz), 4.72 (b, 1H, CH-S), 4.90-4.94 (m, 1H, CH-OP), 6.92 (d, 1H, CH=, $^{3}J_{H-H}$=6.4 Hz), 7.00-7.03 (m, 2H, CH=), 7.22 (d, 2H, CH=, $^{3}J_{H-H}$=8.0 Hz), 7.37 (d, 2H, CH=, $^{3}J_{H-H}$=6.8 Hz). ^{13}C NMR (100.6 MHz, C_6D_6): δ=13.2 (CH_3, Pr), 16.2 (CH_3), 16.5 (CH_3), 20.0 (CH_3), 20.1 (CH_3), 23.0 (CH_2, Pr), 31.3 (CH_3, ^{t}Bu, J_{C-P}=5.3 Hz), 31.4 (CH_3, ^{t}Bu), 33.1 (CH_2, Pr), 34.6 (C, ^{t}Bu), 34.7 (C, ^{t}Bu), 39.2 (d, CH_2, $^{3}J_{C-P}$=3.8 Hz), 56.1 (d, CH-S, $^{3}J_{C-P}$=3.0 Hz), 82.4 (CH-OP), 124.8-146.1 (aromatic carbons). MS HR-ESI [found 613.2903, $C_{36}H_{47}O_3PS$ $(M-Na)^+$ requires 613.2876].

L3b. Yield: 283.6 mg (47%). ^{31}P NMR (161.9 MHz, C_6D_6): δ=134.2 (s). ^{1}H NMR (400 MHz, C_6D_6): δ=1.34 (s, 9H, CH_3, ^{t}Bu), 1.48 (s, 9H, CH_3, ^{t}Bu), 1.58 (s, 9H, CH_3, ^{t}Bu), 1.69 (s, 3H, CH_3), 1.74 (s, 3H, CH_3), 2.05 (s, 3H, CH_3), 2.06 (s, 3H, CH_3), 2.71 (d, 1H, CH_2, $^{2}J_{H-H}$=16.0 Hz), 3.12 (dd, 1H, CH_2, $^{2}J_{H-H}$=16.4 Hz, $^{3}J_{H-H}$=5.2 Hz), 4.56 (b, 1H, CH-S), 5.22-5.25 (m, 1H, CH-OP), 6.83 (d, 1H, CH=, $^{3}J_{H-H}$=7.2 Hz), 6.96-7.21 (m, 1H, CH=), 7.41 (d, 1H, CH=, $^{3}J_{H-H}$

=7.6 Hz). ^{13}C NMR (100.6 MHz, C_6D_6): δ=16.3 (CH_3), 16.5 (CH_3), 20.0 (CH_3), 20.1 (CH_3), 31.4 (CH_3, ^{t}Bu), 34.6 (C, ^{t}Bu), 34.7 (C, ^{t}Bu), 38.8 (CH_2), 43.5 (C, ^{t}Bu), 54.0 (d, CH-S, $^3J_{C-P}$ =3.8 Hz), 83.7 (CH-OP), 124.7-145.7 (aromatic carbons). MS HR-ESI [found 627.3026, $C_{37}H_{49}O_3PS$ $(M-Na)^+$ requires 627.3032].

L3g. Yield: 147,6 mg (31%). ^{31}P NMR (161.9 MHz, C_6D_6): δ=97.7 (s). ^{1}H NMR (400 MHz, C_6D_6): δ=1.24 (s, 9H, CH_3, ^{t}Bu), 2.32 (s, 3H, CH_3, *o*-Tol), 2.41 (s, 3H, CH_3, *o*-Tol), 2.92 (dd, 1H, CH_2, $^2J_{H-H}$ =16.4 Hz, $^3J_{H-H}$ =2.8 Hz), 3.22 (dd, 1H, CH_2, $^2J_{H-H}$ =16.0 Hz, $^3J_{H-H}$ =5.2 Hz), 4.40 (b, 1H, CH-S), 4.82-4.85 (m, 1H, CH-OP), 6.89-7.12 (m, 9H, CH=), 7.39 (d, 1H, CH=, $^3J_{H-H}$ =7.2 Hz), 7.50-7.54 (m, 2H, CH=). ^{13}C NMR (100.6 MHz, C_6D_6): δ=20.2 (d, CH_3, $^3J_{C-P}$ =15.3 Hz), 20.4 (d, CH_3, $^3J_{C-P}$ =16.0 Hz), 31.3 (CH_3, ^{t}Bu), 39.0 (d, CH_2, $^3J_{C-P}$ =6.0 Hz), 43.4 (C, ^{t}Bu), 53.6 (d, CH-S, $^3J_{C-P}$ =6.8 Hz), 88.5 (d, CH-OP, $^3J_{C-P}$ =20.6 Hz), 124.6-142.3 (aromatic carbons). MS HR-ESI [found 457.1731, $C_{27}H_{31}OPS$ $(M-Na)^+$ requires 457.1725].

L4b. Yield: 284.8 mg (41%). ^{31}P NMR (161.9 MHz, C_6D_6): δ=135.3 (s). ^{1}H NMR (400 MHz, C_6D_6): δ=1.44 (s, 9H, CH_3, ^{t}Bu), 1.51 (s, 9H, CH_3, ^{t}Bu), 1.69 (s, 3H, CH_3), 1.77 (s, 3H, CH_3), 2.06 (s, 3H, CH_3), 2.07 (s, 3H, CH_3), 2.73 (d, 1H, CH_2, $^2J_{H-H}$ =16.8 Hz), 2.93 (dd, 1H, CH_2, $^2J_{H-H}$ =17.2 Hz, $^3J_{H-H}$ =5.6 Hz), 4.95 (b, 1H, CH-S), 5.03-5.06 (m, 1H, CH-OP), 6.80-6.82 (m, 1H, CH=), 6.90-7.01 (m, 5H, CH=), 7.21 (d, 2H, CH=, $^3J_{H-H}$ =3.6 Hz), 7.27-7,29 (m, 3H, CH=). ^{13}C NMR (100.6 MHz, C_6D_6): δ=16.2 (CH_3), 16.5 (CH_3), 20.0 (CH_3), 20.1 (CH_3), 31.3 (CH_3, ^{t}Bu), 31.4 (CH_3, ^{t}Bu), 34.5 (C, ^{t}Bu), 34.6 (C, ^{t}Bu), 39.2 (d, CH_2, $^3J_{C-P}$ =3.0 Hz), 58.8 (d, CH-S, $^3J_{C-P}$ =3.8 Hz), 81.6 (d, CH-OP, $^2J_{C-P}$ =4.6 Hz), 124.8-145.7 (aromatic carbons). MS HR-ESI [found 647.2737, $C_{39}H_{45}O_3PS$ $(M-Na)^+$ requires 647.2719].

L5b. Yield: 324.6 mg (42%). ^{31}P NMR (161.9 MHz, C_6D_6): δ=135.7 (s). ^{1}H NMR (400 MHz, C_6D_6): δ=1.42 (s, 9H, CH_3, ^{t}Bu), 1.52 (s, 9H, CH_3, ^{t}Bu), 1.68 (s, 3H, CH_3), 1.79 (s, 3H, CH_3), 2.04 (s, 3H, CH_3), 2.08 (s, 3H, CH_3), 2.31 (s, 6H, CH_3), 2.90 (d, 1H, CH_2, $^2J_{H-H}$ =16.8 Hz), 3.38 (dd, 1H, CH_2, $^2J_{H-H}$ =16.8 Hz, $^3J_{H-H}$ =4.8 Hz), 4.80-4.83 (m, 1H, CH-OP), 4.91 (s, 1H, CH-S), 6.67 (d, 1H, CH=, $^3J_{H-H}$ =7.2 Hz), 6.83 (pt, 1H, CH=, $^3J_{H-H}$ =7.2 Hz), 6.88-7.03 (m, 5H, CH=), 719 (d, 1H, CH=, $^4J_{H-H}$ =2.4 Hz). ^{13}C NMR (100.6 MHz, C_6D_6): δ=16.2 (CH_3), 16.5 (CH_3), 20.0 (CH_3), 20.1 (CH_3), 21.7 (CH_3), 31.2 (CH_3, ^{t}Bu), 31.3 (d, CH_3, ^{t}Bu, J_{C-P} =5.4 Hz), 34.5 (C, ^{t}Bu), 34.6 (C, ^{t}Bu), 39.3 (d, CH_2, $^3J_{C-P}$ =3.8 Hz), 58.0 (d, CH-S, $^3J_{C-P}$ =3.8 Hz), 81.3 (d, CH-OP, $^2J_{C-P}$ =4.6 Hz), 124.8-145.6 (aromatic carbons). MS HR-ESI [found 675.3026, $C_{41}H_{49}O_3PS$ $(M-Na)^+$ requires 675.3032].

L5c. Yield: 276.4 mg (36%). ^{31}P NMR (161.9 MHz, C_6D_6): δ=137.5 (s). ^{1}H NMR (400 MHz, C_6D_6): δ=1.44 (s, 9H, CH_3, ^{t}Bu), 1.56 (s, 9H, CH_3, ^{t}Bu), 1.69 (s, 3H, CH_3), 1.74 (s, 3H, CH_3), 2.05 (s, 3H, CH_3), 2.06 (s, 3H, CH_3), 2.25 (s, 6H, CH_3), 3.19 (d, 1H, CH_2, $^2J_{H-H}$ =16.8 Hz), 3.50 (dd, 1H, CH_2, $^2J_{H-H}$ =17.2 Hz, $^3J_{H-H}$ =4.8 Hz), 4.60 (b, 1H, CH-S), 4.93 (m, 1H, CH-OP), 6.46 (d, 1H, CH=, $^3J_{H-H}$ =7.2 Hz), 6.79 (m, 1H, CH=), 6.86-7.22 (m, 6H, CH=), 7.22 (s, 1H, CH=). ^{13}C NMR (100.6 MHz, C_6D_6): δ=16.2 (CH_3), 16.4 (CH_3), 20.0 (CH_3), 20.7 (CH_3), 31.3 (CH_3, ^{t}Bu), 34.5 (C, ^{t}Bu), 34.6 (C, ^{t}Bu), 40.2 (d, CH_2, $^3J_{C-P}$ =3.0 Hz), 57.5 (d, CH-S, $^3J_{C-P}$ =3.8 Hz), 81.0 (d, CH-OP, $^3J_{C-P}$ =7.6 Hz), 124.8-145.5 (aromatic carbons). MS HR-ESI [found 675.3041, $C_{41}H_{49}O_3PS$ $(M-Na)^+$ requires 675.3032].

L5g. Yield: 260.6 mg (54%). ^{31}P NMR (161.9 MHz, C_6D_6): δ=98.5 (s). ^{1}H NMR (400 MHz, C_6D_6): δ=2.30 (s, 3H, CH_3, *o*-Tol), 2.35 (s, 3H, CH_3, *o*-Tol), 2.44 (s, 6H, CH_3), 3.14 (d, 1H, CH_2, $^2J_{H-H}$ =16.8 Hz), 3.54 (dd, 1H, CH_2, $^2J_{H-H}$ =16.8 Hz, $^3J_{H-H}$ =5.2 Hz), 4.78-4.82 (m, 1H, CH-

OP), 4.83 (b, 1H, CH-S), 6.91-7.14 (m, 12H, CH=), 7.23 (s, 1H, CH=), 7.32-7.35 (m, 1H, CH=), 7.40-7.44 (m, 1H, CH=). ^{13}C NMR (100.6 MHz, C_6D_6): δ=20.1 (d, CH_3, $^3J_{C\text{-}P}$ =6.1 Hz), 20.3 (d, CH_3, $^3J_{C\text{-}P}$ =6.8 Hz), 21.7 (CH_3), 39.4 (d, CH_2, $^3J_{C\text{-}P}$ =6.9 Hz), 58.0 (d, CH-S, $^3J_{C\text{-}P}$ =6.9 Hz), 85.7 (d, CH-OP, $^3J_{C\text{-}P}$ =5.4 Hz), 124.9-143.5 (aromatic carbons).

L6b. Yield: 336.1 mg (52%). ^{31}P NMR (161.9 MHz, C_6D_6): δ=135.6 (s). ^{1}H NMR (400 MHz, C_6D_6): δ=1.41 (s, 9H, CH_3, ^{t}Bu), 1.47 (s, 9H, CH_3, ^{t}Bu), 1.69 (s, 3H, CH_3), 1.74 (s, 3H, CH_3), 2.05 (s, 3H, CH_3), 2.06 (s, 3H, CH_3), 2.67 (d, 1H, CH_2, $^2J_{H\text{-}H}$ =16.8 Hz), 2.99 (dd, 1H, CH_2, $^2J_{H\text{-}H}$ =16.8 Hz, $^3J_{H\text{-}H}$ =6.0 Hz), 4.92 (b, 1H, CH-S), 4.96-5.01 (m, 1H, CH-OP), 6.82-6.84 (m, 1H, CH=), 6.99-7.19 (m, 8H, CH=), 7.24-7.26 (m, 1H, CH=). ^{13}C NMR (100.6 MHz, C_6D_6): δ=16.9 (CH_3), 17.1 (CH_3), 20.6 (CH_3), 20.7 (CH_3), 31.9 (d, CH_3, ^{t}Bu, $^3J_{C\text{-}P}$ =5.3 Hz), 32.0 (CH_3, ^{t}Bu), 35.2 (C, ^{t}Bu), 35.3 (C, ^{t}Bu), 39.6 (CH_2), 58.3 (d, CH-S, $^3J_{C\text{-}P}$ =3.8 Hz), 81.7 (d, CH-OP, $^3J_{C\text{-}P}$ =4.6 Hz), 125.7-146.2 (aromatic carbons). MS HR-ESI [found 715.2610, $C_{40}H_{44}F_3O_3PS$ $(M\text{-}Na)^+$ requires 715.2593].

L7b. Yield: 321 mg (49%). ^{31}P NMR (161.9 MHz, C_6D_6): δ=135.4 (s). ^{1}H NMR (400 MHz, C_6D_6): δ=1.47 (s, 9H, CH_3, ^{t}Bu), 1.55 (s, 9H, CH_3, ^{t}Bu), 1.71 (s, 3H, CH_3), 1.82 (s, 3H, CH_3), 2.07 (s, 3H, CH_3), 2.10 (s, 3H, CH_3), 2.78 (d, 1H, CH_2, $^2J_{H\text{-}H}$ =16.8 Hz), 2.87 (dd, 1H, CH_2, $^2J_{H\text{-}H}$ =16.8 Hz, $^3J_{H\text{-}H}$ =5.6 Hz), 3.16 (s, CH_3, *p*-OMe) 4.88 (b, 1H, CH-S), 5.04-5.07 (m, 1H, CH-OP), 6.54 (d, 2H, CH=, $^3J_{H\text{-}H}$ =8.8 Hz), 6.82 (d, 1H, CH=, $^3J_{H\text{-}H}$ =6.8 Hz), 6.96-7.23 (m, 6H, CH=), 7.31 (d, 1H, CH=, $^3J_{H\text{-}H}$ =7.2 Hz). ^{13}C NMR (100.6 MHz, C_6D_6): δ=16.7 (CH_3), 16.9 (CH_3), 20.4 (CH_3), 20.5 (CH_3), 31.7 (CH_3, ^{t}Bu), 31.8 (CH_3, ^{t}Bu), 35.0 (C, ^{t}Bu), 35.1 (C,^{t}Bu), 39.9 (CH_2), 54.8 (CH_3, *p*-MeO), 60.5 (d, CH-S, $^3J_{C\text{-}P}$ =3.8 Hz), 82.4 (d, CH-OP, $^3J_{C\text{-}P}$ =4.6 Hz), 114.7-160.4 (aromatic carbons). MS HR-ESI [found 677.2851, $C_{40}H_{47}O_4PS$ $(M\text{-}Na)^+$ requires 677.2825].

L8b. Yield: 94.3 mg (27%). ^{31}P NMR (161.9 MHz, C_6D_6): δ=136.1 (s). ^{1}H NMR (400 MHz, C_6D_6): δ=1.28 (s, 9H, CH_3, ^{t}Bu), 1.39 (s, 9H, CH_3, ^{t}Bu), 1.65 (s, 3H, CH_3), 1.79 (s, 3H, CH_3), 2.02 (s, 3H, CH_3), 2.03 (s, 3H, CH_3), 2.91 (d, 1H, CH_2, $^2J_{H\text{-}H}$ =16.8 Hz), 3.45 (dd, 1H, CH_2, $^2J_{H\text{-}H}$ =16.8 Hz, $^3J_{H\text{-}H}$ =5.2 Hz), 4.92-4.95 (m, 1H, CH-OP), 5.22 (b, 1H, CH-S), 6.55-6.63 (m, 2H, CH=), 6.90 (s, 2H, CH=), 7.11-7.28 (m, 6H, CH=), 7.73 (d, 2 H, CH=, $^3J_{H\text{-}H}$ =8,0 Hz), 8.16 (s, 1, CH=), 8.96 (d, 2 H, CH=, $^3J_{H\text{-}H}$ =8,4 Hz). ^{13}C NMR (100.6 MHz, C_6D_6): δ=16.2 (CH_3), 16.6 (CH_3), 20.0 (CH_3), 20.1 (CH_3), 31.1 (CH_3, ^{t}Bu), 31.3 (d, CH_3, ^{t}Bu, $J_{C\text{-}P}$ =5.4 Hz), 34.4 (C, ^{t}Bu), 39.7 (CH_2), 60.1 (CH-S), 81.4 (CH-OP), 124.8-145.7 (aromatic carbons). MS HR-ESI [found 747.3048, $C_{47}H_{49}O_3PS$ $(M\text{-}Na)^+$ requires 747.3028].

L8c. Yield: 102 mg (29%). ^{31}P NMR (161.9 MHz, C_6D_6): δ=134.7 (s). ^{1}H NMR (400 MHz, C_6D_6): δ=1.33 (s, 9H, CH_3, ^{t}Bu), 1.45 (s, 9H, CH_3, ^{t}Bu), 1.66 (s, 3H, CH_3), 1.84 (s, 3H, CH_3), 2.01 (s, 3H, CH_3), 2.07 (s, 3H, CH_3), 2.94 (d, 1H, CH_2, $^2J_{H\text{-}H}$ =16.2 Hz), 3.54 (dd, 1H, CH_2, $^2J_{H\text{-}H}$ =16.2 Hz, $^3J_{H\text{-}H}$ =6.2 Hz), 5.02 (m, 1H, CH-OP), 5.27 (b, 1H, CH-S), 6.64 (m, 2H, CH=), 6.95 (s, 2H, CH=), 7.11-7.27 (m, 6H, CH=), 7.72 (d, 2 H, CH=, $^3J_{H\text{-}H}$ =7.6 Hz), 8.04 (s, 1, CH=), 8.92 (d, 2 H, CH=, $^3J_{H\text{-}H}$ =8.0 Hz). ^{13}C NMR (100.6 MHz, C_6D_6): δ=16.4 (CH_3), 16.5 (CH_3), 20.2 (CH_3), 20.7 (CH_3), 31.4 (CH_3, ^{t}Bu), 31.7 (CH_3, ^{t}Bu), 34.6 (C, ^{t}Bu), 34.8 (C, ^{t}Bu), 40.1 (CH_2), 58.4 (CH-S), 81.4 (CH-OP), 125.2-146.9 (aromatic carbons). MS HR-ESI [found 747.3032, $C_{47}H_{49}O_3PS$ $(M\text{-}Na)^+$ requires 747.3028].

3.4.6. Typical procedure for the allylic alkylation of disubstituted linear (S1, S3-S7) and cyclic (S2, S8-S9) substrates

A degassed solution of $[PdCl(\eta^3\text{-}C_3H_5)]_2$ (0.9 mg, 0.0025 mmol) and the corresponding phosphite/phosphinite-thioether ligand (0.0055 mmol) in dichloromethane (0.5 ml) was stirred for 30 min. Subsequently, a solution of the corresponding substrate (0.5 mmol) in dichloromethane (1.5 ml), nucleophile (1.5 mmol), *N*,*O*-bis(trimethylsilyl)-acetamide (370 ml, 1.5 mmol) and KOAc (3mg, 003 mmol) was added. The reaction mixture was stirred at room temperature. After the desired reaction time the reaction mixture was diluted with Et_2O (5 ml) and saturated NH_4Cl (aq) (25 ml) was added. The mixture was extracted with Et_2O (3 x 10 ml) and the extract dried over $MgSO_4$.

3.4.7. Typical procedure for the allylic alkylation of disubstituted linear substrate S1 using pyrroles

A degassed solution of $[PdCl(\eta^3\text{-}C_3H_5)]_2$ (1.8 mg, 0.005 mmol) and the corresponding phosphite/phosphinite–thioether (0.011 mmol) in dichloromethane (0.5 ml) was stirred for 30 min. Subsequently, a solution of the corresponding substrate (0.5 mmol) in dichloromethane (1.5 ml), the corresponding pyrrole (0.4 mmol), and K_2CO_3 (110 mg, 0.8 mmol) were added. The reaction mixture was stirred at room temperature. After 18 h, the reaction mixture was diluted with Et_2O (5 ml), and saturated NH_4Cl (aq) (25 ml) was added. The mixture was extracted with Et_2O (3 × 10 ml) and the extract dried over $MgSO_4$.

3.4.8. Typical procedure for the allylic etherification and silylation of disubstituted linear substrate S1

A degassed solution of $[PdCl(\eta^3\text{-}C_3H_5)]_2$ (0.9 mg, 0.0025 mmol) and the corresponding ligand (0.0055 mmol) in dichloromethane (0.5 ml) was stirred for 30 min. Subsequently, a solution of *rac*-1,3-diphenyl-3-acetoxyprop-1-ene (**S1**) (31.5 mg, 0.125 mmol) in dichloromethane (1.5 ml) was added. After 10 min, Cs_2CO_3 (122 mg, 0.375 mmol) and the corresponding alcohol or silanol (0.375 mmol) were added. The reaction mixture was stirred at room temperature. After 18 h, the reaction mixture was diluted with Et_2O (5 ml), and saturated NH_4Cl (aq) (25 ml) was added. The mixture was extracted with Et_2O (3 × 10 ml) and the extract dried over $MgSO_4$.

3.4.9. Characterization details and methods for *ee* determination of the substitution products 11-52

Dimethyl 2-(1,3-diphenylallyl)malonate (11).[24] Enantiomeric excess determined by HPLC using Chiralcel OJ-H column (87% hexane/2-propanol, flow 0.5 ml/min, λ= 254 nm). t_R 32.8 min (*R*); t_R 38.6 min (*S*). ^{1}H NMR (400 MHz, $CDCl_3$), δ: 3.52 (s, 3H, CH_3), 3.70 (s, 3H, CH_3), 3.95 (d, 1H, CH, *J*=10.9 Hz), 4.26 (m, 1H, CH), 6.34 (dd, 1H, CH=, *J*=16.0 Hz, *J*=8.4 Hz), 6.48 (d, 1H, CH=, *J*=16.0 Hz), 7.1-7.4 (m, 10H, CH=).

Dimethyl 2-(1,3-cyclohexanylallyl)malonate (12).[25] Enantiomeric excess determined by GC using Chiralsil-Dex CB column (77 kPa H_2, Isotherm at 110 ºC). t_R 20.1 min (*S*); t_R 20.5 min (*R*). ^{1}H NMR (400 MHz, $CDCl_3$), δ: 1.36 (m, 1H, CH_2), 1.56 (m, 1H, CH_2), 1.70 (m, 1H, CH_2), 1.76 (m, 1H, CH_2), 1.99 (m, 2H, CH_2), 3.29 (d, 1H, CH, *J*=9.6 Hz), 3.73 (s, 3H, CH_3), 3.74 (s, 3H, CH_3), 5.22 (m, 1H, CH=), 5.79 (m, 1H, CH=).

Diethyl 2-(1,3-diphenylallyl)malonate (13).[26] Enantiomeric excess determined by HPLC using Chiralcel OJ-H column (87% hexane/2-propanol, flow 0.5 ml/min, λ= 254 nm). t_R 17.6 min (*S*); t_R 20.1 min (*R*). ^{1}H NMR (400 MHz, $CDCl_3$), δ: 1.01 (t, 6H, CH_3, *J*=6.8 Hz), 3.92 (d, 1H, CH, *J*=11.2 Hz), 4.19 (q, 4H, CH_2, *J*=7.2 Hz), 4.23 (m, 1H, CH), 6.34 (dd, 1H, CH=, *J*=20 Hz, *J*=10 Hz), 6.41 (d, 1H, CH=, *J*=18 Hz), 7.1-7.4 (m, 10H, CH=).

Dibenzyl 2-(1,3-diphenylallyl)malonate (14).[26] Enantiomeric excess determined by HPLC using Chiralcel OJ-H column (95% hexane/2-propanol, flow 1 ml/min, λ= 254 nm). t_R 94.0 min (*R*); t_R 107.4 min (*S*). ^{1}H NMR (400 MHz, $CDCl_3$), δ: 4.03 (d, 1H, CH, *J*=9.6 Hz), 4.29 (t, 1H, CH, *J*=10 Hz), 4.92 (s, 2H, CH_2), 5.09 (s, 2H, CH_2), 6.28 (dd, 1H, CH=, *J*=15.6 Hz, *J*=8.4 Hz), 6.40 (d, 1H, CH=, *J*=17 Hz), 7.0-7.4 (m, 20H, CH=).

Dimethyl 2-(1,3-diphenylallyl)-2-methylmalonate (15).[25] Enantiomeric excess determined by HPLC using Chiralcel OD-H column (90% hexane/2-propanol, flow 1 ml/min, λ= 254 nm). t_R 9.9 min (*S*); t_R 12.5 min (*R*). ^{1}H NMR (400 MHz, $CDCl_3$), δ: 1.48 (s, 3H, CH_3), 3.62 (s, 3H, CH_3), 3.71 (s, 3H, CH_3), 4.29 (d, 1H, CH, *J*=8.8 Hz), 6.46 (d, 1H, CH=, *J*=16.0 Hz), 6.68 (dd, 1H, CH=, *J*=16.0 Hz, *J*=8.8 Hz), 7.1-7.4 (m, 10H, CH=).

Dimethyl 2-allyl-2-(1,3-diphenylallyl)malonate (16).[27] Enantiomeric excess determined by HPLC using Chiralcel OJ-H column (87% hexane/2-propanol, flow 0.5 ml/min, λ= 254 nm). t_R 19.4 min (*R*); t_R 26.1 min (*S*). ^{1}H NMR (400 MHz, $CDCl_3$), δ: 2.48 (dd, 1H, CH_2, *J*=14Hz, *J*=8.8 Hz), 2.67 (dd, 1H, CH_2, *J*=14 Hz, *J*=8.0 Hz), 3.66 (s, 3H, CH_3), 3.75 (s, 3H, CH_3), 4.20 (d, 1H, CH, *J*=8.8 Hz), 5.06 (m, 2H, CH_2=), 5.77 (m, 1H, CH=), 6.40 (d, 1H, CH=, *J*=15.6 Hz), 6.77 (dd, 1H, CH=, *J*=16.4 Hz, *J*=8.4 Hz), 7.2-7.4 (m, 10H, CH=).

Diethyl 2-(but-3-en-1-yl)-2-(1,3-diphenylallyl)malonate (17).[4e] Enantiomeric excess determined by HPLC using Chiralcel OJ-H column (87% hexane/2-propanol, flow 0.15 ml/min, λ= 254 nm). t_R 29.9 min (*S*); t_R 34.2 min (*R*). ^{1}H NMR (400 MHz, $CDCl_3$), δ: 1.22 (m, 6H, CH_3), 1.97 (m, 2H, CH_2), 2.08 (m, 2H, CH_2), 3.98 (m, 2H, CH_2), 4.17 (m, 3H, CH_2), 4.89 (m, 2H, CH_2=), 5.68 (m, 1H, CH=), 6.32 (d, 1H, CH=, *J*=16.0 Hz), 6.76 (dd, 1H, CH=, *J*=16.0 Hz, *J*=9.2 Hz), 7.1- 7.4 (m, 10H, CH=).

Diethyl 2-(1,3-diphenylallyl)-2-(pent-4-en-1-yl)malonate (18).[4e] Enantiomeric excess determined by HPLC using Chiralcel IA column (99% hexane/2-propanol, flow 0.5 ml/min, λ= 254 nm). t_R 12.3 min (*S*); t_R 14.4 min (*R*). ^{1}H NMR (400 MHz, $CDCl_3$), δ: 1.20 (t, 3H, CH_3, *J*=6.4 Hz), 1.26 (t, 3H, CH_3, *J*=6.4 Hz), 1.31 (m, 1H, CH_2), 1.45 (m, 1H, CH_2), 1.74 (m, 1H, CH_2), 1.86 (m, 1H, CH_2), 1.96 (m, 2H, CH_2), 4.18 (m, 5H, CH_2-O, CH), 4.94 (m,

2H, CH_2=), 5.72 (m, 1H, CH=), 6.36 (d, 1H, CH=, *J*=15.6 Hz), 6.78 (dd, 1H, CH=, *J*=15.6 Hz, *J*=8.8 Hz), 7.1-7.4 (m, 10H, CH=).

Dimethyl 2-(1,3-diphenylallyl)-2-(prop-2-yn-1-yl)malonate (19).[4e] Enantiomeric excess determined by HPLC using Chiralcel OJ-H column (90% hexane/2-propanol, flow 0.5 ml/min, λ= 254 nm). t_R 19.5 min (*S*); t_R 41.7 min (*R*). ^{1}H NMR (400 MHz, $CDCl_3$), δ: 2.13 (m, 1H, CH), 2.64 (dd, 1H, CH_2, *J*=17.2 Hz, *J*=2.4 Hz), 2.82 (dd, 1H, CH_2, *J*=14.2 Hz, *J*=2.8 Hz), 3.71 (s, 3H, CH_3), 3.78 (s, 3H, CH_3), 4.45 (d, 1H, CH, *J*=8.4 Hz), 6.46 (d, 1H, d, CH=, *J*=15.6 Hz,), 6.79 (t, 1H, CH=, *J*=8.4 Hz), 7.31 (m, 10H, CH=).

(1,3-Diphenylallyl)pentane-2,4-dienone (20).[27] Enantiomeric excess determined by HPLC using Chiralcel OJ-H column (98% hexane/2-propanol, flow 1 ml/min, λ= 254 nm). t_R 53.1 min (*S*); t_R 56.9 min (*R*). ^{1}H NMR (400 MHz, $CDCl_3$), δ: 1.93 (s, 3H, CH_3), 2.25 (s, 3H, CH_3), 4.34 (m, 2H, CH), 6.20 (dm, 1H, CH=, *J*=15.6 Hz), 6.44 (d, 1H, CH=, *J*=15.6 Hz), 7.1-7.4 (m, 10H, CH=).

2-(1,3-Diphenylallyl)malononitrile (21).[18b] Enantiomeric excess determined by HPLC using Chiralcel OJ-H column (70% hexane/2-propanol, flow 1 ml/min). t_R 18.2 min (*R*); t_R 19.4 min (*S*). ^{1}H NMR (400 MHz, $CDCl_3$), δ: 4.07 (m, 2H, CH), 6.47 (dd, 1H, CH=, *J*=15.6 Hz, *J*=8.0 Hz), 6.70 (d, 1H, CH=, *J*=15.6 Hz), 7.2-7.5 (m, 10H, CH=)

Isopropyl 2-cyano-3,5-diphenylpent-4-enoate (22).[28] Enantiomeric excess determined by HPLC using Chiralcel IC column (99% hexane/2-propanol, flow 0.5 ml/min). Major diastereoisomer, t_R 51.0 (*major*) and t_R 53.1 min (*minor*). Minor diastereoisomer, t_R 58.2 (*minor*) and t_R 79.7 min (*major*). ^{1}H NMR (400 MHz, $CDCl_3$), δ: 1.14 (m, 6H, CH_3), 3.86 (dd, 1H, CH, *J*=13.6 Hz, *J*=8.0 Hz), 4.20 (m, 1H, CH), 4.98 (m, 1H, CH), 6.46 (m, 1H, CH=), 6.58 (dd, 1H, CH=, *J*=11.6 Hz, *J*=16.0 Hz), 7.25 (m, 1H, CH=), 7.32 (m, 3H, CH=), 7.53 (m, 6H, CH=).

2-(1,3-Diphenyl-2-propenyl)-5-ethylpyrrole (23).[20] Enantiometic excess determined by HPLC using Chiralpak AD-H column (99% hexane/2-propanol, flow 0.7 ml/min, λ= 254 nm) t_R 12.1 min; t_R 12.9 min. ^{1}H NMR (400 MHz, $CDCl_3$), δ: 1.19 (t, 3H, CH_3, *J*=7.6 Hz), 2.55 (q, 2H, CH_2, *J*=7.6 Hz), 4.81 (d, 1H, CH=, *J*=7.6 Hz), 5.84 (m, 2H, CH=), 6.42 (d, 1H, CH=, *J*=15.6 Hz), 6.58 (dd, 1H, CH=, *J*=15.6 Hz, *J*=7.6 Hz), 7.37−7.18 (m, 10H, CH=), 7.53 (brs, 1H, NH).

3,5-Dimethyl-2-(1,3-diphenyl-2-propenyl)pyrrole (24).[27] Enantiometic excess determined by HPLC using Chiralpak AD-H column (99,5% hexane/2-propanol, flow 0.7 ml/min, λ= 254 nm) t_R 17.8 min; t_R 19.7 min. ^{1}H NMR (400 MHz, $CDCl_3$) δ: 1.96 (s, 3H, CH_3), 2.16 (s, 3H, CH_3), 4.94 (d, 1H, CH=, *J*=6.8 Hz), 5.73 (m, 1H, CH=), 6.31 (d, 1H, CH=, *J*=15.6 Hz), 6.56 (dd, 1H, CH=, *J*=15.6 Hz, *J*= 6.8 Hz), 7.37−7.18 (m, 11H, CH=).

***N*-Benzyl-1,3-diphenylprop-2-en-1-amine (25)**.[29] Enantiomeric excess determined by HPLC using Chiralcel OD-H column (99% hexane/2-propanol, flow 0.5 ml/min, λ= 254 nm). t_R 22.4 min (*R*); t_R 26.2 min (*S*). ^{1}H NMR (400 MHz, $CDCl_3$), δ: 3.77 (d, 1H, NH, *J*=13.2 Hz), 3.80 (d, 1H, CH, *J*=13.2 Hz), 4.41 (m, 2H, CH_2), 6.34 (dd, 1H, CH=, *J*=16.0 Hz, *J*=7.2 Hz), 6.57 (d, 1H, CH=, *J*= 16.0 Hz), 7.1-7.4 (m, 15H, CH=).

***N*-(4-Methoxybenzyl)-1,3-diphenylprop-2-en-1-amine (26)**.[30] Enantiomeric excess determined by HPLC using Chiralcel OD-H column (95% hexane/2-propanol, flow 0.5 ml/min, λ= 254 nm). t_R 19.5 min (*R*); t_R 28.3 min (*S*). ^{1}H-NMR (400 MHz, $CDCl_3$) δ: 3.73

(dd, 2H, *J*=16.9 Hz, *J*=13.2 Hz), 3.81 (s, 3H), 4.39 (d, 1H, *J*=7.2 Hz), 6.36 (dd, 1H, *J* = 15.8, *J*=7.2 Hz), 6.58 (d, 1H, *J*=15.8 Hz), 6.88 (m, 2H), 7.18-7.32 (m, 6H), 7.35 (m, 4H), 7.44 (m, 2H).

1,3-Diphenyl-*N*-(4-(trifluoromethyl)benzyl)prop-2-en-1-amine (27).[30] Enantiomeric excess determined by HPLC using Chiralcel OD-H column (95% hexane/2-propanol, flow 0.5 ml/min, λ= 254 nm). t_R 15.9 min (*R*); t_R 18.0 min (*S*). ^{1}H-NMR (400 MHz, $CDCl_3$) δ: 3.86 (dd, 2H, *J*=17.6 Hz, *J*=14.2 Hz), 4.39 (d, 1H, *J*=7.6 Hz), 6.33 (dd, 1H, *J*=15.9 Hz, *J*=7.6 Hz), 6.59 (d, 1H, *J*=15.9 Hz), 7.23 (m, 1H), 7.27-7.34 (m, 3H), 7.35-7.41 (m, 4H), 7.41-7.51 (m, 4H), 7.57-7-63 (m, 2H). ^{19}F-NMR (375 MHz, $CDCl_3$) δ -62.3 (s, 3F, CF_3).

***N*-(Furan-2-ylmethyl)-1,3-diphenylprop-2-en-1-amine (28)**.[30] Enantiomeric excess determined by HPLC using Chiralcel OJ-H column (95% hexane/2-propanol, flow 0.5 ml/min, λ= 254 nm). t_R 24.9 min (*S*); t_R 39.8 min (*R*). ^{1}H-NMR (400 MHz, $CDCl_3$) δ: 3.79 (s, 2H), 4.39 (d, 1H, *J*=7.6 Hz), 6.17 (dd, 1H, *J*=3.1 Hz, *J*=0.8 Hz), 6.30 (d, 1H, *J*=7.6 Hz), 6.34 (m, 1H), 6.59 (d, 1H, *J*=15.6 Hz), 7.19-7.45 (m, 11H).

4-(1,3-Diphenylallyl)morpholine (29).[30] Enantiomeric excess determined by HPLC using Chiralcel OJ-H column (87% hexane/2-propanol, flow 0.7 ml/min, λ= 254 nm). t_R 10.2 min (*R*); t_R 12.9 min (*S*). ^{1}H-NMR (400 MHz, $CDCl_3$) δ: 2.35-2.46 (m, 2H), 2.49-2.63 (m, 2H), 3.72 (t, 4H, *J*=5.2 Hz), 3.80 (d, 1H, *J*=9.1 Hz), 6.29 (dd, 1H, *J*=15.8 Hz, *J*=9.1 Hz), 6.58 (d, 1H, *J*=15.8 Hz), 7.19-7.38 (m, 8H), 7.43 (m, 2H).

***N*-Allyl-1,3-diphenylprop-2-en-1-amine (30)**.[30] Enantiomeric excess determined by HPLC using Chiralcel OD-H column (99% hexane/2-propanol, flow 1 ml/min, λ= 254 nm). t_R 6.5 min (*S*); t_R 7.1 min (*R*). ^{1}H-NMR (400 MHz, $CDCl_3$) δ: 3.19-3.36 (m, 2H), 4.43 (d, 1H, *J*=7.5 Hz), 5.12-5.17 (m, 1H), 5.18-5.25 (m, 1H), 5.96 (ddt, 1H, *J*=17.1 Hz, *J*=10.2 Hz, *J*=6.0 Hz, 1H), 6.32 (dd, 1H, *J*=15.8 Hz, *J*=7.5 Hz), 6.60 (d, 1H, *J*=15.8 Hz), 7.16-7.50 (m, 10H).

3-Diphenyl-3-(benzyloxy)-1-propene (31).[31] Enantiomeric excess determined by HPLC using Chiralcel OJ-H column (98% hexane/2-propanol, flow 0.75 ml/min, λ= 254 nm). t_R 18.2 min (*S*); t_R 21.5 min (*R*). ^{1}H NMR (400 MHz, $CDCl_3$), δ: 4.64 (m, 2H, CH_2), 5.08 (d, 1H, CH, *J*=6.8 Hz), 6.41 (dd, 1H, CH=, *J*=16.0 Hz, *J*=7.2 Hz), 6.68 (d, 1H, CH=, *J*=16.0 Hz), 7.1-7.5 (m, 15H, CH=).

1,3-Diphenyl-3-(4-methylbenzyloxy)-1-propene (32).[18a] Enantiomeric excess determined by HPLC using Chiralcel OJ-H column (98% hexane/2-propan.ol, flow 0.75 ml/min, λ= 254 nm). t_R 16.8 min (*+*); t_R 24.1 min (-). ^{1}H NMR (400 MHz, $CDCl_3$), δ: 2.44 (s, 3H, CH_3), 4.63 (m, 2H, CH_2), 5.08 (d, 1H, CH, *J*=7.2 Hz), 6.43 (dd, 1H, CH=, *J*=16.4 Hz, *J*=7.6 Hz), 6.70 (d, 1H, CH=, *J*=16.0 Hz), 7.1-7.5 (m, 14H, CH=).

1,3-Diphenyl-3-(4-trifluoromethylbenzyloxy)-1-propene (33).[18a] Enantiomeric excess determined by HPLC using Chiralcel OJ-H column (96% hexane/2-propanol, flow 0.75 ml/min, λ= 254 nm). t_R 20.8 min (*+*); t_R 25.2 min (-). ^{1}H NMR (400 MHz, $CDCl_3$), δ: 4.67 (m, 2H, CH_2), 5.06 (d, 1H, CH, *J*=7.6 Hz), 6.39 (dd, 1H, CH=, *J*=16.4 Hz, *J*=7.2 Hz), 6.70 (d, 1H, CH=, *J*=16.0 Hz), 7.1- 7.7 (m, 14H, CH=).

1,3-Diphenyl-3-(3-methylbenzyloxy)-1-propene (34).[18a] Enantiomeric excess determined by HPLC using Chiralcel OJ-H column (96% hexane/2-propanol, flow 0.75 ml/min, λ= 254 nm). t_R 17.8 min (*+*); t_R 22.6 min (-). ^{1}H NMR (400 MHz, $CDCl_3$), δ: 2.44 (s,

3H, CH_3), 4.62 (m, 2H, CH_2), 5.09 (d, 1H, CH, *J*=7.2 Hz), 6.42 (dd, 1H, CH=, *J*=16.4 Hz, *J*=7.2 Hz), 6.71 (d, 1H, CH=, *J*=16.0 Hz), 7.2-7.5 (m, 14H, CH=).

1,3-Diphenyl-(*E*)-3-(allyloxy)-1-propene (35).[18a] Enantiomeric excess determined by HPLC using Chiralcel OD-H column (99.75% hexane/2-propanol, flow 0.25 ml/min, λ= 254 nm). t_R 35.2 min (*+*); t_R 38.7 min (-). ^{1}H NMR (400 MHz, $CDCl_3$), δ: 4.04 (m, 2H, CH_2), 5.01 (d, 1H, CH, *J*=6.8 Hz), 5.22 (d, 1H, CH_2=, *J*=10.4 Hz), 5.34 (dd, 1H, CH_2=, *J*=17.2 Hz, *J*=2.0 Hz), 6.01 (m, 1H, CH=), 6.33 (dd, 1H, CH=, *J*=16.0 Hz, *J*=7.2 Hz), 6.65 (d, 1H, CH=, *J*=16.4 Hz), 7.2-7.5 (m, 10H, CH=).

((1,3-Diphenylallyl)oxy)triphenylsilane (36).[32] Enantiomeric excess determined by HPLC using Chiralcel OD-H column after desilylation using TBAF (87% hexane/2-propanol, flow 0.5 ml/min, λ= 254 nm). t_R 20.4 min (*S*); t_R 28.1 min (*R*). ^{1}H NMR (400 MHz, $CDCl_3$), δ: 5.54 (d, 1H, CH, *J*=6.4 Hz), 6.32 (dd, 1H, CH=, *J*=16.0 Hz, *J*=6.4 Hz), 6.43 (d, 1H, CH=, *J*=16.0 Hz), 7.3-7.7 (m, 25H, CH=).

Dimethyl 2-(1,3-di-p-tolylallyl)malonate (37).[33] Enantiomeric excess determined by HPLC using Chiralcel OD-H column (95% hexane/2-propanol, flow 0.5 ml/min, λ= 254 nm). t_R 12.4 min (*S*); t_R 13.3 min (*R*). ^{1}H NMR (400 MHz, $CDCl_3$), δ: 2.32 (s, 6H, CH_3), 3.52 (s, 3H, CH_3), 3.68 (s, 3H, CH_3), 3.92 (d, 1H, CH, *J*= 6.2 Hz), 4.21 (m, 1H, CH), 6.14 (dd, 1H, CH=, *J*=16.4 Hz, *J*=10.0 Hz), 6.43 (d, 1H, CH=, *J*=16.4 Hz), 7.10-7.30 (m, 8H, CH=).

Dimethyl 2-allyl-2-(1,3-di-p-tolylallyl)malonate (38).[34] Enantiomeric excess determined by HPLC using Chiralcel IA column (98% hexane/2-propanol, flow 0.2 ml/min, λ= 254 nm). t_R 40.8 min (*S*); t_R 44.0 min (*R*). ^{1}H NMR (400 MHz, $CDCl_3$), δ: 2.47 (s, 6H, CH_3), 2.64 (dd, 1H, CH_2, *J*=14.4 Hz, *J*=8.4 Hz), 2.80 (dd, 1H, CH_2, *J*=14.4 Hz, *J*=6.4 Hz), 3.81 (s, 3H, CH_3), 3.91 (s, 3H, CH_3), 4.09 (m, 1H), 5.19 (m, 2H, CH_2=), 5.94 (m, 1H, CH=), 6.50 (d, 1H, CH=, *J*=15.6 Hz), 6.84 (dd, 1H, CH=, *J*=15.6 Hz, *J*=8.8 Hz), 7.25 (m, 6H, CH=), 7.40 (d, 2H, *J*=8.0 Hz).

Dimethyl 2-(1,3-di-p-bromophenylallyl)malonate (39).[31] Enantiomeric excess determined by HPLC using Chiralcel OJ-H column (87% hexane/2-propanol, flow 0.5 ml/min, λ= 254 nm). t_R 34.4 min (*R*); t_R 49.8 min (*S*). ^{1}H NMR (400 MHz, $CDCl_3$), δ: 3.54 (s, 3H, CH_3), 3.75 (s, 3H, CH_3), 3.92 (m, 1H, CH), 4.23 (m, 1H, CH), 6.30 (dd, 1H, CH=, *J*=15.6 Hz, *J*=8.4 Hz), 6.44 (d, 1H, CH=, *J*=15.6 Hz), 7.10-7.48 (m, 8H, CH=).

Dimethyl 2-(1,3-di-*m*-methoxyphenylallyl)malonate (40).[31] Enantiomeric excess determined by HPLC using Chiralcel OJ-H column (87% hexane/2-propanol, flow 0.5 ml/min, λ= 254 nm). t_R 29.9 min (R); t_R 40.5 min (S). ^{1}H NMR (400 MHz, $CDCl_3$), δ: 2.29 (s, 3H, CH_3), 2.45 (s, 3H, CH_3), 3.53 (s, 3H, CH_3), 3.74 (s, 3H, CH_3), 4.08 (d, 1H, CH, *J*=11.6 Hz), 4.58 (m, 1H, CH), 6.03 (dd, 1H, CH=, *J*=15.6 Hz, *J*=8.4 Hz), 6.68 (d, 1H, CH=, *J*=15.6 Hz), 7.10-7.35 (m, 8H, CH=).

Dimethyl 2-(1,3-di-*o*-tolylallyl)malonate (41).[31] Enantiomeric excess determined by HPLC using Chiralcel OJ-H column (87% hexane/2-propanol, flow 0.5 ml/min, λ= 254 nm). t_R 13.2 min (*R*); t_R 18.8 min (*S*). ^{1}H NMR (400 MHz, $CDCl_3$), δ: 3.54 (s, 3H, CH_3), 3.70 (s, 3H, CH_3), 3.78 (s, 3H, CH_3), 3.79 (s, 3H, CH_3), 3.96 (d, 1H, CH, *J*=10.8 Hz), 4.24 (m, 1H, CH), 6.31 (dd, 1H, CH=, *J*=16.0 Hz, *J*=8.8 Hz), 6.48 (d, 1H, CH=, *J*=16.0 Hz), 6.76 (m, 2H, CH=), 6.85 (m, 2H, CH=), 6.90 (m, 2H, CH=), 7.23 (m, 2H, CH=).

Dimethyl 2-(1,3-diisopropylallyl)malonate (42).[5a] Enantiomeric excess determined by ^{1}H NMR using [Eu(hfc)$_3$] in C_6D_6. ^{1}H NMR (400 MHz, $CDCl_3$), δ: 0.81 (d, 3H, CH_3, *J*=6.8 Hz), 0.87 (d, 3H, CH_3, *J*=6.8 Hz), 0.93 (d, 3H, CH_3, *J*=6.8 Hz), 0.95 (d, 3H, CH_3, *J*=6.8 Hz), 1.69 (m, 1H, CH), 2.25 (m, 1H, CH), 2.58 (m, 1H, CH), 3.51 (d, 1H, CH, *J*=10.0 Hz), 3.66 (s, 3H, CH_3), 3.71 (s, 3H, CH_3), 5.23 (dd, 1H, CH=, *J*=15.2 Hz, *J*=10.0 Hz), 5.44 (dd, 1H, CH=, *J*=15.2 Hz, *J*=6.8 Hz).

Diethyl 2-(1,3-cyclohexanylallyl)malonate (43).[35] Enantiomeric excess determined by HPLC using Chiralpak IC column (98% hexane/2-propanol, flow 0.5 ml/min, λ= 226 nm). t_R 22.4 min (*+*); t_R 23.5 min (-). ^{1}H NMR (400 MHz, $CDCl_3$), δ: 1.22 (t, 6H, CH_3, *J*=7.2 Hz), 1.49 (m, 2H, CH_2), 1.67 (m, 2H, CH_2), 1.93 (m, 2H, CH_2), 2.86 (m, 1H, CH), 3.19 (d, 1H, CH, *J*=9.6 Hz), 4.14 (q, 4H, CH_2, *J*=7.2 Hz), 5.50 (m, 1H, CH=), 5.72 (m, 1H, CH=).

Dibenzyl 2-(1,3-cyclohexanylallyl)malonate (44).[32] Enantiomeric excess determined by HPLC using Chiralpak IA column (90% hexane/2-propanol, flow 0.5 ml/min, λ= 226 nm). t_R 15.1 min (-); t_R 16.3 min (*+*). ^{1}H NMR (400 MHz, $CDCl_3$), δ: 1.41 (m, 2H, CH_2), 1.55 (m, 2H, CH_2), 1.95 (m, 2H, CH_2), 2.96 (m, 1H, CH), 3.40 (d, 1H, CH, *J*=9.6 Hz), 5.15 (s, 4H, CH_2), 5.55 (m, 1H, CH=), 5.75 (m, 1H, CH=), 7.2-7.4 (m, 10H, CH=).

Dimethyl 2-(1,3-cyclohexanylallyl)-2-methylmalonate (45).[36] Enantiomeric excess determined by HPLC using Chiralpak IC column (99.5% hexane/2-propanol, flow 0.5 ml/min, λ= 226 nm). t_R 36.4 min (-); t_R 39.7 min (*+*). ^{1}H NMR (400 MHz, $CDCl_3$), δ: 1.29 (s, 3H, CH_3), 1.51 (m, 2H, CH_2), 1.58 (m, 2H, CH_2), 1.92 (m, 2H, CH_2), 2.99 (m, 1H, CH), 3.68 (s, 6H, CH_3), 5.43 (m, 1H, CH=), 5.74 (m, 1H, CH=).

Dimethyl 2-allyl-2-(1,3-cyclohexanylallyl)malonate (46).[4e] Enantiomeric excess determined by HPLC using Chiralpak IC column (87% hexane/2-propanol, flow 0.5 ml/min, λ= 226 nm). t_R 15.3 min (-); t_R 17.0 min (*+*). ^{1}H NMR (400 MHz, $CDCl_3$), δ: 1.49 (m, 2H, CH_2), 1.77 (m, 2H, CH_2), 1.91 (m, 2H, CH_2), 2.65 (m, 2H, CH_2), 2.86 (m, 1H, CH), 3.65 (s, 3H, CH_3), 3.68 (s, 3H, CH_3), 5.06 (m, 2H, CH_2=), 5.71 (m, 3H, CH=).

Dimethyl 2-propargyl-2-(1,3-cyclohexanylallyl)malonate (47).[7c] Enantiomeric excess determined by GC using Chiraldex β-DM column (90 kPa H_2, 110 ºC, 40 min- 5 ºC/min- 150 ºC). t_R 50.0 min (*S*); t_R 51.2 min (*R*). ^{1}H NMR (400 MHz, $CDCl_3$), δ: 1.33 (m, 2H, CH_2), 1.52 (m, 1H, CH_2), 1.77 (m, 2H, CH_2), 1.92 (m, 1H, CH_2), 2.00 (m, 1H, CH), 3.03 (m, 2H, CH_2), 3.09 (m, 1H, CH), 3.68 (s, 3H, CH_3), 3.72 (s, 3H, CH_3), 5.67 (m, 1H, CH=), 5.74 (m, 1H, CH=).

(1,3-Cyclohexanylallyl)pentane-2,4-dienone (48).[4e] Enantiomeric excess determined by GC using Chiralsil-Dex CB column (77 kPa H_2, Isotherm at 100 ºC). t_R 21.6 min (-); t_R 22.4 min (*+*). ^{1}H NMR (400 MHz, $CDCl_3$), δ: 1.48 (m, 2H, CH_2), 1.62 (m, 2H, CH_2), 1.91 (m, 2H, CH_2), 2.09 (s, 3H, CH_3), 2.12 (s, 3H, CH_3), 2.94 (m, 1H, CH), 3.54 (d, 1H, CH, *J*=10.8 Hz), 5.30 (m, 1H, CH=), 5.70 (m, 1H, CH=).

Dimethyl 2-(1,3-cyclopentanylallyl)malonate (49).[5a] Enantiomeric excess determined by ^{1}H NMR using [Eu(hfc)$_3$] in C_6D_6. ^{1}H NMR (400 MHz, $CDCl_3$), δ: 1.61 (m, 1H, CH_2), 2.15 (m, 1H, CH_2), 2.35 (m, 2H, CH_2), 3.30 (d, 1H, CH, *J*=9.6 Hz), 3.39 (m, 1H, CH), 3.71 (s, 6H, CH_3), 5.65 (m, 1H, CH=), 5.84 (m, 1H, CH=).

Dimethyl 2-propargyl-2-(1,3-cyclopentanylallyl)malonate (50).[34] Enantiomeric excess determined by GC using Chiraldex β-DM column (90 kPa H_2, Isotherm at 110 ºC).

t_R 29.9 min (*R*); t_R 30.9 min (*S*). ^{1}H NMR (400 MHz, $CDCl_3$), δ: 1.70 (m, 1H, CH_2), 2.07 (m, 2H, CH_2, CH), 2.24 (m, 2H, CH_2), 2.81 (m, 2H, CH_2), 3.59 (m, 1H, CH), 3.67 (s, 3H, CH_3), 3.71 (s, 3H, CH_3), 5.74 (m, 1H, CH=), 5.79 (m, 1H, CH=).

Dimethyl 2-(1,3-cycloheptanylallyl)malonate (51).[5a] **Enantiomeric** excess determined by GC using Chiralsil-Dex CB column (90 kPa H_2, Isotherm at 110 ºC). t_R 28.8 min (*S*); t_R 29.7 min (*R*). ^{1}H NMR (400 MHz, $CDCl_3$), δ: 1.33 (m, 1H, CH_2), 1.95 (m, 3H, CH_2), 2.17 (m, 2H, CH_2), 3.05 (m, 2H, CH_2), 3.31 (m, 1H, CH), 3.49 (d, 1H, CH, *J*=8.4 Hz), 3.73 (s, 3H, CH_3), 3.75 (s, 3H, CH_3), 5.60 (m, 1H, CH=), 5.84 (m, 1H, CH=).

Dimethyl 2-propargyl-2-(1,3-cycloheptanylallyl)malonate (52).[34] Enantiomeric excess determined by HPLC using Chiralpak OJ-H column (98% hexane/2-propanol, flow 0.5 ml/min, λ= 226 nm). t_R 11.3 min (*R*); t_R 12.0 min (*S*). ^{1}H NMR (400 MHz, $CDCl_3$), δ: 1.24 (m, 2H), 1.70 (m, 2H, CH_2), 1.83 (m, 1H, CH_2), 2.03 (m, 2H, CH_2, CH), 2.16 (m, 2H, CH_2), 2.84 (m, 2H, CH_2), 3.18 (m, 1H, CH), 3.74 (s, 6H, CH_3), 5.66 (m, 1H, CH=), 5.84 (m, 1H, CH=).

3.4.10. General procedure for the preparation of [Pd(η^{3}allyl)(L)]BF_4 complexes 53 -56

The corresponding ligand (0.05 mmol) and the complex [Pd(μ-Cl)(η^3-1,3-allyl)]$_2$ (0.025 mmol) were dissolved in CD_2Cl_2 (1.5 ml) at room temperature under argon. $AgBF_4$ (9.8 mg, 0.05 mmol) was added after 30 min, and the mixture was stirred for 30 min. The mixture was then filtered over Celite under argon, and the resulting solutions were analyzed by NMR. After the NMR analysis, the complexes were precipitated as pale-yellow solids by adding hexane.

3.4.11. Characterization details for [Pd(η^{3}allyl)(L)]BF_4 complexes 53 - 56

[Pd(η^3-1,3-cyclohexenyl)(L5b)]BF_4 (53). ^{31}P NMR (CD_2Cl_2, 298 K), δ: 106.7 (s, 1P). ^{1}H NMR(CD_2Cl_2, 298 K), δ: 0.78 (m, 1H, CH_2, allyl), 1.03 (m, 1H, CH_2, allyl), 1.39 (s, 9H, CH_3, ^{t}Bu), 1.42-1.56 (m, 2H, CH_2, allyl), 1.52 (s, 9H, CH_3, ^{t}Bu), 1.62-1.71 (m, 2H, CH_2, allyl), 1.81 (s, 3H, CH_3), 1.97 (s, 3H, CH_3), 2.23 (s, 3H, CH_3), 2.41 (s, 3H, CH_3), 2.68 (s, 3H, CH_3, SR group), 2.91 (s, 3H, CH_3, SR group), 3.23 (dd, 1H, CH_2, $^2J_{H-H}$= 12.4 Hz, $^3J_{H-H}$= 7.2 Hz), 3.51 (dd, 1H, CH_2, $^2J_{H-H}$= 12.4 Hz, $^3J_{H-H}$= 6.4 Hz), 4.00 (m, 1H, CH allyl *trans* to S), 4.81 (m, 1H, CH-O), 5.15 (d, 1H, CH-S, $^3J_{H-H}$= 6.8 Hz), 5.24 (m, 1H, CH allyl central), 5.46 (m, 1H, CH allyl *trans* to P), 6.71 (d, 1H, CH=, $^3J_{H-H}$= 6 Hz), 7.18 (m, 1H, CH=), 7.3-7.5 (m, 7H, CH=). ^{13}C NMR (CD_2Cl_2, 298 K), δ: 18.1 (CH_3), 18.2 (CH_3), 20.9 (CH_2 allyl), 21.9 (CH_3), 22.0 (CH_3), 24.5 (CH_3, SR group), 25.7 (CH_3, SR group), 28.6 (CH_2 allyl), 29.6 (CH_2 allyl), 32.9 (CH_3, ^{t}Bu), 33.5 (CH_3, ^{t}Bu), 36.6 (C, ^{t}Bu), 36.9 (C, ^{t}Bu), 39.4 (d, CH_2, J_{C-P}= 6 Hz), 55.2 (CH-S), 83.6 (d, CH-O, J_{C-P}= 4.8 Hz), 84.3 (d, CH allyl *trans* to S, J_{C-P}= 6.5 Hz), 100.6 (d, CH allyl *trans* to P, J_{C-P}= 30.5 Hz), 115.0 (d, CH allyl central, J_{C-P}= 8.7 Hz), 125.5-147.3 (aromatic carbons). MS HR-ESI [found 839.2869, $C_{47}H_{58}O_3PPdS$ $(M\text{-}BF_4)^+$ requires 839.2874].

[Pd(η³-1,3-cyclohexenyl)(L5c)]BF_4 (54). ^{31}P NMR (CD_2Cl_2, 298 K), δ: 106.2 (s, 1P). ^1H NMR(CD_2Cl_2, 298 K), δ: 1.18 (m, 1H, CH_2, allyl), 1.47 (s, 9H, CH_3, ^{t}Bu), 1.55 (s, 9H, CH_3, ^{t}Bu), 1.51-1.72 (m, 3H, CH_2, allyl), 1.84 (s, 3H, CH_3), 1.86 (m, 1H, CH_2, allyl), 2.14 (s, 3H, CH_3), 2.14 (m, 1H, CH_2), 2.38 (s, 3H, CH_3), 2.44 (s, 3H, CH_3), 2.58 (s, 3H, CH_3, SR group), 2.70 (s, 3H, CH_3, SR group), 3.29 (dd, 1H, CH_2, $^2J_{H-H}$= 12.4 Hz, $^3J_{H-H}$= 6.8 Hz), 3.56 (dd, 1H, CH_2, $^2J_{H-H}$= 12.4 Hz, $^3J_{H-H}$= 6 Hz), 4.08 (m, 1H, CH allyl *trans* to S), 5.20 (m, 1H, CH allyl *trans* to P), 5.28 (m, 2H, CH-S and CH allyl central), 5.34 (m, 1H, CH-O), 6.14 (d, 1H, CH=, $^3J_{H-H}$= 6.4 Hz), 7.04 (m, 1H, CH=), 7.3-7.5 (m, 7H, CH=). ^{13}C NMR (CD_2Cl_2, 298 K), δ: 18.1 (CH_3), 18.2 (CH_3), 21.0 (CH_2 allyl), 21.9 (CH_3), 22.0 (CH_3), 24.7 (CH_3, SR group), 24.8 (CH_3, SR group), 29.5 (CH_2 allyl), 30.96 (CH_2 allyl), 33.1 (CH_3, ^{t}Bu), 33.5 (CH_3, ^{t}Bu), 36.6 (C, ^{t}Bu), 36.8 (C, ^{t}Bu), 40.1 (d, CH_2, J_{C-P}= 5.4 Hz), 56.8 (d, CH-S, J_{C-P}= 3.2 Hz), 85.1 (m, CH-O and CH allyl *trans* to S), 103.8 (d, CH allyl *trans* to P, J_{C-P}= 28.6 Hz), 115.0 (d, CH allyl central, J_{C-P}= 7.9 Hz), 125.4-147.0 (aromatic carbons). MS HR-ESI [found 839.2870, $C_{47}H_{58}O_3PPdS$ (M-BF_4)$^+$ requires 839.2874].

[Pd(η³-1,3-diphenylallyl)(L5b)]BF_4 (55). Major isomer (57%): ^{31}P NMR (CD_2Cl_2, 298 K), δ: 102.8 (s, 1P). ^1H NMR(CD_2Cl_2, 298 K), δ: 1.25 (s, 9H, CH_3, ^{t}Bu), 1.59 (s, 9H, CH_3, ^{t}Bu), 1.66 (s, 3H, CH_3), 1.69 (s, 3H, CH_3), 1.97 (s, 3H, CH_3, SR group), 2.18 (s, 3H, CH_3), 2.24 (s, 3H, CH_3), 2.95 (s, 3H, CH_3, SR group), 2.97 (m, 1H, CH_2), 3.41 (dd, 1H, CH_2, $^2J_{H-H}$= 12.4 Hz, $^3J_{H-H}$= 7.2 Hz), 4.70 (m, 1H, CH-S), 4.75 (m, 1H, CH allyl *trans* to S), 4.85 (m, 1H, CH-O), 5.46 (m, 1H, CH allyl *trans* to P), 6.18 (dd, 1H, CH allyl central, $^3J_{H-H}$= 10.8 Hz, $^3J_{H-H}$= 9.2 Hz), 6.36 (d, 1H, CH=, $^3J_{H-H}$= 6.0 Hz), 6.71-7.52 (m, 14H, CH=). ^{13}C NMR (CD_2Cl_2, 298 K), δ: 16.9 (CH_3), 17.3 (CH_3), 20.7 (CH_3), 20.9 (CH_3), 22.5 (CH_3, SR group), 24.0 (CH_3, SR group), 31.5 (CH_3, ^{t}Bu), 32.1 (CH_3, ^{t}Bu), 36.4 (C, ^{t}Bu), 36.6 (C, ^{t}Bu), 37.6 (b, CH_2), 53.6 (CH-S), 80.2 (d, CH allyl *trans* to S, J_{C-P}= 7.3 Hz), 80.4 (d, CH-O, J_{C-P}= 6.8 Hz), 93.0 (d, CH allyl *trans* to P, J_{C-P}= 21.2 Hz), 110.8 (d, CH allyl *trans* to P, J_{C-P}= 8.4 Hz), 122.7-144.5 (aromatic carbons). Minor isomer (43%): ^{31}P NMR (CD_2Cl_2, 298 K), δ: 102.6 (s, 1P). ^1H NMR(CD_2Cl_2, 298 K), δ: 1.50 (s, 9H, CH_3, ^{t}Bu), 1.58 (s, 9H, CH_3, ^{t}Bu), 1.63 (s, 3H, CH_3), 1.80 (s, 3H, CH_3), 2.20 (s, 3H, CH_3, SR group), 2.42 (s, 3H, CH_3), 2.48 (s, 3H, CH_3), 3.14 (s, 3H, CH_3, SR group), 2.97 (m, 1H, CH_2), 3.30 (dd, 1H, CH_2, $^2J_{H-H}$= 12.4 Hz, $^3J_{H-H}$= 7.2 Hz), 4.15 (m, 1H, CH allyl *trans* to S), 4.89 (m, 1H, CH-O), 5.02 (m, 1H, CH-S), 5.39 (m, 1H, CH allyl *trans* to P), 6.36 (d, 1H, CH=, $^3J_{H-H}$= 6.0 Hz), 6.52 (t, 1H, CH allyl central, $^3J_{H-H}$= 9.6 Hz), 6.71-7.52 (m, 14H, CH=). ^{13}C NMR (CD_2Cl_2, 298 K), δ: 16.9 (CH_3), 17.3 (CH_3), 20.8 (CH_3), 20.8 (CH_3), 22.5 (CH_3, SR group), 23.3 (CH_3, SR group), 30.6 (CH_3, ^{t}Bu), 31.0 (CH_3, ^{t}Bu), 36.5 (C, ^{t}Bu), 36.8 (C, ^{t}Bu), 37.6 (b, CH_2), 53.5 (CH-S), 79.8 (d, CH allyl *trans* to S, J_{C-P}= 6.3 Hz), 92.3(d, CH-O, J_{C-P}= 6.2 Hz), 103.2 (d, CH allyl *trans* to P, J_{C-P}= 23 Hz), 112.1 (d, CH allyl *trans* to P, J_{C-P}= 10 Hz), 122.7-144.5 (aromatic carbons). MS HR-ESI [found 951.3184, $C_{56}H_{62}O_3PPdS$ (M-BF_4)$^+$ requires 951.3187].

[Pd(η³-1,3-diphenylallyl)(L5c)]BF_4 (56). Major isomer (70%): ^{31}P NMR (CD_2Cl_2, 298 K), δ: 104.3 (s, 1P). ^1H NMR(CD_2Cl_2, 298 K), δ: 1.41 (s, 9H, CH_3, ^{t}Bu), 1.63 (s, 3H, CH_3), 1.65 (s, 3H, CH_3), 1.77 (s, 12H, CH_3, ^{t}Bu and CH_3), 2.27 (s, 3H, CH_3), 2.47 (s, 3H, CH_3, SR group), 3.06 (s, 3H, CH_3, SR group), 3.01 (m, 1H, CH_2), 3.36 (dd, 1H, CH_2, $^2J_{H-H}$= 12.8 Hz, $^3J_{H-H}$= 6.8 Hz), 5.01 (m, 1H, CH-O), 5.06 (m, 1H, CH-S), 5.12 (m, 1H, CH allyl *trans* to S), 5.26 (d, 1H, CH allyl *trans* to P, $^3J_{H-H}$= 10 Hz), 5.95 (d, 1H, CH=, $^3J_{H-H}$= 6.0 Hz), 6.73 (m, 1H, CH allyl

central), 6.87-7.51 (m, 14H, CH=). ^{13}C NMR (CD_2Cl_2, 298 K), δ: 18.0 (CH_3), 18.4 (CH_3), 21.9 (CH_3), 22.1 (CH_3), 24.4 (CH_3, SR group), 25.8 (CH_3, SR group), 33.8 (CH_3, ^{t}Bu), 34.2 (CH_3, ^{t}Bu), 36.7 (C, ^{t}Bu), 36.9 (C, ^{t}Bu), 40.0 (d, CH_2, $J_{C\text{-}P}$= 6.7 Hz), 56.9 (d, CH-S, $J_{C\text{-}P}$= 2.7 Hz), 84.7 (d, CH-O, $J_{C\text{-}P}$= 5.4 Hz), 88.6 (d, CH allyl *trans* to S, $J_{C\text{-}P}$= 5.2 Hz), 101.5 (d, CH allyl *trans* to P, $J_{C\text{-}P}$= 25.7 Hz), 112.9 (d, CH allyl *trans* to P, $J_{C\text{-}P}$= 8.3 Hz), 124.7-146.9 (aromatic carbons). Minor isomer (30%): ^{31}P NMR (CD_2Cl_2, 298 K), δ: 107.1 (s, 1P). ^{1}H NMR(CD_2Cl_2, 298 K), δ: 1.64 (s, 9H, CH_3, ^{t}Bu), 1.72 (s, 9H, CH_3, ^{t}Bu), 1.74 (s, 3H, CH_3), 1.82 (s, 3H, CH_3), 2.31 (s, 3H, CH_3), 2.33 (s, 3H, CH_3), 2.38 (s, 3H, CH_3, SR group), 2.60 (s, 3H, CH_3, SR group), 3.01 (m, 1H, CH_2), 3.47 (dd, 1H, CH_2, $^2J_{H\text{-}H}$= 12.8 Hz, $^3J_{H\text{-}H}$= 6.8 Hz), 4.85 (d, 1H, CH-S, $^3J_{H\text{-}H}$= 5.6 Hz), 5.21 (m, 1H, CH allyl *trans* to S), 5.51 (m, 1H, CH-O), 5.70 (d, 1H, CH allyl *trans* to P, $^3J_{H\text{-}H}$= 10 Hz), 6.00 (d, 1H, CH=, $^3J_{H\text{-}H}$= 6.0 Hz), 6.58 (m, 1H, CH allyl central), 6.87-7.51 (m, 14H, CH=). ^{13}C NMR (CD_2Cl_2, 298 K), δ: 18.2 (CH_3), 18.3 (CH_3), 21.9 (CH_3), 22.0 (CH_3), 24.2 (CH_3, SR group), 26.1 (CH_3, SR group), 32.8 (CH_3, ^{t}Bu), 34.1 (CH_3, ^{t}Bu), 36.6 (C, ^{t}Bu), 36.7 (C, ^{t}Bu), 39.6 (d, CH_2, $J_{C\text{-}P}$= 7.5 Hz), 58.1 (d, CH-S, $J_{C\text{-}P}$= 2.5 Hz), 86.7 (d, CH-O, $J_{C\text{-}P}$= 7.5 Hz), 95.0 (d, CH allyl *trans* to S, $J_{C\text{-}P}$= 5.4 Hz), 95.9 (d, CH allyl *trans* to P, $J_{C\text{-}P}$= 23.7 Hz), 113.0 (d, CH allyl *trans* to P, $J_{C\text{-}P}$= 9.1 Hz), 124.7-146.9 (aromatic carbons). MS HR-ESI [found 951.3182, $C_{56}H_{62}O_3PPdS$ $(M\text{-}BF_4)^+$ requires 951.3187].

3.4.12. Study of the reactivity of the [Pd(η^3-allyl)(L))]BF_4 with sodium dimethyl malonate by in situ NMR

A solution of in situ prepared [Pd(η^3-allyl)(**L**)]BF_4 (L= phosphite–thioether, 0.05 mmol) in CD_2Cl_2 (1 ml) was cooled in the NMR at −80 °C. At this temperature, a solution of cooled sodium dimethyl malonate (0.1 mmol) was added. The reaction was then followed by ^{31}P NMR. The relative reaction rates were calculated using a capillary containing a solution of triphenylphosphine in CD_2Cl_2 as external standard.

3.4.13. Computational details

All calculations were performed using the Gaussian 09 program.[37] Optimizations of minima and transition states were performed employing the B3LYP[38] density functional and the 6-31G(d) basis set for all elements except for Pd for which LANL2DZ[39] was used.[40] All energies presented correspond to single point calculations with the B3LYP-D3 functional[41] and the larger 6-311+G(d,p)[42] basis set for all elements except Pd. Solvation was taken into account along optimization and single points through the use of the PCM continuum model with the default parameters for dichloromethane.[43] No symmetry constraints were applied. The validity of the model was confirmed by a series of geometry optimizations at the B3LYP-D3 level on the four key transition states. The qualitative trends were unchanged: ligand **L5b** favored the *R* product (corrected ee of 64 vs uncorrected ee of 99.99) and ligand **L5c** favored the *S* product (corrected ee of 99.6 vs uncorrected ee of 97.5). Normal mode analysis of all transition states revealed a

single imaginary frequency corresponding to the expected nucleophilic attack of the nucleophile to one of the two allylic termini carbons. All energies reported are Gibbs free energies in solution at 298.15 K and calculated as $\Delta G_{\text{reported}} = \Delta G_{\text{B3LYP/6-31G(d)}} + (\Delta E_{\text{B3LYP-D3/6-311+G(d,p)}} - \Delta E_{\text{B3LYP/6-31G(d)}})$.

3.5. References

1. (a) *Homogeneous Catalysis with Renewables*. Behr, A.; Vorholt, A. J., Springer: Gewerbestrasse, 2017; (b) van Leeuwen, P. W. N. M.; Chadwick, J. C.,·*Homogeneous Catalysts: Activity-Stability-Deactivation*. Wiley-VCH: Weinheim, 2011.
2. *Catalytic Asymmetric Synthesis*. Ojima, I., Wiley: Hoboken, 2010.
3. (a) *Palladium Reagents and Catalysis: Innovations in Organic Synthesis*. Tsuji, J., Wiley: New York, 1995; (b) Johannsen, M.; Jorgensen, K. A., Allylic Amination. *Chemical Reviews* **1998**, *98*, 1689-1708; (c) *Comprehensive Asymmetric Catalysis, Vol. 2*. Pfaltz, A.; Lautens, M.; Jacobsen, E. N.; Pfaltz, A.; Yamamoto, H., Springer-Verlag: Berlin, 1999; (d) Helmchen, G.; Pfaltz, A., Phosphinooxazolines - A New Class of Versatile, Modular P,N-Ligands for Asymmetric Catalysis. *Accounts of Chemical Research* **2000**, *33*, 336-345; (e) Trost, B. M.; Crawley, M. L., Asymmetric Transition-Metal-Catalyzed Allylic Alkylations: Applications in Total Synthesis. *Chemical Reviews* **2003**, *103*, 2921-2944; (f) Martin, E.; Diéguez, M., Thioether Containing Ligands for Asymmetric Allylic Substitution Reactions. *Comptes Rendus Chimie* **2007**, *10*, 188-205; (g) Lu, Z.; Ma, S., Metal-Catalyzed Enantioselective Allylation in Asymmetric Synthesis. *Angewandte Chemie International Edition* **2008**, *47*, 258-297; (h) Diéguez, M.; Pàmies, O., New Efficient Adaptative Ligands for Pd-Catalyzed Asymmetric Allylic Substitution Reactions. *Accounts of Chemical Research* **2010**, *43*, 312-322; (i) Trost, B. M., Pd- and Mo-Catalyzed Asymmetric Allylic Alkylation. *Organic Process Research & Development* **2012**, *16*, 185-194; (j) Butt, N.; Zhang, W., Transition Metal-Catalyzed Allylic Substitution Reactions with Unactivated Allylic Substrates. *Chemical Society Reviews* **2015**, *44*, 7929-7967; (k) Grange, R. L.; Clizbe, E. A.; Evans, P. A., Recent Developments in Asymmetric Allylic Amination Reactions. *Synthesis* **2016**, *48*, 2911-2968; (l) Butt, N.; Yang, G.; Zhang, W., Allylic Alkylations with Enamine Nucleophiles. *The Chemical Record* **2016**, *16*, 2687-2696.
4. (a) Leeuwen, P. W. N. M. v.; Kamer, P. C. J.; Claver, C.; Pàmies, O.; Diéguez, M., Phosphite-Containing Ligands for Asymmetric Catalysis. *Chemical Reviews* **2011**, *111*, 2077-2118; (b) Pàmies, O.; Diéguez, M.; Claver, C., New Phosphite−Oxazoline Ligands for Efficient Pd-Catalyzed Substitution Reactions. *Journal of the American Chemical Society* **2005**, *127*, 3646-3647; (c) Mata, Y.; Pàmies, O.; Diéguez, M., Pyranoside Phosphite-Oxazoline Ligand Library: Highly Efficient Modular P,N Ligands for Palladium-Catalyzed Allylic Substitution Reactions. A Study of the Key Palladium Allyl Intermediates. *Advanced Synthesis & Catalysis* **2009**, *351*, 3217-3234; (d) Mazuela, J.; Pàmies, O.; Diéguez, M., A New Modular Phosphite-Pyridine Ligand Library for Asymmetric Pd-Catalyzed Allylic Substitution Reactions: A Study of the Key Pd-π-Allyl Intermediates. *Chemistry – A European Journal* **2013**, *19*, 2416-2432; (e) Bellini, R.; Magre, M.; Biosca, M.; Norrby, P. O.; Pàmies, O.; Diéguez, M.; Moberg, C., Conformational Preferences of a Tropos Biphenyl Phosphinooxazoline–a Ligand with Wide Substrate Scope. *ACS Catalysis* **2016**, *6*, 1701–1712; (f) Pàmies, O.; Diéguez, M., Adaptable P-X Biaryl Phosphite/Phosphoroamidite-Containing Ligands for Asymmetric Hydrogenation and C-X Bond-Forming Reactions: Ligand Libraries with Exceptionally Wide Substrate Scope. *The Chemical Record* **2016**, *16*, 2460-2481.

5. (a) Evans, D. A.; Campos, K. R.; Tedrow, J. S.; Michael, F. E.; Gagné, M. R., Application of Chiral Mixed Phosphorus/Sulfur Ligands to Palladium-Catalyzed Allylic Substitutions. *Journal of the American Chemical Society* **2000**, *122*, 7905-7920; (b) Nakano, H.; Okuyama, Y.; Hongo, H., New Chiral Phosphinooxathiane Ligands for Palladium-Catalyzed Asymmetric Allylic Substitution Reactions. *Tetrahedron Letters* **2000**, *41*, 4615-4618; (c) García Mancheño, O.; Priego, J.; Cabrera, S.; Gómez Arrayás, R.; Llamas, T.; Carretero, J. C., 1-Phosphino-2-sulfenylferrocenes as Planar Chiral Ligands in Enantioselective Palladium-Catalyzed Allylic Substitutions. *The Journal of Organic Chemistry* **2003**, *68*, 3679-3686; (d) Enders, D.; Peters, R.; Runsink, J.; Bats, J. W., Novel Ferrocenyl Ligands with Planar and Central Chirality in Pd-Catalyzed Allylic Substitutions. *Organic Letters* **1999**, *1*, 1863-1866; (e) Guimet, E.; Diéguez, M.; Ruiz, A.; Claver, C., Furanoside Thioether–Phosphinite Ligands for Pd-Catalyzed Asymmetric Allylic Substitution Reactions. *Tetrahedron: Asymmetry* **2005**, *16*, 959-963; (f) Caldentey, X.; Pericàs, M. A., Modular P,S-Ligands for Pd-Catalyzed Asymmetric Allylic Substitutions. *The Journal of Organic Chemistry* **2010**, *75*, 2628-2644.

6. (a) Pellissier, H., Chiral Sulfur-Containing Ligands for Asymmetric Catalysis. *Tetrahedron* **2007**, *63*, 1297-1330; (b) Mellah, M.; Voituriez, A.; Schulz, E., Chiral Sulfur Ligands for Asymmetric Catalysis. *Chemical Reviews* **2007**, *107*, 5133-5209; (c) Arrayás, R. G.; Carretero, J. C., Chiral Thioether-Based Catalysts in Asymmetric Synthesis: Recent Advances. *Chemical Communications* **2011**, *47*, 2207-2211.

7. (a) Margalef, J.; Pàmies, O.; Pericàs, M. A.; Diéguez, M., Evolution of phosphorus–thioether ligands for asymmetric catalysis. *Chemical Communications* **2020**, *56*, 10795-10808; (b) Diéguez, M.; Pàmies, O.; Claver, C., Furanoside thioether–phosphinite ligands for Pd-catalyzed asymmetric allylic substitution reactions: Scope and limitations. *Journal of Organometallic Chemistry* **2006**, *691*, 2257-2262; (c) Coll, M.; Pàmies, O.; Diéguez, M., Highly Versatile Pd–Thioether–Phosphite Catalytic Systems for Asymmetric Allylic Alkylation, Amination, and Etherification Reactions. *Organic Letters* **2014**, *16*, 1892-1895; (d) Margalef, J.; Coll, M.; Norrby, P. O.; Pàmies, O.; Diéguez, M., Asymmetric Catalyzed Allylic Substitution Using a Pd/P–S Catalyst Library with Exceptional High Substrate and Nucleophile Versatility: DFT and Pd-π-allyl Key Intermediates Studies. *Organometallics* **2016**, *35*, 3323.

8. Margalef, J.; Coll, M.; Norrby, P. O.; Pàmies, O.; Diéguez, M., Asymmetric Catalyzed Allylic Substitution Using a Pd/P–S Catalyst Library with Exceptional High Substrate and Nucleophile Versatility: DFT and Pd-π-allyl Key Intermediates Studies. *Organometallics* **2016**, *35*, 3323-3335.

9. (a) Vidal-Ferran, A.; Moyano, A.; Pericàs, M. A.; Riera, A., Synthesis of a Family of Fine-Tunable New Chiral Ligands for Catalytic Asymmetric Synthesis. Ligand Optimization through the Enantioselective Addition of Diethylzinc to Aldehydes. *The Journal of Organic Chemistry* **1997**, *62*, 4970-4982; (b) Puigjaner, C.; Vidal-Ferran, A.; Moyano, A.; Pericàs, M. A.; Riera, A., A New Family of Modular Chiral Ligands for the Catalytic Enantioselective Reduction of Prochiral Ketones. *The Journal of Organic Chemistry* **1999**, *64*, 7902-7911; (c) Solà, L.; Reddy, K. S.; Vidal-Ferran, A.; Moyano, A.; Pericàs, M. A.; Riera, A.; Alvarez-Larena, A.; Piniella, J. F., A Superior, Readily Available Enantiopure Ligand for the Catalytic Enantioselective Addition of Diethylzinc to α-Substituted Aldehydes. *The Journal of Organic Chemistry* **1998**, *63*, 7078-7082; (d) Reddy, K. S.; Solà, L.; Moyano, A.; Pericàs, M. A.; Riera, A., Highly Efficient Synthesis of Enantiomerically Pure (S)-2-Amino-1,2,2-triphenylethanol. Development of a New Family of Ligands for the Highly Enantioselective Catalytic Ethylation of Aldehydes. *The Journal of Organic Chemistry* **1999**, *64*, 3969-3974; (e) Rodríguez-Escrich, S.; Solà, L.; Jimeno, C.; Rodríguez-Escrich, C.; Pericàs, M. A., Exploring Structural Diversity in Ligand Design: The Aminoindanol Case. *Advanced Synthesis & Catalysis* **2008**, *350*, 2250-2260.

10. (a) Bayardon, J.; Holz, J.; Schäffner, B.; Andrushko, V.; Verevkin, S.; Preetz, A.; Börner, A., Propylene Carbonate as a Solvent for Asymmetric Hydrogenations. *Angewandte Chemie International Edition* **2007**, *46*, 5971-5974; (b) Schäffner, B.; Holz, J.; Verevkin, S. P.; Börner, A., Organic Carbonates as Alternative Solvents for Palladium-Catalyzed Substitution

Reactions. *ChemSusChem* **2008**, *1*, 249-253; (c) Schäffner, B.; Schäffner, F.; Verevkin, S. P.; Börner, A., Organic Carbonates as Solvents in Synthesis and Catalysis. *Chemical Reviews* **2010**, *110*, 4554-4581.

11. Jacobsen, E. N.; Zhang, W.; Muci, A. R.; Ecker, J. R.; Deng, L., Highly Enantioselective Epoxidation Catalysts Derived from 1,2-Diaminocyclohexane. *Journal of the American Chemical Society* **1991**, *113*, 7063-7064.
12. Takano, S.; Yanase, M.; Ogasawara, K., Nucleophilic Cleavage of (2S,3S)-3-Phenylglycidol. *Heterocycles* **1989**, *29*, 249-252.
13. Palucki, M.; McCormick, G. J.; Jacobsen, E. N., Low temperature asymmetric epoxidation of unfunctionalized olefins catalyzed by (salen)Mn(III) complexes. *Tetrahedron Letters* **1995**, *36*, 5457-5460.
14. (a) Pàmies, O.; Diéguez, M., Adaptable P–X Biaryl Phosphite/Phosphoroamidite-Containing Ligands for Asymmetric Hydrogenation and C–X Bond-Forming Reactions: Ligand Libraries with Exceptionally Wide Substrate Scope. *The Chemical Record* **2016**, *16*, 2460-2481; (b) Farkas, G.; Császár, Z.; Balogh, S.; Szöllősy, A.; Gouygou, M.; Bakos, J., Phosphine–Phosphite Ligands in the Palladium-Catalyzed Asymmetric Allylic Alkylation: Electronic and Steric Effects. *Catalysis Communications* **2013**, *36*, 94-97; (c) Gavrilov, K. N.; Benetsky, E. B.; Boyko, V. E.; Rastorguev, E. A.; Davankov, V. A.; Schäffner, B.; Börner, A., (S)-6-Bromo-BINOL-Based Phosphoramidite Ligand with C1 Symmetry for Enantioselective Hydrogenation and Allylic Substitution. *Chirality* **2010**, *22*, 844-848.
15. (a) Oslob, J. D.; Åkermark, B.; Helquist, P.; Norrby, P. O., Steric Influences on the Selectivity in Palladium-Catalyzed Allylation. *Organometallics* **1997**, *16*, 3015-3021; (b) Hagelin, H.; Åkermark, B.; Norrby, P. O., New Molecular Mechanics (MM3*) Force Field Parameters for Calculations on (η^3-Allyl)palladium Complexes with Nitrogen and Phosphorus Ligands. *Organometallics* **1999**, *18*, 2884-2895; (c) Moberg, C.; Bremberg, U.; Hallman, K.; Svensson, M.; Norrby, P. O.; Hallberg, A.; Larhed, M.; Csoregh, I., Selectivity and Reactivity in Asymmetric Allylic Alkylation. *Pure and Applied Chemistry* **1999**, *71*, 1477-1483.
16. Kleimark, J.; Johansson, C.; Olsson, S.; Håkansson, M.; Hansson, S.; Åkermark, B.; Norrby, P. O., Sterically Governed Selectivity in Palladium-Assisted Allylic Alkylation. *Organometallics* **2011**, *30*, 230-238.
17. (a) Butts, C. P.; Filali, E.; Lloyd-Jones, G. C.; Norrby, P. O.; Sale, D. A.; Schramm, Y., Structure-Based Rationale for Selectivity in the Asymmetric Allylic Alkylation of Cycloalkenyl Esters Employing the Trost 'Standard Ligand' (TSL): Isolation, Analysis and Alkylation of the Monomeric form of the Cationic η^3-Cyclohexenyl Complex $[(\eta^3\text{-c-}C_6H_9)Pd(TSL)]^+$. *Journal of the American Chemical Society* **2009**, *131*, 9945–9957; (b) Fristrup, P.; Ahlquist, M.; Tanner, D.; Norrby, P. O., On the Nature of the Intermediates and the Role of Chloride Ions in Pd-Catalyzed Allylic Alkylations: Added Insight from Density Functional Theory. *Journal of Physical Chemistry A* **2008**, *112*, 12862-12867.
18. (a) Deng, W. H.; Ye, F.; Bai, X. F.; Zheng, Z. J.; Cui, Y. M.; Xu, L. W., Multistereogenic Phosphine Ligand-promoted Palladium-Catalyzed Allylic Alkylation of Cyanoesters. *ChemCatChem* **2015**, *7*, 75-79; (b) Xu, J. X.; Ye, F.; Bai, X. F.; Zhang, J.; Xu, Z.; Zheng, Z. J.; Xu, L. W., Fei-Phos Ligand-Controlled Asymmetric Palladium-Catalyzed Allylic Substitutions with Structurally Diverse Nucleophiles: Scope and Limitations. *RSC Advances* **2016**, *6*, 45495-45502.
19. d'Ischia, M.; Napolitano, A.; Pezzella, A., 3.04 - Pyrroles and their Benzo Derivatives: Applications. In *Comprehensive Heterocyclic Chemistry III*, Katritzky, A. R.; Ramsden, C. A.; Scriven, E. F. V.; Taylor, R. J. K., Eds. Elsevier: Oxford, 2008; pp 353-388.
20. Liu, Y.; Cao, Z.; Du, H., Asymmetric Allylic Alkylation of Pyrroles and 4,7-Dihydroindoles with Alkene–Phosphine Ligands. *The Journal of Organic Chemistry* **2012**, *77*, 4479-4483.
21. (a) Trost, B. M.; Shen, H. C.; Dong, L.; Surivet, J. P., Unusual Effects in the Pd-Catalyzed Asymmetric Allylic Alkylations: Synthesis of Chiral Chromans. *Journal of the American Chemical Society* **2003**, *125*, 9276-9277; (b) Trost, B. M.; Toste, F. D., Asymmetric O- and C-

Alkylation of Phenols. *Journal of the American Chemical Society* **1998**, *120*, 815-816; (c) Trost, B. M.; Toste, F. D., Enantioselective Total Synthesis of (−)-Galanthamine. *Journal of the American Chemical Society* **2000**, *122*, 11262-11263; (d) Uozumi, Y.; Kimura, M., Asymmetric π-Allylic Etherification of Cycloalkenyl Esters with Phenols in Water Using a Resin-Supported Chiral Palladium Complex. *Tetrahedron: Asymmetry* **2006**, *17*, 161-166; (e) Tietze, L. F.; Lohmann, J. K.; Stadler, C., Synthesis of Novel Highly Active Thiophene and Benzothiophene Containing Diphosphine Ligands and their Use in the Asymmetric Allylation of Catechol. *Synlett* **2004**, 1113-1116

22. (a) Deerenberg, S.; Schrekker, H. S.; van Strijdonck, G. P. F.; Kamer, P. C. J.; van Leeuwen, P. W. N. M.; Fraanje, J.; Goubitz, K., New Chiral Phosphine-Phosphite Ligands in the Enantioselective Palladium-Catalyzed Allylic Alkylation. *The Journal of Organic Chemistry* **2000**, *65*, 4810-4817; (b) Fernández, F.; Gómez, M.; Jansat, S.; Muller, G.; Martín, E.; Flores Santos, L.; García, P. X.; Acosta, A.; Aghmiz, A.; Giménez-Pedrós, M.; Masdeu-Bultó, A. M.; Diéguez, M.; Claver, C.; Maestro, M. A., Allylic Alkylations Catalyzed by Palladium Systems Containing Modular Chiral Dithioethers. A Structural Study of the Allylic Intermediates. *Organometallics* **2005**, *24*, 3946-3956.

23. Caldentey, X. Engineering of Modular Ligands for Asymmetric Catalysis: Synthesis and Evaluation. Universitat de Barcelona, 2010.

24. Evans, D. A.; Campoo, K. R.; Tedrow, J. S.; Michael, F. E.; Gagne, M. R., *Journal of the American Chemical Society* **2000**, *122*, 7905.

25. Evans, D. A.; Campos, K. R.; Tedrow, J. S.; Michael, F. E.; Gagné, M. R., Application of chiral mixed phosphorus/sulfur ligands to palladium-catalyzed allylic substitutions. *Journal of the American Chemical Society* **2000**, *122*, 7905.

26. Tanaka, Y.; Mino, T.; Akita, K.; Sakamoto, M.; Fujita, T., Development of Chiral (S)-Prolinol-Derived Ligands for Palladium-Catalyzed Asymmetric Allylic Alkylation: Effect of a Siloxymethyl Group on the Pyrrolidine Backbone. *The Journal of Organic Chemistry* **2004**, *69*, 6679-6687.

27. Dugal-Tessier, J.; Dake, G. R.; Gates, D. P., Chiral Phosphaalkene-Oxazoline Ligands for the Palladium-Catalyzed Asymmetric Allylic Alkylation. *Organic Letters* **2010**, *12*, 4667-4669.

28. Deng, W. H.; Ye, F.; Bai, X. F.; Zheng, Z. J.; Cui, Y. M.; Xu, L. W., Multistereogenic Phosphine ligand-promoted palladium-catalyzed allylic alkylation of cyanoesters. *ChemCatChem* **2015**, *7*, 75.

29. Diéguez, M.; Pàmies, O.; Claver, C., Modular Furanoside Diphosphite Ligands for Pd-Catalyzed Asymmetric Allylic Substitution Reactions: Scope and Limitations. *Advanced Synthesis & Catalysis* **2005**, *347*, 1257.

30. Liu, Q. L.; Chen, W.; Jiang, Q. Y.; Bai, X. F.; Li, Z.; Xu, Z.; Xu, L. W., A D-camphor-based Schiff base as a highly efficient N,P ligand for enantioselective palladium-catalyzed allylic substitutions. *ChemCatChem* **2016**, *8*, 1495.

31. Lam, F. L.; Au-Yeung, T. T. L.; Kwong, F. Y.; Zhou, Z.; Wong, K. Y.; Chan, A. S. C., Palladium–(*S*,p*R*)-FerroNPS-Catalyzed Asymmetric Allylic Etherification: Electronic Effect of Nonconjugated Substituents on Benzylic Alcohols on Enantioselectivity. *Angewandte Chemie International Edition* **2008**, *47*, 1280-1283.

32. Ye, F.; Zheng, Z. J.; Li, L.; Yang, K. F.; Xia, C. G.; Xu, L. W., Development of a Novel Multifunctional N,P Ligand for Highly Enantioselective Palladium-Catalyzed Asymmetric Allylic Etherification of Alcohols and Silanols. *Chemistry – A European Journal* **2013**, *19*, 15452-15457.

33. Mei, L. Y.; Yuan, Z. L.; Shi, M., Chiral imidazoline-phosphine ligands for palladium-catalyzed asymmetric allylic substitutions. *Organometallics* **2011**, *30*, 6466.

34. Magre, M.; Biosca, M.; Norrby, P. O.; Pàmies, O.; Diéguez, M., Theoretical and Experimental Optimization of a New Amino Phosphite Ligand Library for Asymmetric Palladium-Catalyzed Allylic Substitution. *ChemCatChem* **2015**, *7*, 4091-4107.

35. Mazuela, J.; Pàmies, O.; Diéguez, M., A New Modular Phosphite-Pyridine Ligand Library for Asymmetric Pd-Catalyzed Allylic Substitution Reactions: A Study of the Key Pd-π-Allyl Intermediates. *Chem. - Eur. J.* **2013**, *19*, 2416.
36. Leitner, A.; Larsen, J.; Steffens, C.; Hartwig, J. F., Palladium-Catalyzed Addition of Mono- and Dicarbonyl Compounds to Conjugated Dienes. *The Journal of Organic Chemistry* **2004**, *69*, 7552-7557.
37. Frisch, M. J.; Trucks, G. W.; Schlegel, H. B.; Scuseria, G. E.; Robb, M. A.; Cheeseman, J. R.; Scalmani, G.; Barone, V.; Mennucci, B.; Petersson, G. A.; Nakatsuji, H.; Caricato, M.; Li, X.; Hratchian, H. P.; Izmaylov, A. F.; Bloino, J.; Zheng, G.; Sonnenberg, J. L.; Hada, M.; Ehara, M.; Toyota, K.; Fukuda, R.; Hasegawa, J.; Ishida, M.; Nakajima, T.; Honda, Y.; Kitao, O.; Nakai, H.; Vreven, T.; Montgomery, J. A.; Peralta, J. E.; Ogliaro, F.; Bearpark, M.; Heyd, J. J.; Brothers, E.; Kudin, K. N.; Staroverov, V. N.; Kobayashi, R.; Normand, J.; Raghavachari, K.; Rendell, A.; Burant, J. C.; Iyengar, S. S.; Tomasi, J.; Cossi, M.; Rega, N.; Millam, J. M.; Klene, M.; Knox, J. E.; Cross, J. B.; Bakken, V.; Adamo, C.; Jaramillo, J.; Gomperts, R.; Stratmann, R. E.; Yazyev, O.; Austin, A. J.; Cammi, R.; Pomelli, C.; Ochterski, J. W.; Martin, R. L.; Morokuma, K.; Zakrzewski, V. G.; Voth, G. A.; Salvador, P.; Dannenberg, J. J.; Dapprich, S.; Daniels, A. D.; Farkas, O.; Foresman, J. B.; Ortiz, J. V.; Cioslowski, J.; Fox, D. J. *Gaussian 09*, 2009.
38. (a) Lee, C.; Yang, W.; Parr, R. G., Development of the Colle-Salvetti Correlation-Energy Formula into a Functional of the Electron Density. *Physical Review B: Condensed Matter and Materials Physics* **1988**, *37*, 785-789; (b) Becke, A. D., Density-Functional Thermochemistry. III. The Role of Exact Exchange. *Journal of Chemical Physics* **1993**, *98*, 5648-5652.
39. Hay, P. J.; Wadt, W. R., Ab initio Effective Core Potentials for Molecular Calculations. Potentials for K to Au Including the Outermost Core Orbitals. *Journal of Chemical Physics* **1985**, *82*, 299-310.
40. (a) Hehre, W. J.; Ditchfield, R.; Pople, J. A., Self—Consistent Molecular Orbital Methods. XII. Further Extensions of Gaussian—Type Basis Sets for Use in Molecular Orbital Studies of Organic Molecules. *Journal of Chemical Physics* **1972**, *56*, 2257-2261; (b) Hariharan, P. C.; Pople, J. A., The Influence of Polarization Functions on Molecular Orbital Hydrogenation Energies. *Theoretical Chemical Acta* **1973**, *28*, 213-222; (c) Francl, M. M.; Pietro, W. J.; Hehre, W. J.; Binkley, J. S.; Gordon, M. S.; Defrees, D. J.; Pople, J. A., Self-Consistent Molecular Orbital Methods. XXIII. A Polarization-type Basis Set for Second-row Elements. *Journal of Chemical Physics* **1982**, *77*, 3654-3665.
41. (a) Grimme, S.; Antony, J.; Ehrlich, S.; Krieg, H., A Consistent and Accurate Ab Initio Parametrization of Density Functional Dispersion Correction (DFT-D) for the 94 Elements H-Pu. *Journal of Chemical Physics* **2010**, *132*, 154104; (b) Grimme, S.; Ehrlich, S.; Goerigk, L., Effect of the Damping Function in Dispersion Corrected Density Functional Theory. *Journal of Computational Chemistry* **2011**, *32*, 1456-1465.
42. (a) Krishnan, R.; Binkley, J. S.; Seeger, R.; Pople, J. A., Self-Consistent Molecular Orbital Methods. XX. A Basis Set for Correlated Wave Functions. *Journal of Chemical Physics* **1980**, *72*, 650-654; (b) McLean, A. D.; Chandler, G. S., Contracted Gaussian Basis Sets for Molecular Calculations. I. Second Row Atoms, Z = 11–18. *Journal of Chemical Physics* **1980**, *72*, 5639-5648.
43. (a) Miertus, S.; Tomasi, J., Approximate Evaluations of the Electrostatic Free Energy and Internal Energy Changes in Solution Processes. *Chemical Physics* **1982**, *65*, 239-245; (b) Mennucci, B.; Tomasi, J., Continuum Solvation Models: A New Approach to the Problem of Solute's Charge Distribution and Cavity Boundaries. *Journal of Chemical Physics* **1997**, *106*, 5151-5158; (c) Cossi, M.; Barone, V.; Mennucci, B.; Tomasi, J., Ab initio Study of Ionic Solutions by a Polarizable Continuum Dielectric Model. *Chemical Physics Letters* **1998**, *286*, 253-260.

Chapter 4

Application of a phosphite-oxazoline ligand library for Pd-catalyzed asymmetric allylic substitution reactions

4.1. Introduction

The obtention of chiral compounds is essential for many industries such as pharmaceutical, agrochemical or fragrance ones. Their preparation is still nowadays a fruitful research topic.[1] In this aspect, Pd-catalyzed asymmetric allylic substitution has proved to be one of the most efficient methods since it works under mild reaction conditions, it requires usually low catalyst loadings and it has a high functional group tolerance. Furthermore, the presence of a final alkene expands its synthetic application.[2] Although all these advantages, the nucleophile and substrate scope are mainly affected by the nature of the ligand used and usually the more successfully applied ligands do not tolerate well the changes on the substrates. Our group has expertise on the synthesis and application of biaryl phosphite-based ligands.[3] The biaryl phosphite group has been proved to be flexible enough to accommodate well in the chiral pocket the different steric demands on the substrates and therefore increases the substrate versatility. Moreover, phosphites are good π-acceptors which provides higher activity than the standard phosphines. We have previously studied the effect on the substitution of the phosphine group by a biaryl phosphite group in the privileged PHOX ligand.[2d] PHOX ligand **57** works successfully well for hindered substrates such as *rac*-(*E*)-1,3-diphenylallyl acetate (**S1**), but it provides deficient results (racemic) for cyclic substrates, such as benchmark cyclic substrate *rac*-cyclohex-2-en-1-yl acetate (**S2**). In contrast, when the phosphine group is replaced by a biaryl phosphite moiety the Pd-catalyzed allylic alkylation worked very successfully in both of them.[2d, 4]

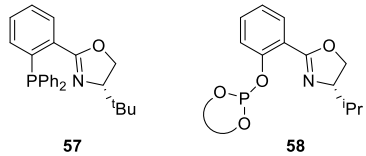

57 **58**

Figure. 4.1. PHOX ligand **57** and the phosphite-oxazoline ligand **58.**

Although ligand **58** has been successfully applied on Pd-catalyzed allylic asymmetric substitution reactions there is still change for improvement in terms of substrate and nucleophile scope. In order to add flexibility to ligand **58**, we have replaced the *o*-phenylene tether by an alkyl backbone chain that connect the oxazoline and the biaryl phosphite group (Figure 4.2). This simple modification allowed us to add new parameters which can be optimized to increase the catalyst performance. In this regard, we have systematically studied the effect on catalytic performance of the substituents and configuration of the oxazoline and biaryl phosphite group respectively, as well as the influence on the substitution and configuration of the substituent on the alkyl backbone chain. In this sense, we have successfully studied their application in Pd-catalyzed asymmetric allylic substitution with linear and cyclic substrates using a several

C-, O- and N-nucleophiles (up to 73 products). DFT calculations as well as NMR studies of the Pd-allyl intermediates allowed us to explain the enantioselectivities observed experimentally.

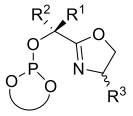

Figure. 4.2. General structure of the new phosphite-oxazoline ligands.

4.2. Results and discussion

4.2.1. Synthesis of the ligands L9-L16a,d-e

The ligands were synthesized in a straightforward manner requiring only of two- to five-steps (Scheme 4.1) starting from readily available compounds. Hence, ligands **L9a**,**d-e**, which are furnished with two methyl groups in the alkyl backbone chain, where synthesized in only two steps from unexpensive α-hidroxyisobutyric acid. The condensation reaction between this acid and (*S*)-phenylglycinol afforded the corresponding hydroxyl-oxazoline. Subsequent reaction with the corresponding phosphochloridite ($ClP(OR)_2$; $P(OR)_2$ = **a**,**d-e**) yielded ligands **L9a**,**d-e**.[5] The phosphochloridites were prepared by reaction of the corresponding BINOL derivative (**a**-**c**) with PCl_3 using pyridine or triethylamine as base.[5b]

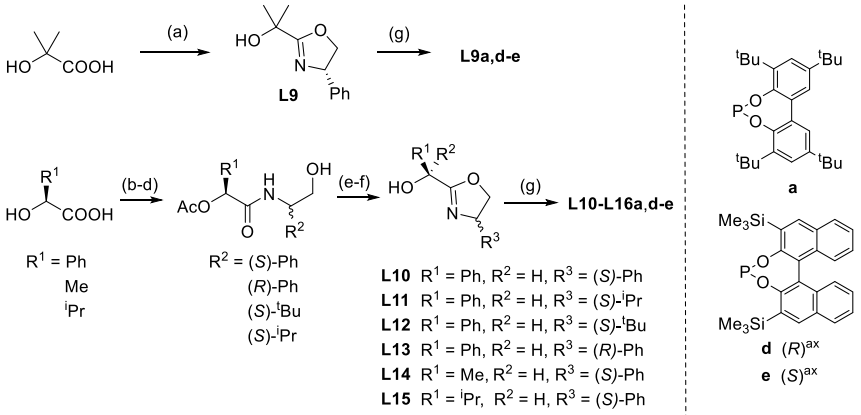

(a) (*S*)-phenylglycinol, xylene, reflux, 16 h. (b) Acetyl chloride, rt, 2 h; (c) Thionyl chloride, dichloromethane, reflux, 3 h. (d) Aminoalcohol, TEA, dichloromethane, 5 h. (e) DAST; potassium carbonate, dichloromethane, from -78 °C to r.t. 3 h. (f) NaOH (aq), ethanol, 0 °C, 3 h. (g) $ClP(OR)_2$, pyridine, toluene, from -78 °C to rt, 16 h.

Scheme 4.1. Synthesis for the preparation of ligands **L9**-**L16a**,**d-e**.

Phosphite-oxazoline ligands (**L10**-**L16a**,**d-e**) which in contrast with the previous ligands have a stereogenic center on the alkyl backbone chain were prepared as we previously reported.[6] In this case and in order to prevent the epimerization of the chiral center on the alkyl backbone chain, the synthesis involved the transformation of the corresponding α-hydroxy-acid to the amide by reaction with the corresponding amino-alcohol. Then the corresponding hydroxy-amides were cyclized by reaction with DAST (dimethylaminosulfur trifluoride) and subsequent standard deprotection yielded hydroxy-oxazolines **L10**-**L15**.[6-7] Finally, the reaction of compounds **L10**-**L15** with the corresponding phosphocloridite afforded the ligands **L10**-**L16a**,**d-e**.

To our delight, ligands **L9**-**L16a**,**d-e** were isolated as white air-stable solids and do not require inert atmosphere for their storage. HRMS-ESI and ^{1}H, ^{13}C and ^{31}P confirmed the formation of the desired compounds.

4.2.2. First ligand screening

With the ligands in hand, we first studied the Pd-catalyzed asymmetric allylic alkylation on the benchmark substrates hindered *rac*-(*E*)-1,3-diphenylallyl acetate (**S1**) and the more challenging cyclic unhindered *rac*-cyclohex-2-en-1-yl acetate (**S2**) using dimethyl malonate as nucleophile. The reaction conditions were chosen to be comparable to our first family of phosphite/oxazoline ligands, therefore, the reaction conditions were the same (23 °C, 0.5 mol% Pd/**L***).[4] The results are summarized in Table 4.1. We have found two ligands, **L9e** and **L14e**, that work well for both hindered substrate **S1** and unhindered substrate **S2** providing enantioselectivities up to 99% and with a high catalytic activity (TOF up to 8640 mol substrate x (mol Pd x h)$^{-1}$) (entries 3 and 14, respectively). The results obtained indicate that the three parameters in our ligands (substituent in alkyl backbone chain, substituent of the oxazoline and the biaryl phosphite used) have an influence in the catalytic results. Nevertheless, the influence of these three parameters in the enantioselectivities observed is different for each substrate type. While ligand **L9e**, furnished with two methyl groups in the alkyl backbone chain, provides the highest enantiomeric excess in the alkylation of cyclic substrate **S2**, its counterpart **L14e** gives the best *ee* values for linear substrate **S1** (entries 3 and 14, respectively).

The enantioselectivities observed with ligands **L9a**,**d-e** with the achiral alkyl backbone chain indicate that these catalytic systems can only control the alkylation well in the linear substrate **S1** (entries 1-3) since for cyclic substrate **S2** it is required to have the match configuration between the biaryl phosphite moiety (with (*S*) configuration) and the oxazoline substituent ((*S*)-phenyl) to attain 99% of *ee* (entry 3 vs 1 and 2). The same trend is observed for ligands **L10**-**L15** where match-mismatch interactions between the chiral alkyl backbone chain, the configuration of the biaryl-phosphite moiety and the substituent of the oxazoline affect to the catalytic performance of our system.

Table 4.1. First ligand screening by using **S1** or **S2**, ligands **L9**-**L16a**,**c-e** and dimethyl malonate as nucleophile.[a]

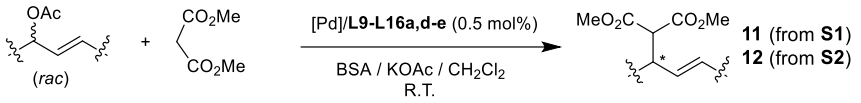

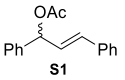

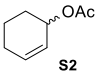

Entry	L	% Conv (h)[b]	%ee[c]	% Conv (h)[b]	%ee[d]
1	**L9a**	100	96 (*S*)	100	60 (*S*)
2	**L9d**	100	86 (*S*)	100	78 (*R*)
3	**L9e**	100	96 (*S*)	100	99 (*S*)
4	**L10a**	100	93 (*S*)	100	40 (*S*)
5	**L10d**	100	40 (*S*)	100	74 (*R*)
6	**L10e**	100	90 (*S*)	100	90 (*S*)
7	**L11a**	100	92 (*S*)	100	7 (*S*)
8	**L12a**	100	73 (*S*)	100	4 (*S*)
9	**L13a**	100	90 (*R*)	100	20 (*R*)
10	**L13d**	100	94 (*R*)	100	81 (*R*)
11	**L13e**	100	55 (*R*)	100	77 (*S*)
12	**L14a**	100	97 (*S*)	100	44 (*S*)
13	**L14d**	100	89 (*S*)	100	65 (*R*)
14	**L14e**	100	99 (*S*)	100	96 (*S*)
15	**L15a**	100	84 (*S*)	100	33 (*S*)
16	**L15d**	100	91 (*S*)	100	60 (*R*)
17	**L15e**	100	90 (*S*)	100	97 (*S*)
18[e]	**L14e**	72	99 (*S*)	41	96 (*S*)

[a] 0.5 mol% $[PdCl(\eta^3\text{-}C_3H_5)]_2$, ligand (0.011 mmol), substrate (1 mmol), CH_2Cl_2 (2 ml), BSA (3 eq), dimethyl malonate (3 eq), KOAc (pinch) at rt for 10 min. [b] Conversion percentage determined by ^{1}H-NMR. [c] determined by HPLC or GC. Absolute configuration drawn in parentheses. [d] Calculated by GC. [e] 5 minutes reaction with 0.1% mol of Pd catalyst.

The influence of the oxazoline substituent was also studied. When the oxazoline ring is furnished by a bulky group, such as *tert*-butyl or isopropyl (**L11** and **L12**) the enantiodiscrimination decreases, especially for cyclic substrate **S2** (entries 7 and 8). On the other hand, when the oxazoline is substituted with a less steric demanding phenyl ring the enantioselectivities observed are better (entry 4). Furthermore, the phenyl substituted oxazoline is more advantageous since it can be synthesized from (*S*)-phenylglycinol which is cheaper than (*S*)-*tert*-leucinol (for **L12a**).

The comparation of the diasteromeric ligands (**L10d-e** and **L13d-e**) stablishes the presence of match and mismatch interactions between the configuration of both the biaryl phosphite moiety and the oxazoline substituent. The match configuration is observed in ligands **L10e** and **L13d** (entries 6 and 10). In this regard, the configuration of the alkylated product using hindered substrate **S1** is mainly controlled by the configuration on the oxazoline ring, whereas for the unhindered cyclic **S2** is the biaryl phosphite group configuration who controls the configuration outcome. Therefore, both

enantiomers of the alkylated substrate are available just by carefully choosing the correct combination of ligand parameters.

The last parameter that we studied was the influence of the substituent in the alkyl backbone. For this, we compared the ligands **L9**, **L10**, **L14** and **L15**, where the alkyl backbone is substituted by a dimethyl-, phenyl-, methyl- or isopropyl-group, respectively. The best performing ligands were **L9** for cyclic substrate **S2** and **L14** for linear substrate **S1** which contains a dimethyl group and a methyl group in the alkyl backbone chain, respectively.

To sum up, the enantioselectivities observed using Pd/**L9e** and Pd/**L14e** catalytic systems are comparable to the obtained with our first family of phosphite/oxazoline ligands (**57**). With the addition that our ligands have provided TOF values three times higher than those with the first family (>8000 *vs* >2400 mol substrate x (mol Pd x h)$^{-1}$).[4]

4.2.3. Substrate scope with linear- and cyclic-type substrates using several C-, O- and N-nucleophiles

With the best performing ligands in hand, we have further studied the Pd-catalyzed asymmetric allylic substitution of different substrates including other linear substrates (unsymmetrical 1,3-disubstituted) and cyclic substrates with different ring sizes. Furthermore, the nucleophiles used include those that are more exciting from a synthetic point of view (amines, β-diketones, substituted malonates, 2-cyanoacetates, pyrroles, aliphatic alcohols, and amines).

First, we studied the nucleophile scope with linear substrate **S1** using Pd/**L14c** catalytic system, which was the best performing using dimethyl nucleophile as nucleophile. To our delight, a range of C-, N- and O-nucleophiles were successfully alkylated with high yields and enantioselectivities.

First, we examinated the C-alkylation of **S1** (Table 4.2). High enantioselectivities, up to >99% and yields were attained when malonates were used (Table 4.2, entries 1-7), even with the substituted ones which can serve as useful intermediates for the preparation of more complex molecules. The alkylation of other dicarbonyl analogues nucleophiles such as acetylacetone and malonitrile (entries 8-9) gave the corresponding alkylated products in excellent yields and enantioselectivities (>99% *ee*). In the case of isopropyl cyanoacetate, we obtained excellent *ee* values albeit the low diastereomeric control (entry 10).

Table 4.2. Nucleophile scope for Pd/**L14e** system using **S1** as substrate.[a]

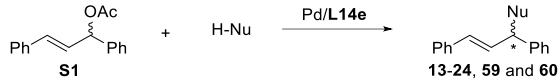

Entry	Product	% Yield[b]	% *ee*[c]	Entry	Product	% Yield[b]	% *ee*[c]
1	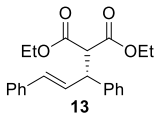 **13**	94	>99 (*S*)	8	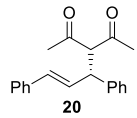 **20**	91	>99 (*S*)
2	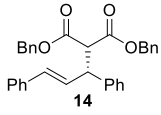 **14**	93	>99 (*S*)	9	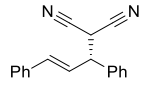 **21**	90	>99 (*S*)
3	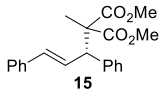 **15**	94	>99 (*R*)	10	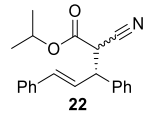 **22**	91 (55:45 *dr*)	99/96
4	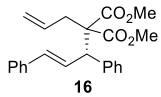 **16**	92	99 (*R*)	11[c]	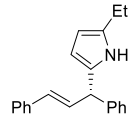 **23**	91	95 (*R*)
5	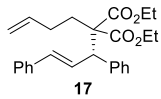 **17**	89	>99 (*R*)	12[c]	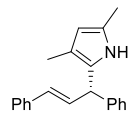 **24**	91	92 (*R*)
6	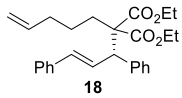 **18**	90	>99 (*R*)	13[c]	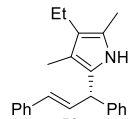 **59**	89	99 (*R*)
7	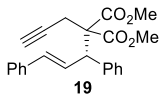 **19**	89	>99 (*R*)	14[d,e]	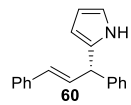 **60**	54	62 (*R*)

[a] 0.5 mol% $[PdCl(\eta^3\text{-}C_3H_5)]_2$, ligand (0.011 mmol), substrate (1 mmol), CH_2Cl_2 (2 ml), BSA (3 eq), Nucleophile (3 eq), KOAc (pinch) at rt for 2 h. [b] Full conversions. [c] Determined by HPLC. [d] Using K_2CO_3 (3 equiv). [e] Reaction at -20 °C for 48 h.

We also attempted the alkylation of pyrrole rings. Pyrrole heterocycle can be found in several interesting molecules as well as in compounds of biologically relevance.[8] As it was previously pointed out in our indene-based P,S-ligand library (see Chapter 3), the benchmark ligands for this transformation such as Trost ligands are not compatible with the use of pyrroles and their use in Pd-AAS has been only reported once requiring low temperatures (-20 °C) to attain high *ee*'s. To our delight, we could attain high levels of enantioinduction for the Pd-AAS of substituted pyrroles using Pd/**L14c** catalytic system (entries 12-14) at room temperature albeit that for non-substituted alkylated pyrrole **60**

the *ee* value observed was some lower and required lower reaction temperature (-20 °C) and a longer reaction time (48 h).

Then, we tried Pd/**L14e** catalytic system in several N- and O-nucleophiles (Table 4.3). This catalytic system performed well when using amines as nucleophiles obtaining enantioselectivities comparable with those obtained with C-nucleophiles. Thus, we could achieve the substitution of several primary and secondary amines (aryl-, alkyl-, and propargyl-substituted amines). In this context, when benzyl- and furfurylamine were used, yields and enantioselectivities remained excellent (entries 15-18). Primary amines also were alkylated with high enantiocontrol (entries 22-23) as well as cyclic secondary amines (entries 19 and 24). The use of aromatic amines such as tosylamine or aniline also provided excellent results (entries 25-26) (*ee* up to >99%). The Pd/**L14e** catalytic system performed better than previously Pd/**58** catalysts, since the latter only provided high levels of enantiocontrol when benzylamine was used as nucleophile.[4]

The excellent enantioselectivities achieved with amines were also obtained when alcohols were used as nucleophiles (entries 13-19). In this regard, the addition of O-nucleophiles gave the corresponding chiral ethers with enantioselectivities comparable with those obtained with dimethyl malonate. In this regard, aliphatic alcohols are of high interest since they can be found in biological active molecules.[9] Nevertheless, successfully applications in Pd-AAS are reported only in few references.[10] In this regard, the success on the enantiodiscrimination is highly affected by the electronic characteristics of the aliphatic alcohol. As can be seen, excellent enantioselectivities were observed with a broad range of benzylic alcohols (entires 27-30) except for the *p*-CF_3 substituted one, which gave some lower *ee*. We also attained the substitution of butanol albeit with lower enantiomeric control (entry 33, *ee* up to 72%). Despite that, enantioselectivities up to 99% were achieved with the addition of less studied allyl alcohol and trihpenylsilanol (entries 31-32).[10d, 11]

In this regard, malonates, including those bearing allyl, pentenyl or propargyl groups, could be used leading to yields and enantioselectivities as high as those obtained with **S1** (entries 1-6, *ee* up to >99%). We also were able to attain excellent results in substrates **S6** and **S7** that are more sterically demanding and are typically obtained with lower levels of enantioinduction (entries 7 and 8, *ee* up to >99%). In addition, our Pd/**L14e** catalytic system was also successfully applied in the less sterically demanding substrate **S10** which only few systems attain this level of enantioinduction with the use of propargyl malonate as nucleophile.

Table 4.3. N- and O-alkylation for Pd/**L14e** system using **S1** as substrate.[a]

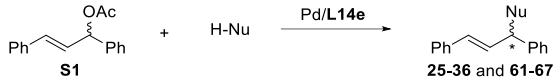

Entry	Product	% Yield[b]	% *ee*[c]	Entry	Product	% Yield[b]	% *ee*[c]
1	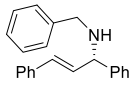 **25**	85	>99 (*R*)	11	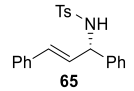 **65**	91	98 (*R*)
2	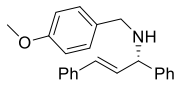 **26**	81	99 (*R*)	12	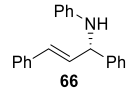 **66**	83	>99 (*R*)
3	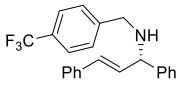 **27**	83	>99 (*R*)	13[d]	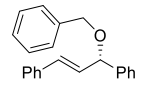 **31**	91	99 (*R*)
4	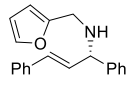 **28**	92	99 (*R*)	14[d]	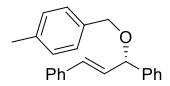 **32**	90	99 (-)
5	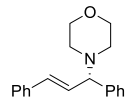 **29**	84	93 (*R*)	15[d]	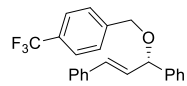 **33**	89	60 (-)
6	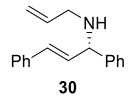 **30**	76	97 (*R*)	16[d]	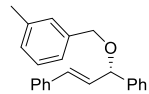 **34**	91	97 (-)
7	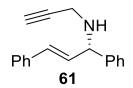 **61**	71	98 (*R*)	17[d]	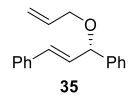 **35**	79	99 (-)
8	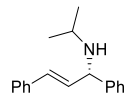 **62**	83	93 (*R*)	18[d]	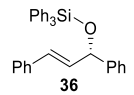 **36**	87	99 (*R*)
9	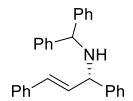 **63**	75	96 (*R*)	19[d]	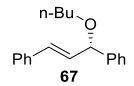 **67**	95	72 (*S*)
10	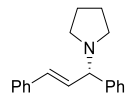 **64**	80	92 (*R*)				

[a] 0.5 mol% $[PdCl(\eta^3\text{-}C_3H_5)]_2$, ligand (0.011 mmol), substrate (1 mmol), CH_2Cl_2 (2 ml), BSA (3 eq), Nucleophile (3 eq), KOAc (pinch) at rt for 2 h. [b] Full conversion. [c] Determined by HPLC. [d] 2 mol% $[PdCl(\eta^3\text{-}C_3H_5)]_2$, 4 mol% of ligand, and $CsCO_3$ (3 eq) as base.

Table 4.4. Substrate and nucleophile scope of different hindered substrates with Pd/**L14e**.[a]

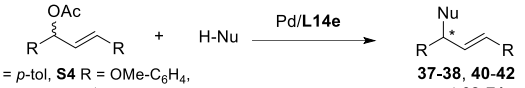

S3 R = *p*-tol, **S4** R = OMe-C_6H_4, **S6** R = *o*-tol, **S7** R = ^{i}Pr, **S10** R = Me

37-38, **40-42** and **68-71**

Entry	Substrate	Product	% Yield[b]	% *ee*[c]
1	**S3**	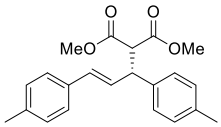 **37**	91	>99 (*S*)
2	**S3**	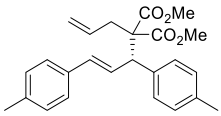 **38**	92	>99 (*R*)
3	**S3**	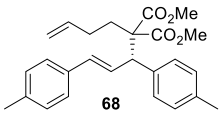 **68**	88	>99 (*R*)
4	**S3**	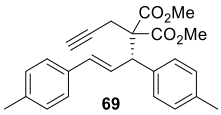 **69**	90	>99 (*R*)
6	**S5**	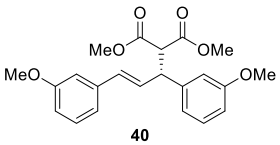 **40**	86	>99 (*S*)
7	**S6**	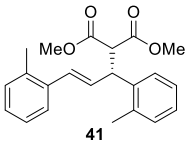 **41**	87	>99 (*S*)
8	**S7**	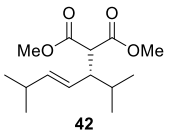 **42**	86	>95 (*S*)
9	**S10**	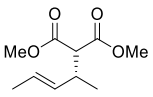 **70**	86	82 (*S*)
10	**S10**	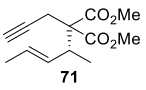 **71**	78	83 (*S*)

[a] 0.5 mol% [PdCl(η^3-C_3H_5)]$_2$, ligand (0.011 mmol), substrate (1 mmol), CH_2Cl_2 (2 ml), BSA (3 eq), Nucleophile (3 eq), KOAc (pinch) at rt. [b] Full conversions were obtained after 2 h except for substrates **S6** and **S7** that required 12 h and **S9** that required 18 h. [c] Determined by HPLC.

The scope was also expanded by studying the Pd-asymmetric allylic alkylation of other challenging linear unsymmetrically disubstituted substrates. For this type of substrates, the regioselectivity of the transformation must be also considered. In this regard, most of the catalytic systems are reported to proceed by a kinetic resolution which limits the yield to 50%.[12] Nevertheless, few examples in which the catalyst is able to epimerize the Pd-allyl intermediate in the reaction conditions and therefore proceed *via* a DYKAT (dynamic kinetic asymmetric transformation) process are found in the literature.[13] We focused in CF_3- substituted substrate **S11** due to the relevance that chiral organofluorine compounds have nowadays (Table 4.5). In this regard, there is only one successful example with substrate **S11**, using a Pd/(*S*)-tol-BINAP catalytic system and requiring 10 mol% Pd, a temperature of 60°C and dioxane as solvent. To our delight, our Pd/**L14e** system was able to promote the epimerization of *rac*-**S11** in the Pd-intermediate and therefore proceed by a DYKAT under mild reaction conditions. Therefore, we were able to alkylate substrate **S11** using several C-nucleophiles including substituted malonates such as allyl or propargyl which can be further derivatize to obtain more complex molecules (see Chapter 5).

Table 4.5. Substrate and nucleophile scope of unsymmetrically disubstituted substrate **S11** with Pd/**L14e**.[a]

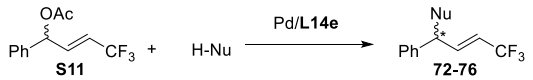

Entry	Product	% Yield[b]	% *ee*[c]
1	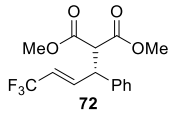 **72**	71	76 (*R*)
2	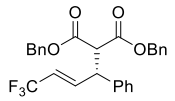 **73**	62	78 (*R*)
3	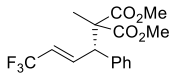 **74**	59	80 (*S*)
4	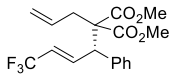 **75**	60	77 (*S*)
5	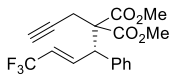 **76**	62	73 (*S*)

[a] 0.5 mol% $[PdCl(\eta^3\text{-}C_3H_5)]_2$, ligand (0.011 mmol), substrate (1 mmol), CH_2Cl_2 (2 ml), BSA (3 eq), Nucleophile (3 eq), KOAc (pinch), 40 °C for 18 h. [b] Full conversions. [c] Determined by HPLC.

As we mentioned before, catalytic systems able to alkylate both hindered and unhindered substrates with excellent enantioselectivities are very difficult to find. In this

regard, our ligand screening showed that Pd/**L9e** catalytic system was able to alkylate benchmark cyclic substrate **S2** with excellent levels of enantioinduction (up to 99% *ee*) using dimethyl malonate as nucleophile (*vide supra,* entry 3, Table 4.1). Encouraged with these results, we further tested our Pd/**L9e** catalytic system in the Pd-AAS of substrates **S2**, **S8** and **S9** which differs in the ring size.

Table 4.6. Allylic alkylation of unhindered cyclic substrates using different C- and N-nucleophiles.[a]

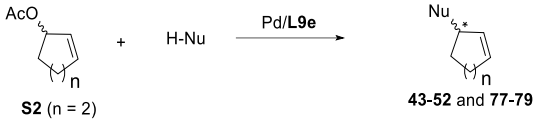

S2 (n = 2)
S8 (n = 1)
S9 (n = 3)

43-52 and **77-79**

Entry	Product	% Yield[b]	% *ee*[c]	Entry	Product	% Yield[b]	% *ee*[c]
1	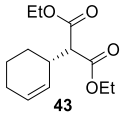 **43**	82	99 (*S*)	8	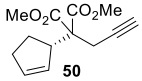 **50**	89	93 (*S*)
2	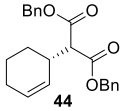 **44**	89	98 (*S*)	9	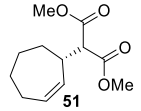 **51**	87	>99 (*S*)
3	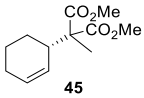 **45**	86	99 (+)	10	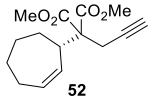 **52**	93	>99 (*S*)
4	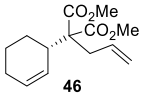 **46**	79	95 (-)	11[d]	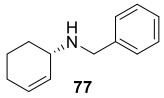 **77**	95	81 (*S*)
5	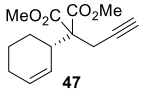 **47**	80	>99 (*S*)	12[d]	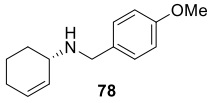 **78**	81	79 (*S*)
6	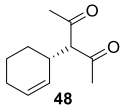 **48**	76	99 (-)	13[d]	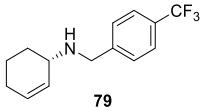 **79**	90	83 (*S*)
7	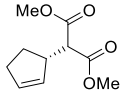 **49**	81	91 (-)				

[a] 0.5 mol% [PdCl(η^3-C_3H_5)]$_2$, ligand (0.011 mmol), substrate (1 mmol), CH_2Cl_2 (2 ml), BSA (3 eq), dimethyl malonate (3 eq), KOAc (pinch) at rt for 2 h. [b] Full conversion. [c] Determined by HPLC or GC. [d] This reaction required the carbonate version of **S2**, *rac*-cyclohex-2-en-1-yl ethyl carbonate, 1 mol% Pd/**L9e** and 18 h.

The application of this system on cyclohexenyl derivative **S2** provided delightful results obtaining excellent yields and enantioselectivities (up to >99%) using several

malonates, even with propargyl malonate which in our reported Pd/**58** catalytic system was obtained in lower enantioselectivity (entries 1-7, *ee's* up to 99%). These excellent results were also attained when cycloheptenyl derivative **S9** was used (entries 9 and 10, *ee's* up to >99%) as well as for the more challenging cyclopentenyl derivative **S8** (entries 7 and 8, *ee's* up to 93%). It is worth to mention that propargyl derivatives **47**, **50** and **52** can further derivatized to more complex chiral molecules (*vide infra,* Chapter 5).

Cyclic substrates can also serve as platforms for the Pd-catalyzed asymmetric allylic amination, although it has been much less studied. In this regard, the systems found in the literature perform worst with amino nucleophiles and they usually provide low enantiomeric excesses.[2b, k, 14] Thus, we further tested our Pd/**L9e** catalytic system in the amination of **S2**. In this regard, we succeeded in the application of our Pd/**L9e** catalytic system using amines as nucleophiles albeit the *ee* were somewhat lower than in the allylic alkylation (entries 11-13). The results obtained showed that the system is hardly influenced by the electronic properties of the group in *para* position of the benzylamine used.

As our catalytic system performed well in 1,3-disubstituted substrates, we wonder if this performance could be retained to the monosubstituted ones. Monosubstituted substrates differs on the 1,3-substituted that the system must control not only the enantioselectivity but also the regioselectivity. Most of the Pd-catalytic systems found in the literature usually give the achiral linear products and therefore the search for a system which can control the regio- and the enantioselectivity on these substrates is still highly needed.[15]

First, we studied the ligand influence in the regioselectivity and the enantioselectivity in the allylic alkylation of benchmark monosubstituted substrate **S12** using dimethyl malonate as nucleophile (Table 4.7).

Table 4.7. Ligand screening for monosubstituted substrate **S12** using dimethyl malonate as nucleophile.[a]

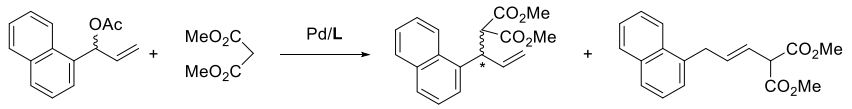

S12 **80a** **80b**

Entry	Ligand	% conv (% yield)[b]	% branched[c]	% *ee*[d]
1	**L9a**	100 (88)	80	64 (*S*)
2	**L9d**	100 (89)	80	37 (*S*)
3	**L9e**	100 (88)	75	88 (*S*)
4	**L10a**	100 (91)	75	64 (*S*)
5	**L10d**	100 (89)	80	34 (*S*)
6	**L10e**	100 (90)	75	91 (*S*)
7	**L13a**	100 (89)	80	45 (*R*)
8	**L13d**	100 (88)	85	87 (*R*)
9	**L13e**	100 (91)	70	45 (*R*)
10	**L14e**	100 (90)	70	93 (*S*)
11[b]	**L15e**	100 (91)	90	98 (*S*)

[a] 1 mol% $[PdCl(\eta^3\text{-}C_3H_5)]_2$, 2.2 mol% ligand, benzene, BSA/KOAc as base at 0°C for 1h. [b] Full conversion. [c] Calculated by NMR from the reaction crude. [d] Determined by HPLC.

We found that the regioselectivity was not substantially affected by the ligand used whereas for the enantioselectivity the ligand used was crucial. The results indicated that the enantioselectivity was affected by both of the oxazoline and the nature of the biaryl phosphite group like in the case of substrate **S1** but the substituent in the alkyl backbone chain affected differently. In this sense, the best performing ligand was **L15e** where the alkyl backbone chain is furnished with a chiral isopropyl group (*ee* up to 98%, entry 8). As it was found for the allylic alkylation of substrate **S1**, the configuration of the resulting product was determined by the configuration of the oxazoline substituent (entries 4-6 *vs* 7-9) whereas the value of the enantioselectivity was dependent on the match or mismatch configurations of the biaryl phosphite moiety and the oxazoline substituent (ligand **L9e** vs ligand **L13d**, entries 6 and 8 respectively).

With the best-performing ligand **L15e** in hand, we further studied different monosubstituted substrates with other steric and electronic demands using several C-nucleophiles (Table 4.8). First, we studied the alkylation of substrates **S13**-**S18** with dimethyl malonate as nucleophile. We observed previously with Pd/**58** catalytic system that the enantioselectivity and the regioselectivity to the branched isomer were reduced when the 1-naphthyl group on **S12** is replace by a phenyl ring (**S13**).[11] Furthermore, the regioselectivity decreasing was more evident when using substrates with electron-withdrawing groups (**S16**). In this sense, we overcame these limitations attaining high enantioselectivities (*ee* up to 96%, entry 5) and regioselectivities (up to 83%, entry 1) using dimethyl malonate as nucleophile regardless the substitution pattern on the substrates. Finally, we also studied the influence of other carbon nucleophiles. When α-substituted malonates were used as nucleophiles, promising high enantioselectivities were attained albeit the regiocontrol was somewhat lower (entries 7-9).

Table 4.8. Substrate and nucleophile scope of unsymmetrically disubstituted substrate **S11** with Pd/**L15e**.[a]

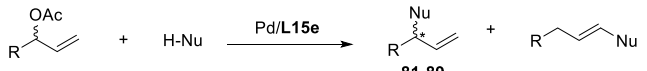

81-89

S13 R = Ph, **S14** R = *p*-tol, **S15** R = *p*-OMe-C_6H_4, **S16** R = *p*-CF_3-C_6H_4, **S17** R = m-OMe-C_6H_4, **S18** R = 2-Napth

Entry	Substrate	Product	% Yield[b] (% branched)[c]	% *ee*[d]
1	**S13**	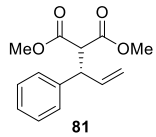 **81**	93 (83)	94 (*S*)
2	**S14**	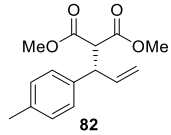 **82**	91 (78)	95 (*S*)

(continuation)

Entry	Substrate	Product	% Yield[b] (% branched)[c]	% *ee*[d]
3	**S15**	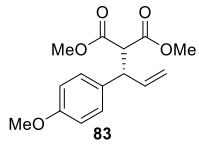 **83**	85 (82)	93 (*S*)
4	**S16**	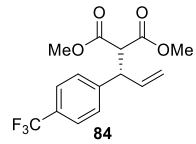 **84**	92 (75)	92 (*S*)
5	**S17**	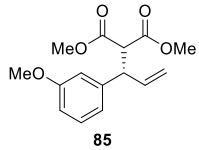 **85**	89 (81)	96 (*S*)
6	**S18**	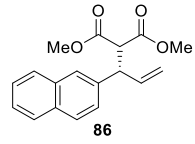 **86**	87 (81)	96 (*S*)
7	**S13**	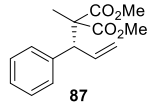 **87**	81 (60)	86 (*R*)
8	**S13**	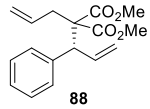 **88**	79 (50)	88 (*R*)
9	**S13**	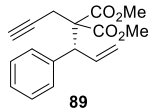 **89**	84 (55)	89 (*R*)

[a] 0.5 mol% $[PdCl(\eta^3\text{-}C_3H_5)]_2$, 1.1 mol% ligand, benzene, BSA/KOAc as base at 0 °C for 2 h. [b] Full conversion. [c] Calculated by NMR from reaction crude. [d] Determined by HPLC.

4.2.4. DFT calculations

Published mechanistic studies regarding Pd/phosphite-oxazoline **58** systems have established that nucleophilic attack, which control enantiomeric output, takes place though an early transition state (TS).[11] Therefore, the enantiomeric outcome is controlled by electrophilicity on the allylic carbons in the TS's. This agrees with the higher *trans* influence of P-group *versus* the oxazoline group and therefore, being the more reactive carbon *trans* to phosphorous.[16] With the objective of determinate the origin of the enantioselectivity we have carried out a DFT studies on the early TS's involving the alkylation of both hindered substrate **S1** and the unhindered one **S2** with

ligands **L9d**, **L9e** and **L14e** (Table 4.9). We have studied the effect on the stereochemical outcome of varying the configuration of the biaryl phosphite group (**L9d** and **L9e**) as well as the effect of having a chiral substituent on the alkyl backbone chain (Ligand **L14e**). The DFT studies were performed using ammonia as nucleophile to speed up the calculations. Furthermore, only the Pd-allyl compounds with *syn-syn* configuration on the allyl were considered (TS_{endo} and TS_{exo}) since the *anti-anti* and *anti-syn* species are higher in energy and they can be neglected.[2c]

Thus, we calculated the most stable TS for each enantiomer respectively ($TS_{(S)}$ and $TS_{(R)}$) with these three ligands. The calculated energies agreed with the enantioselectivities observed experimentally for both substrates. In this regard, the calculations identified that Pd/**L9e** and Pd/**L14e** catalytic systems gave better enantiomeric excesses than Pd/**L9d**. The same results are obtained comparing Pd/**L9e** and Pd/**L9d** systems where the Pd/**L9e** energy gap between the TS's is higher than Pd/**L9d** which is in concordance with the higher enantioselectivity observed experimentally (Table 4.1, 96% (*S*) *ee* for **S1** and 99% (*S*) *ee* for **S2** using **L9e** and 86% (*S*) *ee* for **S1** and 78% (*R*) *ee* for **S2** using **L9d**). Calculated TS also predicted the formation of the opposite enantiomer on **S2** when the opposite configuration on the biaryl phosphite group was used (**L9d** vs **L9e**).

Table 4.9. DFT calculated energies of the most stable TSs with hindered and unhindered benchmark substrates **S1** and **S2** and NH_3.[a]

	Relative Energies of TSs				**Relative Energies of TSs**		
Conformation of the TS	**L9d**	**L9e**	**L14e**	Conformation of the TS	**L9d**	**L9e**	**L14e**
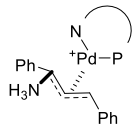 $TS_{(R)}$ endo	16.6[b]	21	14.2	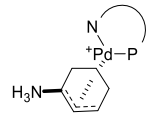 $TS_{(S)}$ endo	5[c]	0	0
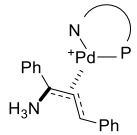 $TS_{(S)}$ exo	5.4[b]	0	0	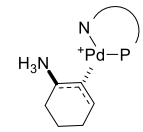 $TS_{(R)}$ exo	4[c]	15.6	13.6

[a] All energies given are relative and in kJ/mol. [b] Relative to $TS_{(R)}$ exo-**L9e** [c] Relative to $TS_{(R)}$ endo-**L9e**.

The analysis of the 3D plotting's of the most stable calculated TS's for ligands **L9d** and **L9e** and substrates hindered **S1** and unhindered **S2** allowed us to evaluate the influence of the configuration of the biaryl phosphite group in the enantioselectivity. As can be seen, in the case of **S1** a repulsive interaction between the oxazoline substituent of both ligands **L9d** and **L9e** with the phenyl substituent of **S1** destabilizes all the *endo* isomers. This repulsive interaction between **S1** and the ligands increases the dihedral angle between the alkyl backbone chain and the oxazoline group (ω C^1-N-C^2-C^3) in TSs

exo respect their counterpart TSs *endo*. Thus, this unfavourable interaction, in the case of TSs *endo*, pushes ultimately away the oxazoline and therefore causing a lower dihedral angle. In contrast, with the cyclic substrate **S2** this repulsive interaction cannot be found. These desestabilizating interactions show why the stereochemical outcome is the same for **S1**.

For hindered substrate **S1** and Pd/**L9e** there is in *exo* $TS_{(s)}$ a CH/π interaction between the biaryl phosphite group and one of the phenyl substituents on **S1** (Figure 4.3) that supplementary stabilizes this TS. This stabilization increases further the energy difference between the TS *exo* and TS *endo* which is therefore translated with the higher levels of enantioinduction observed with Pd/**L9e** respect its counterpart Pd/**L9d**. In the case of Pd/**L9d** there is also a CH/π interaction but in the *endo* $TS_{(R)}$. Thus, the energy gap between both TS's are more similar than its Pd/**L9e** counterpart (see Figure 4.3).

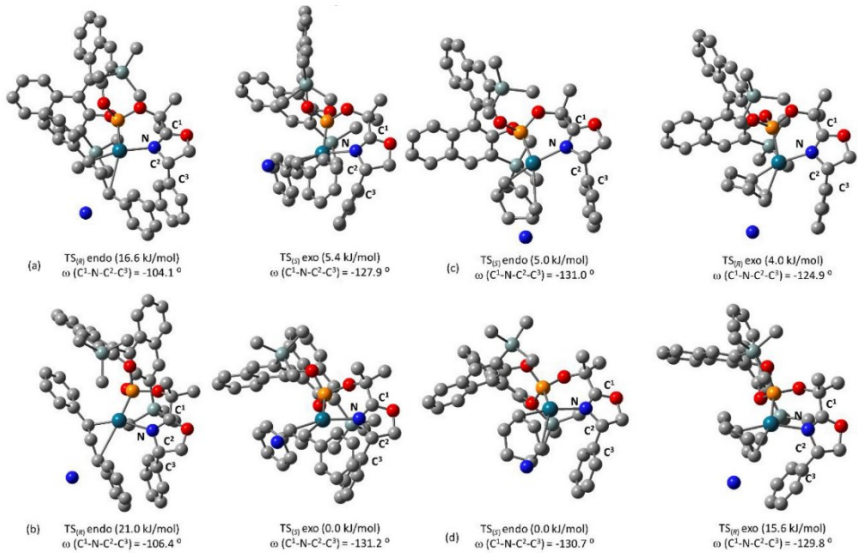

Figure. 4.3. 3D representation of the most stable calculated TSs. $TS_{(S)}$*exo* and $TS_{(R)}$*endo* for **S1** with ligands **L9d** and **L9e**, (a) and (b), respectively, and $TS_{(R)}$ *exo* and $TS_{(S)}$*endo* for **S2** with ligands **L9d** and **L9e**, (c) and (d) respectively.

The analysis of the NCI plots (Non-covalent Interactions) of the TSs regarding **S2** with Pd/**L9d** and Pd/**L9e** systems were more conclusive to explain the stereochemical outcome obtained (Figure 4.4). In this regard, the two most stable TSs with ligands **L9e** and **L9d,** respectively, showed weak stabilizing attractive interactions between the aryl groups of the phosphite moiety and the substrate. When the ligand used had $(R)^{axial}$ configuration on the biaryl phosphite group (ligand **L9d**) the favorable attractive interactions are found in the $TS_{(R)}$-*exo* and therefore, the *R*-enantiomer is produced. In contrast for **L9e**, the interactions found are by far larger in the $TS_{(S)}$-*endo* which leads to the formation of the *S*-enantiomer.

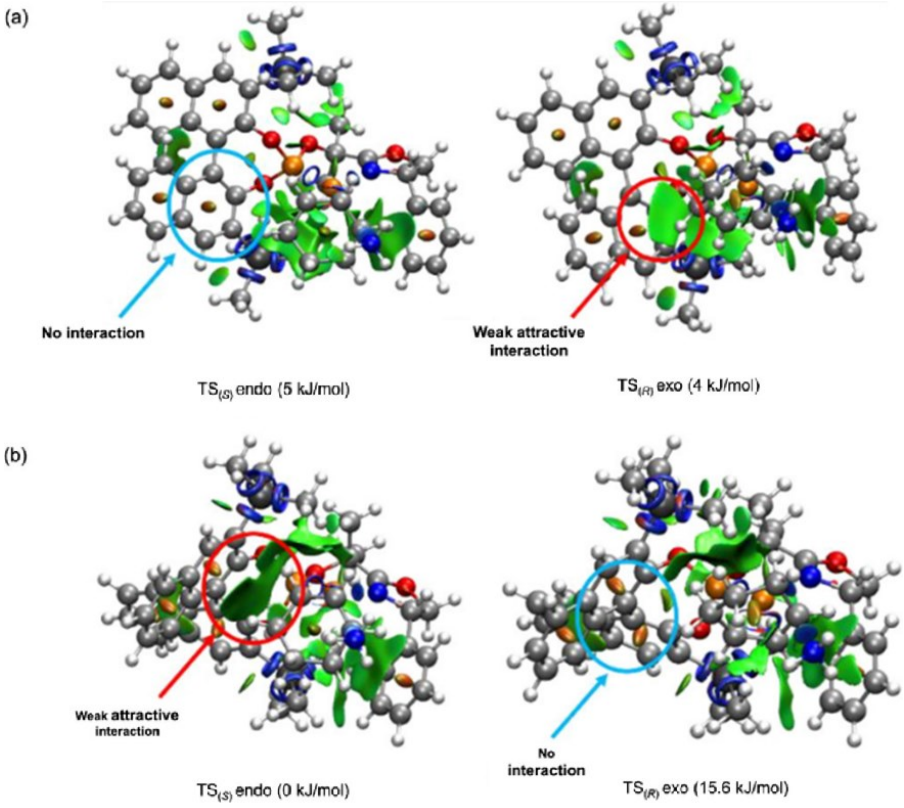

Figure. 4.4. NCI plotting of the most stable TSs for **S2,** $TS_{(R)}$-*endo* and $TS_{(S)}$-*exo*, using ligands **L9d** for (a) and **L9e** for (b). The green color indicates weak attractive interactions, the blue those that are highly attractive and red the highly repulsive interactions.

To sum up, the DFT calculations has stablished that, the enantioselectivity outcome in the cyclic substrate **S2** is controlled by weak interactions between the substrate and the biaryl phosphite moiety. In contrast, for the linear hindered substrate **S1**, the oxazoline ring has also an important role.

4.2.5. Synthesis and preparation of the Pd-allyl intermediates and their study by NMR spectroscopy

As pointed out by DFT calculations, the enantiomeric output is determined during nucleophilic attack by an early transition state. To further study the influence on the enantioselectivity of different groups in the alkyl backbone chain. We prepared Pd-allyl complexes **90**-**93** studied the coordination and reactivity by NMR and VT-NMR experiments.

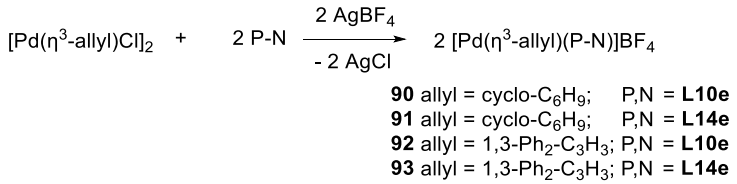

Scheme 4.2. Preparation of the Pd-allyl complexes **90**-**93**.

The Pd-allyl complexes **90**-**93** were prepared analogously to those prepared in Section 3.2.4 for P-S ligands. We choose the ligands **L10e** and **L14e** since they differ on the chiral-substituted alkyl backbone chain between the oxazoline and the biaryl phosphite group, having **L10e** a chiral-phenyl group and **L14e** a chiral-methyl group.

The VT-NMR from (30 to -80 °C) of the Pd- intermediates **90** and **91** show a mixture of *exo* and *endo* at a ratio of 3:1 and 10:1, respectively. No changes in VT-experiment were observed in the range of temperatures studied. This indicates that the equilibria between the two isomers is fast, even at -80°C. The NOE experiments indicate that there is NOE effect between the terminal allylic protons and the ligand therefore indicating a *syn*/*syn* disposition. The NOE experiments were also conclusive to stablish the *exo* and *endo* disposition between them. The ^{13}C-NMR chemical shifts clearly indicated that the most electrophilic allylic terminus carbon atom is *trans* to the phosphite group, which has the higher *trans* effect. As the nucleophile attack occurs in the most electrophilic carbon and the diastereomeric excesses observed in the intermediates differs from the enantiomeric output found experimentally, the major isomer should react faster than the minor isomer. Furthermore, the chemical shift difference between the terminus carbon atoms of the isomers is higher in **90** ($\Delta\delta(^{13}C) \approx 12.4$ ppm) than in **91** ($\Delta\delta(^{13}C) \approx 8$ ppm), therefore, the major isomer of **90** (*exo*) should react faster than the major one (also *exo*) of **91**. Nevertheless, when sodium dimethyl malonate was added at low temperature, they both reacted at a similar rate, being $k_{exo/endo}$ 8 for **90** and 7.5 for the reaction with complex **91**. The higher enantioselectivity obtained by Pd/**L14e** system can be attributed to the higher relative population of the faster reacting isomer. Thus, in **S1**, Pd/**L14e** catalytic system can control better the population of the intermediates as well as the relative electrophilicity in the terminal allyl atoms, both being pivotal to obtain a high enantiocontrol.

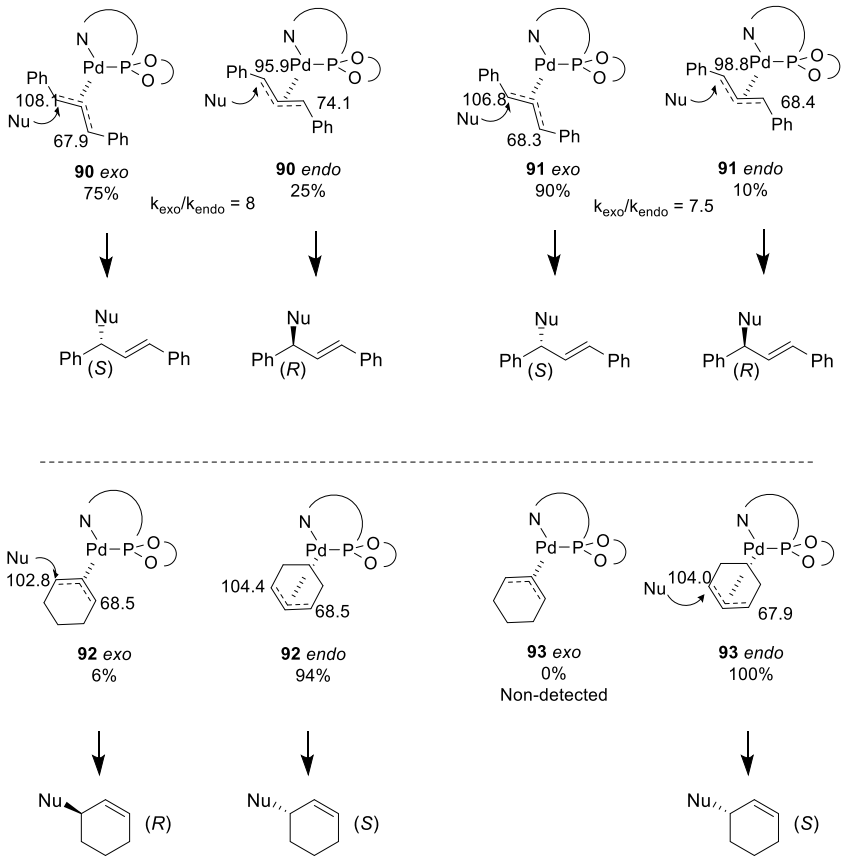

Scheme 4.3. Diastereomeric Pd-allyl intermediates for **S1** and **S2** with ligands **L10e** (**90** and **92**) and **L14e** (**91** and **93**).

The VT-NMR from (30 to -80 °C) of the Pd- intermediates **90** and **91** show a mixture of *exo* and *endo* at a ratio of 3:1 and 10:1, respectively. No changes in VT-experiment were observed in the range of temperatures studied. This indicates that the equilibria between the two isomers is fast, even at -80°C. The NOE experiments indicate that there is NOE effect between the terminal allylic protons and the ligand therefore indicating a *syn*/*syn* disposition. The NOE experiments were also conclusive to stablish the *exo* and *endo* disposition between them. The ^{13}C-NMR chemical shifts clearly indicated that the most electrophilic allylic terminus carbon atom is *trans* to the phosphite group, which has the higher *trans* effect. As the nucleophile attack occurs in the most electrophilic carbon and the diastereomeric excesses observed in the intermediates differs from the enantiomeric output found experimentally, the major isomer should react faster than the minor isomer. Furthermore, the chemical shift difference between the terminus carbon atoms of the isomers is higher in **90** ($\Delta\delta(^{13}C) \approx 12.4$ ppm) than in **91** ($\Delta\delta(^{13}C) \approx 8$ ppm), therefore, the major isomer of **90** (*exo*) should react faster than the major one (also *exo*) of **91**. Nevertheless, when sodium dimethyl malonate was added at low

temperature, they both reacted at a similar rate, being $k_{exo/endo}$ 8 for **90** and 7.5 for the reaction with complex **91**. The higher enantioselectivity obtained by Pd/**L14e** system can be attributed to the higher relative population of the faster reacting isomer. Thus, in **S1**, Pd/**L14e** catalytic system can control better the population of the intermediates as well as the relative electrophilicity in the terminal allyl atoms, both being pivotal to obtain a high enantiocontrol.

In the case of substrate **S2**, the VT-NMR study of the intermediates **92** and **93** showed that the relative population of *exo* and *endo* isomers was 1:15 for **92** and for complex **93** only the *endo* isomer was detected. The major isomers for both complexes were assigned as *endo* due to the NOE effects observed in NOE experiments. As can be seen in Scheme 4.3, the most electrophilic allylic terminus carbon atom shows very similar chemical shift, clearly indicating that both isomers should react at similar rate. So, we can conclude that the enantioselectivity is correlated by the relative ratio of *endo* and *exo* isomers. The higher enantioselectivity observed for Pd/**L14e** catalytic system can be rationalized by the fact that only the *endo* isomer was detected by NMR.

4.3. Conclusions

We have successfully applied a new ligand library based on phosphite-oxazoline ligands for Pd-catalyzed asymmetric allylic substitution reactions. The ligands were synthesized as air-stable solids in three to five steps from the corresponding hydroxy acids. We could successfully substitute several substrates (including symmetrical and unsymmetrical disubstituted and monosubstituted linear substrates as well as different cyclic substrates with different ring sizes) with many C-, O- and N-nucleophiles (up to 73 different combinations). These results surpass the best one reported so far, even the family of ligands included in Chapter 3. We have identified three ligands that work well with a set of substrates, **L14e** for the linear disubstituted, **L15e** for monosubstituted and **L9e** for the cyclic ones. These three ligands, only differs on the substituent on the alkyl backbone chain.

Moreover, the DFT calculations and the NMR study of the Pd-allyl intermediates helped us to establish the origin of the enantioselectivity. These studies stablished that the ratio of the Pd-allyl intermediates which provide each enantiomer is influenced by the ligand parameters and therefore the enantioselectivity is controlled by the relative ratio of *endo* and *exo* isomers. However, unlike what has been published so far with phosphite-N ligands the ligand parameters than governs the ratio of endo and exo isomers for linear substrates also includes the oxazoline substituents. Thus, whereas for cyclic substrates this ratio is mainly controlled by the configuration of the phosphite group for linear substrates the oxazoline substituent also plays a key role.

4.4. Experimental part

All reactions were performed with standard Schlenk techniques using argon. Commercial chemicals were used as received. Solvents were dried by means of standard procedures and stored under inert atmosphere. ^{1}H, $^{13}C\{^{1}H\}$, and $^{31}P\{^{1}H\}$ NMR spectra were recorded using a Varian Mercury 400 MHz spectrometer. Chemical shifts are relative to the signal of $SiMe_4$ (^{1}H and $^{13}C\{^{1}H\}$) or H_3PO_4 ($^{31}P\{^{1}H\}$) as internal standard. Racemic substrates **S1–S12** and **S13–S18,** the ligand precursors, phosphorochloridites, and ligands (except **L9d** and **L9e**) are known compounds and they were synthesized following previously reported procedures.[7a, 11, 17]

The computational details as well the calculated geometries of this Chapter can be found in the electronic supporting information provided with this thesis.

The corresponding NMR copies of new compounds can be found in the electronic supporting information provided.

The characterization details for compounds **11**-**51** can be found in experimental part of Chapter 3.

4.4.1. Typical methodology for the preparation of phosphite-oxazoline ligands

A solution of the desired alcohol-oxazoline (1.0 mmol) and pyridine (0.16 ml, 2.0 mmol) in toluene (6 ml) was added dropwise at −78 °C to a solution of phosphochloridite (1.1 mmol) and pyridine (0.16 ml, 2.0 mmol) in toluene (6 ml). The mixture was left to warm to room temperature and stirred overnight at this temperature. The precipitate formed was filtered under argon, and the solvent was evaporated under vacuum. The residue was purified by flash chromatography (under argon, using neutral alumina and dry toluene as eluent system) to afford the corresponding phosphite-oxazoline **L9**–**L16a**,**d-e** as white solids.

4.4.2. Characterization details for ligands L9d-L9e

L9d. Yield: 398.3 mg (60%). ^{31}P NMR (161.9 MHz, C_6D_6): δ = 153.9 (s). ^{1}H NMR (400 MHz, C_6D_6): δ = 0.52 (s, 9H, CH_3, $SiMe_3$), 0.57 (s, 9H, CH_3, $SiMe_3$), 1.57 (s, 3H, CH_3), 1.74 (s, 3H, CH_3), 3.76 (pt, 1H, CH–O, J_{H-H} = 8.4 Hz), 4.07 (dd, 1H, CH–O, $^{2}J_{H-H}$ = 10.0 Hz; $^{3}J_{H-H}$ = 8.4 Hz), 4.92 (dd, 1H, CH-N, $^{2}J_{H-H}$ = 10.0 Hz, $^{3}J_{H-H}$ = 8.4 Hz), 6.82 (m, 2H, CH═), 6.96–7.13 (m, 7H, CH═), 7.26 (d, 1H, CH═, $^{3}J_{H-H}$= 8.4 Hz), 7.27 (d, 1H, CH═, $^{3}J_{H-H}$ = 8.4 Hz), 7.66 (m, 2H, CH═), 8.09 (s, 1H, CH═), 8.15 (s, 1H, CH═). ^{13}C (100.6 MHz, C_6D_6): δ = −0.3 (d, CH_3, $SiMe_3$, J_{C-P} = 4.5 Hz), 0.4 (CH_3, $SiMe_3$), 28.2 (d, CH_3, $^{3}J_{C-P}$ = 3.8 Hz), 28.7 (d, CH_3, $^{3}J_{C-P}$ = 7.7 Hz), 69.8 (CH-N), 74.9 (CH_2–O), 76.2 (d, C, CMe_2, $^{3}J_{C-P}$= 5.3 Hz), 122.6–152.4 (aromatic

carbons), 169.1 (C═N). TOF-MS (ESI+): *m/z* = 686.2285, calcd for $C_{38}H_{42}NNaO_4PSi_2$ [M + Na]$^+$: 686.2282.

L9e. Yield: 331.9 mg (50%); ^{31}P NMR (161.9 MHz, C_6D_6): δ = 153.6 (s); ^{1}H NMR (400 MHz, C_6D_6): δ = 0.53 (s, 9H, CH_3, $SiMe_3$), 0.59 (s, 9H, CH_3, $SiMe_3$), 1.62 (s, 3H, CH_3), 1.77 (s, 3H, CH_3), 3.55 (pt, 1H, CH–O, J_{H-H} = 8.0 Hz), 4.06 (dd, 1H, CH–O, $^2J_{H-H}$ = 10.8 Hz, $^3J_{H-H}$ = 8.8 Hz), 4.92 (dd, 1H, CH-N, $^2J_{H-H}$ = 10.0 Hz, $^3J_{H-H}$ = 8.0 Hz), 6.81 (m, 2H, CH═), 6.95–7.11 (m, 7H, CH═), 7.26 (m, 2H, CH═), 7.67 (m, 2H, CH═), 8.11 (s, 1H, CH═), 8.15 (s, 1H, CH═). ^{13}C (100.6 MHz, C_6D_6): δ = −0.3 (d, CH_3, $SiMe_3$, J_{C-P} = 4.6 Hz), 0.4 (CH_3, $SiMe_3$), 28.0 (d, CH_3, $^3J_{C-P}$ = 3.9 Hz), 28.7 (d, CH_3, $^3J_{C-P}$ = 6.9 Hz), 69.5 (CH-N), 74.8 (CH_2–O), 75.9 (d, C, CMe_2, $^3J_{C-P}$ = 5.3 Hz), 122.5–152.4 (aromatic carbons), 169.0 (C═N). TOF-MS (ESI+): *m/z* = 686.2280, calcd for $C_{38}H_{42}NNaO_4PSi_2$ [M + Na]$^+$: 686.2282.

4.4.3. General methodology for the preparation of [Pd(η^3-allyl)(P–N)]BF$_4$ complexes 90–93

Compound [Pd(μ-Cl)(η^3-1,3-allyl)]$_2$ (0.025 mmol) and the corresponding ligand (0.05 mmol) were dissolved in CD_2Cl_2 (1.5 ml) at room temperature under argon. After 30 min, $AgBF_4$ (9.8 mg, 0.05 mmol) was added, and the mixture was stirred for 30 min. Silver salts were then removed by filtration over Celite under argon, and the resulting solutions were analyzed by NMR. After the NMR analysis, the [Pd(η^3-allyl)(P–N)]BF_4 complexes were precipitated by adding hexane as pale yellow solids.

4.4.4. Characterization details for [Pd(η^3-allyl)(P–N)]BF$_4$ complexes 90–93

[Pd(η^3-1,3-cyclohexenyl)(L10e)]BF$_4$ (90) Major isomer (95%): ^{31}P NMR (161.9 MHz, CD_2Cl_2): δ = 143.3 (s). ^{1}H NMR (400 MHz, CD_2Cl_2): δ = 0.03 (s, 9H, CH_3, $SiMe_3$), 0.10 (m, 1H, CH_2), 0.61 (s, 9H, CH_3, $SiMe_3$), 0.81 (m, 1H, CH_2), 1.0–1.3 (m, 4H, CH_2), 4.05 (b, 1H, CH═ *trans* to N), 4.53 (m, 1H, CH_2), 5.18 (m, 1H, CH_2), 5.33 (m, 1H, CH_c═), 5.95 (m, 1H, CH-N), 6.09 (m, 1H, CH═ *trans* to P) 6.36 (d, 1H, CH–OP, J_{C-P} = 26.0 Hz), 7.10 (d, 1H, CH═, $^3J_{H-H}$ = 8.8 Hz), 7.11–7.30 (m, 2H, CH═), 7.42–7.60 (m, 14H, CH═), 8.02 (d, 2H, CH═, $^3J_{H-H}$ = 8.4 Hz), 8.24 (s, 1H, CH═). ^{13}C (100.6 MHz, CD_2Cl_2): δ = −0.4 (CH_3, $SiMe_3$), 0.0 (CH_3, $SiMe_3$), 19.9 (CH_2), 27.0 (b, CH_2), 68.5 (d, CH═ *trans* to N, J_{C-P} = 9.1 Hz), 74.5 (CH–OP), 76.4 (CH-N), 78.2 (CH_2), 104.4 (d, CH═ *trans* to P, J_{C-P} = 39.5 Hz), 111.6 (d, CH_c═, J_{C-P} = 10.7 Hz), 122.7–151.0 (aromatic carbons), 169.4 (C═N). Minor isomer (5%): ^{31}P NMR (161.9 MHz, CD_2Cl_2): δ = 139.5 (s). ^{1}H NMR (400 MHz, CD_2Cl_2): δ = 0.08 (s, 9H, CH_3, $SiMe_3$), 0.10 (m, 1H, CH_2), 0.61 (s, 9H, CH_3, $SiMe_3$), 0.81 (m, 1H, CH_2), 1.0–1.3 (m, 4H, CH_2), 3.94 (b, 1H, CH═ *trans* to N), 4.53 (m, 1H, CH_2), 5.21 (m, 2H, CH_2,CH_c═), 5.95 (m, 2H, CH═ *trans* to P, CH-N), 6.34 (d, 1H, CH–OP, J_{C-P} = 21.0 Hz), 7.0–8.2 (m, 20H, CH═).

[Pd(η^3-1,3-cyclohexenyl)(L14e)]BF$_4$ (91) only one isomer observed. ^{31}P NMR (161.9 MHz, CD_2Cl_2): δ = 143.7 (s). ^{1}H NMR (400 MHz, CD_2Cl_2): δ= 0.11 (m, 1H, CH_2), 0.47 (s, 9H, CH_3, $SiMe_3$), 0.54 (s, 9H, CH_3, $SiMe_3$), 0.68 (m, 1H, CH_2), 1.0–1.3 (m, 4H, CH_2), 1.89 (d, 1H,

CH_3, $^3J_{H-H}$ = 6.8 Hz), 4.04 (b, 1H, CH═ *trans* to N), 4.51 (dd, 1H, CH_2, $^2J_{H-H}$ = 9.2 Hz, $^3J_{H-H}$= 8 Hz), 5.15 (dd, 1H, CH_2, $^2J_{H-H}$ = 9.2 Hz, $^3J_{H-H}$ = 10.8 Hz), 5.33 (m, 1H, CHc═), 5.36 (q, 1H, CH, $^3J_{H-H}$ = 6.8 Hz), 5.71 (dd, 1H, CH-N, $^3J_{H-H}$ = 8.0 Hz, $^3J_{H-H}$ = 10.8 Hz), 5.95 (m, 1H, CH═ *trans* to P), 6.99 (d, 1H, CH═, $^3J_{H-H}$ = 8.8 Hz), 7.12 (d, 1H, CH═, $^3J_{H-H}$ = 8.8 Hz), 7.28 (m, 2H, CH═), 7.41–7.50 (m, 7H, CH═), 8.02 (t, 1H, CH═, $^3J_{H-H}$ = 8.8 Hz), 8.23 (d, 1H, CH═, $^3J_{H-H}$ = 7.2 Hz). ^{13}C (100.6 MHz, CD_2Cl_2): δ = −0.1 (CH_3, $SiMe_3$), 0.0 (CH_3, $SiMe_3$), 19.5 (CH_2), 22.9 (d, CH_3, J_{C-P} = 4.5 Hz), 27.1 (b, CH_2), 67.9 (d, CH= *trans* to N, J_{C-P}= 9.2 Hz), 71.6 (CH–OP), 74.3 (CH-N), 78.2 (CH_2), 104.0 (d, CH═ *trans* to P, J_{C-P} = 40 Hz), 111.7 (d, CHc═, J_{C-P} = 10.7 Hz), 121.0–151.0 (aromatic carbons), 171.8 (C═N).

[Pd(η³-1,3-diphenylallyl)(L10e)]BF_4 (92) Major isomer (75%): ^{31}P NMR (161.9 MHz, CD_2Cl_2): δ = 139.5 (s). ^{1}H NMR (400 MHz, CD_2Cl_2): δ = 0.30 (s, 9H, CH_3, $SiMe_3$), 0.54 (s, 9H, CH_3, $SiMe_3$), 4.38 (m, 1H, CH_2), 4.47 (m, 1H, CH═ *trans* to N), 5.01 (m, 2H, CH_2, CH-N), 5.96 (m, 1H, CH_c═), 6.15 (m, 2H, CH–O, CH═ *trans* to P), 7.10–8.21 (m, 30H, CH═). ^{13}C (100.6 MHz, CD_2Cl_2): δ = −0.1 (CH_3, $SiMe_3$), 0.6 (CH_3, $SiMe_3$), 67.7 (CH-N), 67.9 (d, CH═ *trans* to N, J_{C-P} = 10.7 Hz), 76.3 (CH–OP), 78.0 (CH_2), 108.1 (d, CH═ *trans* to P, J_{C-P}= 29.8 Hz), 112.6 (d, CH_c═, J_{C-P} = 9.9 Hz), 120.0–150.0 (aromatic carbons), 169.5 (C═N). Minor isomer (25%): ^{31}P NMR (161.9 MHz, CD_2Cl_2): δ = 140.2 (s). ^{1}H NMR (400 MHz, CD_2Cl_2): δ = 0.20 (s, 9H, CH_3, $SiMe_3$), 0.39 (s, 9H, CH_3, $SiMe_3$), 4.35 (m, 1H, CH_2), 4.74 (m, 1H, CH-N), 5.01 (m, 1H, CH_2), 5.23 (m, 1H, CH═ *trans* to N), 5.27 (m, 1H, CH═ *trans* to P), 5.60 (m, 1H, CH_c═), 6.15 (m, 1H, CH–OP), 7.1–8.2 (m, 25H, CH═). ^{13}C (100.6 MHz, CD_2Cl_2): δ = −0.5 (CH_3, $SiMe_3$), −0.2 (CH_3, $SiMe_3$), 68.9 (CH-N), 74.1 (d, CH═ *trans* to N, J_{C-P} = 10.7 Hz), 75.9 (CH–OP), 77.6 (CH_2), 95.9 (d, CH═ *trans* to P, J_{C-P} = 42 Hz), 109.2 (d, CH_c═, J_{C-P} = 13.0 Hz), 120.0–150.0 (aromatic carbons), 170.2 (C═N).

[Pd(η³-1,3-diphenylallyl)(L14e)]BF_4 (93) Major isomer (91%): ^{31}P NMR (161.9 MHz, CD_2Cl_2): δ ═ 140.3 (s). ^{1}H NMR (400 MHz, CD_2Cl_2): δ = 0.46 (s, 9H, CH_3, $SiMe_3$), 0.74 (s, 9H, CH_3, $SiMe_3$), 1.96 (d, 3H, CH_3, $^3J_{H-H}$ = 6.8 Hz), 4.33 (dd, 1H, CH_2, $^2J_{H-H}$ = 8.8 Hz, $^3J_{H-H}$ = 4.8 Hz), 4.51 (m, 1H, CH═ *trans* to N), 4.88 (m, 1H, CH-N), 5.00 (m, 1H, CH_2), 5.12 (m, 1H, CH–OP), 6.02 (m, 2H, CH_c═, CH═ *trans* to P), 6.3–8.4 (m, 25H, CH═). ^{13}C (100.6 MHz, CD_2Cl_2): δ = −0.1 (CH_3, $SiMe_3$), 0.8 (CH_3, $SiMe_3$), 22.6 (b, CH_3), 67.3 (CH-N), 68.3 (d, CH═ *trans* to N, J_{C-P} = 9.9 Hz), 71.5 (CH–OP), 78.2 (CH_2), 106.8 (d, CH═ *trans* to P, J_{C-P} = 30.4 Hz), 112.2 (d, CH_c═, J_{C-P} = 9.8 Hz), 121.0–150.0 (aromatic carbons), 172.1 (C═N). Minor isomer (9%): ^{31}P NMR (161.9 MHz, CD_2Cl_2): δ = 142.9 (s). ^{1}H NMR (400 MHz, CD_2Cl_2): δ = 0.41 (s, 9H, CH_3, $SiMe_3$), 0.62 (s, 9H, CH_3, $SiMe_3$), 1.75 (d, 3H, CH_3, $^3J_{H-H}$ = 6.8 Hz), 4.39 (dd, 1H, CH_2, $^2J_{H-H}$ = 8.8 Hz, $^3J_{H-H}$ = 4.4 Hz), 4.53 (m, 1H, CH═ *trans* to N), 4.71 (m, 1H, CH_2), 4.88 (m, 1H, CH-N), 5.12 (m, 1H, CH–OP), 5.98 (m, 1H, CH═ *trans* to P), 6.09 (m, 1H, CH_c═), 6.3–8.4 (m, 25H, CH═). ^{13}C (100.6 MHz, CD_2Cl_2): δ = 0.1 (CH_3, $SiMe_3$), 0.3 (CH_3, $SiMe_3$), 22.4 (b, CH_3), 68.1 (CH-N), 68.4 (d, CH═ *trans* to N, J_{C-P} = 9.2 Hz), 70.9 (CH–OP), 78.0 (CH_2), 98.8 (d, CH═ *trans* to P, J_{C-P} = 32.4 Hz), 112.7 (d, CH_c═, J_{C-P} = 9.2 Hz), 121.0–150.0 (aromatic carbons), 172.3 (C═N).

4.4.5. Typical methodology for the allylic alkylation of linear (S1, S3–S9, S12–S18) and cyclic (S2, S10, and S11) substrates

A solution of the desired phosphite-oxazoline ligand (0.011 mmol) and $[PdCl(\eta^3\text{-}C_3H_5)]_2$ (1.8 mg, 0.005 mmol) in CH_2Cl_2 (0.5 ml) was stirred. After 30 min a solution of substrate (1 mmol) in CH_2Cl_2 (1.5 ml), nucleophile (3 mmol), *N,O*-bis(trimethylsilyl)-acetamide (730 µL, 3 mmol), and KOAc (3 mg, 0.03 mmol) were subsequently added. After the desired reaction time the reaction mixture was diluted with Et_2O (5 ml). Saturated NH_4Cl (aq) (25 ml) was then added, the mixture was extracted with Et_2O (3 × 10 ml), and the extract was dried over $MgSO_4$.

4.4.6. Typical methodology for the allylic amination of S1 and S2

A solution of the desired phosphite-oxazoline ligand (0.011 mmol) and $[PdCl(\eta^3\text{-}C_3H_5)]_2$ (1.8 mg, 0.005 mmol) in CH_2Cl_2 (0.5 ml) was stirred. After 30 min, a solution of substrate (1 mmol) in CH_2Cl_2 (1.5 ml) and the corresponding amine (3 mmol) were subsequently added. After the desired reaction time, the reaction mixture was diluted with Et_2O (5 ml). Saturated NH_4Cl (aq) (25 ml) was then added, the mixture was extracted with Et_2O (3 × 10 ml), and the extract was dried over $MgSO_4$.

4.2.6. Typical methodology for the allylic etherification and silylation of S1

A solution of the desired phosphite-oxazoline ligand (0.011 mmol) and $[PdCl(\eta^3\text{-}C_3H_5)]_2$ (1.8 mg, 0.005 mmol) in CH_2Cl_2 (0.5 ml) was stirred. After 30 min, a solution of **S1** (31.5 mg, 0.125 mmol) in CH_2Cl_2 (1.5 ml) was added. After 10 min, Cs_2CO_3 (122 mg, 0.375 mmol) and the corresponding alkyl alcohol or silanol (0.375 mmol) were added. After the desired reaction time, the reaction mixture was diluted with Et_2O (5 ml). Saturated NH_4Cl (aq) (25 ml) was then added, the mixture was extracted with Et_2O (3 × 10 ml), and the extract was dried over $MgSO_4$.

4.2.7. Characterization details for compounds 59-89

2-(1,3-Diphenylallyl)-4-ethyl-3,5-dimethyl-1λ²-pyrrole (59).[18] Enantiometic excess determined by HPLC using Chiralpak AD-H column (99,5% hexane/2-propanol, flow 0.7 ml/min, λ= 254 nm) t_R 17.8 min; t_R 19.7 min. ^{1}H NMR ($CDCl_3$) δ: 1.96 (s, 3H, CH_3), 2.16 (s, 3H, CH_3), 4.94 (d, 1H, CH=, *J*= 6.8 Hz), 5.73 (m, 1H, CH=), 6.31 (d, 1H, CH=, *J*= 15.6 Hz), 6.56 (dd, 1H, CH=, *J*= 15.6 Hz, *J*= 6.8 Hz), 7.37−7.18 (m, 11H, CH=).

2-(1,3-Diphenylallyl)-1λ²-pyrrole (60). [18] Enantiometic excess determined by HPLC using Chiralpak AD-H column (95% hexane/2-propanol, flow 1 ml/min, λ= 254 nm) t_R

49.4 min (*R*); t_R 69.0 min (*S*). ^{1}H NMR ($CDCl_3$) δ: 4.87 (d, 1H, CH=, *J*= 7.6 Hz), 5.97 (s, 1H, CH=), 6.16 (d, 1H, CH=, *J*= 2.6 Hz), 6.43 (d, 1H, CH=, *J*= 15.8 Hz), 6.59 (dd, 1H, CH=, *J*= 15.8 Hz, *J*= 7.6 Hz), 6.72 (s, 1H), 7.2-7.9 (m, 11H, CH=).

1,3-Diphenyl-*N*-(prop-2-yn-1-yl)prop-2-en-1-amine (61).[19] Enantiomeric excess determined by HPLC using Chiralcel AD-H column (95% hexane/2-propanol, flow 0.5 ml/min). t_R 19.6 min (*R*); t_R 21.9 min (*S*). ^{1}H NMR ($CDCl_3$), δ: 2.28 (t, 1H, CH≡, *J*= 2.3 Hz), 3.43 (pdq, 2H, CH_2, *J*= 17.2 Hz, *J*= 2.3 Hz), 4.64 (d, 1H, CH, *J*= 7.7 Hz), 6.29 (dd, 1H, CH=, *J*= 15.8 Hz, *J*= 7.7 Hz), 6.67 (d, 1H, CH=, *J*= 15.8 Hz), 7.30 (m, 10H, CH=).

***N*-Isopropyl-1,3-diphenylprop-2-en-1-amine (62)**.[20] Enantiomeric excess determined by HPLC using Chiralcel OJ-H column (99% hexane/2-propanol, flow 0.5 ml/min). t_R 22.4 min (*R*); t_R 26.2 min (*S*). ^{1}H NMR ($CDCl_3$), □: 1.07 (d, 3H, CH_3, *J*= 6.3 Hz), 1.10 (d, 3H, CH_3, *J*= 6.3 Hz), 1.61 (bs, 1H, NH), 2.81 (pt, 1H, CH, *J*= 6.3 Hz), 4.49 (d, 1H, CH, *J*= 7.4 Hz), 6.30 (dd, 1H, CH=, *J*= 16 Hz, *J*= 7.4 Hz), 6.52 (d, 1H, CH=, *J*= 16 Hz), 7.16-7.22 (m, 1H, CH=), 7.24-7.30 (m, 3H, CH=), 7.31-7.41 (m, 6H, CH=).

***N*-benzhydryl-1,3-diphenylprop-2-en-1-amine (63)**.[20] Enantiomeric excess determined by HPLC using Chiralcel AD-H column (99% hexane/2-propanol, flow 0.5 ml/min). t_R 12.1 min (*S*); t_R 14.5 min (*R*). ^{1}H NMR ($CDCl_3$), δ: 4.30 (d, 1H, CH, *J*= 7.2 Hz), 4.89 (s, 1H, CH), 6.31 (dd, 1H, CH=, *J*= 15.8 Hz, *J*= 7.2 Hz), 6.51 (d, 1H, CH=, *J*= 15.8 Hz), 7.30 (m, 20H, CH=).

1-(1,3-Diphenylallyl)pyrrolidine (64).[20] Enantiomeric excess determined by HPLC using Chiralcel OD-H column (99% hexane/2-propanol, flow 1 ml/min). t_R 4.4 min (*S*); t_R 4.9 min (*R*). ^{1}H NMR ($CDCl_3$), δ: 1.80 (m, 4H, CH_2), 2.40 (m, 4H, CH_2), 3.76 (d, 1H, CH, *J*= 8.5 Hz), 6.42 (dd, 1H, CH=, *J*= 15.6 Hz, *J*= 8.5 Hz), 6.59 (d, 1H, CH=, *J*= 15.6 Hz), 7.25 (m, 8H, CH=), 7.42 (m, 2H, CH=).

***N*-(1,3-Diphenylallyl)-4-methylbenzenesulfonamide (65)**.[21] Enantiomeric excess determined by HPLC using Chiralcel OD-H column (90% hexane/2-propanol, flow 0.5 ml/min). t_R 35.9 min (*R*); t_R 47.5 min (*S*). ^{1}H NMR ($CDCl_3$), δ: 2.32 (s, 3H, CH_3), 5.11 (td, 1H, CH, *J*= 7.3 Hz, *J*= 1.2 Hz), 5.21 (d, 1H, CH, *J*= 7.3 Hz), 6.08 (dd, 1H, CH=, *J*= 15.8 Hz, *J*= 6.8 Hz), 6.34 (dd, 1H, CH=, *J*= 15.8 Hz, *J*= 1.2 Hz), 7.20 (m, 12H, CH=), 7.65 (m, 2H, CH=).

***N*-(1,3-Diphenylallyl)aniline (66)**.[19] Enantiomeric excess determined by HPLC using Chiralcel AD-H column (95% hexane/2-propanol, flow 1 ml/min). t_R 9.5 min (*R*); t_R 12.0 min (*S*). ^{1}H NMR ($CDCl_3$), δ: 5.14 (d, 1H, CH, *J*= 6.1 Hz), 6.45 (dd, 1H, CH, *J*= 15.9 Hz, *J*= 6.1 Hz), 6.69 (m, 3H, CH), 6.76 (tt, 1H, CH=, *J*= 7.5 Hz, *J*= 1.1 Hz), 7.20 (m, 2H, CH=), 7.27 (m, 1H, CH=), 7.34 (m, 3H, CH=), 7.41 (m, 4H, CH=), 7.48 (m, 2H, CH=).

(3-Butoxyprop-1-ene-1,3-diyl)dibenzene (67).[22] Enantiomeric excess determined by HPLC using Chiralcel O*J*-H column (99.5% hexane/2-propanol, flow 0.5 ml/min). t_R 17.5 min (*S*); t_R 22.1 min (*R*). ^{1}H NMR ($CDCl_3$), δ: 0.91 (t, 3H, CH_3, *J*= 7.5 Hz), 1.41 (m, 2H, CH_2), 1.68–1.58 (m, 2H, CH_2), 3.42 (td, 1H, CH_2, *J*= 9.5 Hz, *J*= 6.5 Hz), 3.52 (td, 1H, CH_2, *J*= 9.0 Hz, *J*= 7.0 Hz), 4.88 (d, 1H, CH, *J*= 7.0 Hz), 6.27 (dd, 1H, CH=, *J*= 16.0 Hz, *J*= 7.0 Hz), 6.60 (d, 1H, CH=, *J*= 16 Hz), 7.2-7.4 (m, 10H, CH=).

Diethyl 2-(but-3-en-1-yl)-2-(1,3-di-*p*-tolylallyl)malonate (68).[13h] Enantiomeric excess determined by HPLC using Chiralcel IA column (98% hexane/2-propanol, flow 0.2

ml/min, λ = 254 nm). t_R 39.9 min (*S*); t_R 46.6 min (*R*). ^{1}H NMR ($CDCl_3$), δ: 1.37 (t, 3H, CH_3, *J*= 7.2 Hz), 1.43 (t, 3H, CH_3, *J*= 7.2 Hz), 1.94 (m, 1H, CH_2), 2.09 (m, 2H, CH_2), 2.25 (m, 1H, CH_2), 2.46 (s, 6H, CH_3), 4.32 (m, 5H, CH, CH_2), 5.06 (m, 1H, CH_2=), 5.18 (m, 1H, CH_2=), 5.86 (m, 1H, CH=), 6.49 (d, 1H, CH=, *J*= 12 Hz), 6.86 (dd, 1H, CH=, *J*= 12 Hz, *J*= 9.2 Hz), 7.24 (m, 6H, CH=), 7.38 (d, 2H, *J*= 8 Hz).

Dimethyl 2-(1,3-di-*p*-tolylallyl)-2-(prop-2-yn-1-yl)malonate (69). Enantiomeric excess determined by HPLC using Chiralcel OD-H column (98% hexane/2-propanol, flow 0.5 ml/min, λ= 254 nm). t_R 18.6 min (*R*); t_R 23.4 min (*S*). ^{1}H NMR ($CDCl_3$), δ: 2.03 (t, 1H, CH≡, *J*= 2.6 Hz), 2.23 (s, 6H, 2xCH_3), 2.55 (dd, 1H, CH_2, *J*= 17.1 Hz, *J*= 2.6 Hz), 2.72 (dd, 1H, CH_2, *J*= 17.1 Hz, *J*= 2.6 Hz), 3.63 (s, 3H, CH_3), 3.69 (s, 3H, CH_3), 4.30 (d, 1H, CH, *J*= 8.5 Hz), 6.33 (d, 1H, CH=, *J*= 15.7 Hz), 6.62 (dd, 1H, CH=, *J*= 15.7 Hz, *J*= 8.5 Hz), 7.02 (m, 6H, CH=), 7.16 (m, 2H, CH=). ^{13}C NMR ($CDCl_3$), δ: 21.1 (CH_3), 21.2 (CH_3), 24.5 (CH_2), 51.7 (CH), 52.5 (CH_3), 52.6 (CH_3), 61.8 (C), 71.9 (CH≡), 79.5 (C≡), 126.3 (CH=), 127.8 (CH=), 129.1 (CH=), 129.1 (CH=), 129.1 (CH=), 132.2 (CH=), 134.7 (C=), 135.7 (C=), 137.0 (C=), 137.1 (C=), 169.7 (C=O), 169.8 (C=O).

Dimethyl 2-(1,3-dimethylallyl)malonate (70).[23] Enantiomeric excess determined by GC using Chiralsil-Dex CB column (90 kPa H_2, Isotherm at 65 ºC). t_R 38.6 min (*R*); t_R 39.5 min (*S*). ^{1}H NMR ($CDCl_3$), δ: 1.03 (d, 3H, CH_3, *J*= 6.4 Hz), 1.62 (d, 3H, CH_3, *J*= 6.4 Hz), 2.88 (m, 1H, CH), 3.25 (d, 1H, CH_3, *J*= 9 Hz), 3.68 (s, 3H, CH_3), 3.71 (s, 3H, CH_3), 5.31 (dd, 1H, CH=, *J*= 15.2 Hz, *J*= 8 Hz), 5.50 (m, 1H, CH=).

Dimethyl 2-(pent-3-en-2-yl)-2-(prop-2-yn-1-yl)malonate (71).[24] Enantiomeric excess determined by HPLC using Chiralcel IC column (98% hexane/2-propanol, flow 0.5 ml/min, λ= 254 nm). t_R 13.5 min (*S*); t_R 15.1 min (*R*). ^{1}H NMR ($CDCl_3$), δ: 1.09 (d, 3H, CH_3, *J*= 6.4 Hz), 1.62 (d, 3H, CH_3, *J*= 6.4 Hz), 1.98 (m, 1H, CH), 2.74 (m, 2H, CH_2), 2.98 (m, 1H, CH), 3.70 (m, 3H, CH_3), 3.72 (m, 3H, CH_3), 5.25 (m, 1H, CH=), 5.53 (m, 1H, CH=).

Dimethyl 2-(4,4,4-trifluoro-1-phenylbut-2-en-1-yl)malonate (72).[23] Enantiomeric excess determined by HPLC using Lux-amylose-1 column (95% hexane/2-propanol, flow 1 ml/min, λ= 254 nm). t_R 10.6 min (*R*); t_R 12.1 min (*S*). ^{1}H NMR ($CDCl_3$), δ: 3.52 (s, 3H, OMe), 3.75 (s, 3H, OMe), 3.89 (d, 1H, CH, *J*= 10.7 Hz), 4.21 (pt, 1H, CH, *J*= 9.5 Hz), 5.67 (m, 1H, CH=), 6.56 (m, 1H, CH=), 7.21 (m, 5H, CH=).

Dibenzyl 2-(4,4,4-trifluoro-1-phenylbut-2-en-1-yl)malonate (73).[13h] Enantiomeric excess determined by HPLC using Lux-amylose-1 column (95% hexane/2-propanol, flow 1 ml/min, λ= 254 nm). t_R 15.7 min (*R*); t_R 18.6 min (*S*). ^{1}H NMR ($CDCl_3$), δ: 3.87 (m, 1H, CH), 4.20 (m, 1H, CH), 4.82 (m, 2H, CH_2), 5.05 (m, 2H, CH_2), 5.52 (m, 1H, CH=), 6.45 (m, 1H, CH=), 6.96 (m, 2H, CH=), 7.08 (m, 2H, CH=), 7.22 (m, 11H, CH=).

Dimethyl 2-methyl-2-(4,4,4-trifluoro-1-phenylbut-2-en-1-yl)malonate (74).[13h] Enantiomeric excess determined by HPLC using Lux-amylose-1 column (95% hexane/2-propanol, flow 1 ml/min, λ= 254 nm). t_R 9.0 min (*S*); t_R 9.5 min (*R*). ^{1}H NMR ($CDCl_3$), δ: 1.34 (s, 3H, CH_3), 3.58 (s, 3H, OMe), 3.67 (s, 3H, OMe), 4.11 (dt, 1H, CH, *J*= 7.9 Hz, *J*= 1.4 Hz), 5.53 (dqd, 1H, CH=, *J*= 15.7 Hz, *J*= 6.3 Hz, *J* = 1.4 Hz), 6.81 (ddq, 1H, CH=, *J* = 15.7 Hz, *J*= 7.9 Hz, *J*= 2.1 Hz), 7.10 (m, 2H, CH=), 7.26 (m, 3H, CH=).

Dimethyl 2-allyl-2-(4,4,4-trifluoro-1-phenylbut-2-en-1-yl)malonate (75). Enantiomeric excess determined by HPLC using Lux-amylose-1 column (95% hexane/2-propanol, flow 1 ml/min, λ= 254 nm). t_R 8.1 min (*S*); t_R 8.8 min (*R*). ^{1}H NMR ($CDCl_3$), δ: 2.27 (dd, 1H, CH_2, *J*= 14.3 Hz, *J*= 8.1 Hz), 2.50 (dd, 1H, CH_2, *J*= 14.3 Hz, *J*= 6.5 Hz), 3.64 (s, 3H, OMe), 3.70 (s, 3H, OMe), 4.05 (dt, 1H, CH=, *J*= 6.9 Hz, *J*= 2.1 Hz), 4.95 (m, 2H, CH_2=), 5.37 (dqd, 1H, CH=, *J*= 15.8 Hz, *J*= 6.4 Hz, *J*= 1.6 Hz), 5.63 (dddd, 1H, CH=, *J*= 16.8 Hz, *J*= 10.2 Hz, *J*= 8.1 Hz, *J*= 6.5 Hz), 6.86 (ddq, 1H, CH=, *J*= 15.8 Hz, *J*= 6.4 Hz, *J*= 2.0 Hz), 7.96 (m, 2H, CH=), 7.23 (m, 3H, CH=). ^{13}C NMR ($CDCl_3$), δ: 38.9 (CH_2), 51.5 (CH), 52.3 (OMe), 52.5 (OMe), 62.2 (C), 119.3 (CH_2=), 119.9 (CH=), 128.1 (CH=), 128.8 (CH=), 129.3 (CH=), 132.4 (CH=), 140.4 (m, CH=), 170.1 (C=O), 170.3 (C=O).

Dimethyl 2-(prop-2-yn-1-yl)-2-(4,4,4-trifluoro-1-phenylbut-2-en-1-yl)malonate (76). Enantiomeric excess determined by HPLC using Chiralcel OJ-H column (87% hexane/2-propanol, flow 0.5 ml/min, λ= 254 nm). t_R 9.6 min (*R*); t_R 10.0 min (*S*). ^{1}H NMR ($CDCl_3$), δ: 2.08 (t, 1H, CH≡, *J*= 2.7 Hz), 2.41 (dd, 1H, CH_2, *J*= 17.3 Hz, *J*= 2.7 Hz), 2.71 (dd, 1H, CH_2, *J*= 17.3 Hz, *J*= 2.7 Hz), 3.70 (s, 3H, OMe), 3.73 (s, 3H, OMe), 4.36 (m, 1H, CH), 5.46 (m, 1H, CH=), 6.97 (m, 1H, CH=), 7.10 (m, 2H, CH=), 7.28 (m, 3H, CH=). ^{13}C NMR ($CDCl_3$), δ: 24.2 (CH_2), 49.8 (CH), 52.7 (OMe), 53.0 (OMe), 60.7 (C), 72.83 (C≡), 78.5 (C≡), 120.4 (q, CH=, *J*= 33.5 Hz), 128.2 (CH), 128.8 (CH), 129.3 (C), 136.2 (C), 169.2 (C=O), 169.2 (C=O).

***N*-Benzylcyclohexanamine (77)**.[21] Enantiomeric excess determined by HPLC using Chiralpak OJ-H column (98% hexane/2-propanol, flow 0.5 ml/min, λ= 226 nm). t_R 14.0 min (*S*); t_R 15.5 min (*R*). ^{1}H NMR ($CDCl_3$), δ: 1.31 (b, 1H, NH), 1.52 (m, 2H, CH_2), 1.74 (m, 1H, CH_2), 1.96 (m, 3H, CH_2), 3.22 (m, 1H, CH), 3.85 (m, 2H, CH_2), 5.75 (m, 2H, CH=), 7.12-7.43 (m, 5H, CH=).

***N*-(4-Methoxybenzyl)cyclohexanamine (78)**. Enantiomeric excess determined by HPLC using Chiralpak OJ-H column (98% hexane/2-propanol, flow 0.5 ml/min, λ= 226 nm). t_R 14.5 min (*S*); t_R 15.5 min (*R*). ^{1}H NMR ($CDCl_3$), δ: 1.50 (m, 2H, CH_2), 1.75 (m, 1H, CH_2), 1.93 (m, 3H, CH_2), 3.20 (m, 1H, CH), 3.77 (m, 5H, CH_2, OMe), 5.75 (m, 2H, CH=), 6.85 (m, 2H, CH=), 7.27 (m, 2H, CH=). ^{13}C NMR ($CDCl_3$), δ: 20.3 (CH_2), 25.3 (CH_2), 29.5 (CH_2), 50.4 (CH_2), 52.3 (CH), 55.3 (CH_3), 113.7 (CH=), 128.9 (CH=), 129.3 (CH=), 129.9 (CH=), 132.8 (C=), 158.6 (C=).

***N*-(4-(Trifluoromethyl)benzyl)cyclohexanamine (79)**. Enantiomeric excess determined by HPLC using Chiralpak OD-H column (98% hexane/2-propanol, flow 0.5 ml/min, λ= 226 nm). t_R 8.4 min (*R*); t_R 8.9 min (*S*). ^{1}H NMR ($CDCl_3$), δ: 1.53 (m, 2H, CH_2), 1.75 (m, 1H, CH_2), 1.96 (m, 3H, CH_2), 3.18 (m, 1H, CH), 3.91 (m, 2H, $ArCH_2$), 5.75 (m, 2H, CH=), 7.47 (m, 2H, CH=), 7.57 (m, 2H, CH=). ^{13}C NMR ($CDCl_3$), δ: 20.1 (CH_2), 25.3 (CH_2), 29.4 (CH_2), 50.4 (CH_2), 52.4 (CH), 125.2 (q, CH=, *J*= 3.8 Hz), 128.3 (CH=), 129.3 (C=), 129.6 (CH=), 145.0 (C=).

Dimethyl 2-(1-(naphthalen-1-yl)allyl)malonate (80a).[25] Enantiomeric excess determined by HPLC using Chiralpak OJ-H column (87% hexane/2-propanol, flow 0.7 ml/min, λ= 220 nm). t_R 20.1 min (*S*); t_R 28.9 min (*R*). ^{1}H NMR ($CDCl_3$), δ: 3.38 (s, 3H, CH_3),

3.79 (s, 3H, CH_3), 4.15 (d, 1H, CH, *J*= 10 Hz), 5.03 (dd, 1H, CH, *J*= 10 Hz, *J*= 8.4 Hz), 5.09 (d, 1H, CH=, *J*= 10 Hz), 5.16 (m, 1H, CH=), 6.08 (m, 1H, CH=), 7.3-8.2 (m, 7H, CH=).

Dimethyl 2-(1-phenylallyl)malonate (81).[27] Enantiomeric excess determined by HPLC using Chiralpak OJ-H column (87% hexane/2-propanol, flow 0.7 ml/min, λ= 220 nm). t_R 23.2 min (*S*); t_R 25.0 min (*R*). ^{1}H NMR ($CDCl_3$), δ: 3.39 (m, 3H), 3.65 (m, 3H), 3.79 (d, 1H, CH, *J*= 10.8 Hz), 4.03 (dd, 1H, CH=, *J*= 10.8 Hz, *J*= 8.4 Hz), 5.01 (d, 1H, CH=, *J*= 10 Hz), 5.04 (d, 1H, CH=, *J*= 16.8 Hz), 5.92 (m, 1H, CH=), 7.1-7.3 (m, 5H, CH=).

Dimethyl 2-(1-(p-tolyl)allyl)malonate (82).[26] Enantiomeric excess determined by HPLC using Chiralpak OD-H column (90% hexane/2-propanol, flow 0.7 ml/min, λ= 220 nm). t_R 10.8 min (*R*); t_R 12.0 min (*S*). ^{1}H NMR ($CDCl_3$), δ: 2.30 (s, 3 H), 3.51 (s, 3H), 3.73 (s, 3H), 4.07 (dd, 1H, *J*= 10.9 Hz, *J*= 8.2 Hz), 5.07 (d, 1H, *J*= 9.4 Hz), 5.11 (d, 1H, *J*= 17.0 Hz), 5.98 (ddd, 1H, *J*= 17.1 Hz, *J*= 9.4 Hz, *J*= 8.2 Hz), 7.10 (s, 4H).

Dimethyl 2-(1-(4-methoxyphenyl)allyl)malonate (83).[27] Enantiomeric excess determined by HPLC using Chiralpak OD-H column (90% hexane/2-propanol, flow 0.7 ml/min, λ= 220 nm). t_R 9.4 min (*R*); t_R 10.6 min (*S*). ^{1}H NMR ($CDCl_3$), δ: 3.50 (s, 3H), 3.73 (s, 3H), 3.77 (s, 3H), 3.82 (d, 1H, *J*= 10.9 Hz), 4.06 (dd, 1H, *J*= 10.9 Hz, *J*= 8.3 Hz), 5.06 (d, 1H, *J*= 8.6 Hz), 5.09 (d, 1H, *J*= 15.4 Hz), 5.97 (ddd, 1H, *J*= 17.1 Hz, *J*= 10.1 Hz, *J*= 7.8 Hz), 6.85 (d, 2H, *J*= 8.6 Hz), 7.14 (d, 2H, *J*= 8.6 Hz).

Dimethyl 2-(1-(4-(trifluoromethyl)phenyl)allyl)malonate (84).[28] Enantiomeric excess determined by HPLC using Chiralpak OD-H column (99.5% hexane/2-propanol, flow 0.5 ml/min, λ= 220 nm). t_R 34.5 min (*R*); t_R 35.4 min (*S*). ^{1}H NMR ($CDCl_3$), δ: 3.53 (s, 3H), 3.76 (s, 3H), 3.90 (d, 1H, *J*= 11.1 Hz), 4.19 (dd, 1H, *J*= 10.9 Hz, *J*= 8.6 Hz), 5.12 (s, 1H), 5.16 (d, 1H, *J*= 7.6 Hz), 5.97 (ddd, 1H, *J*= 16.9 Hz, *J*= 10.1 Hz, *J*= 8.1 Hz), 7.36 (d, 2H, *J*= 8.3 Hz), 7.57 (d, 2H, *J*= 8.1 Hz).

Dimethyl 2-(1-(3-methoxyphenyl)allyl)malonate (85).[28] Enantiomeric excess determined by HPLC using Chiralpak OD-H column (99% hexane/2-propanol, flow 0.7 ml/min, λ= 220 nm). t_R 17.8 min (*R*); t_R 20.4 min (*S*). ^{1}H NMR ($CDCl_3$), □: 3.49 (s, 3H), 3.72 (s, 3H), 3.85 (s, 3H), 4.18 (d, 1H, *J*= 10.6 Hz), 4.33 (dd, 1H, *J*= 10.6 Hz, *J*= 8.6 Hz), 5.04 (dd, 1H, *J*= 10.1 Hz, *J*= 0.8 Hz), 5.12 (dt, 1H, *J*= 17.2 Hz, *J*= 1.3 Hz), 6.14 (ddd, 1H, *J*= 17.0 Hz, *J*= 10.1 Hz, *J*= 8.6 Hz), 6.89 (m, 2H), 7.16 (dd, 1H, *J*= 7.6 Hz, *J*= 1.5 Hz), 7.20 (td, 1H, *J*= 7.6 Hz, *J*= 1.8 Hz).

Dimethyl 2-(1-(naphthalen-2-yl)allyl)malonate (86).[28] Enantiomeric excess determined by HPLC using Chiralpak OD-H column (97% hexane/2-propanol, flow 0.5 ml/min, λ= 220 nm). t_R 15.98 min (*R*); t_R 17.2 min (*S*).^{1}H NMR ($CDCl_3$), δ: 3.77 (s, 3H), 3.46 (s, 3H), 4.01 (d, 1H, *J*= 11.1 Hz), 4.30 (dd, 1H, *J*= 9.6 Hz, *J*= 8.4 Hz), 5.04 (d, 1H, *J*= 10.1 Hz), 5.18 (d, 1H, *J*= 17.2 Hz), 6.08 (ddd, 1H, *J*= 17.2 Hz, *J*= 10.4 Hz, *J*= 8.1 Hz), 7.37 (dd, 1H, *J*= 8.6, *J*= 1.5 Hz), 7.47- 7.44 (m, 2H), 7.69 (s, 1H), 7.81–7.79 (m, 3H).

Dimethyl 2-methyl-2-(1-phenylallyl)malonate (87).[13g] Enantiomeric excess determined by HPLC using Chiralpak OJ-H column (87% hexane/2-propanol, flow 0.5 ml/min, λ= 220 nm). t_R 19.3 min (*R*); t_R 22.1 min (*S*). ^{1}H NMR ($CDCl_3$), δ: 1.44 (s, 3H, CH_3), 3.62 (s, 3H, OMe), 3.71 (s, 3H, OMe), 4.15 (d, 1H, CH, *J*= 8.7 Hz), 5.12 (m, 2H, CH=), 6.32 (ddd, 1H, CH=, *J*= 16.9 Hz, *J*= 10.2 Hz, *J*= 8.7 Hz), 7.18- 7.33 (m, 5H, CH=).

Dimethyl 2-allyl-2-(1-phenylallyl)malonate (88).[29] Enantiomeric excess determined by HPLC using Chiralpak OJ-H column (87% hexane/2-propanol, flow 0.5 ml/min, λ= 220 nm). t_R 18.0 min (*R*); t_R 20.5 min (*S*). ^{1}H NMR ($CDCl_3$), δ: 2.34 (dd, 1H, CH_2, *J*= 14.1 Hz, *J*= 8.2 Hz), 2.52 (ddt, 1H, CH_2, *J*= 14 Hz, *J*= 6.2 Hz, *J*= 1.2 Hz), 3.60 (s, 3H, OMe), 3.67 (s, 3H, OMe), 3.94 (d, 1H, CH, *J*= 8.5 Hz), 4.90 – 5.02 (m, 3H, CH=), 5.05 (ddd, 1H, CH=, *J*= 10.2 Hz, *J*= 1.6 Hz, *J*= 0.8 Hz), 5.73 (m, 1H, CH=), 6.32 (ddd, 1H, CH=, *J*= 17 Hz, *J*= 10.2 Hz, *J*= 8.5 Hz), 7.08 (m, 2H, CH=), 7.20 (m, 3H, CH=).

Dimethyl 2-(1-phenylallyl)-2-(prop-2-yn-1-yl)malonate (89).[30] Enantiomeric excess determined by HPLC using Chiralpak OJ-H column (87% hexane/2-propanol, flow 0.5 ml/min, λ= 220 nm). t_R 12.8 min (*R*); t_R 14.6 min (*S*). ^{1}H-NMR ($CDCl_3$), δ: 2.09 (t, 1H, CH≡, *J*= 2.6 Hz), 2.55 (dd, 1H, CH_2, *J* = 17.1 Hz, *J*= 2.6 Hz), 2.75 (dd, 1H, CH_2, *J*= 17.1 Hz, *J*= 2.6 Hz) , 3.72 (s, 3H, OMe), 3.76 (s, 3H, OMe), 4.25 (d, 1H, CH, *J*= 8.2 Hz), 5.15 (m, 2H, CH=), 6.42 (ddd, 1H, CH=, *J*= 17.2 Hz, *J*= 10 Hz, *J*= 8.2 Hz), 7.25 (m, 5H, CH=).

4.4.7. Computational details

All calculations were performed using the Gaussian 09 program.[31] Optimizations of minima and transition states were performed employing the B3LYP[32] density functional and the 6-31G(d) basis set for all elements except for Pd for which LANL2DZ[33] was used.[34] All energies presented correspond to single point calculations with the B3LYP-D3 functional[35] and the larger 6-311+G(d,p)[36] basis set for all elements except Pd. Solvation was taken into account along optimization and single points through the use of the PCM continuum model with the default parameters for dichloromethane.[37] The complexes were treated with charge +1 and in the singlet state. No symmetry constraints were applied. The energies were further refined by performing single point calculations using the above-mentioned parameters, with the exception that the 6-311+G** basis set was used for all elements except palladium for which SDD basis set was employed. All energies reported are Gibbs free energies in solution at 298.15 K and calculated as $\Delta G_{\text{reported}} = \Delta G_{\text{B3LYP/6-31G(d)}} + (\Delta E_{\text{B3LYP-D3/6-311+G(d,p)}} - \Delta E_{\text{B3LYP/6-31G(d)}})$.

4.5. References

1. (a) *Asymmetric Catalysis in Industrial Scale: Challenges, Approaches, and Solutions*. Balser, H. U.; Federsel, H. J., Wiley: Weinheim, 2010; (b) *Comprehensive Asymmetric Catalysis*. Jacobsen, E. N.; Pfaltz, A.; Yamamoto, H., Springer-Verlag: Berlin, 1999; (c) *Applied Homogeneous Catalysis with Organometallics Compounds*. Cornils, B.; Hermann, W. A., Wiley-VCH: Weinhein, 2002; (d) *Catalytic Asymmetric Synthesis*. Ojima, I., Wiley: Hoboken, 2010.

2. (a) *Palladium Reagents and Catalysis: Innovations in Organic Synthesis*. Tsuji, J., Wiley: New York, 1995; (b) Johannsen, M.; Jorgensen, K. A., Allylic Amination. *Chemical Reviews* **1998**, *98*, 1689-1708; (c) *Comprehensive Asymmetric Catalysis, Vol. 2*. Pfaltz, A.; Lautens, M.;

Jacobsen, E. N.; Pfaltz, A.; Yamamoto, H., Springer-Verlag: Berlin, 1999; (d) Helmchen, G.; Pfaltz, A., Phosphinooxazolines - A New Class of Versatile, Modular P,N-Ligands for Asymmetric Catalysis. *Accounts of Chemical Research* **2000**, *33*, 336-345; (e) Trost, B. M.; Crawley, M. L., Asymmetric Transition-Metal-Catalyzed Allylic Alkylations: Applications in Total Synthesis. *Chemical Reviews* **2003**, *103*, 2921-2944; (f) Martin, E.; Diéguez, M., Thioether Containing Ligands for Asymmetric Allylic Substitution Reactions. *Comptes Rendus Chimie* **2007**, *10*, 188-205; (g) Lu, Z.; Ma, S., Metal-Catalyzed Enantioselective Allylation in Asymmetric Synthesis. *Angewandte Chemie International Edition* **2008**, *47*, 258-297; (h) Diéguez, M.; Pàmies, O., New Efficient Adaptative Ligands for Pd-Catalyzed Asymmetric Allylic Substitution Reactions. *Accounts of Chemical Research* **2010**, *43*, 312-322; (i) Trost, B. M., Pd- and Mo-Catalyzed Asymmetric Allylic Alkylation. *Organic Process Research & Development* **2012**, *16*, 185-194; (j) Butt, N.; Zhang, W., Transition Metal-Catalyzed Allylic Substitution Reactions with Unactivated Allylic Substrates. *Chemical Society Reviews* **2015**, *44*, 7929-7967; (k) Grange, R. L.; Clizbe, E. A.; Evans, P. A., Recent Developments in Asymmetric Allylic Amination Reactions. *Synthesis* **2016**, *48*, 2911-2968; (l) Butt, N.; Yang, G.; Zhang, W., Allylic Alkylations with Enamine Nucleophiles. *The Chemical Record* **2016**, *16*, 2687-2696.

3. (a) Diéguez, M.; Pàmies, O., Biaryl Phosphites: New Efficient Adaptative Ligands for Pd-Catalyzed Asymmetric Allylic Substitution Reactions. *Accounts of Chemical Research* **2010**, *43*, 312-322; (b) Diéguez, M.; Ruiz, A.; Claver, C., Chiral Diphosphites Derived from d-Glucose: New Highly Modular Ligands for the Asymmetric Catalytic Hydrogenation. *The Journal of Organic Chemistry* **2002**, *67*, 3796-3801; (c) Diéguez, M.; Jansat, S.; Gomez, M.; Ruiz, A.; Muller, G.; Claver, C., Diphosphites as a promising new class of ligands in Pd-catalysed asymmetric allylic alkylation. *Chemical Communications* **2001**, 1132-1133; (d) Diéguez, M.; Pàmies, O.; Claver, C., Palladium-Diphosphite Catalysts for the Asymmetric Allylic Substitution Reactions. *The Journal of Organic Chemistry* **2005**, *70*, 3363-3368; (e) Leeuwen, P. W. N. M. v.; Kamer, P. C. J.; Claver, C.; Pàmies, O.; Diéguez, M., Phosphite-Containing Ligands for Asymmetric Catalysis. *Chemical Reviews* **2011**, *111*, 2077-2118; (f) Pàmies, O.; Diéguez, M., Adaptable P–X Biaryl Phosphite/Phosphoroamidite-Containing Ligands for Asymmetric Hydrogenation and C–X Bond-Forming Reactions: Ligand Libraries with Exceptionally Wide Substrate Scope. *The Chemical Record* **2016**, *16*, 2460-2481.

4. Pàmies, O.; Diéguez, M.; Claver, C., New Phosphite−Oxazoline Ligands for Efficient Pd-Catalyzed Substitution Reactions. *Journal of the American Chemical Society* **2005**, *127*, 3646-3647.

5. (a) Heldmann, D. K.; Seebach, D., Catalytic Enantioselective Hydrosilylation of Ketones with Rhodium-Phosphite Complexes Containing a TADDOLate and a Dihydrooxazole Unit. *Helvetica Chimica Acta* **1999**, *82*, 1096-1110; (b) Escher, I. H.; Pfaltz, A., New Chiral Oxazoline-Phosphite Ligands for the Enantioselective Copper-Catalyzed 1,4-Addition of Organozinc Reagents to Enones. *Tetrahedron* **2000**, *56*, 2879-2888.

6. Biosca, M.; Magre, M.; Pàmies, O.; Diéguez, M., Asymmetric Hydrogenation of Disubstituted, Trisubstituted, and Tetrasubstituted Minimally Functionalized Olefins and Cyclic β-Enamides with Easily Accessible Ir–P,Oxazoline Catalysts. *ACS Catalysis* **2018**, *8*, 10316-10320.

7. (a) Bolm, V.; Zani, L.; Rudolph, J.; Schiffers, I., New Chiral Ligands Derived from Mandelic Acid: Synthesis and Application in the Asymmetric Phenyl Transfer Reaction to an Aromatic Aldehyde. *Synthesis* **2004**, *13*, 2173-2180 ; (b) Li, Z. T.; Li, X. S.; Li, L. C.; Xu, D. C., Convenient Synthesis of a New Class of Chiral Hydroxymethyldihydrooxazole Ligands and Their Application in Asymmetric Addition of Diethylzinc to Aromatic Aldehydes. *Russian Journal of Organic Chemistry* **2006**, *42*, 545-549.

8. d'Ischia, M.; Napolitano, A.; Pezzella, A., 3.04 - Pyrroles and their Benzo Derivatives: Applications. In *Comprehensive Heterocyclic Chemistry III*, Katritzky, A. R.; Ramsden, C. A.; Scriven, E. F. V.; Taylor, R. J. K., Eds. Elsevier: Oxford, 2008; pp 353-388.

9. Lumbroso, A.; Cooke, M. L.; Breit, B., Catalytic Asymmetric Synthesis of Allylic Alcohols and Derivatives and their Applications in Organic Synthesis. *Angewandte Chemie International Edition* **2013**, *52*, 1890-1932.
10. (a) Iourtchenko, A.; Sinou, D., Asymmetric Palladium(0)-Catalyzed Synthesis of Allylic Ethers. *Journal of Molecular Catalysis A: Chemical* **1997**, *122*, 91-93; (b) Haight, A. R.; Stoner, E. J.; Peterson, M. J.; Grover, V. K., General Method for the Palladium-Catalyzed Allylation of Aliphatic Alcohols. *The Journal of Organic Chemistry* **2003**, *68*, 8092-8096; (c) Lam, F. L.; Au-Yeung, T. T. L.; Kwong, F. Y.; Zhou, Z.; Wong, K. Y.; Chan, A. S. C., Palladium–(*S*,p*R*)-FerroNPS-Catalyzed Asymmetric Allylic Etherification: Electronic Effect of Nonconjugated Substituents on Benzylic Alcohols on Enantioselectivity. *Angewandte Chemie International Edition* **2008**, *47*, 1280-1283; (d) Ye, F.; Zheng, Z. J.; Li, L.; Yang, K. F.; Xia, C. G.; Xu, L. W., Development of a Novel Multifunctional N,P Ligand for Highly Enantioselective Palladium-Catalyzed Asymmetric Allylic Etherification of Alcohols and Silanols. *Chemistry – A European Journal* **2013**, *19*, 15452-15457; (e) Caldentey, X.; Pericàs, M. A., Modular P,S-Ligands for Pd-Catalyzed Asymmetric Allylic Substitutions. *The Journal of Organic Chemistry* **2010**, *75*, 2628-2644; (f) Liu, Z.; Du, H., Development of Chiral Terminal-Alkene-Phosphine Hybrid Ligands for Palladium-Catalyzed Asymmetric Allylic Substitutions. *Organic Letters* **2010**, *12*, 3054-3057; (g) Kato, M.; Nakamura, T.; Ogata, K.; Fukuzawa, S. I., Synthesis of Novel Ferrocenyl-Based P,S Ligands (ThioClickFerrophos) and Their Use in Pd-Catalyzed Asymmetric Allylic Substitutions. *European Journal of Organic Chemistry* **2009**, *2009*, 5232-5238; (h) Feng, B.; Cheng, H. G.; Chen, J. R.; Deng, Q. H.; Lu, L. Q.; Xiao, W. J., Palladium/Sulfoxide–Phosphine-Catalyzed Highly Enantioselective Allylic Etherification and Amination. *Chemical Communications* **2014**, *50*, 9550-9553.
11. Bellini, R.; Magre, M.; Biosca, M.; Norrby, P. O.; Pàmies, O.; Diéguez, M.; Moberg, C., Conformational Preferences of a Tropos Biphenyl Phosphinooxazoline–a Ligand with Wide Substrate Scope. *ACS Catalysis* **2016**, *6*, 1701–1712.
12. (a) Ramdeehul, S.; Dierkes, P.; Aguado, R.; Kamer, P. C. J.; van Leeuwen, P. W. N. M.; Osborn, J. A., Mechanistic Implications of the Observation of Kinetic Resolution in a Palladium-Catalyzed Enantioselective Allylic Alkylation. *Angewandte Chemie International Edition* **1998**, *37*, 3118-3121; (b) Dominguez, B.; Hodnett, N. S.; Lloyd-Jones, G. C., Testing Racemic Chiral Catalysts for Kinetic Resolution Potential. *Angewandte Chemie International Edition* **2001**, *40*, 4289-4291; (c) Lüssem, B. J.; Gais, H. J., Palladium-Catalyzed Deracemization of Allylic Carbonates in Water with Formation of Allylic Alcohols: Hydrogen Carbonate Ion as Nucleophile in the Palladium-Catalyzed Allylic Substitution and Kinetic Resolution. *Journal of the American Chemical Society* **2003**, *125*, 6066-6067; (d) Lei, B. L.; Ding, C. H.; Yang, X. F.; Wan, X. L.; Hou, X. L., Kinetic Resolution of 2,3-Dihydro-2-substituted 4-Quinolones by Palladium-Catalyzed Asymmetric Allylic Alkylation. *Journal of the American Chemical Society* **2009**, *131*, 18250-18251; (e) Cheung, H. Y.; Yu, W. Y.; Au-Yeung, T. T. L.; Zhou, Z. A.; Chan, S. C., Effective Chiral Ferrocenyl Phosphine-Thioether Ligands in Enantioselective Palladium-Catalyzed Allylic Alkylations. *Advanced Synthesis & Catalysis* **2009**, *351*, 1412-1422; (f) Hirakawa, T.; Ikeda, K.; Ikeda, D.; Tanaka, T.; Ogasa, H.; Kawatsura, M.; Itoh, T., Regioselective Synthesis of Trifluoromethyl Group Containing Allylic Amines by Palladium-catalyzed Allylic Amination and Sequential Isomerization. *Tetrahedron* **2011**, *67*, 8238-8247; (g) Mao, B.; Ji, Y.; Fañanás-Mastral, M.; Caroli, G.; Meetsma, A.; Feringa, B. L., Highly Enantioselective Synthesis of 3-Substituted Furanones by Palladium-Catalyzed Kinetic Resolution of Unsymmetrical Allyl Acetates. *Angewandte Chemie International Edition* **2012**, *51*, 3168-3173.
13. (a) Trost, B. M.; Toste, F. D., Regio- and Enantioselective Allylic Alkylation of an Unsymmetrical Substrate: A Working Model. *Journal of the American Chemical Society* **1999**, *121*, 4545-4554; (b) Trost, B. M.; Toste, F. D., Palladium Catalyzed Kinetic and Dynamic Kinetic Asymmetric Transformations of γ-Acyloxybutenolides. Enantioselective Total Synthesis of (+)-Aflatoxin B1 and B2a. *Journal of the American Chemical Society* **2003**, *125*, 3090-3100; (c) Dong, Y.; Teesdale-Spittle, P.; Hoberg, J. O., Regioselective Palladium-catalyzed Allylic

Alkylations. *Tetrahedron Letters* **2005**, *46*, 353-355; (d) Gais, H. J.; Bondarev, O.; Hetzer, R., Palladium-catalyzed Asymmetric Synthesis of Allylic Alcohols from Unsymmetrical and Symmetrical Racemic Alylic Carbonates Featuring C–O-Bond Formation and Dynamic Kinetic Resolution. *Tetrahedron Letters* **2005**, *46*, 6279-6283; (e) Kukkadapu, K. K.; Ouach, A.; Lozano, P.; Vaultier, M.; Pucheault, M., Achieving Chemo-, Regio-, and Stereoselectivity in Palladium-Catalyzed Reaction of γ-Borylated Allylic Acetates. *organic Letters* **2011**, *13*, 4132-4135; (f) Du, L.; Cao, P.; Xing, J.; Lou, Y.; Jiang, L.; Li, L.; Liao, J., Hydrogen-Bond-Promoted Palladium Catalysis: Allylic Alkylation of Indoles with Unsymmetrical 1,3-Disubstituted Allyl Acetates Using Chiral Bis(sulfoxide) Phosphine Ligands. *Angewandte Chemie International Edition* **2013**, *52*, 4207-4211; (g) Kawatsura, M.; Terasaki, S.; Minakawa, M.; Hirakawa, T.; Ikeda, K.; Itoh, T., Enantioselective Allylic Amination of Trifluoromethyl Group Substituted Racemic and Unsymmetrical 1,3-Disubstituted Allylic Esters by Palladium Catalysts. *Organic letters* **2014**, *16*, 2442-2445; (h) Ikeda, K.; Futamura, T.; Hanakawa, T.; Minakawa, M.; Kawatsura, M., Palladium-catalyzed Enantioselective Allylic Alkylation of Trifluoromethyl Group Substituted Racemic and Acyclic Unsymmetrical 1,3-Disubstituted Allylic Esters with Malonate Anions. *Organic & Biomolecular Chemistry* **2016**, *14*, 3501-3505.

14. (a) Coll, M.; Pàmies, O.; Diéguez, M., Highly Versatile Pd–Thioether–Phosphite Catalytic Systems for Asymmetric Allylic Alkylation, Amination, and Etherification Reactions. *Organic Letters* **2014**, *16*, 1892-1895; (b) Evans, D. A.; Campos, K. R.; Tedrow, J. S.; Michael, F. E.; Gagné, M. R., Chiral Mixed Phosphorus/Sulfur Ligands for Palladium-Catalyzed Allylic Alkylations and Aminations. *The Journal of Organic Chemistry* **1999**, *64*, 2994-2995; (c) Zhao, D.; Ding, K., A New Type of C2-Symmetric Bisphospine Ligands with a Cyclobutane Backbone: Practical Synthesis and Application. *Organic Letters* **2003**, *5*, 1349-1351.

15. (a) Prétôt, R.; Pfaltz, A., New Ligands for Regio- and Enantiocontrol in Pd-Catalyzed Allylic Alkylations. *Angewandte Chemie International Edition* **1998**, *37*, 323-325; (b) Hilgraf, R.; Pfaltz, A., Chiral Bis(N-tosylamino)phosphine- and TADDOL-Phosphite-Oxazolines as Ligands in Asymmetric Catalysis. *Synlett* **1999**, *1999*, 1814-1816; (c) You, S. L.; Zhu, X. Z.; Luo, Y. M.; Hou, X. L.; Dai, L. X., Highly Regio- and Enantioselective Pd-Catalyzed Allylic Alkylation and Amination of Monosubstituted Allylic Acetates with Novel Ferrocene P,N-Ligands. *Journal of the American Chemical Society* **2001**, *123*, 7471-7472; (d) Hilgraf, R.; Pfaltz, A., Chiral Bis(N-sulfonylamino)phosphine- and TADDOL-Phosphite-Oxazoline Ligands: Synthesis and Application in Asymmetric Catalysis. *Advanced Synthesis & Catalysis* **2005**, *347*, 61-77; (e) Chen, J. P.; Ding, C. H.; Liu, W.; Hou, X. L.; Dai, L. X., Palladium-Catalyzed Regio-, Diastereo-, and Enantioselective Allylic Alkylation of Acylsilanes with Monosubstituted Allyl Substrates. *Journal of the American Chemical Society* **2010**, *132*, 15493-15495.

16. (a) Oslob, J. D.; Åkermark, B.; Helquist, P.; Norrby, P. O., Steric Influences on the Selectivity in Palladium-Catalyzed Allylation. *Organometallics* **1997**, *16*, 3015-3021; (b) Hagelin, H.; Åkermark, B.; Norrby, P. O., New Molecular Mechanics (MM3*) Force Field Parameters for Calculations on (η^3-Allyl)palladium Complexes with Nitrogen and Phosphorus Ligands. *Organometallics* **1999**, *18*, 2884-2895.

17. (a) Auburn, P. R.; Mackenzie, P. B.; Bosnich, B., Asymmetric Synthesis. Asymmetric Catalytic Allylation Using Palladium Chiral Phosphine Complexes. *Journal of the American Chemical Society* **1985**, *107*, 2033-2046; (b) Jia, C.; Müller, P.; Mimoun, H., Palladium-catalyzed Allylic Acetoxylation of Olefins Using Hydrogen Peroxide as Oxidant. *Journal of Molecular Catalysis A: Chemical* **1995**, *101*, 127-136; (c) Ward, Y. D.; Villanueva, L. A.; Allred, G. D.; Payne, C. C.; Semones, M. A.; Liebeskind, L. S., Synthesis, Characterization, and Configurational Lability of (η^3-Allyl)dicarbonyl[hydrotris(1-pyrazolyl)borato]molybdenum Complexes Bearing Substituents at the Termini: Thermodynamic Preference for the Anti Stereoisomer. *Organometallics* **1995**, *14*, 4132-4156; (d) Allen, J. V.; Williams, J. M. J., Enantiomerically Pure Oxazolines Tethered to Alcohols. Preparation and Use in Asymmetric Catalysis. *Tetrahedron: Asymmetry* **1994**, *5*, 277-282; (e) Buisson, D.; Azerad, R., Preparation and Use of (S)-O-Acetyllactyl Chloride (Mosandl's Reagent) as a Chiral Derivatizing Agent.

Tetrahedron: Asymmetry **1999**, *10*, 2997-3002; (f) Kardassis, G.; Brungs, P.; Nothhelfer, C.; Steckhan, E., Electrogenerated Chiral Cationic Glycine Equivalents — Part 2: Chiral 3-Methoxy-2,5-morpholinediones from (S)-α-Hydroxy Acids and Dimethyl Aminomalonate. *Tetrahedron* **1998**, *54*, 3479-3488; (g) Buisman, G. J. H.; Kamer, P. C. J.; van Leeuwen, P. W. N. M., Rhodium Catalysed Asymmetric Hydroformylation with Chiral Diphosphite Ligands. *Tetrahedron: Asymmetry* **1993**, *4*, 1625-1634; (h) Mazuela, J.; Pàmies, O.; Diéguez, M., Biaryl Phosphite–Oxazoline Ligands from the Chiral Pool: Highly Efficient Modular Ligands for the Asymmetric Pd-Catalyzed Heck Reaction. *Chemistry: A European Journal* **2010**, *16*, 3434-3440.

18. Liu, Y.; Cao, Z.; Du, H., Asymmetric Allylic Alkylation of Pyrroles and 4,7-Dihydroindoles with Alkene–Phosphine Ligands. *The Journal of Organic Chemistry* **2012**, *77*, 4479-4483.

19. Popa, D.; Marcos, R.; Sayalero, S.; Vidal-Ferran, A.; Pericàs, M. A., Towards Continuous Flow, Highly Enantioselective Allylic Amination: Ligand Design, Optimization and Supporting. *Advanced Synthesis & Catalysis* **2009**, *351*, 1539-1556.

20. Wang, A.-E.; Yu, C.-C.; Chen, T.-T.; Liu, Y.-P.; Huang, P.-Q., Enamines as Surrogates of Alkene Carbanions for the Reductive Alkenylation of Secondary Amides: An Approach to Allylamines. *Organic Letters* **2018**, *20*, 999-1002.

21. Yang, H.; Fang, L.; Zhang, M.; Zhu, C., An Efficient Molybdenum(VI)-Catalyzed Direct Substitution of Allylic Alcohols with Nitrogen, Oxygen, and Carbon Nucleophiles. *European Journal of Organic Chemistry* **2009**, *2009*, 666-672.

22. Pàmies, O.; van Strijdonck, G. P. F.; Diéguez, M.; Deerenberg, S.; Net, G.; Ruiz, A.; Claver, C.; Kamer, P. C. J.; van Leeuwen, P. W. N. M., Modular Furanoside Phosphite Ligands for Asymmetric Pd-Catalyzed Allylic Substitution. *The Journal of Organic Chemistry* **2001**, *66*, 8867-8871.

23. Dugal-Tessier, J.; Dake, G. R.; Gates, D. P., Chiral Phosphaalkene-Oxazoline Ligands for the Palladium-Catalyzed Asymmetric Allylic Alkylation. *Organic Letters* **2010**, *12*, 4667-4669.

24. Trost, B. M.; Lautens, M., Cyclization via isomerization: a palladium(2+)-catalyzed carbocyclization of 1,6-enynes to 1,3- and 1,4-dienes. *Journal of the American Chemical Society* **1985**, *107*, 1781-1783.

25. Lloyd-Jones, G. C.; Pfaltz, A., Chiral Phosphanodihydrooxazoles in Asymmetric Catalysis: Tungsten-Catalyzed Allylic Substitution. *Angewandte Chemie International Edition in English* **1995**, *34*, 462-464.

26. Hu, Z.; Li, Y.; Liu, K.; Shen, Q., Bis(perfluoroalkyl) phosphino-oxazoline: a modular, stable, strongly π-accepting ligand for asymmetric catalysis. *Journal of Organic Chemistry* **2012**, *77*, 7957-7967.

27. Alexakis, A.; Polet, D., Very Efficient Phosphoramidite Ligand for Asymmetric Iridium-Catalyzed Allylic Alkylation. *Organic Letters* **2004**, *6*, 3529-3532.

28. Meng, C.-Y.; Liang, X.; Wei, K.; Yang, Y.-R., Enantioselective Ir-Catalyzed Allylic Alkylation of Racemic Allylic Alcohols with Malonates. *Organic Letters* **2019**, *21*, 840-843.

29. Streiff, S.; Welter, C.; Schelwies, M.; Lipowsky, G.; Miller, N.; Helmchen, G., Carbocycles via enantioselective inter- and intramolecular iridium-catalysed allylic alkylations. *Chemical Communications* **2005**, 2957-2959.

30. Farwick, A.; Engelhart, J. U.; Tverskoy, O.; Welter, C.; Umlauf, Q. E.; Rominger, F.; Kerr, W. J.; Helmchen, G., Bicyclic Cyclopentenones via the Combination of an Iridium- Catalyzed Allylic Substitution with a Diastereoselective Intramolecular Pauson–Khand Reaction. *Advanced Synthesis & Catalysis* **2011**, *353*, 349.

31. Frisch, M. J.; Trucks, G. W.; Schlegel, H. B.; Scuseria, G. E.; Robb, M. A.; Cheeseman, J. R.; Scalmani, G.; Barone, V.; Mennucci, B.; Petersson, G. A.; Nakatsuji, H.; Caricato, M.; Li, X.; Hratchian, H. P.; Izmaylov, A. F.; Bloino, J.; Zheng, G.; Sonnenberg, J. L.; Hada, M.; Ehara, M.; Toyota, K.; Fukuda, R.; Hasegawa, J.; Ishida, M.; Nakajima, T.; Honda, Y.; Kitao, O.; Nakai, H.; Vreven, T.; Montgomery, J. A.; Peralta, J. E.; Ogliaro, F.; Bearpark, M.; Heyd, J. J.; Brothers, E.; Kudin, K. N.; Staroverov, V. N.; Kobayashi, R.; Normand, J.; Raghavachari, K.; Rendell, A.;

Burant, J. C.; Iyengar, S. S.; Tomasi, J.; Cossi, M.; Rega, N.; Millam, J. M.; Klene, M.; Knox, J. E.; Cross, J. B.; Bakken, V.; Adamo, C.; Jaramillo, J.; Gomperts, R.; Stratmann, R. E.; Yazyev, O.; Austin, A. J.; Cammi, R.; Pomelli, C.; Ochterski, J. W.; Martin, R. L.; Morokuma, K.; Zakrzewski, V. G.; Voth, G. A.; Salvador, P.; Dannenberg, J. J.; Dapprich, S.; Daniels, A. D.; Farkas, O.; Foresman, J. B.; Ortiz, J. V.; Cioslowski, J.; Fox, D. J. *Gaussian 09*, 2009.

32. (a) Lee, C.; Yang, W.; Parr, R. G., Development of the Colle-Salvetti Correlation-Energy Formula into a Functional of the Electron Density. *Physical Review B: Condensed Matter and Materials Physics* **1988**, *37*, 785-789; (b) Becke, A. D., Density-Functional Thermochemistry. III. The Role of Exact Exchange. *Journal of Chemical Physics* **1993**, *98*, 5648-5652.

33. Hay, P. J.; Wadt, W. R., Ab initio Effective Core Potentials for Molecular Calculations. Potentials for K to Au Including the Outermost Core Orbitals. *Journal of Chemical Physics* **1985**, *82*, 299-310.

34. (a) Hehre, W. J.; Ditchfield, R.; Pople, J. A., Self—Consistent Molecular Orbital Methods. XII. Further Extensions of Gaussian—Type Basis Sets for Use in Molecular Orbital Studies of Organic Molecules. *Journal of Chemical Physics* **1972**, *56*, 2257-2261; (b) Hariharan, P. C.; Pople, J. A., The Influence of Polarization Functions on Molecular Orbital Hydrogenation Energies. *Theoretical Chemical Acta* **1973**, *28*, 213-222; (c) Francl, M. M.; Pietro, W. J.; Hehre, W. J.; Binkley, J. S.; Gordon, M. S.; Defrees, D. J.; Pople, J. A., Self-Consistent Molecular Orbital Methods. XXIII. A Polarization-type Basis Set for Second-row Elements. *Journal of Chemical Physics* **1982**, *77*, 3654-3665.

35. (a) Grimme, S.; Antony, J.; Ehrlich, S.; Krieg, H., A Consistent and Accurate Ab Initio Parametrization of Density Functional Dispersion Correction (DFT-D) for the 94 Elements H-Pu. *Journal of Chemical Physics* **2010**, *132*, 154104; (b) Grimme, S.; Ehrlich, S.; Goerigk, L., Effect of the Damping Function in Dispersion Corrected Density Functional Theory. *Journal of Computational Chemistry* **2011**, *32*, 1456-1465.

36. (a) Krishnan, R.; Binkley, J. S.; Seeger, R.; Pople, J. A., Self-Consistent Molecular Orbital Methods. XX. A Basis Set for Correlated Wave Functions. *Journal of Chemical Physics* **1980**, *72*, 650-654; (b) McLean, A. D.; Chandler, G. S., Contracted Gaussian Basis Sets for Molecular Calculations. I. Second Row Atoms, Z = 11–18. *Journal of Chemical Physics* **1980**, *72*, 5639-5648.

37. (a) Miertus, S.; Tomasi, J., Approximate Evaluations of the Electrostatic Free Energy and Internal Energy Changes in Solution Processes. *Chemical Physics* **1982**, *65*, 239-245; (b) Mennucci, B.; Tomasi, J., Continuum Solvation Models: A New Approach to the Problem of Solute's Charge Distribution and Cavity Boundaries. *Journal of Chemical Physics* **1997**, *106*, 5151-5158; (c) Cossi, M.; Barone, V.; Mennucci, B.; Tomasi, J., Ab initio Study of Ionic Solutions by a Polarizable Continuum Dielectric Model. *Chemical Physics Letters* **1998**, *286*, 253-260.

UNIVERSITAT ROVIRA I VIRGILI
DEVELOPMENT OF TAILOR-MADE CATALYST LIBRARIES FOR THE CONSTRUCTION OF CHIRAL C-X (X= C, N AND O) BONDS. APPLICATION TO THE SYNTHESIS OF COMPLEX MOLECULES
Joan Saltó de la Torre

Chapter 5

Synthetic applications of the resulting Pd-catalyzed allylic substitution products

5.1. Introduction

The sustainable production has become essentially in our society. The reduction of waste or the efficient use of energy are nowadays a must for industrial processes. In the production of enantiopure compounds, asymmetric catalysis plays an important role since with the proper chose of the catalytic system high conversions and excellent enantioselectivities can be obtained.[1] Moreover, their production is growing and the searching for more selective, less expensive, and environmentally friendly processes is today a top research topic. In this regard, enantioselective Pd-catalyzed allylic substitution has become an important strategy for several reasons. First, the enantioselectivities obtained can be excellent with a carefully choice of the ligand. Second, this reaction allows the formation of C-C, C-N and C-O bonds. Third, it has high group tolerance. And finally, the reaction conditions are usually mild. For this reason, its application in synthetic chemistry has grown exponentially.[2] Nevertheless, some of the alkylated products used in Pd-catalyzed asymmetric allylic substitution such as propargylated and alkene-containing products **16**-**19**, **30**, **38**, **46**, **47**, **50** or **52** (*vide supra*) remain in the research studies without any further derivatization. For this reason, we decided to give more value to the alkylated products obtained (from the previous Chapters 3 and 4) by performing several derivatizations with the aim to attain (poly)carbocyclic and heterocyclic compounds. In this Chapter, we present our efforts towards the synthesis of (poly)carbocyclic and heterocyclic compounds by combining in a sequential manner the enantioselective allylic substitution with either Grubbs metathesis or metal-catalyzed cycloisomerizations or Pauson-Khand reactions (Scheme 2.3.1). By following this strategy, a range of (poly)carbocyclic and heterocyclic compounds have been prepared in a straightforward manner. Among them all, we should highlight the high efficiency attained in the synthesis of highly functionalized bi- and tricyclic compounds with multiple stereogenic center.

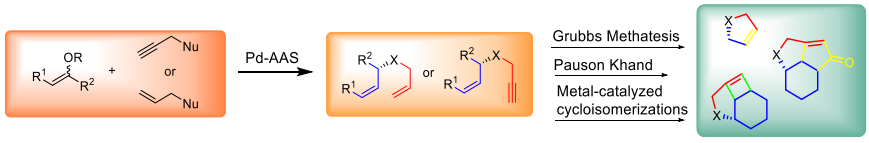

Scheme 5.1. Derivatization of Pd-AAS products to more valuable chiral molecules.

5.2. Results and discussion

5.2.1. Preparation of chiral carbo- and heterocycles via ring closing metathesis

We first studied the use of alkene-containing substitution products obtained in Chapter 3 from the benchmark substrate **S1** and its derivatives for the synthesis of chiral

carbo- and heterocycles via Grubbs metathesis (Table 5.1). Grubbs metathesis involves the exchange of substituents between two different double bonds. The alkenes involving this reaction can be either from two different molecules (intermolecular) or being in the same molecule (intramolecular). In the case of an intramolecular reaction (ring closing metathesis), which have been extensively used in organic synthesis, it leads to the cyclization.[3] In this regard, we thought to use a sequential enantioselective allylic substitution/ring closing metathesis for the formation of chiral functionalized carbo- and heterocyclic compounds.

Table 5.1. Synthesis of chiral functionalized carbo- and heterocyclic compounds **90**-**95**.[a]

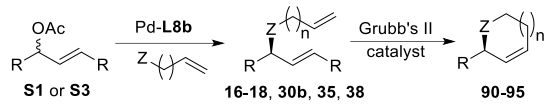

Entry	Substitution product	Cyclic product	% Yield[b]	% *ee*[c]
1	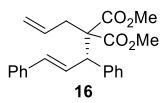 **16**	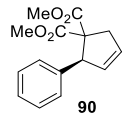 **90**	85	98 (*S*)
2	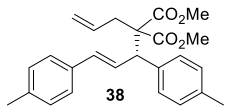 **38**	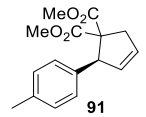 **91**	83	97 (*S*)
3	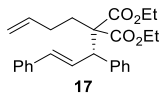 **17**	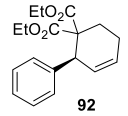 **92**	80	97 (*S*)
4	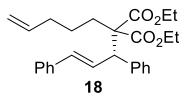 **18**	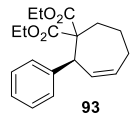 **93**	77	95 (*S*)
5	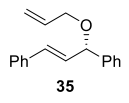 **35**	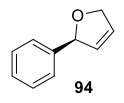 **94**	73	96 (*S*)
6[d]	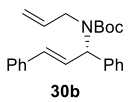 **30b**	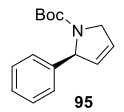 **95**	65	96 (*S*)

[a] Grubbs II (5 mol %), substitution product (1 equiv), dichloromethane, at rt for 16 h. [b] After two consecutive steps. [c] Determined by HPLC or GC. [d] **30b** was obtained in quantitative yields after Boc protection of the corresponding chiral allylamine **30**.

Following this approach, the ring closing metathesis of alkylated products **16**-**18** and **38**, containing vinyl, butenyl and pentenyl groups and prepared using Pd/**L8b** catalytic system, led to the efficient synthesis of 5-, 6- and 7-membered ring carbocycles **90**-**93** in high yields and with complete transfer of the chiral information from the starting materials (Table 5.1, entries 1-4, *ee*'s up to 98%).

The ring closing metathesis reaction was also attempted using the chiral allyl ether **35** yielding with high enantiomeric excess the heterocyclic chiral ether **94** (entry 5, 96% *ee*). Finally, we attempted the cyclization of allyl amine **30**. Unfortunately, compound **30** did not undergo the ring closing metathesis reaction, probably owing to the azophilicity of ruthenium. To overcome this, we decided to use the *tert*-butyl carbamate analog **30b**, which led to the formation of the expected *N*-heterocyclic compound **95** in good yield and with excellent *ee* (entry 6, 96% *ee*).

5.2.2. Preparation of bi- and tricyclic compounds via metal catalyzed cycloisomerization reactions

Initially, we focused on the synthesis of chiral bicyclic compounds with multiple stereogenic centers via a sequential enantioselective allylic substitution/metal-catalyzed cycloisomerization reactions (Tables 5.2 and 5.3). In a first set of experiments chiral 1,6-enynes **47**, **50** and **52**, prepared in Chapter 4 using Pd/**L9e**, were transformed to chiral functionalized bicyclic compounds **96**-**98** by means of the $PtCl_2$ mediated cycloisomerization in the presence of methanol.[4]

Table 5.2. Synthesis of chiral functionalized bicyclic compounds **96**-**98** from the corresponding 1,5-enynes.[a]

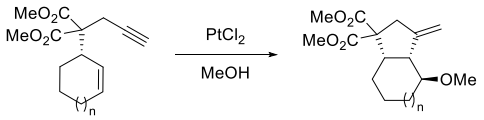

47, **50** and **52** → **96-98**

Entry	Starting material	Product	% Yield[b]	% *ee*[c]
1	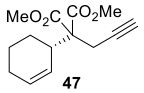 **47**	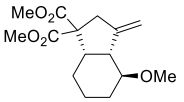 **96**	60	93 (*R,S,S*)
2	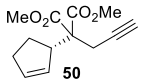 **50**	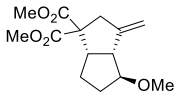 **97**	9	99 (*R,S,S*)
3	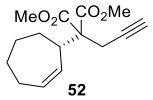 **52**	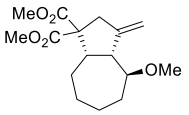 **98**	46	>99 (*R,S,S*)

[a] Enyne (1 mmol), $PtCl_2$ (5 mol%), MeOH, at reflux for 18 h [b] Isolated after flash chromatography. [c] Determined by HPLC.

This cycloisomerization involves the Pt (II) η^2-alkyne coordination and subsequently attack of the alkene to the electrophilic Pt- η^2-alkyne. This leads to the formation of a η^1-alkenyl complex. The nucleophilic addition of MeOH into the carbocation (formed

after attack of the alkene), and protonolysis of the η^1-alkenyl complex, allow the formation of the alkoxylated-bicyclic products with the exocyclic bond.[4b] The results in Table 5.2 indicates that the three chiral alkoxy bicycles **96**-**98** could be attained with an excellent enantiocontrol. The yields ranged from good (for compound **96**) to poor for the more sterically constrained bicyclic product **97**. The low yields obtained in **97** could be explained since the intramolecular attack of the cyclic alkene to the η^2-alkyne-Pt complex is less favourable in the presence of cyclopentene ring. Furthermore, the relative stereochemistry of the products was assigned as previously reported with the achiral version of **96**.[4a]

We then studied the cycloisomerization of chiral 1,6-enynes **47**, **50** and **52**, prepared in Chapter 4 with Pd/**L9e**, using $RuCl_3$ to yield the corresponding unsaturated bicycles **99**-**101** (Table 2.3.3).[5] This cycloisomerization involves the formation of Ru(II)-η^2-alkyne which is further attacked by the double bond. Then, protonolysis followed by β-hydride elimination leads to the formation of the bicyclic desired unsaturated bicycles.[4b, 5] We could obtain **99** and **101** with a delightful enantiocontrol in good yields. However, when **50** was submitted to the same reaction conditions, the reaction only led to the decomposition of the starting material.

Table 5.3. Synthesis of chiral functionalized bicycles **99-101**.[a]

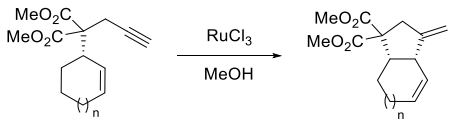

46, **50** and **52** → **99-101**

Entry	Starting material	Product	% Yield[b]	% *ee*[c]
1	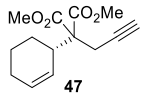 **47**	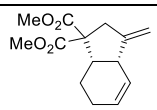 **99**	61	>99 (*R,S*)
2	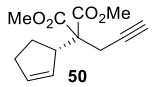 **50**	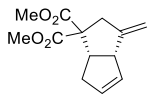 **100**	0	0
3	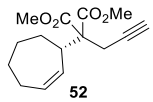 **52**	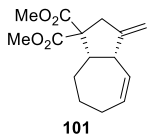 **101**	70	>99 (*R,S*)-

[a] Enyne (1 mmol), $RuCl_3$ (5 mol%), MeOH [b] Isolated after flash chromatography. [c] Determined by chiral HPLC.

In order to further prove the applicability of allylic substitution products we focused in the preparation of chiral tricyclic structures, containing a constrained cyclobutene ring. In this regard, 1,6-enynes and 1,7-enynes has been reported to undergo metal catalyzed cycloisomerization reactions to obtain cyclobutenes (Scheme 5.2),

nevertheless they were obtained as racemates and their chiral version have never been reported.[6] In this sense, Au(I)-JohnPhos and Pt(II) complexes have been reported to catalyze this transformation. Regarding the mechanistic aspects of the reaction, there has been controversy and several mechanistic pathways have been published.[7] Though, in general, MX_n coordinates to the alkyne which after attack of the alkene forms a cyclopropyl-metal carbene. This cyclopropyl-carbene can undergo reductive elimination to form the corresponding ene-products or forming the corresponding cyclobutenes. The cyclobutene formation seems to be favorable when the geometry of the alkene does not allow the corresponding skeletal rearrangement to form the corresponding alder-ene type products.[6a, 7a] Thus, this process can be seen as [2+2]-type cycloaddition reaction. As the reaction pathway does not seem to involve the chiral bound created by Pd-catalyzed asymmetric allylic substitution, we attempted the metal catalyzed cycloisomerization to obtain the corresponding tricyclic chiral cyclobutenes.

Scheme 5.2. General structure of cyclobutene containing compounds.

In order to have more variety of tricyclic structures, we expanded the nucleophile scope studied in Chapter 4 for cyclic substrates **S2**, **S8** and **S9**. In this new nucleophile scope, we focused on the malonate nucleophiles bearing alkynyl groups since they will enable the preparation of more structurally diverse tricyclic scaffolds. For do this, we alkylated the cyclic substrates which differs in the ring size (from five- to seven-membered ring) with a range of substituted propargyl- and butynyl-containing malonate nucleophiles using Pd/**L9c** catalytic system. The results are summarized in Table 5.4.

The alkylation of cyclohexenyl cyclic substrate **S2** proceeded as expected providing the alkylated products **102**, **105** and **111** in good-to-excellent yields and excellent enantioselectivities regardless the substitution pattern on the nucleophile used (*ee*'s up to 99%, entries 1, 4, 7 and 10). These excellent results were maintained for cycloheptenyl cyclic substrate **S9** which provided **103**, **106** and **109** in good yields and with an excellent stereocontrol (ee's up to 99%, entries 3, 6 and 9). Finally, we also attempted this transformation on the more challenging 5-membered ring substrate **S8**. To our delight, we could attain the allylic alkylation products **104**, **105** and **110** in good yields and with enantioselectivities comparable with those obtained for propargyl derivative **50** regardless the nucleophile used (*ee's* up to 93%, entries 2, 5 and 8).

Table 5.4. Expansion of nucleophile scope of cyclic substrates **S2**, **S8** and **S9** with Pd/**L9c** catalytic system.[a]

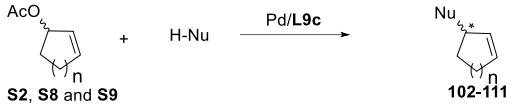

Entry	Substrate	Product	% Yield[b]	% *ee*[c]
1	**S2**	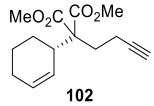 **102**	65	99
2	**S9**	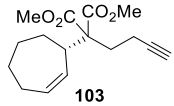 **103**	70	99
3	**S8**	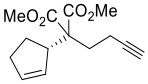 **104**	82	92
4	**S2**	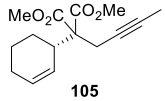 **105**	71	98
5	**S9**	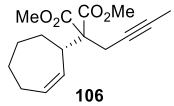 **106**	65	99
6	**S8**	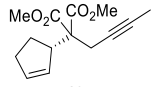 **107**	70	91
7	**S2**	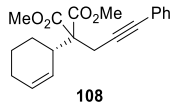 **108**	64	98
8	**S9**	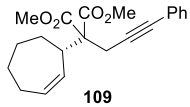 **109**	76	99
9	**S8**	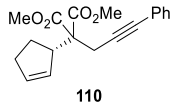 **110**	82	93
10	**S2**	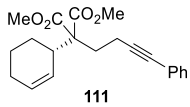 **111**	90	99

[a] 0.5 mol% $[PdCl(\eta^3\text{-}C_3H_5)]_2$, ligand (0.011 mmol), substrate (1 mmol), CH_2Cl_2 (2 ml), BSA (3 eq), dimethyl malonate (3 eq), KOAc (pinch). [b] Full conversions. [c] Measured by HPLC.

Next, we tested the chiral 1,7- and 1,6-enynes **102**-**104** and **108**-**111** in the Au(I)- and Pt(II)-catalyzed cycloisomerizayion reactions (Table 5.5). Thus, the Au(I)-catalyzed

cycloisomerization of 1,7-enyne **102**, with a 6-membered ring, proceeded cleanly to yield tricyclic compound **112** in high yield and excellent selectivity (entry 1). In contrast, the reaction of **102** with the Pt-catalyst led to a complex reaction mixture. In the case of the 7-membered ring substrate **103** the cycloisomerization with gold catalyst led to the clean formation of the bicyclic product **113** rather than the expected tricyclic derivative (entry 2). Again, cycloisomerization of **103** with Pt led to an intractable mixture of cycloisomerized products. For enyne **104**, bearing a 5-memberd ring, no reaction was observed using either gold or platinum catalysis (entry 3).

Table 5.5. Au(I) and Pt(II) catalyzed cycloisomerization reaction on 1,6- and 1,7-enynes.

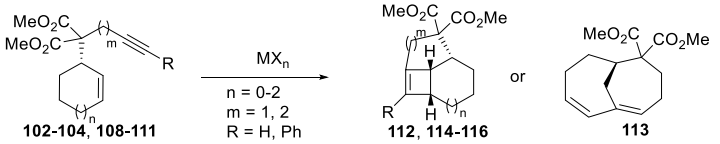

102-104, 108-111 — 112, 114-116 — 113

Entry	Enyne	Catalyst: JohnPhos Au(I)[a]	Catalyst: $PtCl_2/CO$[b]	Yield %[c]	*ee* %[d]
1	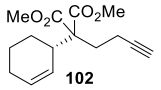 **102**	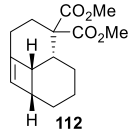 **112**	Complex reaction mixture	75	98
2	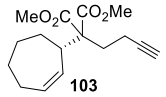 **103**	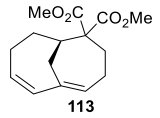 **113**	Complex reaction mixture	65	99
3	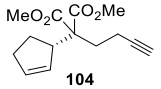 **104**	n.r.[e]	n.r.	-	-
4	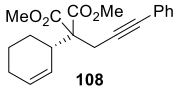 **108**	n.r.	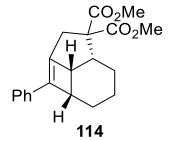 **114**	90	98
5	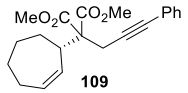 **109**	n.r.	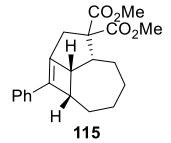 **115**	74	99
6	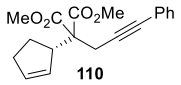 **110**	n.r.	n.r.	-	-

(Continuation)

Entry	Enyne	JohnPhos Au(I)[a]	$PtCl_2$/CO[b]	Yield %[c]	*ee* %[d]
7[f]	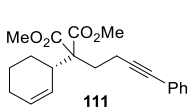 **111**	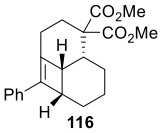 **116**	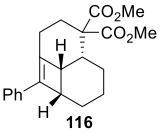 **116**	85/55[h]	98/99[h]

[a] $[Au(P(Cy)_2(C_6H_4\text{-}C_6H_5)(AcCN)](SbF_6)$ (2% mol), enyne (0.2 mmol), 4 Å MS, DCM, 18 h. [b] $PtCl_2$ (10 mol%), enyne (0.2 mmol), toluene, CO atmosphere, at 80 °C for 18 h. [c] After chromatographic isolation. [d] Determined by HPLC. [e] No reaction. [f] In this case, using $PtCl_2$/CO full conversions were not attained even for longer reaction times (72 h). [h] Yields and *ee*'s obtained by Au(I) and Pt(II) catalysis respectively.

For 1,6-enynes **108**, we obtained the corresponding chiral cyclobutene **114** from the 6- membered ring enyne **108** using platinum catalysis (entry 4). In contrast to **103**, the 7-membered ring enyne **109** gave the desired tricyclic compound **115** in good yields and with an excellent *ee* (entry 5). Again, the 5-membered ring enyne **110** did not undergo any transformation using either Au(I) or Pt(II) strategies. The 1,6-enynes were recovered unreacted when we attempted their cycloisomerization reaction using the gold catalyst.

Finally, Ph-substituted 1,7-enyne **111** was cycloisomerized using both gold (I) and $PtCl_2$/CO catalytic systems. In all cases, the resulting relative stereochemistry was assigned as previously described in the literature for the corresponding racemic compounds.[6a, 8]

To sum up, we could prepare 4 different chiral tricyclic structures containing a highly constrained cyclobutene ring using the sequential Pd-catalyzed allylic alkylation and metal catalyzed cycloisomerization reactions.

5.2.3. Preparation of bi- and tricyclic compounds *via* Pauson Khand reaction

In order to extend the applicability of the propargylated compounds obtained by Pd-catalyzed asymmetric allylic substitution, we further tested them in Pauson Khand reactions. Pauson Khand reaction can be described formally as a [2+2+1] cycloaddition of an alkyne, and alkene and a CO.[9] This reaction usually involves the stechiometric coordination of $Co_2(CO)_8$ to the alkyne form a dicobaltocycle which is usually isolable. After that, an alkene can be further coordinated to form a metallacyclopentene complex. After, a migratory insertion of CO in one of Co-C bonds and a subsequently reductive elimination of the complex leads to the formation of cyclopentenones.[10]

In a first set of experiments we focused on the preparation of chiral bicyclopentenones **117**-**120** by sequential reactions involving allylic substitution followed by Pauson-Khand enyne cyclization (Table 5.6). Initially, we attempted the Pauson Khand reaction under thermal conditions by coordination of the enyne **19** with $Co_2(CO)_8$ and subsequent thermal decomposition in refluxing *tert*-butylbenzene.[11] Nevertheless, the corresponding cyclopentenone **117** was attained in poor yields (entry

1). In order to improve the yield, we attempted this transformation using *N*-morpholine oxide (NMO) as promoter at room temperature.[12] Under these conditions, the reaction proceeded as expected obtaining chiral bicyclopentenone **117** in good yield excellent enantiomeric control (Table 5.6, entry 2).

Next, we attempted the derivatization of linear non-symmetric enynes **76** and **89** which led to the expected bicyclopentenones **118** and **119** in moderate yields (entries 3 and 4). The enantioselectivities observed were the same of the enynes, indicating that the chiral information was transferred to the cyclopentenone without any lost during the process. Unfortunately, the Pauson-Khand reaction of enyne **61** did not proceed, being enyne **61** recovered after the reaction. This fact can be explained due to the azaphilicity of cobalt which coordinate first to the amino group rather than to the alkyne moiety.

Table 5.6. Preparation of chiral bicyclopentenones **117**-**120** by sequential reactions involving allylic substitution followed by Pauson-Khand enyne cyclization.

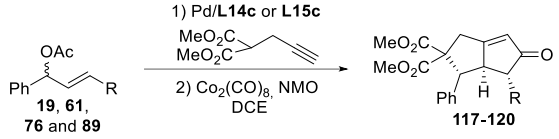

Entry	Enyne	Product	% Yield[a]	% *ee*[b]
1[c]	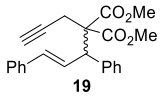 **19**	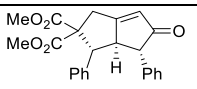 **117**	10	n.d.
2[d]	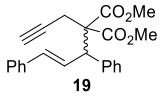 **19**	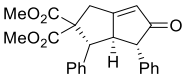 **117**	62	99 (*R,R,S*)
3[d]	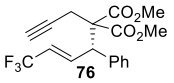 **76**	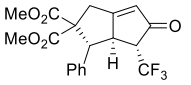 **118**	39	73 (*R,R,R*)
4[d]	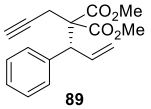 **89**	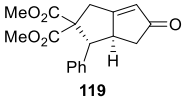 **119**	41	89 (*R,S*)
5[d]	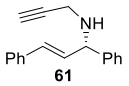 **61**	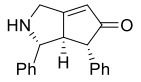 **120**	0	-

[a] Full conversion. [b] Determined by chiral HPLC. [c] $Co_2(CO)_8$ (1.1 equiv), substrate (0.5 mmol), ^{t}Butyl-benzene (1 ml) 1 h, then reflux for 24 h. [d] $Co_2(CO)_8$ (1.1 equiv), substrate (0.5 mmol), DCE (1 ml) 1 h. Then, NMO (6 equiv) until completion (from 1 h to 12 h).

Then, we moved to the preparation of chiral tricyclic cyclopentenones *via* a sequential enantioselective allylic substitution/Pauson-Khand reactions. The use of cyclic enynes such as **47**, **50** and **52** led to the formation of chiral carbocycles containing highly strained trifused-rings. In this regard, we first studied Pauson-Khand reaction with

enynes **47**, **50** and **52**, previously synthesized with Pd/**L9c** catalytic system (*vide supra*, Chapter 4, Table 4.6). Initially, we attempted reaction using the previously reported thermal decomposition conditions.[11] Under these conditions, the tricyclic carbocycles **121**-**123** were obtained in poor-to-moderate yields albeit the enantioselectivities remained excellent during the process (Table 5.7.). With the aim of improve the yields of this reaction we further tested the use of an *N*-methylmorpholine oxide as promoter. Under these conditions, carbocycles **121**-**123** were attained in good yields (up to 75%) and with enantioselectivities comparable to those obtained on the starting materials (*ee's* up to >99%). The relative stereochemistry of tricyclic compounds **121**-**123** has been previously reported and determined by NOE experiments as well as by crystallographic characterization (for compound **123**).[11]

Table 5.7. Synthesis of chiral functionalized fused tricycles **121-123**.

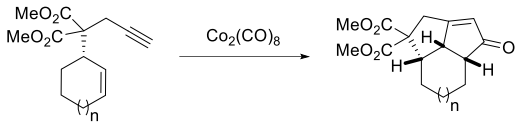

47, **50** and **52** — **121-123**

			Thermal decomposition[a]		Using NMO as promoter[b]	
Entry	Enyne	Product	% Yield[c]	% *ee*[d]	% Yield[c]	% *ee*[d]
1	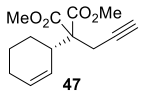 **47**	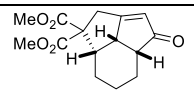 **121**	26	99	52	>99
2	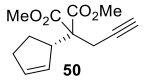 **50**	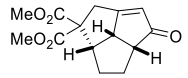 **122**	63	92	75	93
3	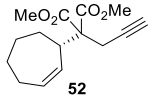 **52**	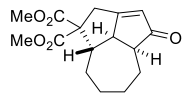 **123**	42	>99	70	99

[a] Alkyne (1 equiv), $Co_2(CO)_8$ (1.3 equiv), *tert*-butylbenzene at reflux for 12 h. [b] Alkyne (1 equiv), $Co_2(CO)_8$ (1.3 equiv), NMO (6 equiv), dichloroethane, until competition (from 2 h to 12 h). [d] After chromatographic isolation. [e] Determined by HPLC.

We then move to study the scope of the Pauson-Khand reaction using enynes **102**-**111** synthesized in Table 5.4. The results are summarized in Table 5.8. Initially, we performed this transformation using 1,7-enynes **102**-**104**. The corresponding tricyclic structures **124**-**126** were obtained in moderate-to-good yields with complete transmission of the chiral information (entries 1-3). It must be mentioned that the resulting relative stereochemistry was the same as observed for **121**-**123**, obtaining **124** and **125** with a *syn-syn* relative stereochemistry and an *anti-syn* for **125**. Next, we

studied the Pauson-Khand reaction of methyl substituted 1,6-enynes **105**-**107**. The reactions proceeded smoothly yielding the corresponding α-methylcyclopentenones **127**-**129** in good yields and excellent enantioselectivities (entries 4-6). The use of phenyl-substituted 1,6-enynes **108**-**110** also led to the formation of the corresponding tryciclic α-phenylcylopentenones in good yields and excellent enantioselectivities (compounds **130**-**132**, entries 7-9). It should be mentioned that for compound **129** the formation of two diastereoisomers at a ratio of 95:5 (*syn-syn*, *syn-anti*, respectively) was attained. Finally, we also studied the Pauson-Khand reaction of phenyl-substituted 1,7-enyne **111**. The corresponding tryciclic α-phenylcylopentenone **133** was attained in 76% yield as a 6:4 diastereomeric mixture of the *syn-syn* and the *anti-syn* isomers, respectively in excellent *ee*'s.

Table 5.8. Pauson-Khand reaction using enynes **102**-**111**.[a]

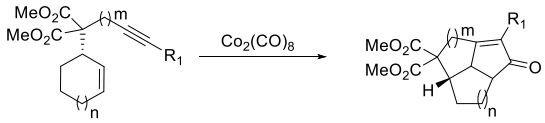

102-111 **124-133**

Entry	Enyne	Product	% Yield[a]	% *ee*[c]
1	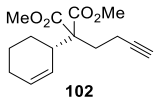 **102**	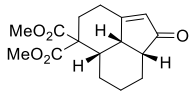 **124**	76	99
2	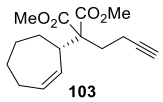 **103**	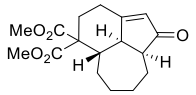 **125**	89	99
3	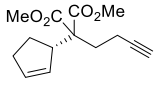 **104**	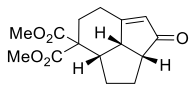 **126**	54	91
4	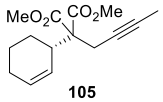 **105**	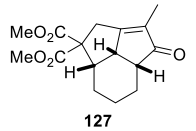 **127**	67	98
5	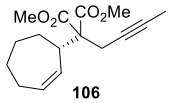 **106**	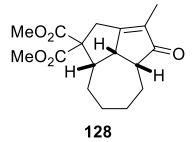 **128**	87	98

(Continuation)

Entry	Enyne	Product	% Yield[a]	% *ee*[c]
6	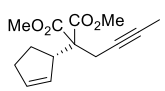 **107**	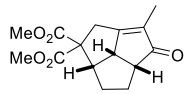 **129**	67	91
7	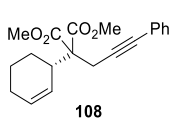 **108**	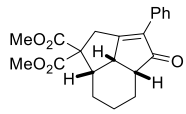 **130**	55 (d.r. 95:5)	98
8	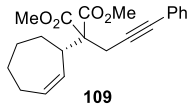 **109**	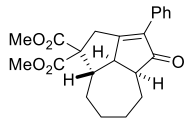 **131**	83	99
9	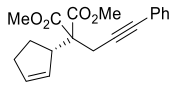 **110**	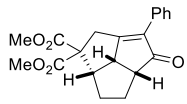 **132**	87	92
10	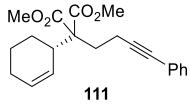 **111**	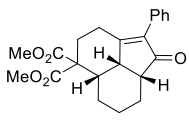 **133**	76 (d.r. 6:4)	98/99

[a] Alkyne (1 equiv), $Co_2(CO)_8$ (1.3 equiv), NMO (6 equiv), dichloroethane. [b] After chromatography isolation. [c] Determined by chiral HPLC.

To sum up, by means of the sequential use of Pd-catalyzed asymmetric allylic substitution and Pauson-Khand, we attained 10 different highly hindered chiral tricyclic cyclopentenones (products **124**-**132**). These tricyclic scaffolds are furnished with different ring sizes in the carbocycle already present in the enyne and in the carbocycle containing the malonate, as well as different substituent at the α-position of the cyclopentenone.

5.3. Conclusions

We have successfully derivatized some of the compounds obtained in Chapters 3 and 4. In this regard, Grubb's metathesis, Pauson-Khand and cycloisomerization reactions produced a range of chiral functionalized (poly)carbocyclic and heterocyclic compounds, with multiple stereogenic centers. From all of them we should highlight for the first time the successful preparation of a range of highly functionalized fused tricyclic

compounds in good yields and excellent selectivities by combining allylic alkylation with either cycloisomerization or Pauson-Khand reactions.

5.4. Experimental part

All reactions were performed with standard Schlenk techniques using argon. Commercial chemicals were used as received. Solvents were dried by means of standard procedures and stored under inert atmosphere. ^{1}H, $^{13}C\{^{1}H\}$, and $^{31}P\{^{1}H\}$ NMR spectra were recorded using a Varian Mercury 400 MHz spectrometer. Chemical shifts are relative to the signal of $SiMe_4$ (^{1}H and $^{13}C\{^{1}H\}$) as internal standard.

The corresponding NMR copies of new compounds can be found in the electronic supporting information provided.

5.4.1. Typical procedure for the preparation of chiral carbo- and heterocyclic compounds 90-95

A solution of Grubbs II catalyst (5 mg, 0.006 mmol) and the corresponding alkylated product (0.12 mmol) in CH_2Cl_2 (3 ml) was stirred for 16 h. The solution was directly purified by flash chromatography (Hex/EtOAc 95:5) to obtain the desired compounds.

5.4.2. Characterization details for compounds 90-95

Dimethyl (*S*)-2-phenylcyclopent-3-ene-1,1-dicarboxylate (90).[13] Enantiomeric excess determined by HPLC using Chiralpak IC column (87% 2-propanol/hexane, flow 0.5 ml/min, λ= 226 nm). t_R 15.3 min (*S*); t_R 17.0 min (*R*). ^{1}H NMR (400 MHz, $CDCl_3$), δ: 2.76 (d, 1H, CH_2, *J* = 17.4 Hz), 3.06 (s, 3 H, CH_3), 3.45 (d, 1H, CH_2, *J* = 17.4 Hz), 3.74 (s, 3H, CH_3), 4.86 (s, 1H, CH), 5.68 (m, 1H, CH=), 5.85 (m, 1H, CH=), 7.1-7.3 (m, 5H, CH=).

Dimethyl (*S*)-2-(p-tolyl)cyclopent-3-ene-1,1-dicarboxylate (91).[13] Enantiomeric excess determined by HPLC using Chiralpak IA column (98% 2-propanol/hexane, flow 0.5 ml/min, λ = 226 nm). t_R 12.1 min (-); t_R 12.8 min (+). ^{1}H NMR (400 MHz, $CDCl_3$), δ: 2.30 (s, 3H, CH_3), 2.81 (bd, 1H, CH_2, *J* = 12.6 Hz), 3.22 (s, 3 H, CH_3), 3.49 (m, 1H, CH_2), 3.76 (s, 3H, CH_3), 4.86 (s, 1H, CH), 5.71 (m, 1H, CH=), 5.87 (m, 1H, CH=), 7.1-7.3 (m, 4H, CH=).

Diethyl 2-phenylcyclohex-3-ene-1,1-dicarboxylate (91).[13] Enantiomeric excess determined by HPLC using Chiralcel OJ-H column (98% 2-propanol/hexane, flow 0.5 ml/min, λ = 220 nm). t_R 12.5 min (-); t_R 17.5 min (+). ^{1}H NMR (400 MHz, $CDCl_3$), δ: 1.25 (t, 6H, CH_3, *J* = 7.2 Hz), 1.9-2.3 (m, 4H, CH_2), 3.91 (m, 1H, CH), 4.19 (m, 4H, CH_2), 5.76 (m, 1H, CH=), 5.90 (m, 1H, CH=), 7.1-7.4 (m, 5H, CH=).

Diethyl 2-phenylcyclohept-3-ene-1,1-dicarboxylate (93).[13] Enantiomeric excess determined by HPLC using Chiralcel OJ-H column (98% 2-propanol/hexane, flow 0.5 ml/min, λ = 220 nm). t_R 11.2 min (-); t_R 13.8 min (+). ^{1}H NMR (400 MHz, $CDCl_3$), δ: 0.99 (t, 3H, CH_3, *J* = 7.2 Hz), 1.26 (t, 3H, CH_3, *J* = 7.2 Hz), 1.52 (m, 2H, CH_2), 2.3 (m, 2H, CH_2), 3.80

(m, 2H, CH_2), 4.03 (m, 4H, CH_2), 4.05 (m, 1H, CH), 5.88 (m, 1H, CH=), 5.92 (m, 1H, CH=), 7.0-7.3 (m, 4H, CH=).

(*S*)-2-Phenyl-2,5-dihydrofuran (94).[14] Enantiomeric excess determined by GC using Chiralsil-Dex CB column (105 kPa H_2, 90 °C for 30 min, 10 °C/min, to 180 °C). t_R 17.4 min (*S*); t_R 18.3 min (*R*).^{1}H NMR (400 MHz, $CDCl_3$), δ: 4.76 (m, 1H), 4.87 (m, 1H), 5.79 (m, 1H), 5.88 (m, 1H), 6.03 (m, 1H), 7.2-7.4 (m, 5H).

***tert*-Butyl (*S*)-2-phenyl-2,5-dihydro-1H-pyrrole-1-carboxylate (95)**.[15] Enantiomeric excess determined by HPLC using Chiralpak IC column (hexane/2-propanol=95/5, 0.5 ml/min, λ = 210 nm). t_R 18.3 min (*R*); t_R 19.9 min (*S*). ^{1}H NMR (400 MHz, $CDCl_3$), δ: 1.21 (s, 9H), 4.33 (s, 2H), 5.37 (s, 1H), 5.73 (s, 1H), 5.84 (s, 1H), 7.1-7.3 (m, 5H).

5.4.3. Typical procedure for the preparation of bicyclic compounds 96-100

A mixture of the enyne (1 mmol) and $PdCl_2$ or $RuCl_3$ (0.05 mmol) in MeOH (5 ml) was heated at reflux for 24 h. The solution was then cooled down, the solvent was removed in vacuo, and the residue was purified by column chromatography (hexane:EtOAc mixtures) to give the desired carbobicycle.

5.4.4. Characterization details for bicyclic compounds 96-100

Dimethyl 4-methoxy-3-methylenehexahydropentalene-1,1(2*H*)-dicarboxylate (96). Enantiomeric excess determined by HPLC using Chiralcel OJ-H column (95% hexane/2-propanol, flow 0.5 ml/min, λ= 220 nm). t_R 13.3 min; t_R 13.9 min. ^{1}H NMR ($CDCl_3$), δ: 1.17 (m, 1H, CH_2), 1.62 (m, 1H, CH_2), 1.84 (m, 2H, CH_2), 2.69 (dq, 1H, CH_2, *J*= 16.7 Hz, *J* = 1.3 Hz), 3.05 (dq, 1H, CH_2, *J*= 16.7 Hz, *J*= 1.3 Hz), 3.13 (m, 1H, CH), 3.29 (m, 1H, CH), 3.34 (s, 3H, CH_3), 3.60 (m, 1H, CH), 3.69 (s, 3H, CH_3), 3.71 (s, 3H, CH_3), 4.93 (m, 1H, CH_2=), 4.98 (m, 1H, CH_2=). ^{13}C NMR ($CDCl_3$), δ: 26.1 (CH_2), 32.0 (CH_2), 39.4 (CH_2), 47.6 (CH), 52.5 (CH_3), 52.7 (CH_3), 54.1 (CH), 56.8 (CH), 62.9 (C), 90.1 (CH), 109.1 (CH_2=), 149.9 (C=), 170.6 (C=O), 172.0 (C=O).

Dimethyl 4-methoxy-3-methyleneoctahydroazulene-1,1(2*H*)-dicarboxylat (97). Enantiomeric excess determined by HPLC using Chiralcel OJ-H column (95% hexane/2-propanol, flow 0.5 ml/min, λ= 220 nm). t_R 11.3 min; t_R 12.7 min. ^{1}H NMR ($CDCl_3$), δ: 1.11 (m, 1H, CH_2), 1.30 (m, 2H, CH_2), 1.58 (m, 1H, CH_2), 1.87 (m, 3H, CH_2), 2.92 (m, 3H, 2xCH, CH_2), 3.13 (m, 1H, CH_2), 3.19 (m, 2H, CH, CH_2), 3.32 (s, 3H, CH_3), 3.68 (s, 3H, CH_3), 3.70 (s, 3H, CH_3), 4.97 (m, 1H, CH_2=), 5.14 (m, 1H, CH_2=). ^{13}C NMR ($CDCl_3$), δ: 27.2 (CH_2), 27.5 (CH_2), 30.0 (CH_2), 30.9 (CH_2), 38.5 (CH_2), 47.4 (CH), 52.4 (CH), 52.6 (CH_3), 52.9 (CH_3), 55.6 (CH), 64.1 (C), 86.4 (CH), 107.9 (CH_2=), 150.3 (C=), 170.4 (C=O), 171.7 (C=O).

Dimethyl 4-methoxy-3-methyleneoctahydro-1*H*-indene-1,1-dicarboxylat (98).[4a] Enantiomeric excess determined by HPLC using Chiralcel OJ-H column (95% hexane/2-propanol, flow 0.5 ml/min, λ= 220 nm). t_R 18.0 min; t_R 20.2 min. ^{1}H NMR ($CDCl_3$), δ: 0.88 (m, 1H, CH_2), 1.31 (m, 1H, CH_2), 1.39 (m, 1H, CH_2), 1.41 (m, 1H, CH_2), 1.58 (m, 1H, CH_2),

1.74 (m, 1H, CH_2), 2.91 (m, 1H, CH_2), 2.92 (m, 1H, CH), 3.03 (bs, 1H, CH), 3.31 (m, 1H, CH_2), 3.36 (s, 3H, CH_3), 3.63 (dd, 1H, CH, *J* = 5.4 Hz, *J* = 2.8 Hz,), 3.71 (s, 3H, CH_3), 3.72 (s, 3H, CH_3), 4.79 (dd, 1H, CH_2=, *J* = 5 Hz, *J* = 2.6 Hz), 5.02 (dd, CH_2=, *J* = 5 Hz, *J* = 2.6 Hz).

Dimethyl (3a*S*, 7a*R*)-3-methylene-2,3,3a,6,7,7a-hexahydro-1H-indene-1,1-dicarboxylate (99).[16] Enantiomeric excess determined by HPLC using Chiralcel OJ-H column (95% hexane/2-propanol, flow 0.5 ml/min, λ= 210 nm). t_R 10.5 min; t_R 11.4 min. ^{1}H NMR ($CDCl_3$), δ: 1.13 (m, 1H, CH_2), 1.32 (m, 1H, CH_2), 2.03 (m, 2H, CH_2), 2.86 (m, 2H, CH, CH_2), 3.21 (m, 1H, CH), 3.32 (m, 1H, CH_2), 3.71 (s, 3H, CH_3), 3.73 (s, 3H, CH_3), 4.84 (m, 1H, CH_2=), 4.98 (m, 1H, CH_2=), 5.76 (m, 1H, CH=), 5.86 (m, 1H, CH=).

Dimethyl (3a*S*,8a*R*)-3-methylene-3,3a,6,7,8,8a-hexahydroazulene-1,1(2H)-dicarboxylate (101).[16] Enantiomeric excess determined by HPLC using Chiralcel OJ-H column (95% hexane/2-propanol, flow 0.5 ml/min, λ= 210 nm). t_R 11.6 min; t_R 12.5 min. ^{1}H NMR ($CDCl_3$), δ: 1.27 (m, 1H, CH_2), 1.76 (m, 1H, CH_2), 2.23 (m, 5H, CH_2), 2.75 (m, 1H, CH_2), 3.11 (d, 1H, CH_2, *J* = 17.3 Hz), 3.25 (d, 1H, CH, *J* = 11.3 Hz), 3.62 (pt, 1H, CH, *J* = 7.4 Hz), 3.72 (s, 3H, CH_3), 3.75 (s, 3H, CH_3), 4.92 (m, 1H, CH_2=), 4.98 (m, 1H, CH_2=), 5.79 (m, 1H, CH=), 5.87 (m, 1H, CH=).

5.4.5. Typical procedure for synthesis of compounds 102-111 via asymmetric Pd-catalyzed allylic alkylation

A solution of the **L9c** (0.011 mmol) and $[PdCl(\eta^3\text{-}C_3H_5)]_2$ (1.8 mg, 0.005 mmol) in CH_2Cl_2 (0.5 ml) was stirred. After 30 min a solution of substrate (1 mmol) in CH_2Cl_2 (1.5 ml), nucleophile (3 mmol), *N,O*-bis(trimethylsilyl)-acetamide (730 µL, 3 mmol), and KOAc (3 mg, 0.03 mmol) were subsequently added. After the desired reaction time the reaction mixture was diluted with Et_2O (5 ml). Saturated NH_4Cl (aq) (25 ml) was then added, the mixture was extracted with Et_2O (3 × 10 ml), and the extract was dried over $MgSO_4$. Then the reaction crude was subjected to flash chromatography (petroleum ether/ethyl acetate) to obtain the desired enynes.

5.4.6. Characterization details for enynes 102-111

Dimethyl 2-(but-3-yn-1-yl)-2-(cyclohex-2-en-1-yl)malonate (102).[6a] Enantiomeric excess determined by HPLC using Chiralcel OJ-H column (98% 2-propanol/hexane, flow 0.5 ml/min, λ = 220 nm). $t_{R(minor)}$ 13.4 min; $t_{R(major)}$ 16.1 min. ^{1}H-NMR ($CDCl_3$), δ: 1.29 – 1.38 (m, 1H), 1.50 – 1.60 (m, 1H), 1.74 – 1,84 (m, 2H), 1.99 (m, 3H), 2.16 – 2.28 (m, 4H), 2.88 – 2,95 (m, 1H), 3.72 (s, 3H), 3.74 (m, 3H), 5.64 (d, 1H, *J* = 10.4 Hz), 5.72 – 5.78 (m, 1H).

Dimethyl 2-(but-3-yn-1-yl)-2-(cyclohept-2-en-1-yl)malonate (103). Enantiomeric excess determined by HPLC using Chiralcel OJ-H column (98% 2-propanol/hexane, flow 0.5 ml/min, λ = 220 nm). $t_{R(minor)}$ 12.3 min; $t_{R(major)}$ 13.1 min. ^{1}H-NMR ($CDCl_3$), δ: 1.18 (m, 2H, CH_2), 1.65 (m, 3H, 2xCH_2, CH_2), 1.94 (s, 1H, CH≡), 2.01 (m, 1H, CH_2), 2.13 (m, 4H,

2xCH_2), 2.22 (m, 2H, CH_2), 2.91 (m, 1H, CH), 3.71 (ap. m, 6H, 2xCH_3), 5.64 (m, 1H, CH=), 5.82 (m, 1H, CH=). ^{13}C-NMR (100.6 Hz, $CDCl_3$) δ 14.6 (CH_2), 26.0 (CH_2), 27.9 (CH_2), 30.1 (CH_2), 31.6 (CH_2), 33.1 (CH_2), 44.2 (CH), 52.2 (CH_3), 52.3 (CH_3), 68.5 (CH≡), 83.6 (C≡), 132.2 (CH=), 132.8 (CH=), 171.0 (CO), 171.1 (CO).

Dimethyl 2-(but-3-yn-1-yl)-2-(cyclopent-2-en-1-yl)malonate (104). Enantiomeric excess determined by HPLC using Chiralcel OJ-H column (98% 2-propanol/hexane, flow 0.5 ml/min, λ = 220 nm). $t_{R(minor)}$ 16.9 min; $t_{R(major)}$ 17.7 min. ^{1}H-NMR (400 Hz, $CDCl_3$), δ: 1.69 (m, 1H, CH_2), 1.96 – 2.37 (m, 8H, CH_2, CH≡), 3.41 (m, 1H, CH), 3.69 (s, 3H, CH_3), 3.71 (s, 3H, CH_3), 5.70 (m, 1H, CH=), 5.79 (m, 1H, CH=). ^{13}C-NMR (100.6 Hz, $CDCl_3$) δ 14.5 (CH_2), 25.3 (CH_2), 31.8 (CH_2), 32.1 (CH_2), 49.9 (CH), 52.2 (CH_3), 52.3 (CH_3), 60.4 (C), 68.6 (CH≡), 83.5 (C≡), 130.8 (CH=), 132.8 (CH=), 171.1 (CO), 171.2 (CO).

Dimethyl 2-(but-2-yn-1-yl)-2-(cyclohex-2-en-1-yl)malonate (105). Enantiomeric excess determined by HPLC using Chiralpak AD column (98% 2-propanol/hexane, flow 0.5 ml/min, λ = 220 nm). $t_{R(minor)}$ 11.5 min; $t_{R(major)}$ 12.2 min.^{1}H-NMR ($CDCl_3$), δ: 1.21 – 1.34 (m, 1H, CH_2), 1.45 – 1.57 (m, 1H, CH_2), 1.67 – 1.85 (m, 5H, including a triplet (*J* = 2.6Hz) at 1.70, 2xCH_2, CH_3), 1.85 – 1.96 (m, 2H, CH_2), 2.77 (ap qq, 2H, CH_2, *J* = 10.0 Hz, 2.6 Hz), 3.06 (m, 1H, CH), 3.66 (s, 3H, CH_3), 3.70 (s, 3H, CH_3), 5.65 – 5.73 (m, 2H, CH=). ^{13}C-NMR (100.6 Hz, $CDCl_3$) δ 3.5 (CH_3), 22.3 (CH_2), 22.9 (CH_2), 24.1 (CH_2), 24.8 (CH_2), 8.7 (CH), 52.1 (CH_3), 52.3 (CH_3), 60.6 (C), 73.7 (C≡), 78.6 (C≡), 127.6 (CH=), 128.7 (CH=), 170.3 (CO), 170.5 (CO),

Dimethyl 2-(but-2-yn-1-yl)-2-(cyclohept-2-en-1-yl)malonate (106). Enantiomeric excess determined by HPLC using Chiralcel OJ-H column (98% 2-propanol/hexane, flow 0.5 ml/min, λ = 220 nm). $t_{R(minor)}$ 11.7 min; $t_{R(major)}$ 12.4 min. ^{1}H-NMR (400 MHz $CDCl_3$) δ 1.08 – 1.27 (m, 2H, CH_2), 1.55 – 1.84 (m including a triplet (*J* = 2.8 Hz) at 1.72, 6H, CH_3, CH_2), 1.94 – 2.04 (m, 1H, CH_2), 2.08 – 2.17 (m, 2H, CH_2), 2.76 (q, 2H, CH_2, *J* = 2.6 Hz), 3.14 (m, 1H, CH), 3.70 (s, 6H, CH_3), 5.67 (m, 1H, CH=), 5.78 (m, 1H, CH=). ^{13}C-NMR (100.6 Hz, $CDCl_3$) δ 3.5 (CH_3), 23.9 (CH_2), 26.0 (CH_2), 27.9 (CH_2), 29.6 (CH_2), 31.4 (CH_2), 42.9 (CH), 52.3 (CH_3), 52.4 (CH_3), 60.8 (C), 73.9 (C≡), 78.6 (C≡), 131.8 (CH=), 132.8 (CH=), 170.6 (CO), 170.6 (CO).

Dimethyl 2-(but-2-yn-1-yl)-2-(cyclopent-2-en-1-yl)malonate (107). Enantiomeric excess determined by HPLC using Chiralpak AD column (98% 2-propanol/hexane, flow 0.5 ml/min, λ = 220 nm). $t_{R(minor)}$ 10.9 min; $t_{R(major)}$ 12.5 min. ^{1}H-NMR ($CDCl_3$), δ: 1.64 – 1.77 (m including a triplet (*J* = 2.6 Hz) at 1.77, 4H, CH_3. CH_2), 2.05 (m, 1H, CH_2), 2.26 (m, 2H, CH_2), 2.75 (app q, 2H, CH_2, *J* = 2.6 Hz), 3.61 (m, 1H, CH), 3.69 (s, 3H, CH_3), 3.73 (s, 3H, CH_3), 5.77 (m, 2H, CH=).^{13}C-NMR (100.6 Hz, $CDCl_3$) δ 3.5 (CH_3), 23.6 (CH_2), 25.2 (CH_2), 31.7 (CH_2), 48.8 (CH), 52.3 (CH_3), 52.5 (CH_3), 60.4 (C), 73.8 (C≡), 78.6 (C≡), 131.2 (CH=), 132.4 (CH=), 170.6 (CO), 170.8 (CO).

Dimethyl 2-(cyclohex-2-en-1-yl)-2-(3-phenylprop-2-yn-1-yl)malonate (108).[6b] Enantiomeric excess determined by HPLC using Chiralcel OJ-H column (98% 2-propanol/hexane, flow 0.5 ml/min, λ = 220 nm). $t_{R(major)}$ 23.8 min; $t_{R(minor)}$ 26.6 min. ^{1}H-NMR (400 MHz $CDCl_3$) δ 1.34 – 1.48 (m, 1H, CH_2), 1.50 – 1.65 (m, 1H, CH_2), 1.75 – 1,93

(m, 2H, CH_2), 1.97 (m, 2H, CH_2), 3.06 (ap q, *J* = 14.6 Hz, 2H, CH_2), 3.20 (m, 1H, CH), 3.73 (s, 3H, CH_3), 3.76 (s, 3H, CH_3), 5.77 (m, 2H, CH=), 7.26 (m, 3H, CH=), 7.35 (m, 2H, CH=).

Dimethyl 2-(cyclohept-2-en-1-yl)-2-(3-phenylprop-2-yn-1-yl)malonate (109).[6b] Enantiomeric excess determined by HPLC using Chiralcel OJ-H column (98% 2-propanol/hexane, flow 0.5 ml/min, λ = 220 nm). $t_{R(major)}$ 22.4 min; $t_{R(minor)}$ 24.8 min. ^{1}H-NMR (400 MHz $CDCl_3$) δ 1.18 – 1.33 (m, 2H, CH_2), 1.60 – 1.78 (m, 2H, CH_2), 1.85 – 1,95 (m, 1H, CH_2), 2.00 – 2.10 (m, 1H, CH_2), 2.17 (m, 2H, CH_2), 3.07 (s, 2H, CH_2), 3.28 (m, 1H, CH), 3.76 (s, 3H, CH_3), 3.77 (s, 3H, CH_3), 5.76 (m, 1H, CH=), 5.86 (m, 1H, CH=), 7.27 (m, 3H, CH=), 7.36 (m, 3H, CH=).

Dimethyl 2-(cyclopent-2-en-1-yl)-2-(3-phenylprop-2-yn-1-yl)malonate (110). Enantiomeric excess determined by HPLC using Chiralcel OJ-H column (98% 2-propanol/hexane, flow 0.5 ml/min, λ = 220 nm). $t_{R(major)}$ 24.7 min; $t_{R(minor)}$ 28.2 min. ^{1}H-NMR (400 MHz $CDCl_3$) δ 1.72 – 1.86 (m, 1H, CH_2), 2.05 – 2.18 (m, 1H, CH_2), 2.29 (m, 2H, CH_2), 3.02 (s, 2H, CH_2), 3.71 (m, 1H, CH), 3.71 (s, 3H, CH_3), 3.74 (s, 3H, CH_3), 5.82 (m, 2H, CH=), 7.25 (m, 3H, CH=), 7.34 (m, 2H, CH=). ^{13}C-NMR (100.6 Hz, $CDCl_3$) δ 23.9 (CH_2), 25.2 (CH_2), 31.8 (CH_2), 49.1 (CH), 52.4 (CH_3), 52.6 (CH_3), 60.5 (C), 83.2 (C≡), 85.0 (C≡), 123.3 (C=), 127.9 (C=), 128.2 (2xCH=), 131.1 (CH=), 131.6 (2xCH=), 132.7 (CH=), 170.4 (CO), 170.6 (CO).

Dimethyl 2-(cyclohex-2-en-1-yl)-2-(4-phenylbut-3-yn-1-yl)malonate (111). Enantiomeric excess determined by HPLC using Chiralpak AD column (98% 2-propanol/hexane, flow 0.5 ml/min, λ = 220 nm). $t_{R(minor)}$ 16.4 min; $t_{R(major)}$ 17.8 min. ^{1}H-NMR (400 MHz, $CDCl_3$) δ 1.26 (m, 2H, CH_2), 1.80 (m, 2H, CH_2), 1.96 (m, 2H, CH_2), 2.26 (m, 2H, CH_2), 2.44 (m, 2H, CH_2), 2.94 (m, 1H, CH), 3.65 (s, 3H, CH_3), 3.67 (s, 3H, CH_3), 5.61 (m, 1H, CH=), 5.67 (m, 1H, CH=), 7.20 (m, 3H, CH=), 7.31 (m, 2H, CH=).^{13}C-NMR (100.6 Hz, $CDCl_3$) δ 15.6 (CH_2), 22.4 (CH_2), 24.5 (CH_2), 24.8 (CH_2), 31.9 (CH_2), 40.2 (CH), 52.1 (CH_3), 52.3 (CH_3), 60.7 (C), 80.8 (C≡), 89.1 (C≡), 123.7 (C=), 127.6 (CH=), 127.7 (CH=), 128.2 (2xCH=), 128.7 (CH=), 131.5 (2xCH=), 170.8 (CO), 171.1 (CO).

5.4.7. Typical preparation of cyclobutenes by $PtCl_2$/CO system

To a solution containing the corresponding enyne (0.2 mmol) and $PtCl_2$ (10% mol) in 1 ml of toluene, CO was bubbled for 5 min. Then, the flask was closed and stirred at 80 °C for 18h. Then, the solvent was removed at vacuum and the reaction mixture chromatographed (petroleum ether/ethyl acetate) to afford the corresponding cyclobutenes.

5.4.8. Typical preparation of cyclobutenes by JohnPhos Au(I) system

To a solution of the corresponding enyne (0.2 mmol) in 1ml of dichloromethane, JohnPhosAu SbF_6 complex (2% mol) and a punch of 4 Å MS were added and the resulting

suspension stirred until TLC showed competition (0.5 – 4h). After that, the solvent was removed at vacuum and the reaction crude chromatographed (petroleum ether/ethyl acetate) to obtain the corresponding cyclobutenes.

5.4.9. Characterization details for cyclobutene-containing compounds 112, 114-116 and bicyclic compound 113

Dimethyl (1a1S,4aR,7aR)-1a1,2,3,4a,5,6,7,7a-octahydro-4H-cyclobuta[de]naphthalene-4,4-dicarboxylate (112).[6a] Enantiomeric excess determined by HPLC using Chiralcel OD column (87% 2-propanol/hexane, flow 0.5 ml/min, λ = 220 nm). $t_{R(major)}$ 8.7 min; $t_{R(minor)}$ 9.5 min. ^{1}H-NMR (400 MHz, $CDCl_3$) δ 1.00 (m, 1H), 1.34 (m, 2H), 1.63 (m, 1H), 1.75 (m, 2H), 1.92 (td, 1H, *J* = 13.6 Hz, 4.6 Hz), 2.17 (m, 3H), 2.64 (m, 1H), 2.85 (m, 1H), 2.95 (m, 1H), 3.62 (s, 3H), 3.68 (s, 3H), 5.59 (m, 1H).

Dimethyl (*R*)-bicyclo[4.4.1]undeca-5,7-diene-2,2-dicarboxylate (113). Enantiomeric excess determined by HPLC using Chiralcel OD column (87% 2-propanol/hexane, flow 0.5 ml/min, λ = 220 nm). $t_{R(major)}$ 8.7 min; $t_{R(minor)}$ 9.5 min. ^{1}H-NMR (400 MHz, $CDCl_3$) δ 0.91 (m, 1H, CH_2), 1.40 (m, 4H, CH_2), 1.69 (m, 1H, CH_2), 2.03 (m, 1H, CH_2), 2.26 (dt, 1H, CH_2, *J* = 18.6 Hz, 6.5 Hz), 2.75 (d, 1H, CH_2, *J* = 17.7 Hz), 3.17 (d, 1H, CH_2, *J* = 17.7 Hz), 3.59 (m, 1H, CH), 3.65 (s, 3H, CH_3), 3.66 (s, 3H, CH_3), 5.40 (s, 1H, CH=), 5.61 (ddd, 1H, CH=, *J* = 11.3 Hz, 6.0 Hz, 3.5 Hz), 5.98 (d, 1H, CH=, *J* = 11.3 Hz). ^{13}C-NMR (100.6 Hz, $CDCl_3$) δ 24.6 (CH_2), 30.2 (CH_2), 30.6 (CH_2), 31.8 (CH_2), 44.4 (CH_2), 50.4 (CH), 52.4 (CH_3), 52.8 (CH_3), 62.5 (C), 125.9 (CH=), 130.0 (CH=), 134.1 (C=), 135.1 (CH=), 170.4 (CO), 172.7 (CO).

Dimethyl (1aS,1a1S,4aR)-1-phenyl-1a,2,3,4,4a,6-hexahydrocyclobuta[cd]indene-5,5(1a1H)-dicarboxylate (114). Enantiomeric excess determined by HPLC using Chiralpak AD column (98% 2-propanol/hexane, flow 0.5 ml/min, λ = 220 nm). $t_{R(major)}$ 17.4 min; $t_{R(minor)}$ 18.7 min. ^{1}H-NMR (400 MHz, $CDCl_3$) δ 1.27 (m, 1H, CH_2), 1.55 (m, 3H, CH_2), 2.28 (dd, *J* = 14.2 Hz, 7.8 Hz, 1H, CH_2), 2.42 (m, 1H, CH_2), 2.49 (dd, 1H, CH_2, *J* = 14.2 Hz, 7.8 Hz), 2.62 (m, 1H, CH_2), 2.83 (m, 1H, CH), 3.20 (m, 1H, CH), 3.37 (m, 1H, CH), 3.57 (s, 3H, CH_3), 3.72 (s, 3H, CH_3), 7.23 (m, 3H, H-Ar), 7.33 (m, 2H, H-Ar). ^{13}C-NMR (100.6 Hz, $CDCl_3$) δ 21.5 (CH_2), 23.5 (CH_2), 25.9 (CH_2), 34.1 (CH_2), 41.0 (CH), 42.5 (CH), 46.3 (CH), 52.1 (CH_3), 52.7 (CH_3), 68.7 (C), 125.4 (2xCH=), 126.7 (C=), 128.4 (2xCH=), 134.7 (C=), 141.8 (C=), 142.7 (C=), 170.7 (CO), 173.2 (CO).

Dimethyl (1a1S,3aR,7aS)-1-phenyl-1a1,2,3a,4,5,6,7,7a-octahydro-3H-cyclobuta[cd]azulene-3,3-dicarboxylate (115). Enantiomeric excess determined by HPLC using Chiralcel OJ column (98% 2-propanol/hexane, flow 0.5 ml/min, λ = 220 nm). $t_{R(major)}$ 14.2 min; $t_{R(minor)}$ 17.8 min. ^{1}H-NMR (400 MHz, $CDCl_3$) δ 1.43 (m, 4H, CH_2), 1.80 (m, 2H, CH_2), 2.21 (m, 2H, CH_2), 2.35 (m, 2H, CH_2), 2.75 (m, 1H, CH), 3.25 (tdd, 1H, CH, *J* = 7.5 Hz, 4.7 Hz, 2.2 Hz), 3.52 (dd, 1H, CH, *J* = 8.2 Hz, 4.8 Hz), 3.63 (s, 3H, CH_3), 3.75 (s, 3H, CH_3), 7.21 (m, 2H, H-Ar), 7.31 (3H, H-Ar). ^{13}C-NMR (100.6 Hz, $CDCl_3$) δ 27.4 (2xCH_2), 28.6 (CH_2), 29.5 (CH_2), 32.1 (CH_2), 40.8 (CH), 42.7 (CH), 49.6 (CH), 52.2 (CH_3), 52.7 (CH_3), 71.3 (C),

125.7 (2xCH=), 126.7 (CH=), 128.4 (2xCH=), 134.9 (C=), 140.3 (C=), 145.3 (C=), 170.1 (CO), 172.8 (CO).

Dimethyl (1a1S,4aR,7aS)-1-phenyl-1a1,2,3,4a,5,6,7,7a-octahydro-4H-cyclobuta[de]naphthalene-4,4-dicarboxylate (116). Enantiomeric excess determined by HPLC using Chiralcel OJ-H column (98% 2-propanol/hexane, flow 0.5 ml/min, λ = 220 nm). $t_{R(minor)}$ 18.5 min; $t_{R(major)}$ 21.8 min. ^{1}H-NMR (400 MHz, $CDCl_3$) δ 1.06 (m, 1H, CH_2), 1.20 (m, 1H, CH_2), 1.52 (m, 1H, CH_2), 1.62 (m, 2H, CH_2), 2.01 (m, 2H, CH_2), 2.27 (m, 1H, CH_2), 2.68 (m, 3H, 2xCH_2, CH), 3.00 (dd, 1H, CH, *J* = 7.2 Hz, 5.0 Hz), 3.16 (dtd, 1H, CH, *J* = 9.8 Hz, 5.0 Hz, 2.6 Hz), 3.63 (s, 3H, CH_3), 3.72 (s, 3H, CH_3), 7.11 (m, 1H, H-Ar), 7.21 (m, 4H, H-Ar). ^{13}C-NMR (100.6 Hz, $CDCl_3$) δ 22.7 (CH_2), 23.4 (CH_2), 24.2(CH_2), 26.2 (CH_2), 26.5 (CH_2), 35.5 (CH), 36.8 (CH), 39.6 (CH), 52.5 (CH_3), 52.4 (CH_3), 58.8 (C), 125.9 (2xCH=), 126.5 (2xCH=), 128.5 (CH=), 134.7 (C=), 139.1 (C=), 140.3 (C=), 171.1 (CO), 171.3 (CO).

5.4.10. Typical methodology for the preparation of bicyclopentenones 117–120

Under an atmosphere of argon, a solution of the enyne (1.0 mmol) and $Co_2(CO)_8$ (359 mg, 1.05 mmol) in dry CH_2Cl_2 (0.06 M) was stirred at room temperature until TLC monitoring indicated full conversion. $Me_3NO{\cdot}2H_2O$ (3–10 mmol) was then added in one portion. Stirring was continued until TLC monitoring showed complete consumption of the cobalt-alkyne complex. The solvent was then evaporated under reduced pressure, and the residue was purified by column chromatography (petroleum ether/ethyl acetate) to give the desired bicyclopentenone.

5.4.11. Characterization details for bicyclopentenones 117-119

Dimethyl (3*S*,3a*R*,4*S*)-5-oxo-3,4-diphenyl-3,3a,4,5-tetrahydropentalene-2,2(1H) -dicarboxylate (117). Enantiomeric excess determined by HPLC using Chiralpak IA column (87% hexane/2-propanol, flow 0.7 ml/min, λ= 220 nm). t_R 16.4 min; t_R 25.0 min. ^{1}H NMR ($CDCl_3$), δ: 3.12 (ddd, 1H, CH_2, *J* = 18.7 Hz, 2.3 Hz, 1.2 Hz), 3.17 (s, 3H, CH_3), 3.27 (d, 1H, CH, *J*= 3.3 Hz), 3.75 (pdt, 1H, CH, *J* = 12.9 Hz, 3.3 Hz, 1.3 Hz), 3.78 (s, 3H, CH_3), 3.84 (d, 1H, CH, *J* = 12.9 Hz), 3.86 (d, 1H, CH_2, *J* = 18.7 Hz), 6.11 (ptd, 1H, CH=, *J* = 2.3 Hz, 1.2 Hz), 6.85 (m, 2H, CH=), 7.08 – 7.22 (m, 8H, CH=). ^{13}C NMR ($CDCl_3$), δ: 36.7 (CH_2), 52.5 (CH_3), 53.0 (CH_3), 55.3 (CH), 56.9 (CH), 59.5 (CH), 65.6 (C), 125.1 (CH=), 126.9 (CH=), 127.7 (CH=), 128.0 (CH=), 128.3 (CH=), 128.5 (CH=), 128.6 (CH=), 135.8 (C=), 138.1 (C=), 170.6 (C=O), 171.2 (C=O), 181.9 (C=), 208.9 (C=O).

Dimethyl (3*S*,3a*S*,4*R*)-5-oxo-3-phenyl-4-(trifluoromethyl)-3,3a,4,5-tetrahydro-pentalene-2,2(1H)-dicarboxylate (118). Enantiomeric excess determined by HPLC using Chiralcel OJ-H column (87% hexane/2-propanol, flow 0.5 ml/min, λ= 220 nm). t_R 39.5 min; t_R 53.5 min. ^{1}H NMR ($CDCl_3$), δ: 2.80 (dq, 1H, CH, *J* = 9.8 Hz, 3.4 Hz), 3.07 (d, 1H, CH_2, *J* = 18.7 Hz), 3.20 (s, 3H, CH_3), 3.70 (s, 3H, CH_3), 3.73 (m, 2H, 2xCH), 3.84 (d, 1H, CH2, *J* =

18.7 Hz), 6.01 (m, 1H, CH=), 7.25 (m, 5H, CH=). ^{13}C NMR ($CDCl_3$), δ: 36.5 (CH_2), 49.5 (CH), 52.8 (CH_3), 53.2 (CH_3), 54.7 (CH), 54.9 (q, CH, *J*= 27.4 Hz), 65.5 (C), 125.5 (CH=), 128.2 (CH=), 128.2 (CH=), 128.7 (CH=), 135.2 (C=), 170.4 (C=O), 170.9 (C=O), 182.1 (C=O).

Dimethyl (3*S*,3a*R*)-5-oxo-3-phenyl-3,3a,4,5-tetrahydropentalene-2,2(1H)-dicarboxylate (119).[17] Enantiomeric excess determined by HPLC using Chiralcel OJ-H column (87% hexane/2-propanol, flow 0.5 ml/min, λ= 220 nm). t_R 24.6 min; t_R 29.2 min. ^{1}H NMR ($CDCl_3$), δ: 2.04 (dd, 1H, CH_2, *J* = 18.6 Hz, 2.3 Hz), 2.54 (dd, 1H, CH_2, *J* = 18.1 Hz, 5.5 Hz), 3.05 (d, 1H, CH, *J* = 18.6 Hz), 3.15 (s, 3H, CH_3), 3.61 (m, 2H, CH_2), 3.74 (s, 3H, CH_3), 3.80 (d, 1H, CH, *J*= 18.6 Hz), 5.96 (s, 1H, CH=), 7.24 (m, 5H, CH=).

5.4.12. Typical methodology for the preparation of tricyclic cyclopentenones 121-133

Under an atmosphere of argon, a solution of the enyne (1.0 mmol) and $Co_2(CO)_8$ (359 mg, 1.05 mmol) in dry CH_2Cl_2 (0.06 M) was stirred at room temperature until TLC monitoring indicated full conversion. NMO (6 mmol) was then added portion wise at 0 °C. Stirring was continued at room temperature until TLC monitoring showed complete consumption of the cobalt-alkyne complex. The solvent was then evaporated under reduced pressure, and the residue was purified by flash chromatography (petroleum ether/ethyl acetate) to give the desired tricyclic cyclopentenones.

2.3.3.1. Characterization details tricyclic cyclopentenones 121-133

Dimethyl (2a1S,4aR,7aS)-4-oxo-2,2a1,4,4a,5,6,7,7a-octahydro-1H-cyclopenta[cd]indene-1,1-dicarboxylate (121).[11] Enantiomeric excess determined by HPLC using Chiralcel OJ-H column (87% 2-propanol/hexane, flow 0.5 ml/min, λ = 220 nm). $t_{R(major)}$ 33.0 min; $t_{R(minor)}$ 53.1. ^{1}H-NMR (400 MHz, $CDCl_3$) δ 0.68 (dq, 1H, *J* = 12.8 Hz, 2.6 Hz), 1.01 (tdd, 1H, *J* = 13.6 Hz, 9.9 Hz, 3.8 Hz), 1.25 (m, 1H), 1.44 (m, 1H), 1.64 (m, 1H), 2.04 (m, 1H), 2.70 (td, 1H, *J* = 9.5 Hz, 6.1 Hz), 2.96 (ddd, 1H, *J* = 13.3 Hz, 7.8 Hz, 6.4 Hz), 3.15 (ddd, 1H, *J* = 20.7 Hz, 2.2 Hz, 1.1 Hz), 3.36 (t, *J* = 7.3 Hz), 3.62 (dt, 1H, *J* = 20.7 Hz, 2.0 Hz), 3.76 (s, 3H), 3.77 (s, 3H), 5.84 (s, 1H).

Dimethyl (2a1R,4aS,8aS)-4-oxo-2a1,4,4a,5,6,7,8,8a-octahydrocyclopenta[cd]azulene-1,1(2H)-dicarboxylate (122).[11] Enantiomeric excess determined by HPLC using Chiralcel OJ-H column (87% 2-propanol/hexane, flow 0.5 ml/min, λ = 220 nm). $t_{R(major)}$ 23.7 min; $t_{R(minor)}$ 27.5 min. ^{1}H-NMR (400 MHz, $CDCl_3$) δ 1.20 (m, 3H), 1.41 (m, 1H), 1.95 (m, 1H), 2.09 (m, 3H), 2.22 (m, 1H), 2.55 (ddd, 1H, *J* = 12.9 Hz, 7.7 Hz, 5.7 Hz), 3.00 (dt, 1H, *J* = 18.5 Hz, 1.1 Hz), 3.16 (dddt, 1H, *J* = 13.3 Hz, 7.1 Hz, 2.2 Hz, 1.4 Hz), 3.58 (ddt, 1H, *J* = 18.5 Hz, 2.2 Hz,1.1 Hz), 3.77 (s, 3H), 3.78 (s, 3H), 5.86 (td, 1H, *J* = 2.1 Hz, 1.1 Hz).

Dimethyl 4-oxo-2a^1,4,4a,5,6,6a-hexahydrocyclopenta[*cd*]pentalene-1,1(2*H*)-dicarboxylate (123).[11] Enantiomeric excess determined by HPLC using Chiralcel OJ-H

column (87% 2-propanol/hexane, flow 0.5 ml/min, λ = 220 nm). $t_{R(major)}$ 45.5 min; $t_{R(minor)}$ 66.5 min. ^{1}H-NMR (400 MHz, $CDCl_3$) δ = 0.92 (tdd, 1H, *J* = 12.9 Hz, 11.5 Hz, 7.0 Hz), 1.58 (dt, 1H, *J* = 12.9 Hz, 7.0 Hz), 1.79 (dd, 1H, *J* = 13.3 Hz, 7.0 Hz), 1.94 (tdd, 1H, *J* = 13.3 Hz, 10.1 Hz, 6.8 Hz), 2.84 (dd, 1H, *J* = 10.1 Hz, 5.3 Hz), 2.91 (ddd, 1H, *J* = 17.5 Hz, 2.0 Hz, 1.2 Hz), 3.13 (dt, 1H, *J* = 11.5 Hz, 7.4 Hz), 3.55 (t, 1H, *J* = 6.2 Hz), 3.66 (d, 1H, *J* = 17.5 Hz), 3.71 (s, 3H), 3.78 (s, 3H), 6.02 (t, 1H, *J* = 2.0 Hz).

Dimethyl (2a1S,5aS,8aR)-1-oxo-2a1,3,4,5a,6,7,8,8a-octahydroacenaphthylene-5,5(1H)-dicarboxylate (124). Enantiomeric excess determined by HPLC using Chiralcel OJ-H column (87% 2-propanol/hexane, flow 0.5 ml/min, λ = 220 nm). $t_{R(major)}$ 26.0 min; $t_{R(minor)}$ 33.4 min. ^{1}H-NMR (400 MHz, $CDCl_3$) δ 1.50 (m, 3H, CH_2), 1.70 (m, 3H, 2xCH_2, CH), 1.87 (m, 1H, CH_2), 2.41 (q, 1H, CH, *J* = 7.6 Hz), 2.60 (m, 3H, 2xCH_2, CH), 2.75 (m, 1H, CH_2), 3.66 (m, 4H, CH_3, CH), 3.75 (s, 3H, CH_3), 5.80 (s, 1H, CH=). ^{13}C-NMR (100.6 Hz, $CDCl_3$) δ 21.3 (CH_2), 22.1 (CH_2), 27.9 (CH_2), 24.1 (CH_2), 35.6 (CH_2), 43.6 (CH), 45.7 (CH), 46.9 (CH), 52.3 (CH_3), 52.7 (CH_3), 58.9 (C), 125.4 (CH=), 170.6 (CO), 171.3 (CO), 181.0 (C=), 210.6 (CO).

Dimethyl (2a1R,5aS,9aS)-1-oxo-1,2a1,3,4,5a,6,7,8,9,9a-decahydro-5H-benzo[cd]azulene-5,5-dicarboxylate (125). Enantiomeric excess determined by HPLC using Chiralcel OJ-H column (90% 2-propanol/hexane, flow 0.5 mL/min, λ = 220 nm). $t_{R(major)}$ 12.2 min; $t_{R(minor)}$ 19.0 min. ^{1}H-NMR (400 MHz, $CDCl_3$) δ 1.24 (m, 2H, CH_2), 1.64 (m, 2H, CH_2), 1.85 (m, 3H, CH_2), 2.03 (m, 3H, 2xCH_2, CH_3), 2.51 (m, 3H, 2xCH_2, CH_3), 2.79 (m, 1H, CH_2), 2.97 (dd, 1H, CH, *J* = 12.7 Hz, 6.6 Hz), 3,74 (s, 3H, CH_3), 3.78 (s, 3H, CH_3), 5.88 (t, 1H, CH=, *J* = 1.9 Hz). ^{13}C-NMR (100.6 Hz, $CDCl_3$) δ 27.1 (CH_2), 28.8 (CH_2), 29.7 (CH_2), 30.7 (CH_2), 33.0 (CH_2), 33.5 (CH_2) 46.3 (CH), 48.3 (CH), 51.7 (CH), 52.3 (CH_3), 52.8 (CH_3), 60.4 (C), 126.9 (CH=), 170.5 (CO), 172.1 (CO), 179.7 (C=), 210.5 (CO).

Dimethyl (2aR,2a1S,7aS)-3-oxo-1,2,2a,2a1,3,5,6,7a-octahydro-7H-cyclopenta[cd]indene-7,7-dicarboxylate (126). Enantiomeric excess determined by HPLC using Chiralcel OJ-H column (87% 2-propanol/hexane, flow 0.5 ml/min, λ = 220 nm). $t_{R(major)}$ 29.4 min; $t_{R(minor)}$ 45.0 min. ^{1}H-NMR (400 MHz, $CDCl_3$) δ 1.22 (m, 2H, CH_2), 1.81 (m, 2H, CH_2), 2.12 (m, 2H, CH_2), 2.44 (m, 1H, CH_2), 2.79 (m, 3H, 2xCH, CH_2), 3.74 (m, 1H, CH), 3.71 (s, 3H, CH_3), 3.81 (s, 3H, CH_3), 5.95 (s, 1H, CH=). ^{13}C-NMR (100.6 Hz, $CDCl_3$) δ 24.2 (CH_2), 27.5 (CH_2), 27.7 (CH_2), 28.6 (CH_2), 43.6 (CH), 48.2 (CH), 50.0 (CH), 52.7 (CH_3), 53.0 (CH_3), 55.8 (C), 129.7 (CH=), 170.5 (CO), 171.5 (CO), 180.1 (C=), 211.6 (CO).

Dimethyl (2a1S,4aR,7aS)-3-methyl-4-oxo-2,2a1,4,4a,5,6,7,7a-octahydro-1H-cyclopenta[cd]indene-1,1-dicarboxylate (127).[18] Enantiomeric excess determined by HPLC using Chiralcel OJ column (87% 2-propanol/hexane, flow 0.5 ml/min, λ = 220 nm). $t_{R(major)}$ 20.6 min; $t_{R(minor)}$ 28.3 min. ^{1}H-NMR (400 MHz, $CDCl_3$) δ 0.63 (dq, 1H, CH_2, *J* = 12.8 Hz, 2.5 Hz), 0.93 (m, 1H, CH_2), 1.20 (m, 1H, CH_2), 1.39 (m, 1H, CH_2), 1.63 (m, 1H, CH_2), 1.71 (m, 3H, CH_3), 2.00 (m, 1H, CH_2), 2.71 (m, 1H, CH), 2.94 (m, 1H, CH), 3.01 (d, 1H, CH_2, *J* = 20.4 Hz), 3.22 (br.s, 1H, CH), 3.51 (d, 1H, CH_2, *J* = 20.4 Hz), 3.75 (s, 3H, CH_3), 3.77 (s, 3H, CH_3).

Dimethyl (2a1S,4aR,8aS)-3-methyl-4-oxo-2a1,4,4a,5,6,7,8,8a-octahydrocyclopenta[cd]azulene-1,1(2H)-dicarboxylate (128). Enantiomeric excess

determined by HPLC using Chiralcel OJ column (87% 2-propanol/hexane, flow 0.5 ml/min, λ = 220 nm). $t_{R(major)}$ 16.9 min; $t_{R(minor)}$ 20.8 min. ^{1}H-NMR (400 MHz, $CDCl_3$) δ 1.01 – 1.38 (m, 4H, CH_2), 1.67 (br. s, 3H, CH_3), 1.86 – 2.23 (m, 5H, CH_2, CH), 2.52 (m, 1H, CH), 2.88 (d, 1H, CH_2, *J* = 18.4 Hz), 3.01 (m 1H, CH), 3.45 (d, 1H, CH_2, *J* = 18.4 Hz), 3.76 (s, 3H, CH_3), 3.77 (s, 3H, CH_3). ^{13}C-NMR (100.6 Hz, $CDCl_3$) δ 8.5 (CH_3), 27.3 (CH_2), 28.2 (CH_2), 30.2 (CH_2), 30.4 (CH_2), 35.2 (CH_2), 48.7 (CH), 48.9 (CH), 51.9 (CH), 52.7 (CH_3), 52.8 (CH_3), 62.4 (C), 132.0 (C=), 171.4 (CO), 171.6 (CO), 175.1 (C=), 211.2 (CO).

Dimethyl (2aS,2a1S,4aR)-6-methyl-5-oxo-2a,2a1,3,4,4a,5-hexahydrocyclopenta[cd]pentalene-2,2(1H)-dicarboxylate (129). Enantiomeric excess determined by HPLC using Chiralcel OJ column (87% 2-propanol/hexane, flow 0.5 ml/min, λ = 220 nm). $t_{R(major)}$ 30.9 min; $t_{R(minor)}$ 45.0 min. ^{1}H-NMR (400 MHz, $CDCl_3$) δ 0.77 (m, 1H, CH_2), 1.51 (dt, 1H, CH_2, *J* = 13.6 Hz, 6.9 Hz), 1.71 (ps. t, 3H, CH_3, *J* = 1.8 Hz), 1.75 (m, 1H, CH_2), 1.92 (tdd, 6.8 Hz, 1H, CH_2, *J* = 13.6 Hz, 10.0 Hz), 2.80 (d, 1H, CH_2, *J* = 18.0 Hz), 2.84 (m, 1H, CH), 3.08 (dt, 1H, CH, *J* = 11.4 Hz, 7.3 Hz), 3.41 (m, 1H, CH), 3.60 (d, 1H, CH_2, *J* = 18.0 Hz) 3.69 (s, 3H, CH_3), 3.76 (s, 3H, CH_3). ^{13}C-NMR (100.6 Hz, $CDCl_3$) δ 8.7 (CH_3), 25.4 (CH_2), 31.1 (CH_2), 34.4 (CH_2), 46.2 (CH), 50.4 (CH), 52.7 (CH_3), 53.1 (CH_3), 55.3 (CH), 62.6 (C), 136.7 (C=), 170.1 (CO), 172.4 (CO), 176.1 (C=), 212.0 (CO).

Dimethyl (2a1S,4aR,7aS)-4-oxo-3-phenyl-2,2a1,4,4a,5,6,7,7a-octahydro-1H-cyclopenta[cd]indene-1,1-dicarboxylate (130).[18] Enantiomeric excess determined by HPLC using Chiralcel OJ column (87% 2-propanol/hexane, flow 0.5 ml/min, λ = 220 nm). $t_{R(major)}$ 24.1 min; $t_{R(minor)}$ 30.2 min. Major diastereoisomer: ^{1}H-NMR (400 MHz, $CDCl_3$) δ 1.40 (m, 1H), 1.59 (m, 1H), 1.90 (m, 4H), 2.80 (m, 3H), 2.99 (d, 1H, *J* = 17.9 Hz), 3.67 (s, 3H), 3.80 (s, 3H), 3.93 (d, 1H, *J* = 17.9 Hz), 7.37 (m, 3H), 7.56 (m, 2H).

Dimethyl (2a1R,4aS,8aS)-4-oxo-3-phenyl-2a1,4,4a,5,6,7,8,8a-octahydrocyclopenta[cd]azulene-1,1(2H)-dicarboxylate (131). Enantiomeric excess determined by HPLC using Chiralcel OD column (87% 2-propanol/hexane, flow 0.5 ml/min, λ = 220 nm). $t_{R(major)}$ 14.3 min; $t_{R(minor)}$ 17.2 min. ^{1}H-NMR (400 MHz, $CDCl_3$) δ 1.25 (m, 4H, CH_2), 1.97 (m, 1H, CH_2), 2.12 (m, 2H, CH_2, CH), 2.71 (m, 1H, CH), 2.99 (d, 1H, CH_2, *J* = 18.8 Hz), 3.19 (dd, 1H, CH, *J* = 13.3 Hz, 7.1 Hz), 3.71 (s, 3H, CH_3), 3.81 (s, 3H, CH_3), 3.83 (d, 1H, CH_2, *J* = 18.8 Hz), 7.37 (m, 3H, CH=), 7.56 (m, 2H, CH=). ^{13}C-NMR (100.6 Hz, $CDCl_3$) δ 27.6 (CH_2), 28.2 (CH_2), 30.2 (CH_2), 30.3 (CH_2), 37.1 (CH_2), 48.3 (CH), 49.7 (CH), 52.0 (CH), 52.8 (2xCH_3), 62.6 (C), 128.1 (CH=), 128.3 (CH=), 128.4 (CH=), 131.2 (C=), 134.6 (C=), 171.2 (CO), 171.4 (CO), 177.0 (C=), 209.9 (CO).

Dimethyl (2aS,2a1S,4aR)-5-oxo-6-phenyl-2a,2a1,3,4,4a,5-hexahydrocyclopenta[cd]pentalene-2,2(1H)-dicarboxylate (132). Enantiomeric excess determined by HPLC using Chiralcel OD column (87% 2-propanol/hexane, flow 0.5 ml/min, λ = 220 nm). $t_{R(major)}$ 27.3 min; $t_{R(minor)}$ 30.4 min. ^{1}H-NMR (400 MHz, $CDCl_3$) δ 0.88 (m, 1H, CH_2), 1.61 (m, 1H, CH_2), 1.90 (dd, 1H, CH_2, *J* = 13.5 Hz, 7.0 Hz), 2.06 (ap tdd, 1H, CH, *J* = 13.5 Hz, 10.2 Hz, 7.0 Hz), 3.05 (dd, 1H, CH, *J* = 10.2 Hz, 5.3 Hz), 3.14 (dt, 1H, CH, *J* = 11.5 Hz, 7.2 Hz), 3.23 (dd, 1H, CH_2, *J* = 18.3 Hz, 1.7 Hz), 3.61 (m, 1H, CH), 3.68 (s, 3H, CH_3), 3.71 (dd, 1H, CH_2, *J* = 18.3 Hz, 1.1 Hz), 3.82 (s, 3H, CH_3), 7.40 (m, 3H, H-Ar), 7.52 (m, 2H, H-Ar). ^{13}C-NMR (100.6 Hz, $CDCl_3$) δ 25.6 (CH_2), 31.2 (CH_2), 36.1 (CH_2), 46.4 (CH), 51.8

(CH), 52.7 (CH_3), 53.2 (CH_3), 55.7 (CH), 63.1 (C), 128.4 (CH=), 128.5 (2xCH=), 128.5 (2xCH=), 130.8 (C=), 139.2 (C=), 169.9 (CO), 172.4 (CO), 177.9 (C=), 209.8 (CO).

Dimethyl (2a1S,5aS,8aR)-1-oxo-2-phenyl-2a1,3,4,5a,6,7,8,8a-octahydroacenaphthylene-5,5(1H)-dicarboxylate (133) Enantiomeric excess determined by HPLC using Chiralcel OD column (87% 2-propanol/hexane, flow 0.5 ml/min, λ = 220 nm). $t_{R(major)}$ 19.9 min; $t_{R(minor)}$ 25.2 min. ^{1}H-NMR (400 MHz, $CDCl_3$) δ 1.33-3.02 (m, 10xCH_2, 6xCH), 3.66 (s, 3H, CH_3, major), 3.69 (s, 3H, CH_3, major), 3.72 (s, 3H, CH_3, minor), 3.77 (s, 3H, CH_3, minor), 7.21-7.37 (m, 10xCH=).^{13}C-NMR (100.6 Hz, $CDCl_3$) δ 21.5-58.7 (CH, CH_2), 52.2 (CH_3, minor), 52.4 (CH_3, minor), 52.7 (CH_3, major), 57.7 (CH_3, major), 127.3-173.7 (CH=, C=), 170.3 (CO, major), 170.7 (CO, major), 171.4 (CO, minor), 171.6 (CO, minor), 205.0 (CO, major), 207.9 (CO, minor).

5.5. References

1. (a) *Asymmetric Catalysis in Industrial Scale: Challenges, Approaches, and Solutions*. Balser, H. U.; Federsel, H. J., Wiley: Weinheim, 2010; (b) *Catalytic Asymmetric Synthesis*. John Wiley & Sons: Hoboken, 2010; (c) *Catalysis from A to Z: A Concise Encyclopedia*. Cornils, B.; Herrmann, W. A.; Xu, J. H.; Zanthoff, H. W., 5th ed.; Wiley-VCH: Weinheim, 2019.
2. (a) Pàmies, O.; Margalef, J.; Cañellas, S.; James, J.; Judge, E.; Guiry, P. J.; Moberg, C.; Bäckvall, J.-E.; Pfaltz, A.; Pericàs, M. A.; Diéguez, M., Recent Advances in Enantioselective Pd-Catalyzed Allylic Substitution: From Design to Applications. *Chemical Reviews* **2021**, *121*, 4373-4505; (b) Lu, Z.; Ma, S., Metal-Catalyzed Enantioselective Allylation in Asymmetric Synthesis. *Angewandte Chemie International Edition* **2008**, *47*, 258-297; (c) Trost, B. M.; Crawley, M. L., Asymmetric Transition-Metal-Catalyzed Allylic Alkylations: Applications in Total Synthesis. *Chemical Reviews* **2003**, *103*, 2921-2944; (d) *Comprehensive Asymmetric Catalysis*. Jacobsen, E. N.; Pfaltz, A.; Yamamoto, H., Springer-Verlag: Berlin, 1999; (e) Johannsen, M.; Jorgensen, K. A., Allylic Amination. *Chemical Reviews* **1998**, *98*, 1689-1708; (f) Tsuji, J.,·*Palladium Reagents and Catalysis: Innovations in Organic Synthesis*. Wiley: New York, 1995.
3. (a) Ogba, O. M.; Warner, N. C.; O'Leary, D. J.; Grubbs, R. H., Recent advances in ruthenium-based olefin metathesis. *Chemical Society Reviews* **2018**, *47*, 4510-4544; (b) Hanson, P. R.; Maitra, S.; Chegondi, R.; Markley, J. L., General Ring-Closing Metathesis. In *Handbook of Metathesis*, Wiley-VCH Verlag: Weinheim, 2015; pp 1-170.
4. (a) Méndez, M.; Muñoz, M. P.; Echavarren, A. M., Platinum-Catalyzed Alkoxy- and Hydroxycyclization of Enynes. *Journal of the American Chemical Society* **2000**, *122*, 11549-11550; (b) Méndez, M.; Muñoz, M. P.; Nevado, C.; Cárdenas, D. J.; Echavarren, A. M., Cyclizations of Enynes Catalyzed by $PtCl_2$ or Other Transition Metal Chlorides: Divergent Reaction Pathways. *Journal of the American Chemical Society* **2001**, *123*, 10511-10520.
5. Trost, B. M.; Mueller, T. J. J.; Martinez, J., Ruthenium Catalyzed Synthesis of Butenolides and Pentenolides via Contra-Electronic .alpha.-Alkylation of Hydroxyalkynoates. *Journal of the American Chemical Society* **1995**, *117*, 1888-1899.
6. (a) Nieto-Oberhuber, C.; López, S.; Muñoz, M. P.; Cárdenas, D. J.; Buñuel, E.; Nevado, C.; Echavarren, A. M., Divergent Mechanisms for the Skeletal Rearrangement and [2+2] Cycloaddition of Enynes Catalyzed by Gold. *Angewandte Chemie International Edition* **2005**, *44*, 6146-6148; (b) Fürstner, A.; Davies, P. W.; Gress, T., Cyclobutenes by Platinum-Catalyzed Cycloisomerization Reactions of Enynes. *Journal of the American Chemical Society* **2005**, *127*, 8244-8245.

7. (a) Jiménez-Núñez, E.; Echavarren, A. M., Gold-Catalyzed Cycloisomerizations of Enynes: A Mechanistic Perspective. *Chemical Reviews* **2008**, *108*, 3326-3350; (b) Zhang, L.; Sun, J.; Kozmin, S. A., Gold and Platinum Catalysis of Enyne Cycloisomerization. *Advanced Synthesis & Catalysis* **2006**, *348*, 2271-2296.
8. Fürstner, A.; Stelzer, F.; Szillat, H., Platinum-Catalyzed Cycloisomerization Reactions of Enynes. *Journal of the American Chemical Society* **2001**, *123*, 11863-11869.
9. (a) Blanco-Urgoiti, J.; Añorbe, L.; Pérez-Serrano, L.; Domínguez, G.; Pérez-Castells, J., The Pauson–Khand reaction, a powerful synthetic tool for the synthesis of complex molecules. *Chemical Society Reviews* **2004**, *33*, 32-42; (b) Lindsay, D. M.; Kerr, W. J., Recent Advances in the Pauson–Khand Reaction. In *Cobalt Catalysis in Organic Synthesis: Methods and Reactions*, Hapke, M.; Hilt, G., Eds. Wiley-VCH Verlag: 2019.
10. Magnus, P.; Principe, L. M., Origins of 1,2- and 1,3-stereoselectivity in dicobaltoctacarbonyl alkene-alkyne cyclizations for the synthesis of substituted bicyclo[3.3.0]octenones. *Tetrahedron Letters* **1985**, *26*, 4851-4854.
11. Biosca, M.; Margalef, J.; Caldentey, X.; Besora, M.; Rodríguez-Escrich, C.; Saltó, J.; Cambeiro, X. C.; Maseras, F.; Pàmies, O.; Diéguez, M.; Pericàs, M. A., Computationally Guided Design of a Readily Assembled Phosphite–Thioether Ligand for a Broad Range of Pd-Catalyzed Asymmetric Allylic Substitutions. *ACS Catalysis* **2018**, *8*, 3587-3601.
12. Shambayani, S.; Crowe, W. E.; Schreiber, S. L., N-oxide promoted pauson-khand cyclizations at room temperature. *Tetrahedron Letters* **1990**, *31*, 5289-5292.
13. Magre, M.; Biosca, M.; Norrby, P. O.; Pàmies, O.; Diéguez, M., Theoretical and Experimental Optimization of a New Amino Phosphite Ligand Library for Asymmetric Palladium-Catalyzed Allylic Substitution. *ChemCatChem* **2015**, *7*, 4091-4107.
14. Mazuela, J.; Pàmies, O.; Diéguez, M., Biaryl Phosphite–Oxazoline Ligands from the Chiral Pool: Highly Efficient Modular Ligands for the Asymmetric Pd-Catalyzed Heck Reaction. *Chemistry: A European Journal* **2010**, *16*, 3434-3440.
15. Wu, C.; Zhou, J., Asymmetric Intermolecular Heck Reaction of Aryl Halides. *Journal of the American Chemical Society* **2014**, *136*, 650-652.
16. Sole, D.; Cancho, Y.; Llebaria, A.; Moreto, J. M.; Delgado, A., Intramolecular Nitrogen Assistance in the Nickel-Promoted Tandem Cyclization-Capture of Amino-Tethered Vinyl Bromides and Alkenes. *Journal of the American Chemical Society* **1994**, *116*, 12133-12134.
17. Farwick, A.; Engelhart, J. U.; Tverskoy, O.; Welter, C.; Umlauf, Q. E.; Rominger, F.; Kerr, W. J.; Helmchen, G., Bicyclic Cyclopentenones via the Combination of an Iridium- Catalyzed Allylic Substitution with a Diastereoselective Intramolecular Pauson–Khand Reaction. *Advanced Synthesis & Catalysis* **2011**, *353*, 349.
18. Hicks, F. A.; Kablaoui, N. M.; Buchwald, S. L., Scope of the Intramolecular Titanocene-Catalyzed Pauson–Khand Type Reaction1. *Journal of the American Chemical Society* **1999**, *121*, 5881-5898.

UNIVERSITAT ROVIRA I VIRGILI
DEVELOPMENT OF TAILOR-MADE CATALYST LIBRARIES FOR THE CONSTRUCTION OF CHIRAL C-X (X= C, N AND O) BONDS. APPLICATION TO THE SYNTHESIS OF COMPLEX MOLECULES
Joan Saltó de la Torre

Chapter 6

Synthesis of heterodonor phosphabarrelene/5-phosphasemibullvalene-pyridine ligands and metal complexes

6.1. Introduction

Phosphabarrelenes are two fused six-membered rings with a bicyclo[2.2.2]octa-2,5,7-triene (barrelene) structure where one or more of the carbons are substituted by phosphorous atom. The most common structure found in the literature is the 1-phosphabarralene (Figure 6.1), although there are few examples regarding other structures such as 1,4-diphosphabarralene or 2-phosphabarralene.[1]

Figure 6.1. Different types of phosphabarrelenes.

1-Phosphabarrelenes are prepared by [4+2] cycloaddition to the corresponding phosphinine ring which acts as a diene and an alkyne (Scheme 6.1).[2] In this regard, there are few examples of successful derivatization which involves the use of extremely reactive dienophiles in particular those bearing highly electron-withdrawing groups (such as $-CF_3$ or -CN) or highly strained alkynes (benzyne derivatives, cyclooctyne, etc.). The first example of a successful preparation was attained by reacting 2,4,6-triphenylphosphinine with hexafluoro-2-butyne gas at 100 °C in methyl cyclohexane.[2]

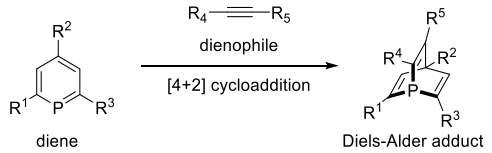

Scheme 6.1. Preparation of 1-phosphabarrelene derivatives.

Despite that, there are two strategies to allow Diels-Alder reaction using other less dienophilic alkynes. The first one is by reducing the aromaticity of the phosphinine ring, for example by the oxidation of the λ^3-phosphinine to a λ^5-phosphinine by reaction with molecular sulfur (**134**) or by using phosphininium cations (**135**).[3] The second strategy is by coordination with a metal center prior the cycloaddition step (**136**). In this case, the reduced aromaticity of the system either allows cycloaddition reaction with other alkenes such as N-phenylmaleimide and cyclopentadiene or the alkyne counterpart dimethyl acetylenedicarboxylate.[4] In Figure 6.2 is shown some examples of 1-phosphabarrelenes achieved using these strategies.

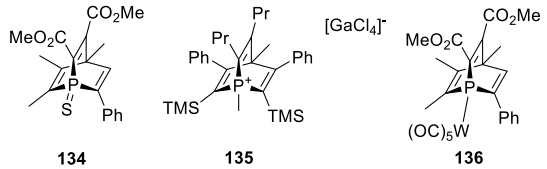

Figure 6.2. Phosphabarralenes **134**-**136** obtained by other strategies.

The electronic and steric properties of phosphabarrelene compounds have not been extensively studied. Nevertheless, there are some insights in the literature than can help to elucidate them. The reported CO stretching in monodentate phosphabarrelene containing complexes such as *trans*-[L_2RhCl(CO)] are in the range of 1971-1993 cm^{-1}, whereas the corresponding triphenylphosphine, triphenylphosphinite or the phosphite (P[O(2-^{t}Bu$C_6H_4)_3$]) analogues have frequencies of 1965, 1999 and 2013 cm^{-1}, respectively.[5] Therefore, the electronic properties are in between phosphines and phosphinites or phosphites. Regarding the steric properties of 1-phosphabarrelene ligands there are some estimated Tolman cone angle from the respective *trans*-[L_2RhCl(CO)] complexes with values about 161-181° which are similar to those reported for bulky phosphines analogues (P(^{t}Bu)$_3$ and P(Cy)$_3$, 182° and 170°, respectively).[5c, 6] Nevertheless, the estimation on other complexes such as Fe(II) o Ru(II) changed substantially the values obtained for Rh-complexes counterpart.[7] This fact could indicate that despite their rigidity, the steric exerted by 1-phosphabarrelenes can be modulated depending on their coordination environment.

To the best of our knowledge, the application of 1-phosphabarrelenes compounds as ligands in metal-catalyzed transformations are anecdotic.[8] In this regard, monodentate phosphabarrelene ligands have been applied successfully in non-asymmetric version of Pd-catalyzed cross coupling reactions (**137**),[9] Pt-catalyzed hydrosilylation of alkenes (**137**),[10] and Rh-hydroformylation(**138**) (Figure 6.3).[5c]

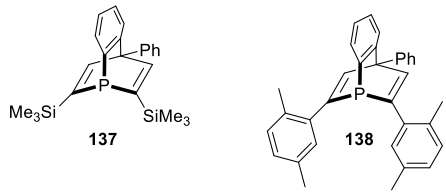

Figure 6.3. 1-Phosphabarrelene ligands **137** and **138** applied in metal catalyzed reactions.

In this respect, there is only one application of chiral phosphabarrelene containing ligands in asymmetric catalysis.[11] Thus, Breit et al. reported the synthesis and use of several phosphabarrelene-phosphite ligands **139**-**142** in the asymmetric hydrogenation of dehydroamino acid derivatives and dimethyl itaconate (Figure 6.4). While high *ee*'s (up to 90%) were attained in the hydrogenation of dehydroamino acid derivatives, low enantioselectivity was attained with dimethyl itaconate (*ee*'s up to 19%). It should be

pointed out that the use of the analogous monodentate phosphabarrelene derivatives **143**-**145** only provided low enantiocontrol in these reactions.

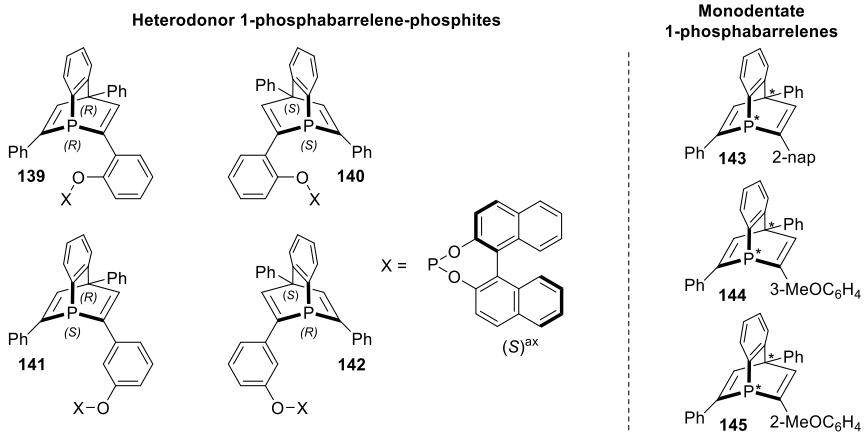

Figure 6.4. 1-Phosphabarrelene-phosphite ligands **139**-**142** and monodentate 1-phosphabarrelene ligands **143**-**145**.

Despite chiral phosphabarrelene-ligands have been scarcely used, related phosphanorbornadienes have found some interesting applications in asymmetric catalysis (Figure 6.5). In this sense, the C_2-symmetric phosphanorbornadiene ligand **146** has been successfully used in the Rh-catalyzed hydrogenation of some α-acetamidocinnamic acids with *ee*'s up to >98%.[12] Also, the heterodonor phosphanorbornadiene-oxazoline ligand **147** provided high enantioselectivities in the Pd-catalyzed asymmetric allylic substitution and intermolecular Heck reactions (*ee*'s up to 94% and 93%, respectively).[13]

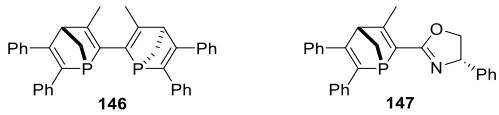

Figure 6.5. C_2-symmetric phosphanorbornadiene ligand **146** and its heterodonor counterpart phosphanorbornadiene-oxazoline ligand **147**.

Encouraged by the promising results attained with heterodonor phosphabarrelene-based ligands **139**-**142**, Müller group published the first example of a heterodonor phosphabarrelene-pyridine ligand **L16**, synthesized from the corresponding phosphinine **148** with hexafluorobutyne (Scheme 6.2).[14] Although, the Diels-Alder with arynes was also evaluated, the pyridyl derivative only allowed the functionalization with this highly reactive dienophile.[14] They also reported the coordination of **L16** to Rh and W (**149** and **150** respectively, Scheme 6.2).[14]

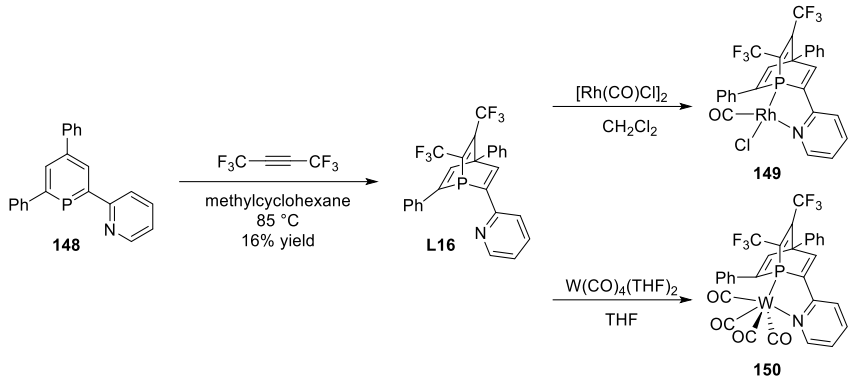

Scheme 6.2. Preparation of the 1-phosphabarrelene-pyridine ligand **L16** and its coordination to Rh and W.

The photochemical transformation of barrelenes are also known.[15] In this regard, the photoirradiation on barrelene yields semibullvalenes. Nevertheless, this type of rearrangement usually is not selective leading to the formation of several isomers. Furthermore, these semibullvalene derivatives were not stable showing decomposition over the time.[15] In 2016, Müller's group published the first example of photoirradiation of the phosphabarrelene **151** to form the 5-phosphasemivullvalene derivative **152** (Scheme 6.3).[16] In contrast with the barrelene counterpart, the phosphorous analogue yielded a single 5-phosphasemibullvalene, by a di-π-methane rearrangement, as a stable solid.

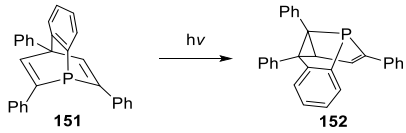

Scheme 6.3. Irradiation of the 1-phosphabarrelene **151** to form the 5-phosphasemibullvalene derivative **152**.

Later in 2019, the same group disclosed the selective photoirradiation of previously mentioned Rh- and W-complexes containing the 1-phosphabarrelene-pyridine ligand **L16** (Scheme 6.2), which yielded the corresponding 5-phosphasemibullvalene-pyridine complexes **153** and **154**, respectively (Figure 6.6).[14] Nevertheless, the direct photoirradiation of the single ligand **L16** has not been reported.

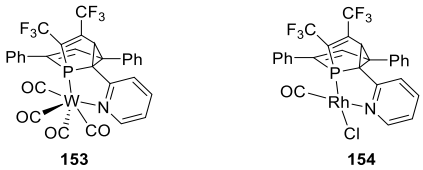

Figure 6.6. 5-Phosphasemibullvalene complexes **153** and **154** prepared *via* photoirradiation of complexes **149** and **150**, respectively.

In addition, ligand **L16** and the corresponding 5-phosphasemibullvalene derivative have never been tested in catalysis. For this reason, the preparation of a group of 1-phosphabarrelene/5-phosphasemibullvalene-pyridine ligands is of high interest since their isolation as single enantiomer would lead to chiral ligands with a P-stereogenic center. The molecules containing a P-stereogenic element are of high importance to increase the ligand portfolio in asymmetric catalysis.[17] To continue our quest in finding new improved ligand classes for asymmetric catalysis we include here the development of new 1-phosphabarrelene/5-phosphasemibullvalene-pyridine compounds (Figure 6.7). In addition, we also improved the yield of the previously synthesized ligand **L18** by optimization of the reaction conditions.

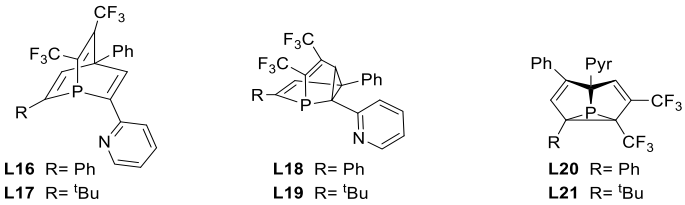

Figure 6.7. 1-Phosphabarrelene-pyridine ligands **L16** and **L17** and 5-phosphasemibullvalenes-pyridine ligands **L18**-**L21**.

6.2. Results and discussion

6.2.1. Preparation of a new phosphinine-pyridine compound 155

Following the methodology reported by Müller group for the preparation of phosphinine-pyridine compound **148** (Scheme 6.2),[18] we also prepared the phosphinine-pyridine compound **155** with differ in the presence of a *tert*-butyl group at the *ortho* position of the phosphinine moiety (Scheme 6.4). For this, we synthesized the corresponding (*E*)-benzylidenepinacolone **156** by condensation reaction between pinacolone and benzaldehyde. With this chalcone derivative we synthesized the corresponding diketone **157** by condensation with 2-acetylpyridine in quantitative

yields. The reaction of **157** with $HBF_4{\cdot}OEt_2$ yielded the corresponding pyrylium salt **158** in 85% yield after recrystallization. Then, the reaction of **158** with $P(TMS)_3$ gave the corresponding phosphinine-pyridine compound **155** in 30% yield after flash chromatography isolation.

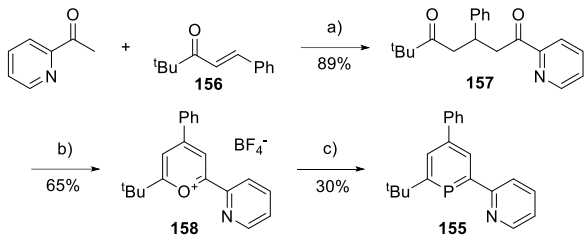

a) ^{t}Bu-Chalcone **156** (1 equiv), 2-acetylpyridine (1 equiv), NaOH (1 equiv). 30 min. b) **157** (1 equiv), chalcone (1 equiv), $HBF_4{\cdot}OEt_2$ (8 equiv). 3 h at 70 °C. c) **158** (1 equiv), $P(TMS)_3$ (2.1 equiv), 6 h acetonitrile reflux.

Scheme 6.4. Preparation of phosphinine-pyridine compound **155**.

6.1.1. Preparation of ligands L16 and L17

With compounds **148** and **155** in hand, we next studied their derivatization to 1-phosphabarrelene-pyridine ligands **L16** and **L17** by Diels-Alder reaction (Scheme 6.5).

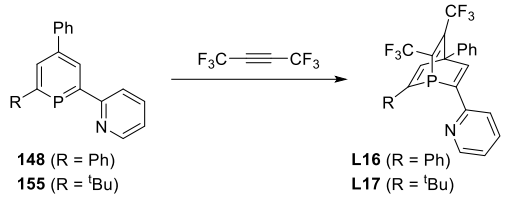

Scheme 6.5. Diels Alder reaction on phosphinines **148** and **155** to yield **L16** and **L17**, respectively.

As already commented in the introduction, the preparation of **L16** was already reported by Müller's group.[14] Thus, the reaction of **148** with hexafluorobutyne in methylcyclohexane at 85 °C for 3 days yielded the **L16**, but in only 17% yield after recrystallization (20% conversion by $^{31}P\{^1H\}$-NMR, Scheme 6.2). To improve the yield, we decided to change the solvent to toluene since it allows to work at higher temperatures. We first increased the temperature to 100 °C achieving 34% of conversion. To our delight, when temperature was increased to 120 ° and the reaction time was increased to 5 days, we attained an 80% of conversion.

We also studied the use of methylcyclohexane as solvent. However, we found as already reported that at temperatures higher than 85 °C the retro Diels-Alder product (formed after the release of phenylacetylene) is also attained in this solvent.[14]

With these optimized conditions, we then attempted the synthesis of the 1-phosphabarralene derivative with a ^{t}Bu group (ligand **L17**). In this regard we could attain the Diels-Alder of 2-*tert*-butyl phosphinine-pyridine **155** to afford the corresponding 1-phosphabarrelene ligand **L17** in 55% yield.

In order to confirm that the ligand **L17** was racemic we prepared the corresponding (+)-camphorsulfonic diastereomeric acid-base adduct **159** (Figure 6.8). For this, we prepared an equimolar mixture of **L17** and (+)-camphorsulfonic and we analyzed it by ^{1}H- and ^{31}P{^{1}H}-NMR using d^{6}-benzene as solvent. We could not observe any splitting of the signals in ^{1}H-NMR. Nevertheless, the ^{31}P{^{1}H}-NMR was more indicative, showing two quartets one of each diastereoisomer in a 1:1 ratio.

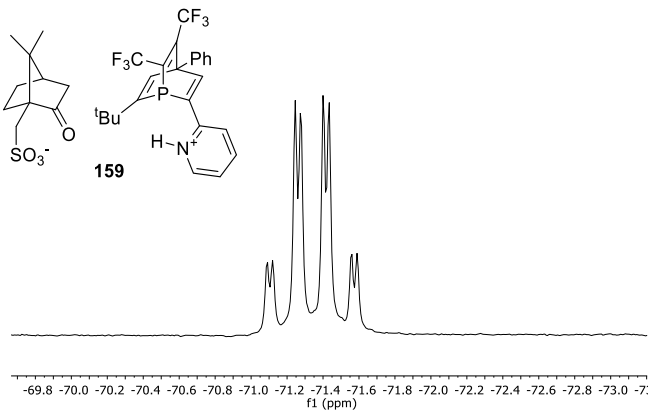

Figure 6.8. ^{31}P{^{1}H}-NMR showing the two signals regarding the diastereiomeric acid-base adduct **159**.

The next step for their application in asymmetric catalysis was to attempt the separation of the two enantiomers of each ligand. For this, we performed an HPLC study. Initially, we studied the stability of the 1-phosphabarrelene ligands towards their oxidation in solution. The respective ^{31}P{^{1}H}-NMR analysis of an isopropanol solution of **L16** and **L17** indicated that the ligands were robust enough to be separated by chiral semipreparative HPLC since no oxidation was observed even for 5 days. After testing different chiral columns (Chiralcel OJ-H and OD-H as well as Chiralpak IA, IB, IC and AD columns) and conditions, we found that the separation of ligands can be achieved by using semipreparative Chiralcel OD-H column.

6.2.2. Preparation of metal complexes of ligand L16 and L17

The first complex that we attempted to prepare was the [Rh(COD)**L17**]BF_4 **160** (COD=1,5-cyclooctadiene) since we can compare its structure with the analogous with ligand **L16** already prepared in Müller's group.[14] We chose this complex since this type

of cationic complexes are usually used as catalyst precursors for the hydrogenation of functionalized olefines.[19] In this respect, we reacted equimolarly **L17** with $[Rh(COD)_2]BF_4$ in CH_2Cl_2 (Scheme 6.6). The coordinated complex was immediately detected by $^{31}P\{^1H\}$-NMR showing a $J_{P\text{-}Rh}$ = 170 Hz and a $J_{P\text{-}F}$ = 10 Hz.

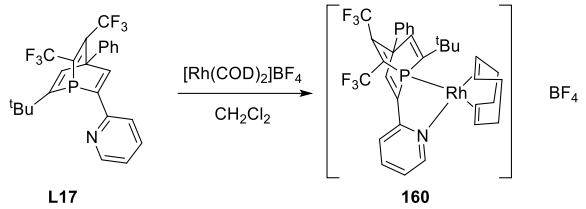

L17 **160**

Scheme 6.6. Preparation of Rh (I) complex **160**.

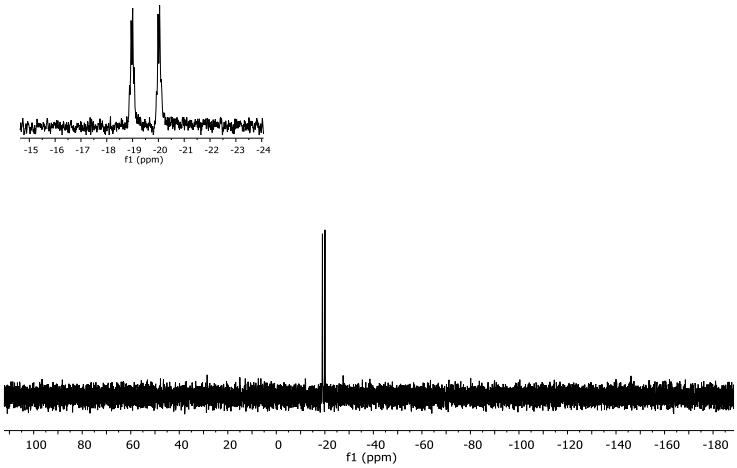

Figure 6.9. $^{31}P\{^1H\}$-NMR of Rh(I) complex **160**.

A crystal suitable for x-ray diffraction were obtained by slow diffusion of toluene into fluorobenzene solution of **160** (Figure 6.10). The geometry of the metal center is a slightly distorted square plane (P1-Rh1-C29: 154.1°, P1-Rh1-C28: 169.1°, N1-Rh1-C25: 154.2°, N1-Rh1-C32: 168.7°, C25-Rh1-C28: 78.9°, C29-Rh1-C32: 80.7°). For comparation purposes a selected set of angles are shown in Table 6.1 and compared with the analogous complex with ligand **L16**.

Comparing with the analogue complex with **L16**[14] we could observe a more open angle between the C1-P1-C5 whereas the angle for C1-P1-Rh1 decreased. This indicate that the presence of the *tert*-butyl pushes slightly the rest of the molecule towards the pyridine. This fact could be also observed when the bond distances are analyzed. Whereas for **149**, the values of Rh1-N1 are 2.161Å for the complex **160** with **L16** is

2.163Å. A higher difference is found for P1-Rh1 distance. Also, for complex **161,** we found a P1-Rh1 distance of 2.284Å which are larger than the reported with the Ph-derivative is 2.240Å.

Table 6.1. Comparation between the published Rh complex of **L16** and those obtained for **160**.

Angle	Value for **160**	Published value for Rh complex of **L16**
C1-P1-C5	98.1	97.2
C6-P1-C1	97.2	98.9
C6-P1-C5	95.5	91.9
P1-Rh-N1	81.7	81.6
C6-P1-Rh1	128.3	128.3
C1-P1-Rh1	101.8	104.5

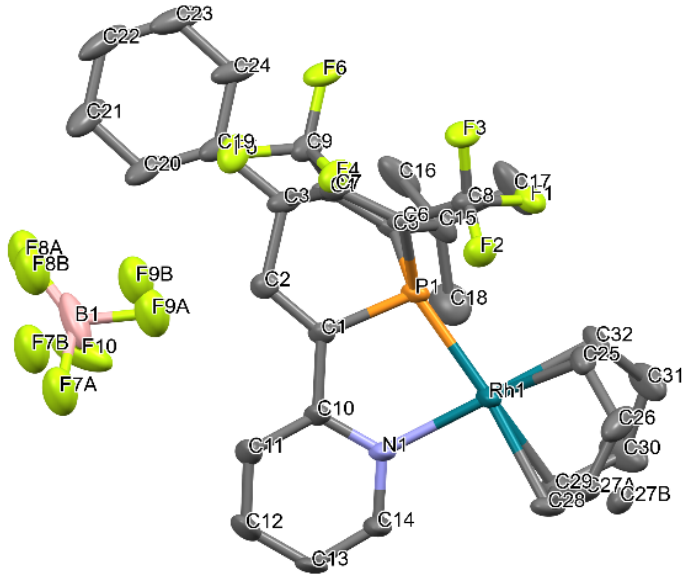

Figure 6.10. XR-structure of **160** in the crystal. Hydrogens are omitted for clarity.

We next attempted the synthesis of Re(I) complex of **L17** (Scheme 6.7). For this, we reacted **L17** with $Re(CO)_5Br$ overnight at 80 °C in toluene. Then, the solvent was evaporated, and the complex washed with pentane to afford **161** as a white solid. To our delight, we could attain a suitable crystal for x-ray by slow diffusion of pentane to a solution of **161** in dichloromethane (Figure 6.11). The crystallographic analysis of Re(I) complex **161** indicated that the shape on the metal center has a slightly octahedral geometry (Br1-Re1-C26: 96.0°, C25-Re1-C26: 88.1°, C26-Re1-C27: 90.0°, Br1-Re1-N1:

82.7°, Br1-Re1-P1: 80.65°). We could observe the same effect of the *tert*-butyl group of the Rh-complex **160** since this group pushes one of the equatorial CO groups causing the distortion observed. The bond distances on the 1-phosphabarrelene were comparable to those obtained with the Rh(I) complex **160**.

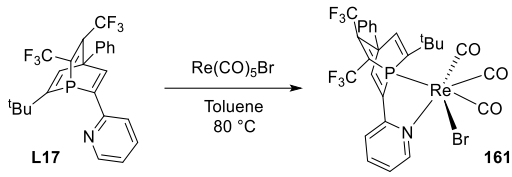

Scheme 6.7. Preparation of Re(I) complex **161**.

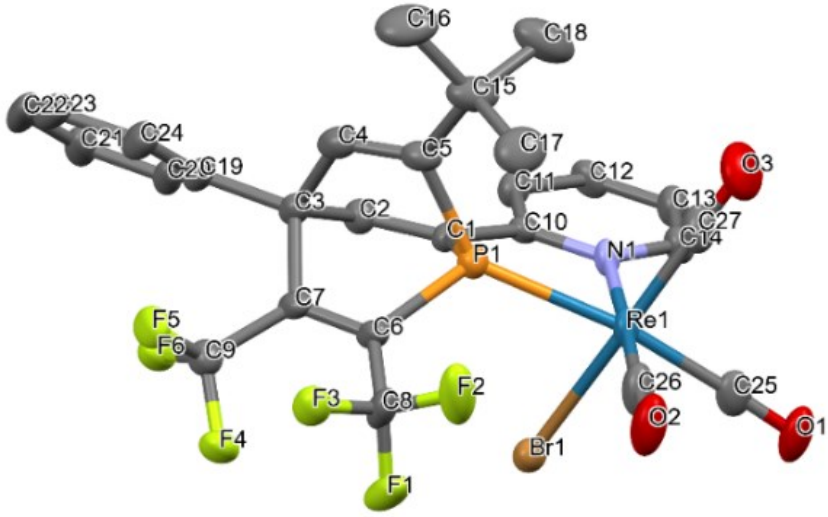

Figure 6.11. XR-structure of **161** (hydrogens are omitted for clarity).

We next prepared [W(CO)$_4$**L17**] complex **162** following also the methodology described by Müller's group using **L16**.[14] For this, we first prepared the corresponding precursor W(CO)$_4$(THF)$_2$ by UV irradiation of W(CO)$_6$ in a THF solution.[20] Then, we reacted **L17** with the freshly prepared precursor in a equimolar 1:1 ratio at 50 °C in THF for 12 h (Scheme 6.8). Then, the reaction mixture was analyzed by ^{19}F and ^{31}P NMR. We could observe the formation of the desired product **162**, which shows the expected satellites due to the P-W coupling in ^{31}P{^{1}H} (Figure 6.12), but in contrast with the reported W/**L16** complex, we also observed the presence of the 5-phosphasemibullvalene derived complex **163** (at signal 89.5 ppm (10%)), which indicated that compound **162** reacts with light.

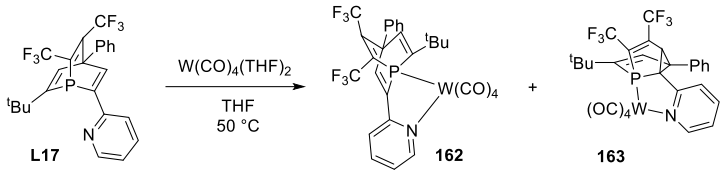

Scheme 6.8. Preparation of W(0) complex with **L17**.

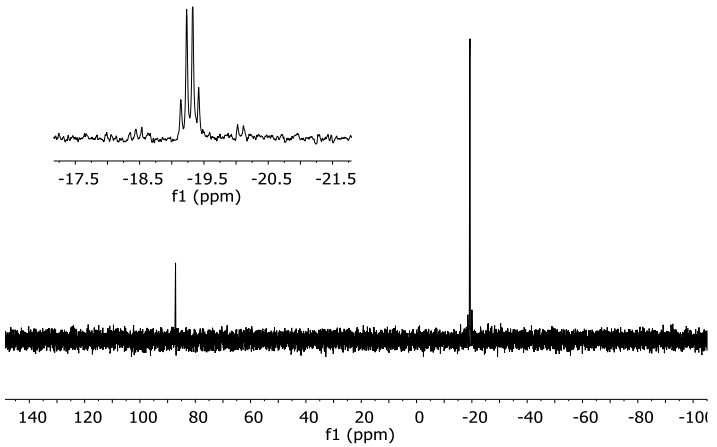

Figure 6.12. $^{31}P\{^{1}H\}$-NMR of W(0) complex **162** showing the P-W satellites and the W/5-phosphasemibullvalene by-product **163**.

Then, we decided to study for the first time the coordination of both phosphabarrelene-pyridine ligands (**L16** and **L17**) to Ir and Pd, since our initial intention was to evaluate the catalytic performance of ligands **L16** and **L17** in the Ir-catalyzed asymmetric hydrogenation of unfunctionalized olefins and Pd-catalyzed asymmetric allylic substitution reactions. For the synthesis of the Ir-complexes, we first reacted the corresponding ligand **L16** and **L17** with the iridium precursor $[Ir(COD)Cl]_2$ in dichloromethane. After 30 minutes, the chloride anion was exchanged with $NaBAr_F$ and both reactions were purified by flash chromatography (Scheme 6.9) to yield the corresponding iridium complexes **164** and **165** in excellent yields. It should be mentioned that for the preparation of these iridium complexes, the reaction and the purification should be done at dark since these complexes reacted in solution under sunlight. Complexes **164** and **165** were characterized by $^{31}P\{^{1}H\}$, $^{19}F\{^{1}H\}$, ^{1}H and $^{13}C\{^{1}H\}$ NMR spectra and MS spectrometry. All data agreed with the assigned structures. Unfortunately, we were unable to obtain crystal of sufficient quality to perform X-ray diffraction measurements. With the aim to achieve good crystals, we also prepared the corresponding complexes with other counterions: BF_4^-, Cl^- and PF_6^-. Nevertheless, any of them afforded a suitable crystal for x-ray diffraction.

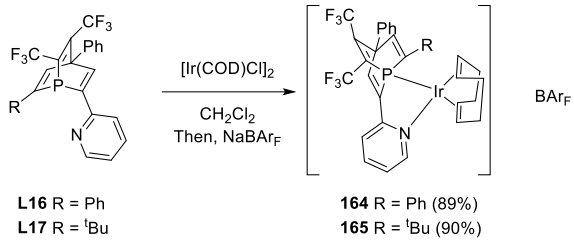

L16 R = Ph
L17 R = ^{t}Bu

164 R = Ph (89%)
165 R = ^{t}Bu (90%)

Scheme 6.9. Preparation of Ir(I)-complexes **164** and **165**.

Finally, we initiated the complexation studies to Pd. For this, we reacted a 1:1 molar ratio of **L17** with $Pd(COD)Cl_2$ in CH_2Cl_2. Then, the solvent was evaporated, and the complex washed several times with pentane to afford **166** in 92% yield as a pale-yellow solid (Scheme 6.10). To our delight, we could attain crystals suitable for x-ray measurement by slow diffusion of pentane over a CH_2Cl_2 solution of **166** (Figure 6.13).

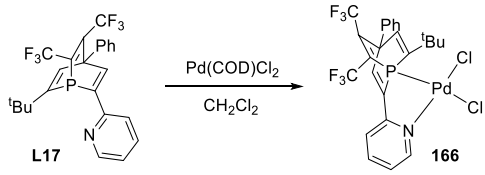

L17 **166**

Scheme 6.10. Preparation of Pd(II) complex **166**.

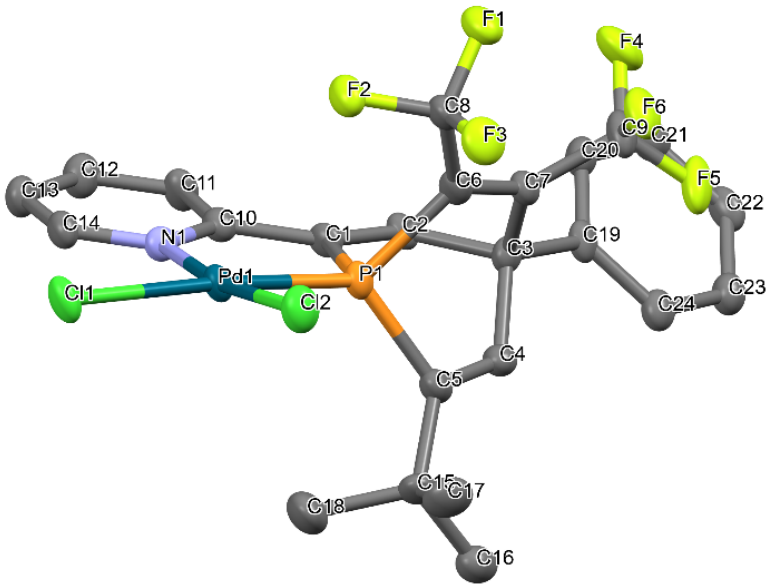

Figure 6.13. XR-structure of **166** in the crystal. Hydrogens are omitted for clarity.

The angle analysis indicated that the metal center is slightly distorted square planar (N1-Pd1-P1: 83.6, Cl2-Pd1-P1: 89.52, Cl1-Pd1-N1: 95.8, Cl1-Pd1-Cl2: 91.58). This distortion seems to be caused for the presence of the *tert*-butyl group which pushes the Cl-2 atom up to the equatorial plane. The distances found on the ligand were comparable with those found for Rh(I) complex **160**.

6.2.3. Irradiation studies of 1-phosphabarrelenes L16 and L17 and their complexes. Preparation of 5-phosphasemibullvalene-pyridine analogues

As commented in the introduction of this chapter, barrelenes undergo di-π-rearrangement when irradiated with UV light to yield the corresponding semibullvalenes.[15, 21] it is reported that the rearrangement on CF_3-substitued barrelene **167** yields at least 3 different products **168**-**170** in a proportion of 4:2:1, respectively (Scheme 6.11). This reaction has shown to be more selective with phosphabarrelenes, especially when the 1-phosphabarrelene is coordinated to a metal center.[14, 16]

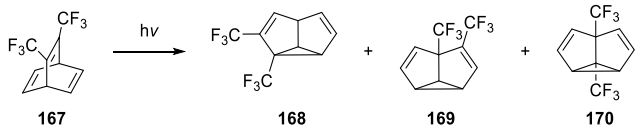

Scheme 6.11. Photochemical rearrangement of CF_3-disubstituted barrelene **167**.

The proposed mechanism for the rearrangement on 1-phosphabarrelenes agrees with the radical mechanism studied by Zimmerman for the barrelenes counterpart (see Scheme 6.12).[16, 22] The higher selectivity observed for the phosphorous analogues has been attributed to the fact that α-aryl groups to the phosphorous helps to stabilize the corresponding radicals formed during the rearrangement. Therefore, the presence of a α- *tert*-butyl group to the phosphorous could be even more beneficial for this process since the *tert*-butyl group can help to further stabilize the radical and therefore the reaction could proceed more selectively.

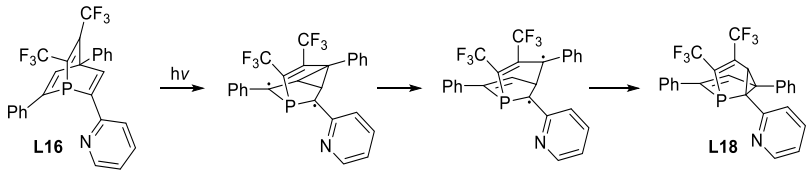

Scheme 6.12. Proposed mechanism for the irradiation of **L16** to yield 5-phosphasemibullvalene-pyridine **L18**.

First, we studied the irradiation of [Rh(CO)Cl(**L17**)] **171** complex analogously as reported for [Rh(CO)Cl(**L16**)]. Complex **171** was prepared in situ by reaction of **L17** with

$[Rh(CO)_2Cl]_2$ in CH_2Cl_2. Then, the complex was irradiated with UV light for 30 minutes. The $^{31}P\{^1H\}$-NMR spectrum showed the formation of a new Rh specie corresponding to [Rh(CO)Cl(**L19**)] (Figure 6.14). In contrast with the irradiation of [Rh(CO)Cl(**L16**)] that yields a mixture of [Rh(CO)Cl(**L18**)] and an unidentified product at a ratio of 10:1[14], the irradiation of [Rh(CO)Cl(**L17**)] was much more selective forming exclusively the new semibullvalene complex [Rh(CO)Cl(**L19**)] **172**.

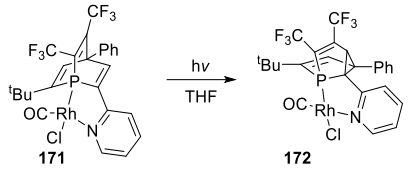

Scheme 6.13. Preparation of Rh(I) semibullvalene complex **172**.

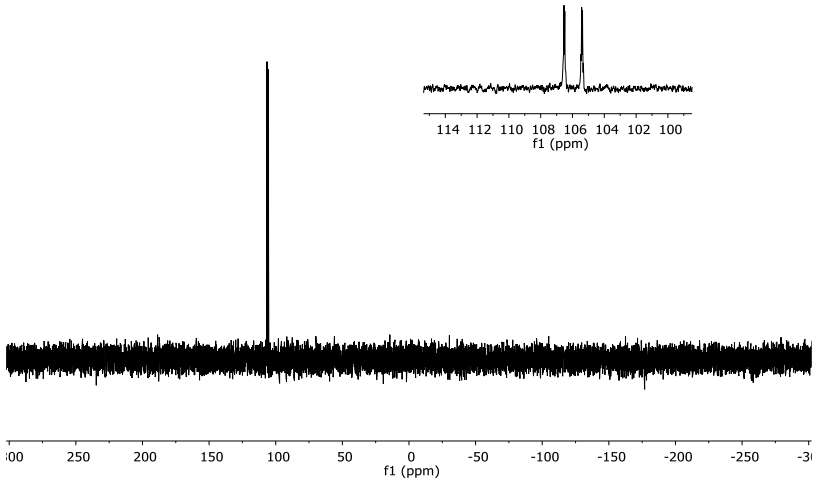

Figure 6.14. $^{31}P\{^1H\}$-NMR of irradiated Rh(I) complex **172**.

To confirm the increased selectivity of the transformation when ligand **L17** is used instead of **L16**, we also studied the irradiation of W-complex **162** (Scheme 6.14). To our delight, the irradiation of **162** was also selective affording the corresponding complex $[W(CO)_4$(**L19**)] **163**.

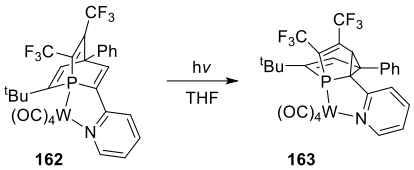

Scheme 6.14. Irradiation of the W(0) complex **162**.

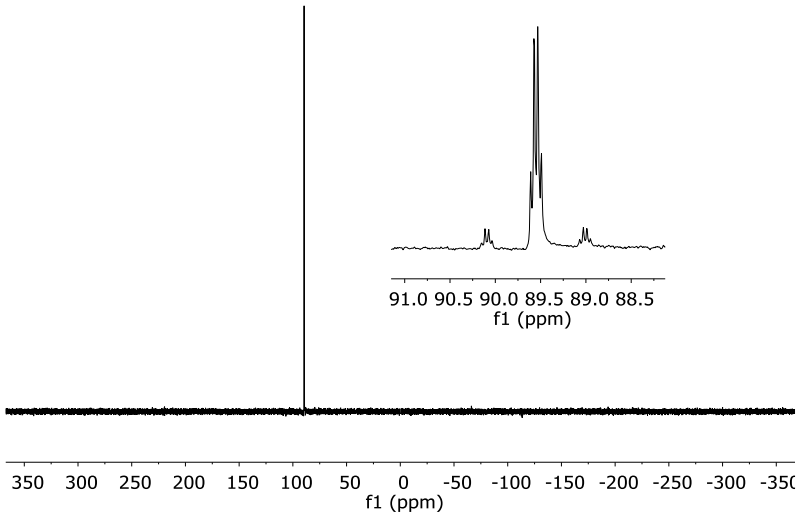

Figure 6.15. $^{31}P\{^{1}H\}$-NMR of irradiated W(0) complex **163**.

Taking into account the highly selective transformation of complexes containing ligand **L17** to the corresponding 5-phosphasemibullvalene derivative, we envisaged the synthesis of 5-phosphasemibullvalene **L19** using the cheapest Cu-complex. For this, we prepared in situ and irradiated the copper complex Cu(**L17**)$_2$PF$_6$ **173** for 30 min (see Experimental Section for the synthesis of copper complexes). After that, we added the strongly chelating ligand dppp (1,3-bis(diphenylphosphino)propane) and we observed the decomplexation of **L19** (reaction followed by ^{31}P-NMR). Finally, the 5-phosphasemibullvalene **L19** were easily isolated by flash chromatography (60 % yield).

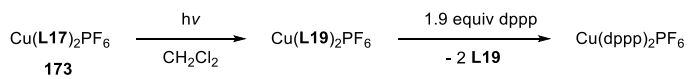

Scheme 6.15. Irradiation and decomplexation of copper complex **173**.

Following the same methodology, we also synthesized the copper complex with **L16** counterpart $Cu(\mathbf{L16})_2PF_6$ **174**. Nevertheless, in this case the reaction was less selective attaining **L18** and the same 5-phosphabarrelene isomer already reported by Müller *et al*.[14]

Finally, we decided to do the direct irradiation of the 1-phosphabarrelene ligands **L16** and **L17** (Scheme 6.15). We first irradiated **L17**, which we expect to be more selective. After 12 h, the formation of two species at a ratio of 1:1 was observed by $^{31}P\{^1H\}$-NMR (Figure 6.15a). One of the species corresponds to the expected 5-phosphasemibullvalene-pyridine **L19** while the other species has been attributed to 5-phosphasemibullvalene-pyridine **L21.** The latter appears down-shield shifted in the $^{31}P\{^1H\}$ NMR, which indicate that the ligand suffered a Cope-rearrangement. Both compounds were easily separated by column chromatography. When **L16** was irradiated we observed the presence of two major species analogues to those observed for **L17**, which has been attributed to 5-phosphasemibullvalene-pyridines **L18** and **L20**, and another four minor species (in a proportion 3:7 respect to the major species; Figure 6.15b)**.**

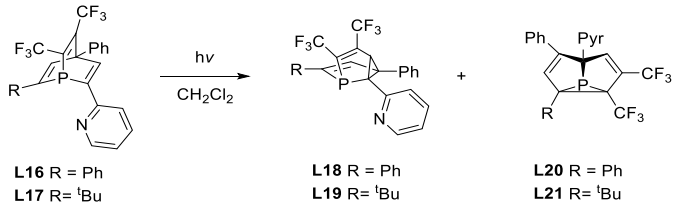

L16 R = Ph
L17 R= ^{t}Bu

L18 R = Ph
L19 R= ^{t}Bu

L20 R = Ph
L21 R= ^{t}Bu

Scheme 6.16. Irradiation of the ligands **L16** and **L17**.

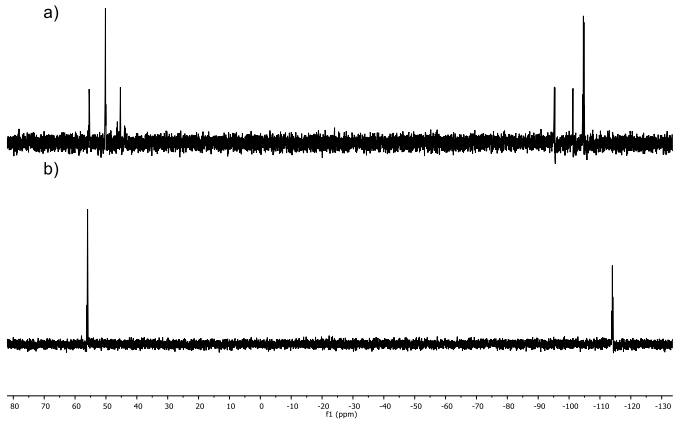

Figure 6.16. $^{31}P\{^1H\}$-NMR spectra of a) irradiation of **L16**, b) irradiation of **L17** in CH_2Cl_2.

6.3. Conclusions

We have developed for the first time the synthesis of a reduced but valuable chiral phosphabarralene-pyridine family of ligands designed to be applied in the near future in some asymmetric catalytic processes. We managed to improve the synthetic yield of previous phosphabarralene-pyridine by optimization of the reaction conditions. These optimizations were also successfully applied to the synthesis of another phosphabarralene-pyridine ligand, with different substituent decorating the phosphabarrelene moiety. The study of the irradiation of phosphabarrelene-pyridine containing complexes indicated that two new set of 5-phosphasemibullvalene ligands could be obtained. Furthermore, the irradiation of the ligands indicated that whereas for the reported ligand the irradiation was less selective, the new ^{t}Bu ligand showed to be more promising since only two species were formed.

6.4. Experimental Part

All reactions were carried out using standard Schlenk techniques under an argon atmosphere. Commercial chemicals were used as received. Solvents were dried by means of standard procedures and stored under argon. NMR spectra were recorded with a *JEOL ECX 600* (^{1}H NMR 600 MHz), a *JEOL ECX400,* a *JEOL ECAII* 400 NMR Spectrometer (^{1}H NMR 400 MHz), *JEOL ECP 500* NMR Spectrometer (^{1}H NMR 500 MHz) or a *Brucker AVANCE III 700* NMR Spectrometer (^{1}H NMR 700 MHz). Chemical shifts are relative to that of $SiMe_4$ (^{1}H and $^{13}C\{^1H\}$) as an internal standard. The NMR copies can be found in the electronic supporting information provided with this thesis. For reactions under UV radiation a Osram Ultra Vitalux 300W lamp was used. Chalcone **157** was prepared as reported.[23]

6.4.1. Preparation of 1,5-diketone 157

Chalcone **156** (3.77 g, 20 mmol), NaOH (0.80 g, 20 mmol) and 2-acetylpyridine (2.42 g, 20 mmol) were mixed in a mortar for 20 minutes until a sticky white solid were obtained. After that, the solid was dissolved with H_2O and Et_2O and transferred to an extraction funnel. Then, the organic phase was separated, and the aqueous phase extracted twice with Et_2O. The combined organic phase was washed with brine, dried with $MgSO_4$ and evaporated under reduced pressure to afford **157** as white solid (5.54 g, 89%).

6.4.2. Characterization details for 1,5-diketone 157

^{1}H NMR (600 MHz, $CDCl_3$), δ: 1.00 (s, 9H, ^{t}Bu), 2.86 (dd, 1H, CH_2, *J* = 17.5 Hz, 6.8 Hz), 2.93 (dd, 1H, CH_2, *J* = 17.5 Hz, 7.2 Hz), 3.46 (dd, 1H, CH_2, *J* = 17.4 Hz, 6.8 Hz), 3.70 (dd, 1H, CH_2, *J* = 17.4 Hz, 7.2 Hz), 3.95 (ap p, 1H, CH, *J* = 7.1 Hz), 7.11 (m, 1H, CH=), 7.24 (m, 4H, CH=), 7.40 (m, 1H, CH=), 7.75 (t, 1H, CH=, *J* = 7.6 Hz), 7.92 (d, 1H, CH=, *J* = 7.9 Hz), 8.62 (d, 1H, CH=, *J* = 4.7 Hz). ^{13}C NMR (151 MHz, $CDCl_3$), δ: 26.2 (^{t}Bu), 36.1 C^{t}Bu), 43.4 (CH_2), 43.6 (CH), 44.1 (CH_2), 121.9 (CH=), 126.4 (CH=), 127.1 (CH=), 127.7 (2xCH=), 128.4 (2xCH=), 136.9 (CH=), 144.7 (C=), 148.9 (CH=), 153.5 (C=), 200.1 (CO), 213.9 (CO).

6.4.3. Preparation of pyrilium salt 158

$HBF_4{\cdot}OEt_2$ (62.7 g, 387.8 mmol) was added to a mixture of 1,5-diketone **157** (15 g, 48.5 mmol) and (*E*)-Chalcone (10 g, 48.48 mmol) at room temperature. Then, the reaction mixture was stirred at 70 °C for 3 h. After allowing the reaction mixture to cool down to room temperature Et_2O was added and the yellow precipitate was collected, washed several times with Et_2O and recrystallized from hot methanol to obtain the pyrilium salt **158** as yellow needles (11.8 g. 65%).

6.4.4. Characterization details for pyrilium salt 158

^{1}H NMR (500 MHz, $CDCl_3$), δ: 1.68 (s, 9H, ^{t}Bu), 7.67 (m, 4H, CH=), 8.08 (td, 1H, CH=, *J* = 7.8 Hz, 1.7 Hz), 8.17 (m, 2H, CH=), 8.23 (d, 1H, CH=, *J* = 1.8 Hz), 8.37 (dt, 1H, CH=, *J* = 7.9 Hz, 1.0 Hz), 8.85 (ddd, 1H, CH=, *J*=4.7 Hz, 1.7 Hz, 0.9 Hz), 9.05 (d, 1H, CH=, *J*=1.8 Hz). ^{13}C NMR(126 MHz, $CDCl_3$): δ = 28.6 (^{t}Bu), 39.5 (C^{t}Bu), 116.1 (CH=), 116.9 (CH=), 124.2 (CH=), 128.6 (CH=), 129.9 (2xCH=), 130.5 (2xCH=), 132.9 (CH=), 135.7 (CH=), 138.5 (CH=), 146.3 (C=) 151.1 (C=), 168.4 (C=), 169.7 (C=), 186.7 (C=).

6.4.5. Preparation of phosphinine 155

To a solution of the corresponding pyrylium salt (10 g, 26.5 mmol) in dry acetonitrile (70 ml) was added dropwise $P(TMS)_3$ (14 g, 55.7 mmol) under argon. After that, the resulting red solution was stirred for 6 h under reflux. After that, the solvent was evaporated, and the reaction mixture dissolved in THF and packed with dry SiO_2 under argon. The purification by flash chromatography of the reaction crude (gradient 100% hexanes to 8:2 hexanes:EtOAc) afforded the corresponding phosphinine ligands as a red solid (2.4 g, 30%).

6.4.6. Characterization details of 155

2-(6-(*tert*-Butyl)-4-phenylphosphinin-2-yl)pyridine (155). $^{31}P\{^1H\}$ NMR (242.95 Hz, CD_2Cl_2), δ: 190.7 (s). ^1H NMR (564.73, CD_2Cl_2), δ: 1.59 (d, 9H, ^tBu, *J* = 1.5 Hz), 7.27 (dt, 1H, CH=, *J* =7.4 Hz, 2.9 Hz), 7.43 (m, 1H), 7.51 (m, 2H, CH=), 7.71 (dd, 2H, CH=, *J* = 8.3 Hz, 1.3 Hz), 7.76 (td, 1H, CH=, *J* = 7.7 Hz, 1.3 Hz), 7.98 (dd, 1H, CH=, *J* = 8.0 Hz, 1.2 Hz), 8.19 (dd, 1H, CH=, *J* = 6.5 Hz, 1.3 Hz), 8.59 (dd, 1H, CH=, *J* = 5.5 Hz, 1.3 Hz), 8.70 (ddd, 1H, CH=, *J* = 4.8 Hz, 1.9 Hz). ^{13}C NMR (125.77 MHz, CD_2Cl_2), δ: 32.9 (d, ^tBu, *J* = 12.4 Hz), 39.2 (d, C-^{t}Bu, *J* = 21.3 Hz), 121.3 (d, CH=, *J* = 14.4 Hz), 122.6 (d, CH=, *J* = 1.8 Hz), 127.9 (CH=), 127.9 (d, 2xCH=, *J* = 1.6 Hz), 129.0 (2xCH=), 130.8 (ap t, 2xCH=, *J* = 12 Hz), 136.9 (CH=), 142.8 (d, C=, *J* =3.1 Hz), 143.4 (d, C=, *J* =14 Hz), 149.9 (CH=), 159.9 (d, C=, *J* = 25.4 Hz), 168.0 (d, C=, *J* = 49.9 Hz), 185.5 (d, C=, *J* = 57.7 Hz).

6.4.7. Preparation of phosphabarrelene L17

A solution of **156** (4.5 g, 12.8 mmol) in toluene (25 ml) was degassed 3 times under freeze-pump cycles. After that, the flask was immersed into a liquid N_2 bath and hexafluorobutyne (3.7 g, 23 mmol) condensed into the reaction flash. Then, the reaction mixture was allowed to reach room temperature and stirred for 3 days at 120 °C. After that, the solvent was evaporated and reaction mixture was purified by flash chromatography (gradient 300:1 to 5:1 hexanes:EtOAc) to afford the corresponding phosphabarrelene as a pale yellow solid (3.8 g, 55%).

6.4.8. Characterization details for L17

7-(*tert*-Butyl)-4-phenyl-5,6-bis(trifluoromethyl) bicyclo [2.2.2] octa-2,5,7-trien-2-yl) pyridine (L17). $^{31}P\{^1H\}$ NMR (242.95 Hz, CD_2Cl_2), δ: -70.23 (q, *J* = 38.2 Hz). $^{19}F\{^1H\}$ NMR (564.73 MHz, CD_2Cl_2) δ: -55.15 (m, 3F, CF_3), -54.75 (m, 3F, CF_3). ^1H NMR (400 MHz, CD_2Cl_2) δ: 1.21 (s, 9H, ^tBu), 7.19 (ddd, 1H, CH, *J* = 6.8 Hz, 4.8 Hz, 1.8 Hz), 7.37 (dd, 1H, CH, *J* = 7.2 Hz, 1.8 Hz), 7.44 (m, 1H, CH), 7.52 (dd, 2H, CH, *J* = 8.5 Hz, 6.8 Hz), 7.70 (m, 2H, CH), 7.80 (d, 2H, CH, *J* =7.8 Hz), 8.59 (dd, 1H, CH, *J* = 4.8 Hz, 1.5 Hz), 8.65 (dd, 1H, CH, *J* = 5.9 Hz, 2.3 Hz). ^{13}C NMR (101.40 MHz, CD_2Cl_2), δ: 28.8 (d, ^tBu, *J* = 8.6 Hz), 36.5 (d, C-^{t}Bu, *J* =24.0 Hz), 66.1 (d, 1H, CH, *J* = 5.1 Hz), 120.4 (d, *J* = 12.9), 122.9, 128.1, 128.7, 129.4, 136.9, 169.4, 144.8, 149.8, 152.7 (m), 154.8 (d, CH, *J* = 27.2 Hz), 164.3 (d, *J* = 22.6 Hz).

6.4.9. Preparation of rhodium(I) cyclooctadiene complex 160

To a solution of $Rh(COD)_2BF_4$ (16 mg, 0.039 mmol) in CH_2Cl_2 (2 ml), **L17** (18 mg, 0.039 mmol) was added, and the resulting orange solution stirred for 10 min. After that, the

solvent was evaporated, and the crude complex was washed with pentane (3 x 1 ml) and dried under high vacuum to afford the corresponding Rh complex **160** as a yellow solid (29 mg, 98%). Crystals suitable for x-ray were obtained by diffusion of toluene into a fluorobenzene solution of **160**.

6.4.10. Preparation of rhenium(I) complex 161

To a solution of $Re(CO)_5Br$ (18 mg, 0.044 mmol) in toluene (1 ml) was added **L17** (21 mg, 0.044). Then, the reaction mixture was stirred overnight at 80 °C. After that, the toluene was evaporated to afford the corresponding Re(I) complex **161** (33 mg, 89%).

6.4.11. Preparation of tungsten (0) complex 162

To a solution of a freshly prepared $W(CO)_4(THF)_2$ (26 mg, 0.058 mmol) in THF (1 ml), **L17** was added (27 mg, 0.058 mmol) and the resulting mixture stirred overnight at 80 °C. After that, the solvent was evaporated, and the crude complex washed with pentane (2 x 1 ml) and dried under high vacuum. The complex was obtained as a yellow solid which contained a mixture of $W(CO)_4$(**L17**) **162** and $W(CO)_4$(**L19**) **163** in a proportion 9:1, respectively, as detected by ^{31}P NMR.

6.4.12. Preparation of iridium complexes 164 and 165

To a light protected solution of $[Ir(COD)Cl]_2$ precursor (0.5 equiv) in CH_2Cl_2, the corresponding ligand **L16** or **L17** was added (1 equiv). After stirring at room temperature for 30 min, $NaBAr_F$ (1.1 equiv) and water were added. The biphasic mixture was stirred for a further 30 min. Then, the aqueous phase was decanted, and the organic phase dried over $MgSO_4$. Flash chromatography (CH_2Cl_2) at dark of the organic phase afforded the corresponding Ir complexes **164** or **165** as a red-orange solids.

6.4.13. Preparation of Pd (II) complex 166

To a solution of $Pd(COD)Cl_2$ (12 mg, 0.042 mmol) in CH_2Cl_2 was added **L17** (20 mg, 0.042 mmol). After stirring for 30 minutes, the solvent was evaporated, and the crude complex washed with pentane to afford the corresponding Pd **166** complex as a yellow solid (24 mg, 92%). Crystals suitable for x-ray diffraction were obtained by slow diffusion of pentane into a CH_2Cl_2 solution of **166**.

6.4.14. Characterization details of metal complexes 160-166

[Rh(COD)L17]BF_4 (160). $^{31}P\{^1H\}$ NMR (242.95 Hz, CD_2Cl_2), δ: -18.56 (dq, *J* = 170 Hz, 10.14 Hz). $^{19}F\{^1H\}$ NMR (564.73, CD_2Cl_2), δ: -152.3 (s, 3F, BF_4), -152.2 (s, 1F, BF_4), -54.51 (ap q, 1F, CF_3, *J* = 12.4 Hz), -53.52 (q, 1F, CF_3, *J* = 12.4 Hz). ^1H NMR (564.73, CD_2Cl_2), δ: 1.47 (s, 9H, ^{t}Bu), 2.41 (m, 4H, CH_2), 2.62 (m, 4H, CH_2), 5.03 (m, 1H, CH=), 5.22 (m, 1H, CH=), 5.53 (m, 1H, CH=), 5.85 (m, 1H, CH=), 7.36 (d, 1H, CH), 7.56 (m, 2H, CH), 7.63 (m, 1H, CH), 7.77 (m, 3H, CH), 8.03 (d, 1H, CH, *J* = 6 Hz), 8.14 (m, 2H, CH), 8.87 (d, 1H, CH, *J* = 15 Hz). ^{13}C NMR (564.73, CD_2Cl_2), δ: 27.7-32.6 (CH_2-COD), 29.9 (CH_3, ^{t}Bu), 36.5 (d, C-^{t}Bu, J = 15.1 Hz), 63.9 (d, CH, *J* = 12.6), 79.2-84.3 (CH-COD), 122.1-160.0 (Aromatic carbons, CF_3, C-P). MS HR-ESI [found 678.1232, C32H32F6NPRh (M-BF4)+ requires 678.1245].

Re(CO)(L17)Br (161). $^{31}P\{^1H\}$ NMR (162 MHz, CD_2Cl_2) δ: -19.67 (br. m). $^{19}F\{^1H\}$ NMR (375 MHz, CD_2Cl_2) δ: -55.73 (q, 3F, CF_3, *J* = 13.4 Hz), -48.72 (dq, 3F, CF_3, *J* = 16.8 Hz, 13.2 Hz). ^1H NMR (400 MHz, CD_2Cl_2) δ: 1.35 (s, 9H, ^{t}Bu), 7.33 (ddd, 1H, CH, *J* = 7.3 Hz, 5.8 Hz, 1.8 Hz), 7.51 (d, 1H, CH, *J* = 19.2 Hz), 7.58 (m, 1H, CH), 7.63 (m, 2H, CH), 7.85 (m, 2H, CH), 7.97 (m, 2H, CH), 8.87 (d, 1H, CH, *J* = 14.4 Hz), 9.16 (ddd, 1H, CH, *J* = 5.8 Hz, 1.6 Hz, 0.9 Hz).

$W(CO)_4$(L17) (162). $^{31}P\{^1H\}$ NMR (161.8 MHz, THF-d^8) δ: -17.48 (q, *J* = 15.0 Hz, P-W satellite 124.0 Hz). $^{19}F\{^1H\}$ NMR (376.1 MHz, THF-d^8) δ: -55.10 (q, 3F, CF_3, *J* = 12.6 Hz), -51.91 (m, 3F, CF_3). ^1H NMR (400 MHz, CD_2Cl_2) δ: 1.39 (s, 9H), 7.27 (ddd, 1H, *J* = 7.2 Hz, 5.7 Hz, 1.4 Hz), 7.35 (d, 1H, *J* = 18.6 Hz), 7.59 (m, 1H), 7.60 (m, 2H), 7.94 (m, 3H), 8.14 (dt, 1H, *J* = 8.2 Hz, 1.1 Hz), 9.26 (ddd, 1H, *J* = 5.6 Hz, 1.7 Hz, 0.8 Hz), 9.29 (d, 1H, *J* = 12.7 Hz).

[Ir(COD)(L16)]BAr_F (164). 89% Yield.$^{31}P\{^1H\}$ NMR (162 MHz, CD_2Cl_2) δ: -13.5 (q, $J^3_{P\text{-}F}$ = 13.4 Hz). $^{19}F\{^1H\}$ NMR (375 MHz, CD_2Cl_2) δ: -62.75 (s, 24F, CF_3, BAr_F), -54.19 (q, *J* = 13 Hz, 3F, CF_3), -53.90 (ap p, *J* = 13.5 Hz, 3F, $\underline{CF_3}$-C-P). ^1H NMR (700 MHz, CD_2Cl_2) δ: 1.77 (m, 2H, CH_2, cod), 1.98 (m, 1H, CH_2, cod), 2.16 (m, 1H, CH_2, cod), 2.27 (m, 1H, CH_2, cod), 2.37 (m, 1H, CH_2, cod), 2.46 (m, 1H, CH_2, cod), 2.53 (m, 1H, CH_2, cod), 3.63 (m, 1H, CH=, cod), 4.74 (m, 1H, CH=, cod), 5.28 (m, 1H, CH=, cod), 5.83 (m, 1H, CH=, cod), 7.47 (m, 3H, CH=), 7.56 (m, 8H, CH=), 7.61 (m, 2H, CH=), 7.73 (m, 10H, CH=), 7.97 (dt, 1H, CH=, *J* = 8.1 Hz, 0.6 Hz), 8.09 (m, 2H, CH=), 8.47 (dd, 1H, N-$\underline{CH=}$, *J* = 6.1, 0.9 Hz), 8.52 (d, 1H, P-C-$\underline{CH=}$, *J* = 17.0 Hz). ^{13}C NMR (176 MHz, CD_2Cl_2) δ: 26.9 (CH_2, cod), 31.0 (d, CH_2, cod, , *J* = 2.7 Hz), 31.2 (CH_2), 35.5 (d, CH_2, cod, *J* = 6.0 Hz), 65.7 (d, *J* = 14.4 Hz, C_q-Ar) 68.2 (CH=, cod), 69.5 (CH=, cod), 98.5 (d, *J* = 15.9 Hz, CH=, cod), 100.7 (d, CH=, cod, *J* = 9.2 Hz), 118.1 – 160.2 (aromatic and CF_3 carbons), 162.3 (q, C_q-B, BAr_F, $^1J_{C\text{-}B}$ = 49.8 Hz). MS HR-ESI [found 788.1499, $C_{34}H_{28}F_6NPIr$ (M-BAr_F)+ requires 788.1493].

[Ir(COD)(L17)]BAr_F (165). 90% yield. $^{31}P\{^1H\}$ NMR (162 MHz, CD_2Cl_2) δ: -17.89 (q, *J* = 8.7 Hz). $^{19}F\{^1H\}$ NMR (375 MHz, CD_2Cl_2) δ: -62.74 (s, 24F, CF_3, BAr_F), -54.65 (dq, 3F, CF_3, *J* = 13.0 Hz, 8.8 Hz), -53.89 (q, 3F, CF_3, *J* = 13.1 Hz). ^1H NMR (700 MHz, CD_2Cl_2) δ: 1.33 (s, 9H, ^{t}Bu), 2.01 (m, 2H, CH_2, cod), 2.20 (m, 1H, CH_2, cod), 2.43 (m, 5H, CH_2, cod), 4.85 (m, 1H, CH=, cod), 4.93 (m, 1H, CH=, cod), 5.27 (m, 1H, CH=, cod), 5.47 (m, 1H, CH=, cod),

7.36-7.14 (m, 19H), 7.91 (dd, 1H, CH, *J* = 8.2 Hz, 1.6 Hz), 8.00 (m, 1H, CH), 8.27 (d, 1H, CH, *J* = 6.1 Hz), 8.71 (d, 1H, CH, *J* = 16.1 Hz). ^{13}C NMR (176 MHz, CD_2Cl_2) δ: 27.5-32.6 (CH, cod), 29.9 (^{t}Bu), 36.6 (C-^{t}Bu, *J* = 15.1 Hz), 63.9 (d, C, *J* = 12.6 Hz), 79.6 (CH=, cod), 83.8 (CH=, cod), 104.7 (CH=, cod), 105.21 (CH=, cod), 119.4-157.95 (aromatic and CF_3 carbons), 159.9(q, C_q-B, BAr_F, $^1J_{C-B}$ = 49.8 Hz). MS HR-ESI [found 768.1819, $C_{32}H_{32}F_6NPIr$ (M-BAr_F)+ requires 768.1806].

Pd(L17)Cl$_2$ (166). $^{31}P\{^1H\}$ NMR (162 MHz, CD_2Cl_2) δ: -7.21 (q, *J* = 13.2 Hz). $^{19}F\{^1H\}$ NMR (375 MHz, CD_2Cl_2) δ: -57.37 (q, 3F, CF_3, *J* = 13.9 Hz), -51.99 (ap. p, 3F, CF_3, *J* = 13.8 Hz). ^{1}H NMR (400 MHz, CD_2Cl_2) δ: 1.59 (s, 9H, ^{t}Bu), 7.55 (m, 3H, CH), 7.66 (m, 2H, CH), 7.80 (m, 3H, CH), 8.03 (m, 1H, CH), 8.43 (d, 1H, CH, *J* = 17.5 Hz), 10.09 (d, 1H, CH, *J* = 6.1 Hz).

6.4.15. Preparation and irradiation of Rh(CO)Cl(L17) 171 to obtain complex 172

To a solution of $[Rh(CO)_2Cl]_2$ (15 mg, 0.039 mmol) in CH_2Cl_2 (1 ml) **L17** (36 mg, 0.077 mmol) was added. After stirring at dark for 10 minutes, NMR indicated the formation of complex **171**. Then, the solvent was removed and THF (1 ml) was added, and the resulting solution irradiated with UV light for 30 minutes. Then, the solvent was evaporated, and the complex washed with pentane (2 x 2 ml) to obtain the corresponding complex **172** as an orange solid (47 mg, 97%).

6.4.16. Preparation of tungsten complex 163

To a solution of a freshly prepared $W(CO)_4(THF)_2$ (26 mg, 0.058 mmol) in THF (1 ml), **L17** was added (27 mg, 0.058 mmol) and the resulting mixture stirred overnight at 80 °C. After that, the solvent was evaporated, and the crude complex washed with pentane (2 x 1 ml) and dried under high vacuum. Then, the complex was dissolved in THF and irradiated for 30 min. Then, the solvent was evaporated to obtain the corresponding W complex **163** as a yellow solid (42 mg, 98%).

6.4.17. Characterization details for complexes 171, 172 and 163

Rh(CO)Cl(L17) (171). $^{31}P\{^1H\}$ NMR (162 MHz, CD_2Cl_2) δ: 12.44 (dq, *J* = 192.8 Hz, 12.8 Hz). $^{19}F\{^1H\}$ NMR (375 MHz, CD_2Cl_2) δ: -54.24 (q, 3F, CF_3, *J* = 13.2 Hz), -54.42 (p, 3F, CF_3, *J* = 13.0 Hz). ^{1}H NMR (400 MHz, CD_2Cl_2) δ: 1.46 (s, 9H, ^{t}Bu), 7.19 (dd, 1H, *J* = 21.8 Hz, 1.4 Hz), 7.51 (m, 2H), 7.60 (m, 2H), 7.92 (br. d, 2H, *J* = 7.7 Hz), 8.03 (m, 1H), 8.16 (m, 1H), 9.21 (d, 1H, CH, *J* = 15.6 Hz).

Rh(CO)Cl(L19) (172). $^{31}P\{^1H\}$ NMR (162 MHz, THF-d^8) δ: 104.09 (dq, *J* = 180.5 Hz, 8.4 Hz). $^{19}F\{^1H\}$ NMR (375 MHz, THF-d^8) δ: -64.37 (q, 3F, CF_3), -53.47 (m, 3F, CF_3). ^{1}H NMR

(700 MHz, CD_2Cl_2) δ: 1.47 (s, 9H, ^{t}Bu), 4.79 (d, 1H, CH, *J* = 6.7 Hz), 6.14 (d, 1H, CH, *J* = 8.1 Hz), 6.24 (dd, 1H, CH, *J* = 28.9 Hz, 1.1 Hz), 7.34 (ddd, 1H, CH, *J* = 7.3 Hz, 5.8 Hz, 1.4 Hz), 7.40 (m, 2H, CH), 7.48 (m, 3H, CH), 7.60 (m, 1H, CH), 9.80 (dd, 1H, CH, *J* = 5.8 Hz, 1.6 Hz). ^{13}C NMR (176 MHz, CD_2Cl_2) δ: significative signals: 30.8 (d, ^{t}Bu, *J* = 4.3 Hz), 35.2 (d, C-^{t}Bu, *J* = 11.8 Hz), 53.9 (CH), 54.18 (q, CH, *J* = 3.0 Hz), 118.6–158-9 (aromatics, CH= and CF_3 carbons).

W(CO)4(L19) (163). $^{31}P\{^1H\}$ NMR (243 MHz, THF-d^8) δ: 89.55 (q, *J* = 10.1 Hz, P-W satellite *J* = 263.8 Hz). $^{19}F\{^1H\}$ NMR (565 MHz, THF-d^8) δ: -62.28 (q, 3F, CF_3, *J* = 10.9 Hz), -51.79 (ap. p, 3F, CF_3, *J* = 10.9 Hz). ^{1}H NMR (700 MHz, THF-d^8) δ: 1.47 (s, 9H, ^{t}Bu), 4.62F (dd, 1H, CH, *J* = 5.2 Hz, 1.3 Hz), 6.05 (ddd, 1H, CH, *J* = 8.2 Hz, 1.4 Hz, 0.8 Hz), 6.29 (d, 1H, CH, *J* = 23.0 Hz), 7.06 (ddd, 1H, CH, *J* = 7.3 Hz, 5.7 Hz, 1.4 Hz), 7.44 (m, 5H, CH), 9.16 (ddd, 1H, CH, *J* = 5.7 Hz, 1.6 Hz, 0.8 Hz). ^{13}C NMR (176 MHz, CD_2Cl_2) δ: significative signals: 29.8 (d, ^{t}Bu, *J* = 4.2 Hz), 33.0 (d, C-^{t}Bu, *J* = 12.8 Hz), 53.5 (CH), 118.7-158.0 (aromatic, CH= and CF_3 carbons), 200.2 (d, CO, *J* = 8.4 Hz), 201.4 (d, CO, *J* = 5.5 Hz), 206.8 (d, CO, *J* = 5.1 Hz), 208.2 (d, CO, *J* = 32.2 Hz).

6.4.18. Preparation and irradiation of Cu complexes 173 and 174

To a solution of $Cu(AcCN)_4PF_6$ (0.5 equiv) in CH_2Cl_2 the respective ligand (1 equiv) was added **L16** or **L17**. After 10 min, the full complexation of ligands was detected as judged by $^{31}P\{^1H\}$-NMR. Then, the respective complexes were irradiated for 4 h to attain the corresponding 5-phosphasemibullvalenes (full conversion). Finally, dppp (0.9 equiv) was added. After 5 minutes, the complexes were analysed by NMR which showed the corresponding $Cu(dppp)_2PF_6$ and the corresponding **L18** and **L19** as non-coordinated ligands.

6.4.19. Characterization details for Cu complexes 173-174

$Cu(L17)_2PF_6$ (173). ^{1}H NMR only showed broad signals. $^{31}P\{^1H\}$ NMR (162 MHz, CD_2Cl_2) δ: -143.30 (sep, PF_6, *J* = 710.5 Hz), -66.80 (br. m, P(III)). $^{19}F\{^1H\}$ NMR (565 MHz, CD_2Cl_2) δ: -73.08 (d, 6F, PF_6, *J* = 710.5 Hz), -55.41 (br. q, 6F, CF_3, *J* = 15.1 Hz). Data for irradiated complex: $^{31}P\{^1H\}$ NMR (162 MHz, CD_2Cl_2) δ: -145.51 (sep, PF_6, *J* = 710.4 Hz), 42.80 (br. m, P(III)). $^{19}F\{^1H\}$ NMR (565 MHz, CD_2Cl_2) δ: -74.50 (d, 6F, PF_6, *J* = 710.4 Hz), -63.11 (br. m, 3F, CF_3), -52.80 (br. m, 3F, CF_3).

$Cu(L16)_2PF_6$ (174). ^{1}H NMR only showed broad signals. $^{31}P\{^1H\}$ NMR (162 MHz, CD_2Cl_2) δ: -143.84 (sep, PF_6, *J* = 710.6 Hz), -58.45 (br. m, P(III)). $^{19}F\{^1H\}$ NMR (565 MHz, CD_2Cl_2) δ: -73.14 (d, 6F, PF_6, *J* = 710.6 Hz), -54.55 (br. m, 6F, CF_3). Data for irradiated complex: $^{31}P\{^1H\}$ NMR (162 MHz, CD_2Cl_2) δ: -145.73 (sep, PF_6, *J* = 710.4 Hz), -42.90 (br. m, P(III)). $^{19}F\{^1H\}$ NMR (565 MHz, CD_2Cl_2) δ: -74.40 (d, 6F, PF_6, *J* = 710.4 Hz), -62.69 (br. m, 3F, CF_3), -59.20 (br. m, 3F, CF_3).

6.4.20. Preparation of L19 and L21 by irradiation of the corresponding 1-phosphabarrelene ligands

A solution of the corresponding 1-phosphabarrelene (0.3500 mmol) in dichloromethane (4 ml) was irradiated with UV light for 12h. After that, the solvent was evaporated and the product purified by flash chromatography (gradient 100% hexanes – 9:1 hexane:EtOAc).

6.4.21. Characterization details for L19 and L21

2-(1-(*tert*-Butyl)-2a–phenyl-3,4-bis(trifluoromethyl)- 2a,2b–dihydro-2a1H-4a-phosphacyclopropa[cd]pentalen-2a1-yl)pyridine (L19). White solid. 37% yield. $^{31}P\{^{1}H\}$ NMR (243 MHz, CD_2Cl_2) δ: 56.63 (q, *J* = 10.1 Hz). $^{19}F\{^{1}H\}$ NMR (565 MHz, CD_2Cl_2) δ: -61.83 (q, 3F, CF_3, *J* = 10.9 Hz), -51.88 (m, 3F, CF_3). ^{1}H NMR (600 MHz, CD_2Cl_2) δ: 1.27 (s, 9H, ^{t}Bu), 4.58 (m, 1H, CH), 6.05 (d, 1H, CH=, *J* = 6.9 Hz), 6.91 (1H, CH=, *J* = 7.9 Hz), 6.77 (ddd, 1H, CH=, *J* = 7.5 Hz, 4.9 Hz, 1.1 Hz), 7.09 (m, 2H, CH=), 7.14 (m, 3H, CH=), 7.43 (td, 1H, CH=, *J* = 7.7 Hz, 1.9 Hz), 8.29 (ddd, 1H, CH=, *J* = 4.9 Hz, 1.9 Hz, 1.0 Hz). ^{13}C NMR (176 MHz, CD_2Cl_2) δ: 31.5 (d, ^{t}Bu, *J* = 5.5 Hz), 35.3 (d, C-^{t}Bu, *J* = 15.8 Hz), 51.7 (dd, CH, *J* = 7.2 Hz), 64.5 (d, C, *J* = 7.4 Hz), 67.2 (C), 121.4 (d, CH=, *J* = 7.2 Hz), 121.7 (CH=), 127.6 (CH=), 128.2 (2xCH=), 129.7 (2xCH=), 136.0 (CH=), 136.1 (d, CH=, *J* = 3.3 Hz), 137.1 (C=), 149.1 (C=), 155.0 (d, C=, *J* = 24.9 Hz), 163.7 (d, C=, *J* = 29.7 Hz).

2a-(*tert*-Butyl)–1–phenyl-2b,3–bis(trifluoromethyl)-2a,2b–dihydro- 4aH-2a1-phosphacyclopropa[cd]pentalen-4a-yl)pyridine (L21). White solid. 28%. $^{31}P\{^{1}H\}$ NMR (243 MHz, CD_2Cl_2) δ: 56.63 (q, *J* = 10.1 Hz). $^{19}F\{^{1}H\}$ NMR (565 MHz, CD_2Cl_2) δ: -61.83 (q, 3F, CF_3, *J* = 10.9 Hz), -51.88 (m, 3F, CF_3). ^{1}H NMR (600 MHz, CD_2Cl_2) δ: 1.04 (s, 9H, ^{t}Bu), 4.72 (m, 1H, CH=), 6.4 (s, 1H, CH=), 7.21 (ddd, 1H, CH=, *J* = 7.6 Hz, 4.8 Hz, 1.2 Hz), 7.36 (m, 5H, CH=), 7.51 (m, 2H, CH=), 7.66 (td, 1H, CH=, *J* = 7.7 Hz, 1.8 Hz), 8.58 (ddd, 1H, CH=, *J* = 4.8 Hz, 1.9 Hz, 1.0 Hz). ^{13}C NMR (176 MHz, CD_2Cl_2) δ: 30.1 (d, ^{t}Bu, *J* = 8.5 Hz), 35.7 (d, C-^{t}Bu, *J* = 11.8 Hz), 68.9 (d, CH, *J* = 6.2 Hz), 72.1 (d, C, *J* = 22.8 Hz), 88.2 (d, C, *J* = 48.5 Hz), 122.8 (CH=), 124.2 (d, CH=, *J* = 8.8 Hz), 126.4 (CH=), 127.6 (2xCH=), 128.4 (2xCH=), 128.4 (CH=), 129.7 (CH=), 132.8 (C=), 136.6 (CH=), 142.1 (C=), 149.9 (CH=), 157.2 (d, C=, *J* = 11.6 Hz).

6.5. References

1. (a) Kobayashi, Y.; Kumadaki, I.; Ohsawa, A.; Hamana, H., 1,3-Dipolar cycloaddition reactions of a diphosphabarrelene. *Tetrahedron Letters* **1977**, *18*, 867-868; (b) Annen, U.; Regitz, M., Phosphabarrelene mit λ3σ2-phosphor. *Tetrahedron Letters* **1987**, *28*, 5141-5144.
2. (a) Märkl, G.; Lieb, F., Substituted 1-Phosphabarrelenes (1-Phospha[2.2.2]octa-2,5,7-trienes). *Angewandte Chemie International Edition in English* **1968**, *7*, 733-733; (b) Märkl, G.;

Heier, K. H., Benzo- und dibenzo-phosphabarrelene. *Tetrahedron Letters* **1974**, *15*, 4369-4372.
3. Alcaraz, J.-M.; Mathey, F., Generation and trapping of a phosphinine sulphide. *Journal of the Chemical Society, Chemical Communications* **1984**, 508-509.
4. Alcaraz, J.-M.; Mathey, F., Accroissement de la reactivite des phosphorines en tant que dienes et philodienes par complexation du phosphore. *Tetrahedron Letters* **1984**, *25*, 207-210.
5. (a) Moloy, K. G.; Petersen, J. L., N-Pyrrolyl Phosphines: An Unexploited Class of Phosphine Ligands with Exceptional .pi.-Acceptor Character. *Journal of the American Chemical Society* **1995**, *117*, 7696-7710; (b) Breit, B.; Winde, R.; Mackewitz, T.; Paciello, R.; Harms, K., Phosphabenzenes as Monodentate π-Acceptor Ligands for Rhodium-Catalyzed Hydroformylation. *Chemistry – A European Journal* **2001**, *7*, 3106-3121; (c) Fuchs, E.; Keller, M.; Breit, B., Phosphabarrelenes as Ligands in Rhodium-Catalyzed Hydroformylation of Internal Alkenes Essentially Free of Alkene Isomerization. *Chemistry – A European Journal* **2006**, *12*, 6930-6939; (d) Fernández, E.; Ruiz, A.; Claver, C.; Castillón, S.; Polo, A.; Piniella, J. F.; Alvarez-Larena, A., Regio- and Stereoselective Hydroformylation of Glucal Derivatives with Rhodium Catalysts. *Organometallics* **1998**, *17*, 2857-2864.
6. Tolman, C. A., Steric effects of phosphorus ligands in organometallic chemistry and homogeneous catalysis. *Chemical Reviews* **1977**, *77*, 313-348.
7. Wallis, C.; Edwards, P. G.; Hanton, M.; Newman, P. D.; Stasch, A.; Jones, C.; Tooze, R. P., Coordination chemistry of 2,6-dixylyl-4-phenylphosphabarrelene with selected transition metals. *Dalton Transactions* **2009**, 2170-2177.
8. Müller, C.; Vogt, D., Phosphinines as ligands in homogeneous catalysis: recent developments, concepts and perspectives. *Dalton Transactions* **2007**, 5505-5523.
9. Blug, M.; Guibert, C.; Le Goff, X.-F.; Mézailles, N.; Le Floch, P., 1-Phosphabarrelene complexes of palladium and their use in Suzuki–Miyaura coupling reactions. *Chemical Communications* **2008**, 201-203.
10. Blug, M.; Le Goff, X.-F.; Mézailles, N.; Le Floch, P., A 14-VE Platinum(0) Phosphabarrelene Complex in the Hydrosilylation of Alkynes. *Organometallics* **2009**, *28*, 2360-2362.
11. Breit, B.; Fuchs, E., Chiral Phosphabarrelene Ligands: Synthesis and Evaluation in Rhodium-Catalyzed Asymmetric Hydrogenation. *Synthesis* **2006**, *2006*, 2121-2128.
12. Robin, F.; Mercier, F.; Ricard, L.; Mathey, F.; Spagnol, M., BIPNOR: A New, Efficient Bisphosphine Having Two Chiral, Nonracemizable, Bridgehead Phosphorus Centers for Use in Asymmetric Catalysis. *Chemistry – A European Journal* **1997**, *3*, 1365-1369.
13. Gilbertson, S. R.; Genov, D. G.; Rheingold, A. L., Synthesis of New Bicyclic P−N Ligands and Their Application in Asymmetric Pd-Catalyzed π-Allyl Alkylation and Heck Reaction. *Organic Letters* **2000**, *2*, 2885-2888.
14. Bruce, M.; Papke, M.; Ehlers, A. W.; Weber, M.; Lentz, D.; Mézailles, N.; Slootweg, J. C.; Müller, C., Pyridyl-Functionalized 1-Phosphabarrelene: Synthesis, Coordination Chemistry and Photochemical di-π-Methane Rearrangement. *Chemistry – A European Journal* **2019**, *25*, 14332-14340.
15. Zimmerman, H. E.; Grunewald, G. L., The Chemistry of Barrelene. III. A Unique Photoisomerization to Semibullvalene. *Journal of the American Chemical Society* **1966**, *88*, 183-184.
16. Rigo, M.; Weber, M.; Müller, C., Expanding the phosphorus–carbon analogy: formation of an unprecedented 5-phosphasemibullvalene derivative. *Chemical Communications* **2016**, *52*, 7090-7093.
17. (a) Lemouzy, S.; Giordano, L.; Hérault, D.; Buono, G., Introducing Chirality at Phosphorus Atoms: An Update on the Recent Synthetic Strategies for the Preparation of Optically Pure P-Stereogenic Molecules. *European Journal of Organic Chemistry* **2020**, *2020*, 3351-3366; (b) Grabulosa, A.,·*P-Stereogenic Ligands in Asymmetric Catalysis*. RSC Publishing: Cambridge, 2011; (c) Grabulosa, A.; Granell, J.; Muller, G., Preparation of optically pure P-stereogenic

trivalent phosphorus compounds. *Coordination Chemistry Reviews* **2007**, *251*, 25-90; (d) Kolodiazhnyi, O. I., Recent Advances in Asymmetric Synthesis of P-Stereogenic Phosphorus Compounds. *Topics in Current Chemistry* **2015**, *360*, 161-236.

18. Müller, C.; Wasserberg, D.; Weemers, J. J. M.; Pidko, E. A.; Hoffmann, S.; Lutz, M.; Spek, A. L.; Meskers, S. C. J.; Janssen, R. A. J.; van Santen, R. A.; Vogt, D., Donor-Functionalized Polydentate Pyrylium Salts and Phosphinines: Synthesis, Structural Characterization, and Photophysical Properties. *Chemistry – A European Journal* **2007**, *13*, 4548-4559.

19. Etayo, P.; Vidal-Ferran, A., Rhodium-catalysed asymmetric hydrogenation as a valuable synthetic tool for the preparation of chiral drugs. *Chemical Society Reviews* **2013**, *42*, 728-754.

20. Darensbourg, D. J.; Draper, J. D.; Frost, B. J.; Reibenspies, J. H., Structural and Spectroscopic Studies of 16-Electron, Unsaturated Derivatives of Low-Valent, Group 6 Carbonyl Complexes Containing π-Donor Ligands. *Inorganic Chemistry* **1999**, *38*, 4705-4714.

21. (a) Zimmerman, H. E.; Armesto, D., Synthetic Aspects of the Di-π-methane Rearrangement. *Chemical Reviews* **1996**, *96*, 3065-3112; (b) Liu, R. S. H., 2,3-Bis(perfluormethyl)bicyclo[2.2.2]octa-2,5,7-trienes and their photorearrangement reactions. *Journal of the American Chemical Society* **1968**, *90*, 215-216.

22. Zimmerman, H. E.; Binkley, R. W.; Givens, R. S.; Grunewald, G. L.; Sherwin, M. A., Mechanistic and exploratory organic photochemistry. XLIV. The barrelene to semibullvalene transformation. Correlation of excited-state potential energy surfaces with reactivity. *Journal of the American Chemical Society* **1969**, *91*, 3316-3323.

23. Wu, Y.; Zhou, G.; Meng, Q.; Tang, X.; Liu, G.; Yin, H.; Zhao, J.; Yang, F.; Yu, Z.; Luo, Y., Visible Light-Induced Aerobic Epoxidation of α,β-Unsaturated Ketones Mediated by Amidines. *The Journal of Organic Chemistry* **2018**, *83*, 13051-13062.

UNIVERSITAT ROVIRA I VIRGILI
DEVELOPMENT OF TAILOR-MADE CATALYST LIBRARIES FOR THE CONSTRUCTION OF CHIRAL C-X (X= C, N AND O) BONDS. APPLICATION TO THE SYNTHESIS OF COMPLEX MOLECULES
Joan Saltó de la Torre

Chapter 7

General conclusions

The general conclusions of this thesis are:

1. We have synthetized two families of easily accessible and air stable heterodonor ligand libraries that surpass the best results reported so far in the Pd-AAS. The simplicity of the first family allowed us to use DFT calculations to optimize the ligand parameters. In this respect, the application of the optimized P-thioether ligand has overcome the substrate specificity and the low nucleophilic scope in this transformation. The second family of ligands, a set of phosphite-oxazoline compounds, surpass the best results reported with the previous commented Pd/P-thioether catalyst. Moreover, and in contrast to Pd/phosphite-N ligands previously reported in the literature, the mechanistic studies showed that the enantioselectivities are not only governed by the biaryl phosphite moieties but also by the oxazoline substituents.

2. To show the synthetic applicability of Pd-AAS reactions, some of the compounds resulting from the application of the previous two family of ligands have been applied in subsequent sequential derivatizations, such as Grubb's metathesis, Pauson-Khand or cycloisomerization reactions, to produce a range of chiral functionalized (poly)carbocyclic and heterocyclic compounds, with multiple stereogenic centers. From all of them we should highlight for the first time the successful preparation of a range of highly functionalized fused tricyclic compounds in good yields and excellent selectivities by combining allylic alkylation with either cycloisomerization or Pauson-Khand reactions.

3. Finally, to expand the current portfolio of ligands for asymmetric catalysis, we have developed for the first time the synthesis of a reduced but valuable chiral phosphabarralene/5-phosphasemibullvalene-pyridine family of ligands designed to be applied in the near future in some asymmetric catalytic processes. We managed to improve the synthetic yield of a previous synthetized phosphabarralene-pyridine ligand by optimization of the reaction conditions. These optimizations were also successfully applied to the synthesis of other phosphabarralene-pyridine ligands, with different substituent decorating the phosphabarrelene moiety. The study of the irradiation of phosphabarrelene-pyridine containing complexes indicated that two new set of 5-phosphasemibullvalene ligands could be obtained. Furthermore, the irradiation of the ligands indicated that whereas for the reported ligand the

irradiation was less selective, the new ^{t}Bu-based phosphabarrralene-pyridine ligand showed to be more promising since only two species were formed.

UNIVERSITAT ROVIRA I VIRGILI
DEVELOPMENT OF TAILOR-MADE CATALYST LIBRARIES FOR THE CONSTRUCTION OF CHIRAL C-X (X= C, N AND O) BONDS. APPLICATION TO THE SYNTHESIS OF COMPLEX MOLECULES
Joan Saltó de la Torre

UNIVERSITAT ROVIRA I VIRGILI
DEVELOPMENT OF TAILOR-MADE CATALYST LIBRARIES FOR THE CONSTRUCTION OF CHIRAL C-X (X= C, N AND O) BONDS. APPLICATION TO THE SYNTHESIS OF COMPLEX MOLECULES
Joan Saltó de la Torre

UNIVERSITAT ROVIRA I VIRGILI
DEVELOPMENT OF TAILOR-MADE CATALYST LIBRARIES FOR THE CONSTRUCTION OF CHIRAL C-X (X= C, N AND O) BONDS. APPLICATION TO THE SYNTHESIS OF COMPLEX MOLECULES
Joan Saltó de la Torre

UNIVERSITAT ROVIRA I VIRGILI
DEVELOPMENT OF TAILOR-MADE CATALYST LIBRARIES FOR THE CONSTRUCTION OF CHIRAL C-X (X= C, N AND O) BONDS. APPLICATION TO THE SYNTHESIS OF COMPLEX MOLECULES
Joan Saltó de la Torre

UNIVERSITAT ROVIRA I VIRGILI
DEVELOPMENT OF TAILOR-MADE CATALYST LIBRARIES FOR THE CONSTRUCTION OF CHIRAL C-X (X= C, N AND O) BONDS. APPLICATION TO THE SYNTHESIS OF COMPLEX MOLECULES
Joan Saltó de la Torre

UNIVERSITAT
ROVIRA i VIRGILI